The Interaction of HIV with Cellular Trafficking Pathways

Justine E. Alford

Thesis submitted in partial fulfilment of the requirements for the degree of

Doctor of Philosophy

University of Warwick, School of Life Sciences

October 2013

Contents

CHAPTER 2: MATERIALS AND METHODS

CHAPTER 3: DOES HIV-1 PROTEIN EXPRESSION ALTER THE LEVELS/LOCALISATION OF THE ADAPTOR PROTEINS

CHAPTER 4: DO THE ADAPTOR PROTEINS AFFECT HIV-1 GENE EXPRESSION?

CHAPTER 5: WHAT IS THE EFFECT OF ADAPTOR PROTEIN DEPLETION ON HIV-1 GAG TRAFFICKING?

CHAPTER 6: INVESTIGATING HIV-2 TRAFFICKING AND THE ROLE OF THE MATRIX DOMAIN IN HIV-1 AND HIV-2 TRAFFICKING

Acknowledgements

There are numerous people that I wish to thank for supporting me throughout this PhD. Firstly, I would like to thank my supervisor Dr Emma Anderson, for not only providing me with this incredible academic opportunity, but for her unparalleled guidance as a supervisor. Without her patience, advice and support, none of this work would have been possible.

I would also like to thank my second supervisor Professor David Evans for his helpful advice throughout my PhD, but also particularly during Emma's absence. My collaborators, Dr Robert Spooner and Dr Yuriy Pankratov, made some of the most interesting pieces of work in this thesis possible, and I thank them for donating me their valuable time and expertise.

I am exceedingly grateful for the helpful technical advice, tips, protocols and constant lending of reagents and equipment from members of the Virology labs; Gemma Watkins, Michela Marongiu, Phil Gould, Jordan Wright and Andy Tuplin in particular.

My family; Mum, Dad, Stepdad, Brother and Grandparents always believed in me even when I didn't, and taught me to have faith in my own abilities. My friends, and of course John, also encouraged me every step of the way and cheered me up no end during the tough times, for which I am eternally grateful.

I would finally like to thank the University of Warwick for the provision of excellent research and learning facilities, and the Medical Research Council for their generous funding.

Declaration

This work was completed at the University of Warwick between October 2010 and September 2013, and has not been submitted for another degree. I declare that the work is original and, unless otherwise stated in the text, has been completed by the author.

Justine Elizabeth Alford October 2013

Summary

HIV-1 hijacks cellular trafficking pathways in order to transport newly synthesised viral subunits, such as the structural polyprotein Gag, to virion assembly sites. HIV-1 Gag has been reported to interact with clathrin adaptor proteins (AP) 1-3, which function to assist clathrin mediated cargo transport. AP-1 and AP-3 assist viral particle release, whereas AP-2 inhibits viral particle release. How these APs facilitate HIV protein trafficking and particle assembly, and the consequences of HIV infection on the function of these trafficking pathways, has not been elucidated. The interaction of these pathways with the closely related virus, HIV-2, has also not been defined.

Confocal immunofluorescence microscopy revealed HIV-1 and HIV-2 Gag have different intracellular localisations; HIV-1 displayed a mainly diffuse cytoplasmic location, whereas HIV-2 predominantly localised to intracellular compartments. Further investigation through microscopy found that HIV-2, unlike HIV-1, heavily colocalised with AP-3, which functions in endosomal cargo trafficking. siRNA mediated knockdown of the APs also deduced that HIV-2 is more dependent on AP-3 than AP-1 to facilitate particle assembly, whereas HIV-1 had similar dependencies on both. HIV-2 also strongly colocalised with, and redistributed clathrin.

Initial investigation of adaptor protein dependent trafficking pathways deduced that HIV-2 interrupted the trafficking of Diphtheria toxin, which traffics in an AP-3 dependent manner through endosomal compartments, to a greater extent than HIV-1. Taken together, these results suggested that these viruses adopt different pathways to reach assembly sites, and that particle assembly likely occurs at different localisations between these viruses; the plasma membrane, via an endosomal intermediate, for HIV-1, and predominantly intracellular compartments for HIV-2. Furthermore, it was found that the matrix domain of Gag, which contains AP binding sites, was not sufficient to drive this different Gag localisation in mutant chimeric viruses.

Finally, the interruption of AP dependent trafficking pathways was investigated in astrocytes. HIV-1 displayed a striking perturbation of vesicle endocytosis events, indicating a global negative effect on these AP dependent pathways and suggesting a putative mechanism for the development of neurological symptoms, in particular short-term memory loss, during HIV infection.

Abbreviations

Ab	Antibody
AEA	Anandamide
Ag	Antigen
AIDS	Acquired immune deficiency syndrome
AMPA	2-amino-3-(3-hydroxy-5-methyl-isoxazol-4-yl) propanoic acid
AP	Adaptor Protein
ARV	Antiretroviral
ATP	Adenosine-5'-triphosphate
BAF	Barrier to auto integration factor
BBB	Blood brain barrier
BFA	Brefeldin A
BSA	Bovine serum albumin
CA	Capsid
CDK	Cyclin dependent kinase
cDNA	Complementary DNA
CD4	Cluster of differentiation 4
CD63	Cluster of differentiation 63
CMV	Cytomegalovirus
CNS	Central nervous system
COP	Coat protein complex
CRFs	Circulating recombinant forms
CTD	Carboxy terminal domain
CypA	Cyclophillin A
DAPI	4',6-diamidino-2-phenylindole dihydrochloride
DMEM	Dulbecco's modified eagle's medium
DMSO	Dimethyl sulfoxide
DNA	Deoxyribonucleic acid
dsRNA	Double stranded RNA
DTx	Diphtheria toxin
E. coli	*Escherichia coli*
ECL	Enhanced chemiluminescence
EDTA	Ethylenediamine tetraacetic acid
EMEM	Eagle's minimum essential medium
Env	Envelope glycoprotein
ESCRT	Endosomal sorting complex required for transport
ER	Endoplasmic reticulum
Fc	Fragment crystallisable
FCS	Foetal calf serum
Gag	Group specific antigen
GFAP	Glial fabrillary acidic protein
GFP	Green fluorescent protein
GluR	Glutamate receptor
HAART	Highly active antiretroviral therapy
HAD	HIV associated dementia
HAND	HIV associated neurocognitive disorders
HIV	Human immunodeficiency virus
HLA	Human leukocyte antigen
HRP	Horse radish perixodase
HTLV	Human T-lymphotrophic virus
IDU	Injecting drug user
IL	Interleukin
IN	Integrase
IP	Immunoprecipitation
kB	Kilobase
kDa	Kilodaltons
LB	Lysogeny broth
LEDGF	Lens epithelium-derived growth factor
LTR	Long terminal repeats
µCi	Microcurie
MA	Matrix
MHC	Major histocompatibility complex
MPR	Mannose-6-phosphate receptor
mRNA	Messenger RNA
MVB	Multivesciular body
NC	Nucleocapsid
NEB	New England Biolabs

Nef	Negative factor
NFκB	Nuclear factor kappa-light-chain-enhancer of activated B cells
NIBSC	National Institute for Biological Standards Control
NIH	National Institutes for Health
NLS	Nuclear localisation signal
NNRTI	Non-nucleoide reverse transcriptase inhibitor
NPC	Nuclear pore complex
NRTI	Nucleoside reverse transcriptase inhibitor
Nt	Nucleotide
ONPG	Ortho-nitrophenyl-β-galactopyranoside
OPV	Oral polio vaccine
ORF	Open reading frame
PBS	Phosphate buffered saline
PCR	Polymerase chain reaction
PEG	Polyethylene glycol
PIC	Pre-integration complex
PKR	Protein kinase R
PKRi	Protein kinase R inhibitor
PLB	Passive lysis buffer
PM	Plasma membrane
PPT	Polypurine tract
PR	Protease
RER	Rough endoplasmic reticulum
Rev	Regulator of virion expression
RIPA	Radio immunoprecipitation assay
RL	Renilla luciferase
RNA	Ribonucleic acid
RPM	Revolutions per minute
RRE	Rev responsive element
RT	Reverse transcriptase
rt	Room temperature
RTx	Ricin toxin
SD	Splice donor
SDS	Sodium dodecyl sulphate
SDS-PAGE	Sodium dodecyl sulphate polyacrylamide gel electrophoresis
siRNA	Short interfering RNA
SIV	Simian immunodeficiency virus
SOC	Super optimal broth with catabolite repression
SP	Spacer peptide
STD	Sexually transmitted disease
SU	Surface
SQV	Saquinavir
TAK	Tat-associated kinase
TAR	*trans*-activation response element
Tat	Trans-activator of transcription
TBS-T	Tris-buffered saline tween
TCA	Trichloroacetic acid
TfR	Transferrin receptor
TFLLR	Trifluoroacetate salt
TGF	Transforming growth factor
TGN	Trans-Golgi network
TM	Transmembrane
TRBP	Human immunodeficiency virus transactivating response RNA-binding protein
UTP	Uridine-5’-triphosphate
UTR	Untranslated region
Vif	Virion infectivity factor
Vpr	Viral protein R
Vpu	Viral protein U
Vpx	Viral protein X
VSV-G	Vesicular stomatitis glycoprotein/ts045-VSV-G-EGFP

CHAPTER 1: INTRODUCTION

1.1 The Origin of HIV

Human immunodeficiency virus (HIV) is a retrovirus belonging to the genus Lentivirus, and is the causative agent of the degenerative disease acquired immune deficiency syndrome (AIDS). There are 3 main groups of Retrovirus; spumaviruses, with human foamy virus as the prototype within the *Spumavirus* genus (Delelis et al., 2003); oncoretroviruses, such as the human T-lymphotrophic virus type 1 (HTLV-1) (Mahieux and Gessain, 2003) and lentiviruses. Lentiviruses are characterised by long incubation periods, causing chronic and persistent infections in mammals (Gifford, 2012). This is due to their inherent ability to stably integrate their genome into that of the host, therefore establishing a latent infection that may be reactivated at a later stage to produce new viral particles (Schild and Minor 1990). Lentiviruses have been isolated from various animal species such as horses, cats, monkeys and cattle, for example the well characterised equine infectious anaemia virus (EIAV) but HIV is the only known Lentivirus to infect humans (Coffin et al, 1997; Leroux et al., 2004; Sharp and Hahn, 2011). There are also numerous other immunodeficiency viruses; the simian immunodeficiency viruses (SIV) which infect apes and monkeys, bovine immunodeficiency viruses (BIV) that infect cattle, and feline immunodeficiency viruses (FIV) which infect cats (Yamamoto et al., 2010; Chahroudi et al., 2012; Bhatia et al., 2013).

There are two types of HIV; HIV-1 and HIV-2. HIV-1 is the dominant virus worldwide, whereas HIV-2 is largely confined to West African countries, and those with links to West Africa such as France and Portugal. HIV-2 is separated into eight groups, A-H, with A the most prevalent worldwide. Until recently, HIV-1 has been

organised into 3 groups; M (Main) which is responsible for the majority of infections worldwide, N (Non-M, Non-O) and O (Outlier) (Coffin et al., 1997). The M group is then further divided into 9 subtypes, or clades, of A-D, F-H, J and K which dominate in different geographical areas worldwide (see Figure 1) (Coffin et al., 1997; Tebit and Arts, 2011). Clade C, which is prevalent in Africa and Asia, is responsible for over 50% of new infections worldwide (Geretti et al., 2006). Inter-subtype recombination events have also resulted in numerous CRFs (circulating recombinant forms) worldwide, with at least 49 recorded so far (Castro-Nallar et al., 2012). A new HIV-1 variant, closely related to the simian immunodeficiency virus SIVgor, which is found in wild-living gorillas, has been found in a Cameroonian woman which is distinct from the established 3 HIV-1 groups, and has been designated into a novel group; P (Plantier et al., 2009).

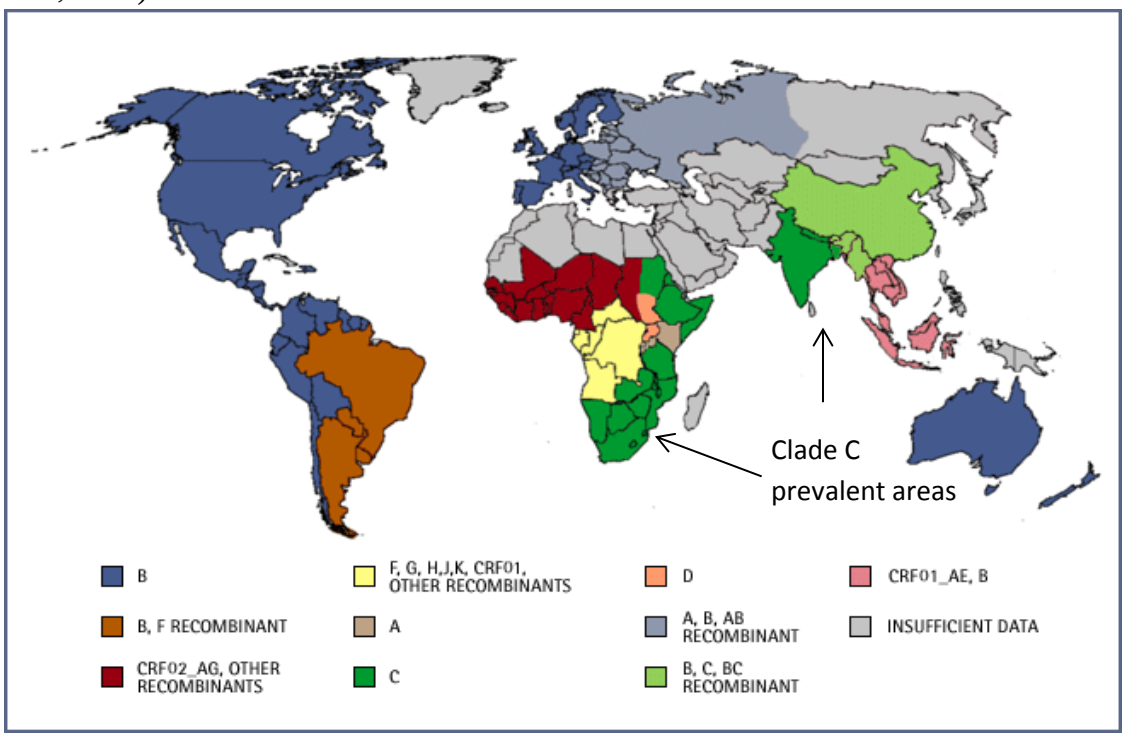

Figure 1: The global distribution of HIV-1. The map below displays the global distribution of the 9 HIV-1 clades and the common circulating recombinant forms (adapted from http://www.pbs.org/wgbh/pages/frontline/aids/atlas/clade.html accessed 01.2012).

Phylogenetic data has shown that the closest lentiviral relatives of HIV are the collectively known simian immunodeficiency viruses (SIVs) which infect non-human primates, but unlike HIV they do not usually cause disease in their hosts; however some species do exhibit very high infection rates (Sharp et al., 2001). More than 40 species of African primates have been found to harbour SIVs and geographical correlations exist between SIVs in their different primate hosts and HIV. Data such as this provided undeniable evidence that HIV arose through cross-species transmission from primates in Africa (Sharp et al., 2001; Castro-Nallar et al., 2012).

HIV-1 and HIV-2 arose from independent transmission events and therefore have different lineages (Sharp et al., 1995). Closely related SIVs to HIV-2 have been found in sooty mangabeys (*Cercocebus atys*; SIVsm) and three different macaque species (SIVmac). The only macaques found to harbour SIVmac have been in captivity as they are not naturally infected; wild sooty mangabeys however have been found to carry SIVsm in Western Africa, the only region to which HIV-2 is endemic (Sharp et al., 2001; Castro-Nallar et al., 2012). Specifically, the eight groups of HIV-2 arose from eight independent transmissions from SIVsm infected sooty mangabeys in West Africa (Sharp and Hahn, 2011).

HIV-1 has a slightly more complicated lineage; however, each group arose from a single transmission event. Groups M and N have been traced to originate from SIV-infected chimpanzees of the *Pan troglodytes troglodytes* species (SIVcpz), whereas the closest SIV relatives of O and P are in gorillas (SIVgor) (Tebit and Arts, 2011; Ayouba et al., 2013). Most cross-species transmission events of SIVs into humans gave rise to a virus with limited replicative ability in humans; the single transmission event of SIVcpz which gave rise to group M, however, is largely responsible for the AIDS epidemic (Sharp and Hahn, 2011). A diagrammatic representation of transmission

events and relationships between HIV and SIVs is shown in Figure 2 (reproduced with permission by Elsevier).

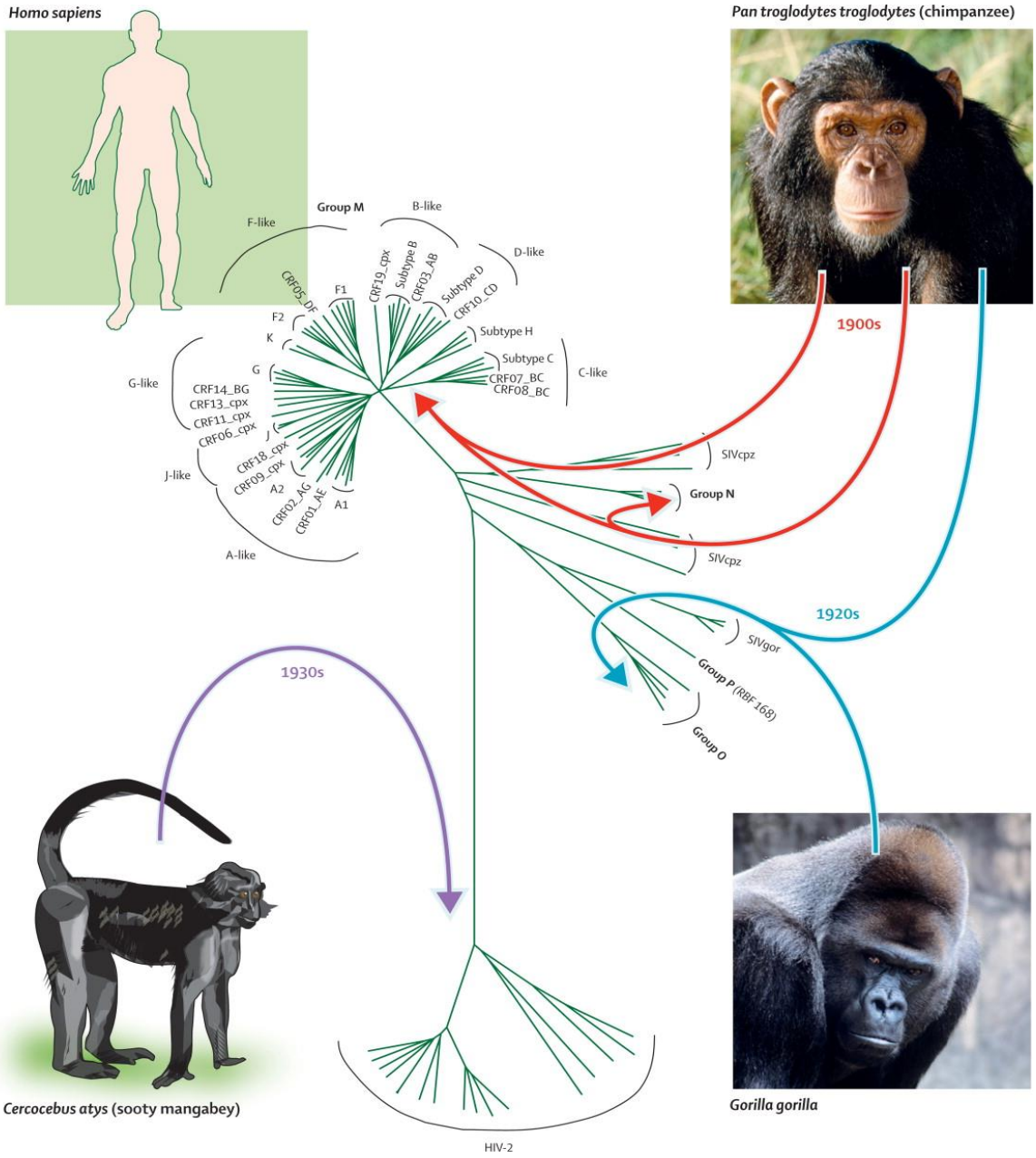

Figure 2: A diagram showing the relationships between the HIV-1 groups, M, N, O and P, HIV-2 and the SIVs, and transmission events between primates and humans (Tebit and Arts, 2011).

In order to determine when HIV entered the population by cross-species transmission, scientists gathered viral sequence data over time, using this to calibrate a "molecular clock" based on the rate of change of nucleotides. This can then be used to infer the rate of sequence evolution (Wertheim and Worobey, 2009). The time of most recent

common ancestor (tMRCA) of HIV-1 group M was estimated to be 1908; the highest probability distribution was estimated to be between 1884 and 1924 (Worobey et al., 2008). The tRMCA of group O was estimated at 1920 (1890-1940) (Lemey et al., 2004). The two epidemic subtypes of HIV-2, A and B, were also investigated, and the tRMCAs were found to be approximately 1940 (1924-1956) and 1945 (1931-1959), respectively (Lemey et al., 2003). Differences in estimates arise from recombination events, which are frequent in HIV (Schierup and Hein, 2000). HIV-1 and HIV-2 in their present forms share only 40% nucleotide sequence identity (Dilley et al., 2011).

But how did these viruses get into the human population? The simplest suggestion is via direct exposure to infected blood or mucosal secretions from infected animals (Sharp et al., 2001), which is logical because indigenous sooty mangabeys, for example, are kept as pets or butchered for food in West Africa, the same geographic region to which HIV-2 is most prevalent (Gao et al., 1999; Sharp et al., 1999). The rise in logging in Africa also opened up previously inaccessible wildlife habitats, leading to an increase in the resulting "bushmeat" being sold (Robinson et al., 1999). The consumption of improperly cooked meats or exposure to infected secretions whilst butchering the animals seems a plausible pathway of entrance.

Another popular theory of the origin of HIV is that it has always been present in the population, but at such low prevalence that it was unrecognised. Changes to society, for example urbanisation and the beginnings of world travel may have introduced the virus into previously uninfected countries. An increase in promiscuity, intravenous drug use and the liberation of gay people would have encouraged rapid spread of the virus through the human population (Coffin et al., 1997).

1.1.1 Restriction Factors and Crossing the Species Barrier

The immune system can be separated into two subsystems; the adaptive and innate systems. Innate responses are non-specific and form the first line of defence to an incoming pathogen. They rely on features that are common to many pathogens but not present in the host, and evoke 2 forms of response; an inflammatory response, which is mediated in part by cytokines, and phagocytosis (the engulfment of a particular object) by cells such as macrophages. The adaptive immune response is more specific and complex, providing long-term protection against pathogens by immunologic memory and is split into two responses; humoral (antibody) or cell-mediated. The humoral response is mediated by a class of lymphocytes called B cells which produce the antibodies; whereas the cell-mediated response is facilitated by T cells, of which there are many types including helper T cells which release cytokines, and cytotoxic T cells (Janeway et al., 2001; Alberts et al., 2002). Both of these responses are important features of HIV infection.

Primate hosts, including humans, have evolved numerous restriction factors as part of the innate immune response as a barrier to various pathogens; the virus in-turn evolves mechanisms to counteract these; however, these are often species-specific. Therefore, the virus needs to develop new ways in which to counteract these restriction factors (Sharp and Hahn, 2011). Three classes of restriction factors are known to exist, which provide obstacles to SIV cross-species transmission. These are BST-2 (tetherin), which forms protein tethers expressed on the cell surface that prevent virus release (Neil et al., 2008), APOBEC3G (apolipoprotein B mRNA-editing, enzyme-catalytic, polypeptide-like 3G) which inhibits reverse transcription (Mehle et al., 2004), and TRIM5α that prevents uncoating (Kajaste-Rudnitski et al., 2010). These classical restriction factors have been shown to be up-regulated by the antiviral cytokine interferon-alpha (IFN-α)

(Sakuma et al., 2007; Wang et al., 2008; Homann et al., 2011. Tetherin has had a large effect on the success of the viruses introduced into the human population by cross-species transmission (Sharp and Hahn, 2011).

Selection pressures imposed during cross-species transmission have resulted in the emergence of different anti-tetherin responses; the majority of SIV strains use Nef to counteract tetherin, whereas HIV-1 uses Vpu (see chapter 1.4.7iv for a description of these HIV proteins) (Neil et al., 2008; Jai et al., 2009). However, this also in-turn drives host evolution; indeed, the human tetherin has a deletion in the cytoplasmic domain, which was sufficient to render the SIVcpz Nef ineffective at counteracting tetherin. This meant that SIVcpz needed to develop other mechanisms to counteract tetherin, which was not always successful. When HIV-1 groups were investigated, it was found that only group M viruses possessed strong anti-tetherin responses, which likely provides some explanation for the fact that group M is responsible for the majority of the AIDS epidemic (Sauter et al., 2009; Sharp and Hahn, 2011). Indeed, the 2 viruses within the newly discovered P group are also unable to antagonise tetherin (Sauter et al., 2011).

TRIM5α is a ubiquitin ligase expressed by all primate species, and restricts HIV infection by prematurely destabilising the viral capsid through acting as a pattern recognition receptor for the capsid lattice, meaning reverse transcription cannot ensue (Stremlau et al., 2004; Pertel et al., 2011). It has also been found to promote innate immune signalling through initiating a signal transduction cascade (Stremlau et al., 2004; Takeuchi et al., 2013). Since chimpanzees are relatively closely related to humans, it was likely that HIV-1 did not require significant adaptations to counteract TRIM5α; HIV-2 on the other hand originated from sooty mangabeys, which are less closely related to humans. It was therefore suggested that one of the reasons that HIV-2

is less pathogenic than HIV-1 is through an inability to counteract TRIM5α; indeed, it was discovered that the CA domain of HIV-2 is more susceptible to TRIM5α than HIV-1 (Takeuchi et al., 2013).

There are also two other restriction factors of HIV infection; SAMHD1 (SAM domain and HD domain-containing protein 1) and the recently described REAF (RNA-associated Early-stage Anti-viral factor) (Marno et al., 2014). SAMHD1 restricts HIV-1 infection in primary macrophages, dendritic cells and resting $CD4^+$ T cells early in cell infection by degrading the pool of dNTPs which are required for reverse transcription. HIV-2 and SIV encode an accessory protein called Vpx which counteracts SAMHD1 restriction by targeting it for degradation (Descours et al., 2012; Lahouassa et al., 2012). REAF inhibits HIV-1, HIV-2 and SIV infection early in the replication cycle. Although a limited amount is known so far, it is thought that it may inhibit reverse transcription since it associates with viral nucleic acids (Marno et al., 2014).

1.2 HIV Pathogenesis

1.2.1 Epidemiology of HIV

In 2010, it was estimated that 33.3 million people worldwide are living with HIV; 30.8 million of these are adults. An astonishing 2.6 million individuals are newly infected with HIV per year, and 1.8 million infected people die of AIDS every year (UNAIDS, 2010). The burden of HIV worldwide differs extensively between geographic regions (see Figure 3).

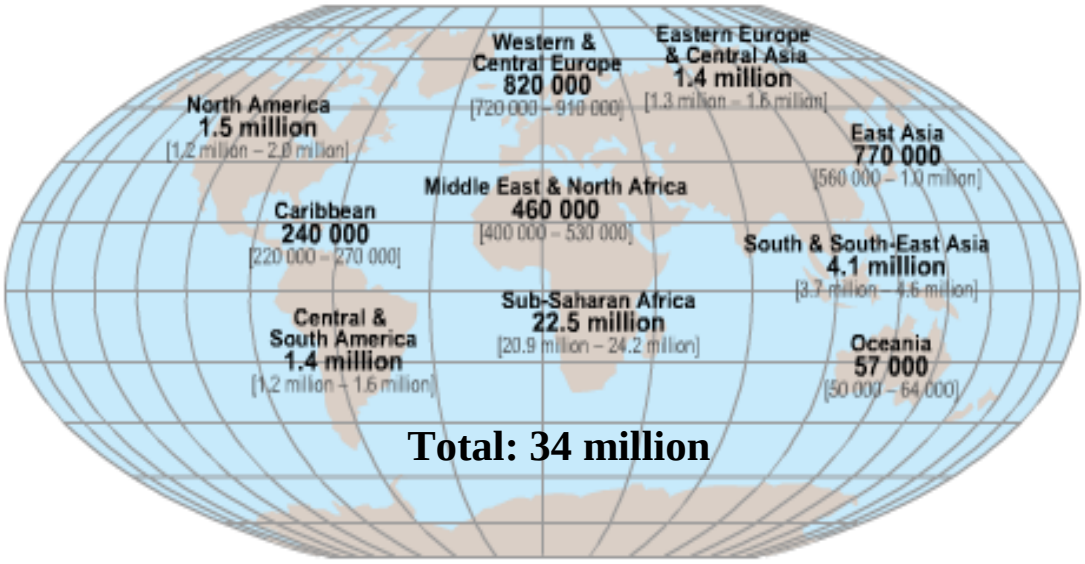

Figure 3: Adults and children estimated to be living with HIV by geographic area in 2009 (adapted from UNAIDS 2010).

There are numerous reasons for the differences observed across continents. For example, in Sub-Saharan Africa, poor education about safe sex and a lack of freely available contraception, resulting in a high percentage of STIs (sexually transmitted infections) in the population, means that HIV spreads rapidly between the heterosexual population, accounting for 80-90% of infections among adults (Stratigos and Tzala, 2000). In contrast, in more developed nations, access to healthcare and education programmes results in an overall lower prevalence of infection. (Quinn, 1996). A lack of healthcare provision in Sub- Saharan Africa also means that pre-exposure prophylaxis has not always been available to give to mothers pre-birth to prevent mother-child transmission. Little/no access to clean water also means that almost all children are breastfed, leading to more infections of children (Stratigos and Tzala, 2000). However, new initiatives to prevent mother-to-child transmission by the provision of antiretroviral prophylaxis during pregnancy, childbirth and breastfeeding has reduced new infections of children by 43% between 2003 and 2011 (UNAIDS 2012).

1.2.2 Transmission

As discussed, the epidemiology of HIV varies greatly worldwide, and this is in part due to the mode of transmission which predominates in that region. There are 3 recognised routes of transmission of HIV; sexual, perinatal and parenteral (Quinn, 1996).

Sexual transmission remains the most common route of infection. HIV is found in infected mononuclear cells in semen as well as cell-free virus; it is also found in cervical smears and vaginal fluid. It has been estimated that the probability of an infected male passing HIV into an uninfected female from vaginal intercourse is 0.2%; the probability of infection from a woman to man is even less likely. The likelihood of infection from receptive male intercourse is, however, much higher due to associated tissue trauma and the fact that only a thin mucosal membrane in the rectum separates deposited semen from target cells beneath. HIV has rarely been transmitted through oral sex (Coffin et al., 1997).

The risk of HIV transmission from infected individuals with ulcerative genital lesions caused by syphilis or herpes is four fold higher than those without, whereas non-ulcerative STDs (sexually transmitted diseases) such as chlamydia or gonorrhoea pose only a two-three fold greater risk (Laga et al., 1994). This is due to a higher probability of virus entering the blood through broken mucosal barriers caused by the lesions and the higher number of $CD4^+$ cells present due to inflammation (Greenspan and Castro, 1990; Coffin et al., 1997). The association between HIV and STDs is shown below in Table 1; the areas with the greatest numbers of HIV infections, Sub-Saharan Africa and South East Asia are also the areas with the highest number of STD infections (Quinn, 1996).

Region	Prevalent curable STDs	Prevalent HIV infections	Cumulative HIV infections
Africa	60 million	13·0 million+	16·0 million+
Asia	138 million	4·0 million+	4·1 million+
Europe	16 million	500000	650000
Latin America and Caribbean	24 million	1·7 million+	2·0 million
North America	8 million	750000	1·3 million
Oceania/Pacific	4 million	70000+	75000+
Global total	250 million	20 million+	24·0 million+

Table 1: Worldwide distribution of curable STDs (gonorrhoea, syphilis, chlamydia and trichomoniasis) and HIV among young adults in 1995 (adapted from Quinn, 1996).

Meta-analyses have clearly shown that condom use severely reduces HIV transmission, which is therefore an important preventative measure in the control of HIV spread. Yet in a survey of 745 African Americans in 1999, only 40% knew that condoms were effective in preventing HIV transmission, meaning education is half the battle (Weller, 1993; Rodgers-Farmer, 1999).

Parenteral transmission, which includes blood transfusions, exchange of blood through needles by IDUs (injecting drug users) and infection of healthcare workers through inadequately sterilised medical equipment (Quinn, 1996). In Bangkok, as many as 50% of known IDUs have been found to be HIV positive (Des Jarlais et al., 1992). Before HIV was established as the causative agent of AIDS, one of the main routes of transmission was contaminated blood products and a large number of haemophiliacs became infected due to inadequate screening (Lowe, 1987). Infection from blood transfusions has decreased significantly since the introduction of HIV screening in the late 1980s and prevention of high-risk individuals from donating blood, and now rarely occurs (Coffin et al., 1997).

Perinatal transmission can occur *in utero* when the maternal blood enters the foetal circulation, although this is rare, during delivery via mucosal exposure to virus, or postnatally from breastfeeding. A number of factors are associated with an increased risk of perinatal transmission, including chorioamnionitis, the presence of other sexually transmitted diseases, viral load and low titres of antibody to the HIV-1 envelope (Peckham and Gibb, 1995; Quinn, 1996).

Breastfeeding adds an additional 14% risk over the risk of infection pre/during delivery (Dunn et al., 1992). Infected mothers are advised to bottle feed their babies in order to reduce the risk of transmission, however this is often not possible in developing countries where there is poor sanitation and little/no access to clean water (Quinn, 1996). Specific antipartum and intrapartum regimens of 5'azidothymidine (AZT) or zidovudine have been found to reduce the risk of perinatal HIV transmission by about two thirds (Peckham and Gibb, 1995; Coffin et al., 1997).

1.2.3 Host Cellular Targets

Although HIV has been found to infect numerous different cell types *in vitro*, including eosinophils, cervical cells, columnar epithelial cells, astrocytes and B cells, the main cells that are consistently infected *in vivo* are $CD4^+$ effector memory T lymphocytes and macrophage-lineage cells. This is because the primary receptor used by HIV for cell entry is CD4, which is present on both of the above cell types and various other cells. The presence of CD4 is necessary but not sufficient for HIV infection, which suggested the necessity for another cofactor for virus entry (Coffin et al., 1997).

HIV also primarily uses one of two co-receptors for entry; the chemokine co-receptor CCR5 or CXCR4 (Veazey et al., 2001; Grossman et al., 2006). CCR5 is the initial choice of target in the majority of cases (Douek et al., 2003). This choice of co-receptor

is not accidental, since there is a large reservoir of $CCR5^+$ $CD4^+$ T cells within and immediately below the genital epithelial cell layers, where sexual transmission occurs. This population of cells is continually maintained by the proliferation or differentiation of $CCR5^-$ cells, making this a highly available and abundant target cell population (Picker, 2006). Mucosal tissue layers are also rife with inflammatory cytokines, which can propagate the activation of resting $CD4^+$ T cells and therefore facilitate HIV infection of these cells (Douek et al., 2003).

It has also been demonstrated that HIV can use the fragment crystallisable receptor (FcR) to infect cells of the macrophage/monocyte lineage. Infection of $CD4^-$ lineages is also observed which is mediated by a variety of factors, such as galactosyl ceramide on colonic epithelium. HIV replication in $CD4^-$ cell lines is, however, limited in comparison to $CD4^+$ cells (Coffin et al., 1997).

1.2.4 Cellular Tropism Determinants

Two phenotypes of HIV-1 have been distinguished, based on the cell types they are able to replicate within *in vitro*. T-tropic viruses are those which can replicate in T-cell lines, but not macrophages or monocytes, whereas M-tropic viruses have reverse specificity (Coffin et al., 1997). This tropism is influenced by the co-receptor which HIV-1 Env binds to and utilises for entry (Sterjovski at al., 2010). T-tropic viruses preferentially use CXCR4 (X4) co-receptors for entry into cells, for example thymocytes, whereas M-tropic viruses use CCR5 (R5) co-receptors (Berkowitz et al., 1998). Viruses are often referred to by their preferred co-receptor; X4 and R5 viruses. Some variants are also able to use both co-receptors (R5X4 viruses), and are further classified according to the efficiency of receptor usage; Dual-R (more efficient usage of R5) and Dual-X4 (vice versa) (Bunnik et al., 2011). R5 viruses often predominate early

in HIV infection; however a phenotypic switch occurs in most individuals late in infection to X4 viruses, possibly because of an increased turnover of naïve T cells which X4 viruses preferentially utilise (Ribeiro et al., 2006). The replicative capacity of these viruses is, however, not specifically defined by their tropism; some R5 viruses cannot infect macrophages, and some X4 viruses can (Duncan and Sattentau, 2011). Therefore, the underlying determinants for HIV-1 tropism cannot solely be due to co-receptor specificity (Sterjovski et al., 2010).

1.2.5 The Course of HIV Infection

Although there is often considerable variation of disease presentation between HIV infected individuals, a common pattern of disease progression has been shown in almost all cases (see Figure 4). During the early stages of infection, the host is unable to mount significant adaptive responses such as the production of neutralising antibodies, therefore the adaptive immune system is relied on. Here, toll-like receptors (TLR), which are proteins expressed on the surface of macrophages and dendritic cells, are activated. This results in the production of numerous cytokines in an acute-phase cytokine storm, such as TNF-α and IL-10, which are potent suppressors of viral infection (Borrow et al., 2010; Perera and Saksena, 2012). Interestingly, HIV is able to down-regulate the TLR pathway which results in a decrease in the production of cytokines, which is associated with disease progression (Nicol et al., 2008). Natural killer cells, which also form part of the innate immune response, increase dramatically in number during this acute phase and assist in the control of HIV replication (Chang and Altfield, 2010).

After the acute response, significant humoral and cellular responses ensue, followed by a prolonged period of asymptomatic clinical latency (normally approximately ten

years). During this phase, $CD4^+$ T cell numbers begin to increase after an initial drop. These cells play numerous roles during HIV infection, including homeostasis of $CD8^+$ cells, which initiate cytolytic killing of infected cells, and antibody producing B cells. $CD4^+$ cells are thus one of the most important cells in dealing with HIV infection (Perera and Saksena, 2012). The humoral response also kicks in during this phase, resulting in the production of neutralising antibodies, for example to the viral Envelope, which exert significant pressure on HIV. Thus, escape variants with mutations in the areas to which antibodies bind in Envelope eventually arise (Haigwood and Stamatatos, 2003).

After this chronic phase, alongside severe immune depletion including loss of $CD4^+$ cells, various syndromes will appear as the disease becomes clinically apparent, and death usually occurs within 2 years without treatment (Pantaleo et al., 1993).

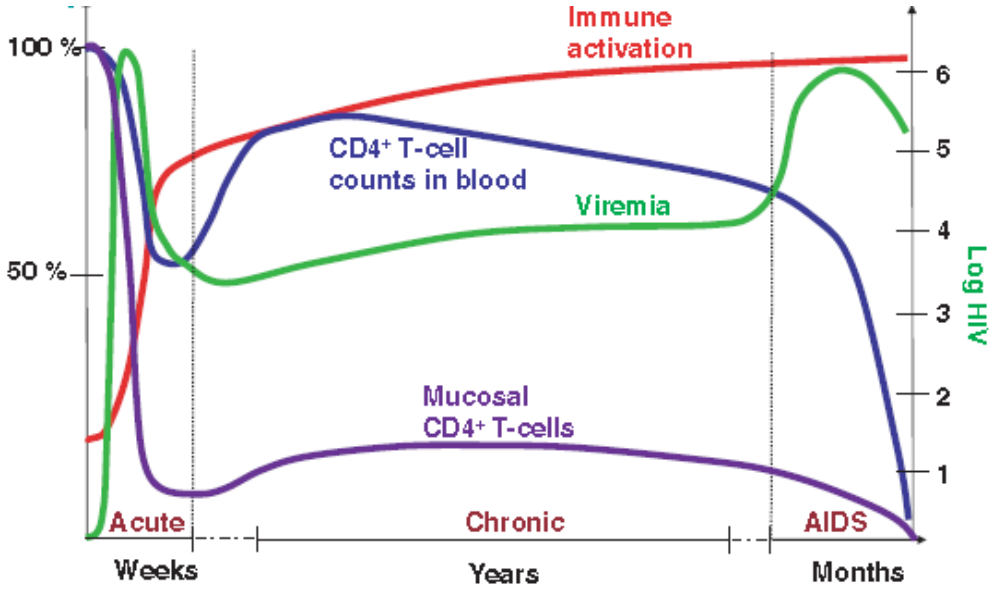

Figure 4: HIV disease progression depicting changes in mucosal and blood $CD4^+$ numbers and viraemia levels. During the acute phase, as viraemia (green) rapidly increases, mucosal $CD4^+$ cell levels drop dramatically. $CD4^+$ cells within the blood initially experience a decline, then stabilise at a subnormal level. The immune system becomes highly activated (red). During the chronic phase, $CD4^+$ cells steadily decline as virus levels continue to escalate. At the onset of AIDS, $CD4^+$ cells are virtually abolished and virus levels continue to rise until death (adapted from Grossman et al., 2006).

1.2.5i Acute Phase

After initial infection, tissue dendritic cells most likely facilitate the spread of infection around the body. Efficient replication of the small viral inoculum at the site of exposure dramatically increases viral load, and around 6 days post infection a huge systemic infection of target T cells ensues. Any pre-existing inflammation at the site of exposure, for example from sexually transmitted diseases, amplifies the efficiency of systemic infection (Picker, 2006). Mucosal $CD4^+$ T cells, particularly those within the gut, are the primary target for HIV proliferation due to the high expression of CCR5 and their activated state, and are consequently the largest site of T cell depletion during the acute phase. At the peak of infection, around 10 days post exposure, 30-60% of memory $CD4^+$ T cells are found to be infected, and most of these are destroyed within 4 days (Mattapallil et al., 2005). This, combined with apoptosis of cells which have interacted with the virus in a receptor/ co-receptor dependent manner, accounts for the massive loss in $CD4^+$ cells (Picker, 2006).

In the majority of infections, an acute mononucleosis-like syndrome appears approximately 1-3 weeks after initial infection, associated with the high levels of virus (Pantaleo et al., 1993). Symptoms may include headache, muscle aches, low/high grade fever, malaise and swollen lymph nodes. Although these symptoms only last a few weeks, lethargy and lymphadenopathy may persist for many months (Levy, 1993). During this high period of viral replication, up to 10^7 virions per ml in cell-free plasma can be detected, although only a small percentage of these are infectious (Coffin et al., 1997).

Around 3-6 weeks post infection antiviral immune responses can be detected, combined with a significant decrease in viremia and simultaneous appearance of strong

antibodies to the viral proteins Env and Gag, resolution of the clinical syndrome and a temporary stabilisation of $CD4^+$ cell level. This is probably due to a combination of responses from both the innate and adaptive systems and the exhaustion of susceptible target cells (Clark et al., 1991; Coffin et al., 1997).

1.2.5ii Clinical Latency

Following the immune response observed during the acute phase, a prolonged period of "clinical latency" ensues (see Figure 5 overleaf), which usually lasts some years (Coffin et al., 1997). The term "latency" can be misleading, as the immune status of the majority of patients continually gradually declines due to the gradual, progressive attrition of $CD4^+$ cells (Fauci, 1998; Pantaleo et al., 1993). This decline is not seen in a minority of infected individuals, who are termed "long term non-progressors" (Coffin et al., 1997)

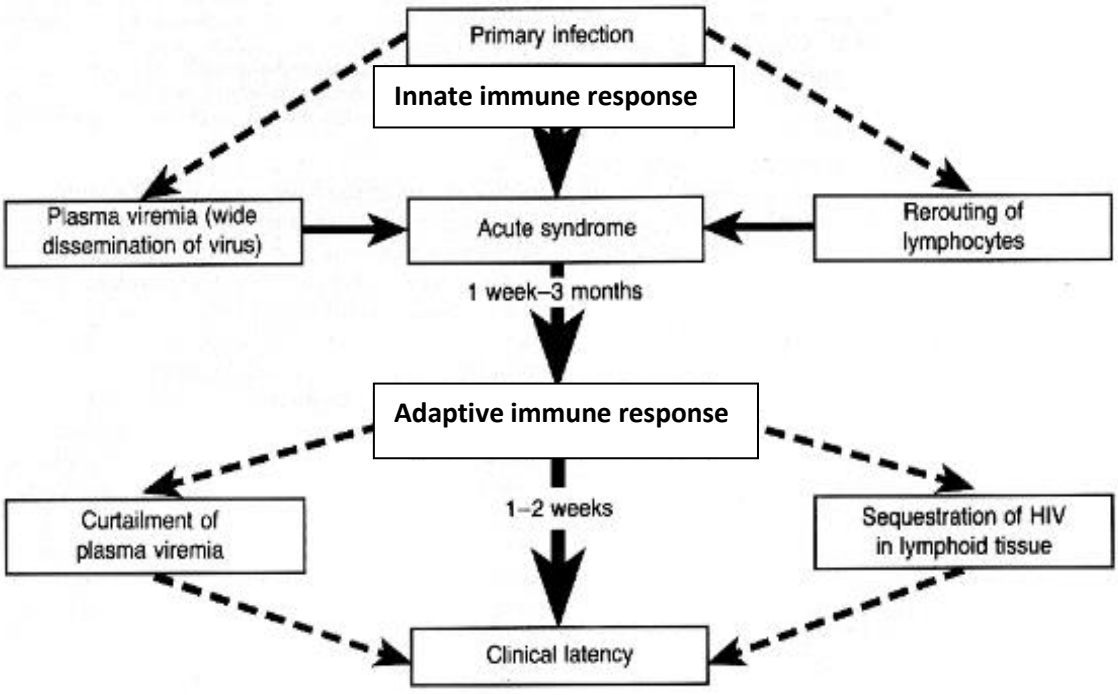

Figure 5: A schematic of the progression from HIV infection to the development of clinical disease (Adapted from Pantaleo et al., 1993).

During this stage, the majority of cells that die are bystander cells by apoptosis; most of the apoptotic T cells in the lymph nodes and peripheral blood of HIV positive individuals are uninfected (Kynsz et al., 2010). This is caused by a combination of activation-induced cell death of mature T cells following chronic activation, and by direct effects of HIV viral proteins. Some studies have indicated that both *in vivo* and *in vitro*, only 0.0001 to 0.01% of HIV virions produced are actually infectious, therefore non-infectious virions contribute largely to the $CD4^+$ decline via the induction of bystander apoptosis (Dimitrov et al., 1993; Holm and Gabuzda, 2005).

1.2.5iii Clinical stage (AIDS)

The inevitable outcome for the majority of HIV infected patients is clinically apparent disease (Panteleo et al., 1993). When the $CD4^+$ T cell count drops below the normal range (from 600-1200/µl blood) to around 500, and the first disease symptoms start to become apparent (see Table 2 on page 16).

There has been speculation over the years as to how to define the onset of AIDS, and now the generally accepted definition is a patient whose $CD4^+$ cell count is at or below 200 cells per microlitre of blood. Prior to using actual T cell counts, the "gold standard" of AIDS diagnosis was seropositivity in conjunction with one or more AIDS defining illnesses, such as Kaposi's sarcoma (see Figure 6A) or *Pneumocystis jirovecii* pneumonia (see Figure 6B) (Kerdel and Pennys, 1989).

At this stage, the patient is susceptible to a number of AIDS-defining opportunistic infections and neoplasms. Many patients within this advanced stage will also experience a range of neurocognitive problems due to infection of cells within the central nervous system (CNS), such as microglia and astrocytes, coined HIV associated neurocognitive disorders (HAND). Studies have shown similar features between the

development of HAND and other neurodegenerative diseases such as Alzheimer's, including the appearance of amyloid plaques (Kaul, 2009)

This stage will continue until the T cells are virtually absent in the body, and the patient will eventually die from one of a number of conditions as shown in Table 2 (Coffin et al., 1997).

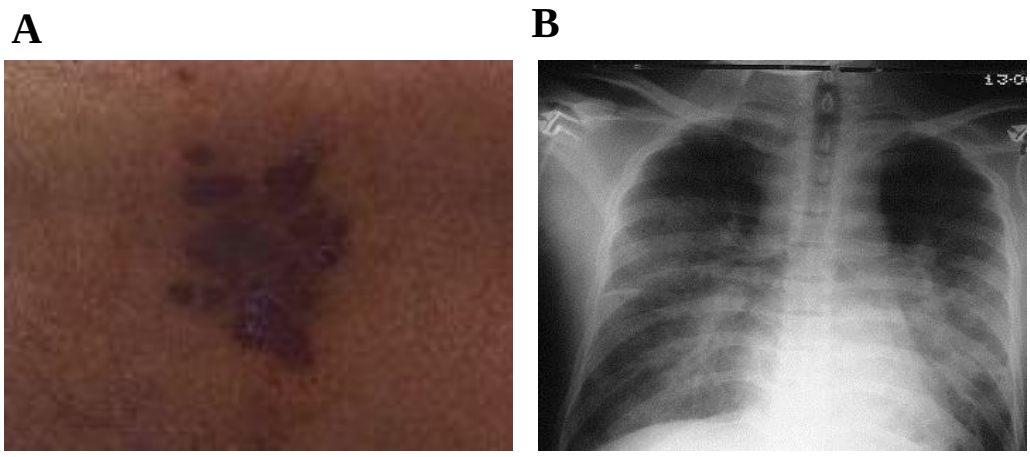

Figure 6: A- An example of a typical cutaneous lesion seen in Kaposi's sarcoma. Patients present discrete, non-pruritic and non-tender pink/purple papules which are often asymmetrical. B- *Pneumocystis jirovecii* pneumonia chest X-ray demonstrating bilateral mid and lower zone infiltrates (Lewthwaite and Wilkins, 2009).

Primary Infection	**Mononucleosis-like syndrome;** Fever, malaise, pharyngitis, lymphadenopathy, arthralgias, maculopapular rash
Clinical Latency	Fatigue, mild weight loss, thrush, generalised lympadenopathy
Clinical Disease (200-500 $CD4^+$T cells/µl)	Oral lesions (thrush, hairy leukoplakia) shingles, thrombocytopenia, reactivation of latent *M. tuberculosis*
Clinical Disease (<200 $CD4^+$T cells/µl)	**Protozoal infections;** *Pneumocystis jirovecii, Toxoplasma gondii, Isospora belli* **Bacterial infections**; *Treponema pallidum.* **Fungal infections**; *Candida albicans, Cryptococcus neoformans*. **Viral infections and malignancies**; cytomegalovirus, lymphoma (Epstein-Barr virus), Kaposi's sarcoma (human herpes virus 8), non-Hodgkin's lymphoma, invasive cervical cancer. **Neurological symptoms**; aseptic meningitis, myopathy, HAD

	(HIV associated dementia), sensory ataxia, and peripheral neuropathies.

Table 2: Pathologic conditions associated with HIV infection/ AIDS (Coffin et al., 1997, Bower et al., 2006)

Since up to 90% of HIV infections occur in the developing world, and tuberculosis is prevalent in 30-50% in the AIDS clinical series of many of these countries, tuberculosis became one of the most common AIDS defining illnesses. The HIV epidemic caused more than a 2-fold increase in tuberculosis cases across Sub-Saharan Africa and Asia. The presentation of tuberculosis in AIDS patients is, however, different from those without HIV infection; it occurs in younger aged individuals, there are a higher proportion of smear-negative pulmonary disease and extrapulmonary tuberculosis, and a considerably higher 12 month mortality rate exists (Dore and Cooper, 2001).

Cancer risk is increased with various types of immune deficiencies, including immunosuppression following organ transplants and congenital disorders. HIV patients have an alarmingly high risk of developing an unusual array of cancers (Goedert et al., 2012). Although late stage HIV infection can cause numerous cancers, several "AIDS-defining" cancers exist; Kaposi's sarcoma, non-Hodgkin's lymphoma and cervical cancer. Kaposi's sarcoma is the most common AIDS related malignancy, and is caused by human herpes virus 8 (Lewthwaite and Wilkins, 2009). Other cancers that HIV patients are at a higher risk of developing include Hodgkin's disease, anal cancer, lip cancer, leukaemia and multiple myeloma. It is, however, important to note that since HIV patients will be undergoing increased medical surveillance, that some cancers may have been diagnosed when they would have otherwise not been apparent, therefore it can be difficult to judge whether there is an actual increased risk of particular cancers. Medical immunosuppression has been shown to cause similar cancers to those observed in HIV patients that are usually caused by viral infections (Grulich et al., 1999).

1.3 HIV Treatment

Prior to 1996, few treatment options were available to HIV+ patients. Standard regimes included prophylaxis against opportunistic infections and management of AIDS related illnesses, i.e. treating symptoms not the cause. HIV treatment was revolutionised in the 1990's by the introduction of inhibitors of two of HIV's key enzymes; protease and reverse transcriptase (RT). The first antiretroviral (ARV) drugs developed were administered as monotherapy, but since this was found to be ineffective due to the rapid emergence of resistant strains, treatment regimens evolved to the administration of a cocktail of 3 or more drugs targeting different stages of the HIV life cycle (Arts and Hazuda, 2012). This combination therapy, still used today, was named HAART (highly active antiretroviral therapy) and has been critical to reducing HIV associated mortality and morbidity (Collier et al., 1996).

Although HIV drugs have become more advanced and sophisticated since their introduction in the mid 1990's, no drugs can actually yet "cure" patients of HIV, i.e. abolish all viral particles and prevent the onset of the disease stage. They are, however, effective at reducing viral load and prolonging life. Five major classes of antiretroviral drugs exist, targeting different stages of the HIV life cycle:

- Nucleoside Reverse Transcriptase Inhibitors (NRTIs)
- Non-Nucleoside Reverse Transcriptase Inhibitors (NNRTIs)
- Protease Inhibitors
- Entry Inhibitors
- Integrase Inhibitors

More recently, inhibitors of viral assembly and production have been added to the list

HIV infection is characterised by continuous, high rate viral replication. RTs lack of proof-reading during the synthesis of viral DNA, married with HIVs capacity for

genetic recombination, is the reasoning behind HIVs high mutability. This also allows immune evasion resulting in the emergence and selection of drug resistant variants (Pauwels, 2004).

1.3.1 Highly Active Antiretroviral Therapy (HAART)

The advent of combination therapy, or HAART, revolutionised HIV treatment, reducing both morbidity and mortality associated with HIV infection, allowing patients to resume a near-normal quality of life. Typically, 3 ARVs are administered, targeting at least two different molecular targets; this is essential in delaying the onset of drug resistance. HAART dramatically suppresses viral replication, reducing viral load to almost undetectable levels in plasma, allowing the immune system to rebuild (Arts and Hazuda, 2012).

HAART has transformed HIV infection, turning it into a chronic manageable condition in many as opposed to an inevitably fatal disease. Despite its success, however, there still remains a large proportion of individuals who do not respond to their first line of treatment. This means that the patients are at a high risk of virologic rebound, and may be less responsive to further treatment options (Vella and Palmisano, 2000).

1.4 The HIV-1 Life Cycle

1.4.1 The HIV-1 Genome and Virion

The HIV-1 genome, as with all other lentiviruses, is complex. All retroviruses have RNA genomes and contain 3 benchmark genes; *gag*, *pol* and *env*. HIV-1 contains an additional 6 genes, making up a 9.8 kb genome containing 9 open reading frames (ORFs), flanked by long terminal repeats (LTRs). These genes can be organised into 3

distinct groups; *tat* and *rev* are regulatory; *gag*, *pol* and *env* are structural and/or enzymatic; *nef*, *vif*, *vpu* and *vpr* are accessory. These genes encode 15 viral proteins.

A summary of the HIV-1 genome and viral proteins produced shown in Figure 7.

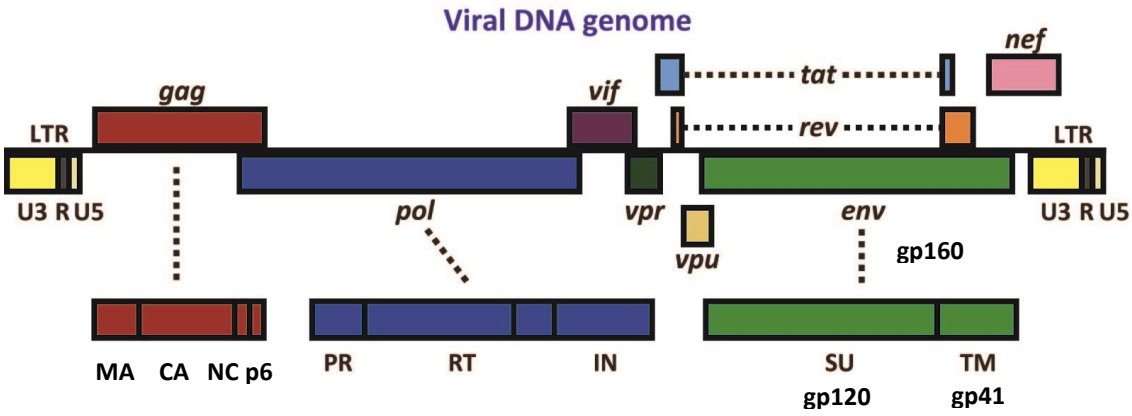

Figure 7: The HIV-1 genome and the proteins encoded by these genes. MA (matrix), CA (capsid), NC (nucleocapsid), PR (protease), RT (reverse transcriptase, IN (integrase), SU (surface), TM (transmembrane) (adapted from Suzuki and Suzuki, 2001).

Mature, infectious HIV particles possess a characteristic conical core encasing the viral RNA and replication proteins, which is the most distinctive feature of the mature virion (Briggs et al., 2003; Sundquist and Kräusslich, 2012). The mature virion is composed of "shell" like layers of Gag; matrix (MA) lies beneath the lipid membrane and composes the outer shell. The transmembrane (TM) portion of Env passes through the membrane and contacts MA in a non-specific manner, whereas the outer portion contacts the surface (SU) domain. Numerous host proteins are also incorporated into the lipid membrane, such as the MHC proteins. Inside the virion, the capsid (CA) portion of Gag forms the outer core, the capsid domain. The location of p6 (located on the carboxy terminus of Gag) is assumed to lie just outside the core. Within the centre of the core lies the viral RNA, bound to the nucleocapsid (NC), which are associated

with some RT and IN molecules (Coffin et al., 1997). A diagram of a mature particle is shown in Figure 8.

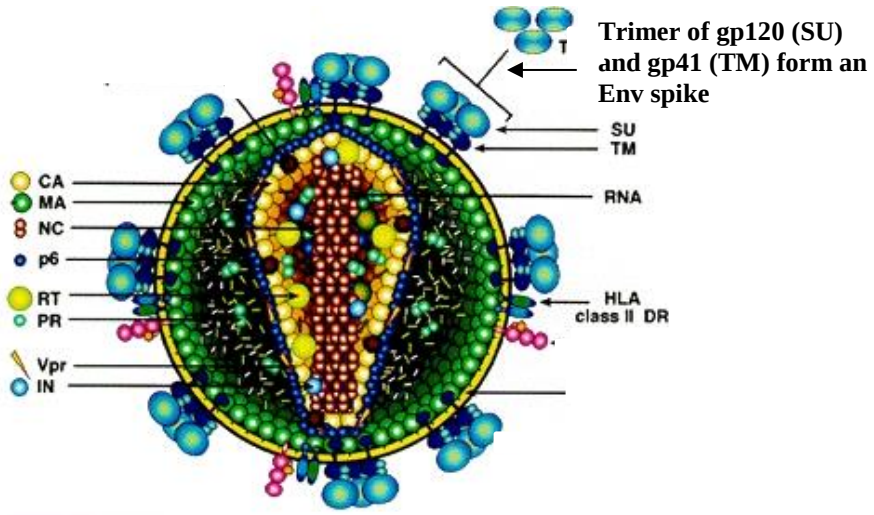

Figure 8: The mature HIV-1 virion, showing structure and protein organisation. CA (capsid), MA (matrix), NC (nucleocapsid), RT (reverse transcriptase), PR (protease), IN (integrase), Env (envelope), SU (surface), TM (transmembrane). (adapted from Coffin et al., 1997).

1.4.2 Stages of the HIV Life Cycle

The HIV-1 life cycle represents a complex, multi-step process, involving a collaboration of events from both the host and the virus (Adamson and Freed, 2010). A brief summary of the life cycle is represented overleaf in Figure 9.

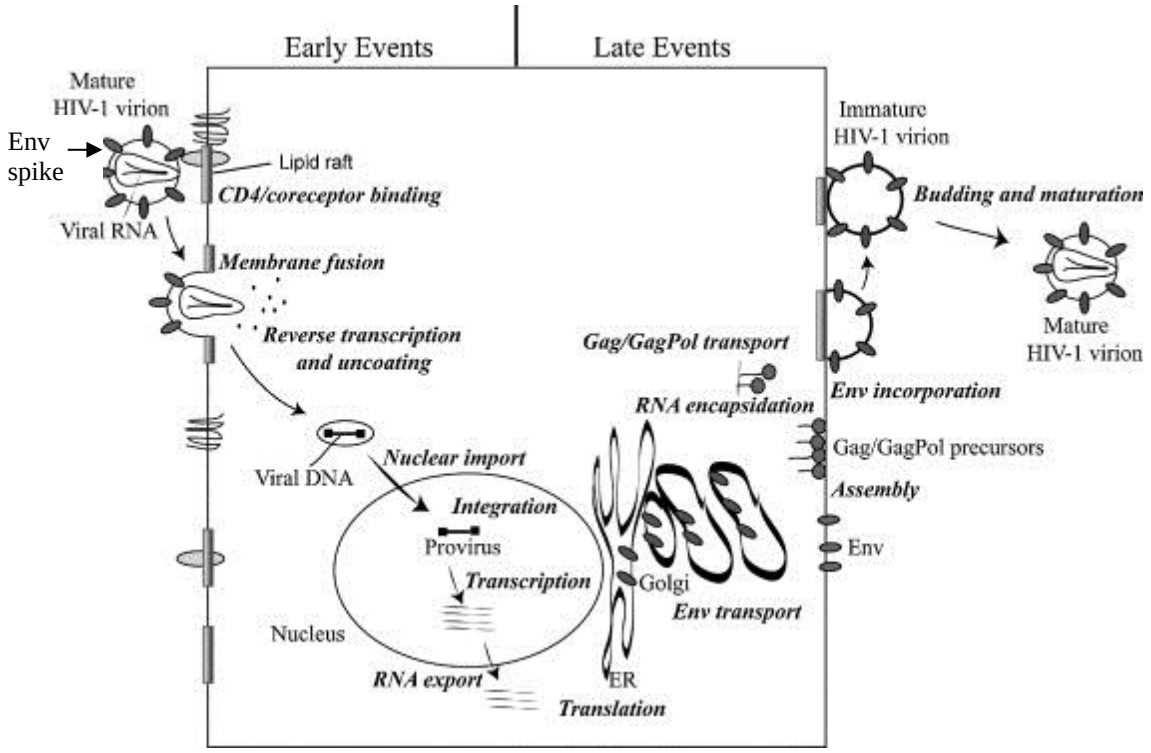

Figure 9: **A schematic of the main events occurring during the HIV-1 life cycle (adapted from Adamson and Freed, 2010).**

The life cycle begins with viral entry where the virus binds, mediated by gp120 of the Env spike, to the CD4 receptor and the appropriate co-receptor (CCR5 or CXCR4); a conformational change in gp41 of Env results in fusion of the envelope to the cellular membrane, releasing the viral core (composed of the capsid, nucleocapsid and the single stranded, dimeric RNA genome) into the cytoplasm. After uncoating, the viral reverse transcriptase (RT) produces double stranded DNA from the RNA genome, which migrates into the nucleus and stably integrates into the host genome, mediated by viral integrase (IN). Proviral DNA is transcribed by cellular RNA polymerase II into full-length progeny RNA and numerous spliced mRNA transcripts which are exported by viral Tat and Rev. Translation, mediated by cellular polysomes, results in the synthesis of viral subunits which, together with full-length genomic RNA, are transported to assembly sites. After virion assembly, budding occurs, releasing immature non-infectious particles which are then proteolytically processed by viral

protease to produce mature, infectious particles (Sierra et al., 2005; Adamson and Freed, 2010). These events will be described in detail in following sections.

1.4.3 Viral Entry and Uncoating

The entry of HIV-1 is the first step in the infection process, and involves series of tightly controlled steps that ultimately result in the fusion of the viral and cellular membranes and the release of the viral genome into the cytoplasm of the infected cell (Gomez and Hope, 2005). As mentioned in chapter 1.2.3, HIV-1 utilises host CD4 receptors (a member of the immunoglobulin super family) expressed on monocytes, macrophages, dendritic cells and subsets of T cells, and chemokine receptors CCR5 and CXCR4 to enter cells (Tilton and Doms, 2010).

The entry process is facilitated by viral Env; the *env* gene encodes a glycoprotein, gp160, which is post-translationally cleaved by a cellular protease (furin) to produce gp120 (SU, surface subunit) and gp41 (TM, transmembrane portion) which are non-covalently joined into a trimeric structure (Lu et al., 1995; Gomez and Hope, 2005). The first stage of entry involves Env gp120 engaging CD4, upon which various important conformational changes in gp120 occur; the V1/V2 and V3 loops become exposed, two sets of separated β-sheets come together to form a bridging sheet and the orientation is changed in such a way that the bridging sheet and V3 face the cellular membrane, thereby allowing stabilising interactions with the co-receptor (CCR5 or CXCR4). Following co-receptor binding, further Env conformational changes result in the exposure of the hydrophobic fusion peptide of gp41, which is subsequently inserted into the host membrane. After this, the heptad regions of gp41 rearrange into a six helix bundle, forcing the TM region toward the fusion peptide, and this is subsequently also inserted into the host membrane, forming a fusion pore (Esté and Telenti, 2007; Chan

et al., 1997; Sackett and Shai, 2002; Tilton and Doms, 2010). The entry process is summarised below in Figure 10.

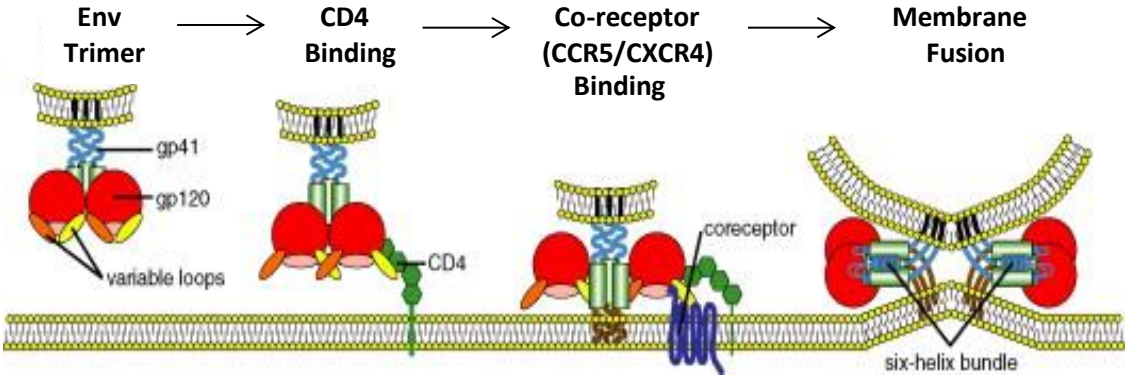

Figure 10: The multi-step process of HIV-1 entry. CD4 and co-receptors are found on the host (bottom) membrane, whilst gp120 and gp41 are associated with the viral membrane (top) (adapted from Tilton and Doms, 2010).

The viral capsid enters the host cytoplasm through the fusion pore. The process of uncoating involves both cellular factors and viral proteins; MA, Nef and Vif (Sierra et al., 2005). Uncoating is defined as the dissociation of the viral Capsid core from the ribonucleoprotein complex (Forshey et al., 2002).

Recently, it was discovered that phosphorylation of CA within the virion acted as a "molecular switch" to trigger uncoating, although the kinase is currently unknown. Once phosphorylation of a specific serine/threonine residue followed by a proline has taken place, a cellular protein Pin1 (a peptidyl-prolyl isomerase involved in transcriptional regulation) is able to assist uncoating and binds to this phosphorylated region of CA and isomerises the proline (Musumi et al., 2010). Cyclophilin A (CypA), another cellular peptidyl-prolyl isomerase, which may be incorporated into virions, is also thought to aid uncoating (Li et al., 2009) by destabilising core formation through an interaction with specific CA residues G89 and P90 (Friedrich et al., 2011), and also contributes to virion infectivity.

1.4.4 Reverse Transcription and Nuclear Import

The HIV life cycle, as with that of all retroviruses, requires integration of a DNA copy of its genome into a host chromosome, in order to instigate stable replication. Since the HIV genome is positive single stranded RNA, it must therefore generate a DNA copy before integration can occur (Sleiman et al., 2012). The process involved is reverse transcription (RTN), and is shared by retroviruses, retrotransposons and hepadnaviruses (Abbink and Berkhout, 2008).

RTN requires both packaged cellular and viral factors; minimally, the HIV RT and a cellular $tRNA^{Lys3}$ primer which is packaged into virions by $Pr55^{Gag}$ and $Pr160^{Pol}$ (Harrich and Hooker, 2002). The HIV-1 RT is encoded by the *pol* gene with its embedded RNaseH (ribonuclease H) activity, alongside integrase and protease. It is an asymmetrical heterodimer composed of 2 subunits; p66 and p51. The RNaseH is located on the carboxy terminus of the p66 subunit, and is not present on the C-terminally truncated p51 subunit (see below for further detail of RNaseH activity) (Sarafianos et al., 2009).

RTN occurs in the cytoplasm of the host cell; specifically, within a nucleoprotein complex which is only permeable to small molecules such as dNTPs, preventing the loss of RT or other essential factors (Sleiman et al., 2012). A specific RTN initiation complex (RTNIC) is formed by base pairing between $tRNA^{Lys3}$ and the viral RNA, which is postulated to prevent RTN until after infection (Harrich and Hooker, 2002). Specifically, the 3'-terminal 18 nucleotides (nts) of $tRNA^{Lys3}$ base pair with a complementary region of viral genomic RNA called the primer binding site (PBS), which is located at the 5' end of the viral RNA. The 3'-OH of the tRNA primes template-dependent DNA synthesis (Abbink and Berkhout, 2008).

DNA synthesis begins at the 5' end of the viral genome, alongside the extension of the 3' end of the tRNA. The first DNA product is minus (-) sense, and termed the "minus strand strong stop DNA"; a short length of DNA resulting from copying from the primer to the 5'-end of the viral RNA (see Figure 11 part A). This short piece of DNA then translocates to a site near the 3'-end, via a homologous repeat (minus strand transfer); this is required to complete the minus strand synthesis (Figure 11 part B) (Goff, 1990). A second transfer is also required to produce the plus (+) strand. RNaseH is required for strand transfer as degradation of the RNA template strand from the extending DNA strand frees a single stranded region that is capable of annealing to the second site (Figure 11 part C) (Basu et al., 2008). (-) strand transfer originates from a region at the 5'-end called R region, to an equivalent region at the 3'-end. This region consists of a TAR hairpin and a poly(A) hairpin.

As elongation of the (-) strand continues, RNaseH degrades RNA from the RNA:DNA hybrid, which dissociates from the nascent DNA, except for 2 fragments which are resistant due to their possession of a polypurine tract (PPT). These RNA oligomers; 3'-PPT and central PPT (cPPT) act as primers for the synthesis of the (+) strand. (+) strand synthesis begins at the 3'-PPT and continues to the 5'-end, using the PBS as a template, to produce (+) strand strong stop DNA (Figure 11 part D). This strand must then transfer to the 3'-end of the (-) strand to complete the process (Figure 11 parts E and F) (Goff, 1990; Charneau et al., 1994; Basu et al., 2008).

This double stranded DNA, which is longer than HIV RNA due to extended LTRs which are critical for integration and transcription, must then be imported into the nucleus for integration into the host genome, and subsequent DNA replication. A summary of reverse transcription is shown overleaf in Figure 11.

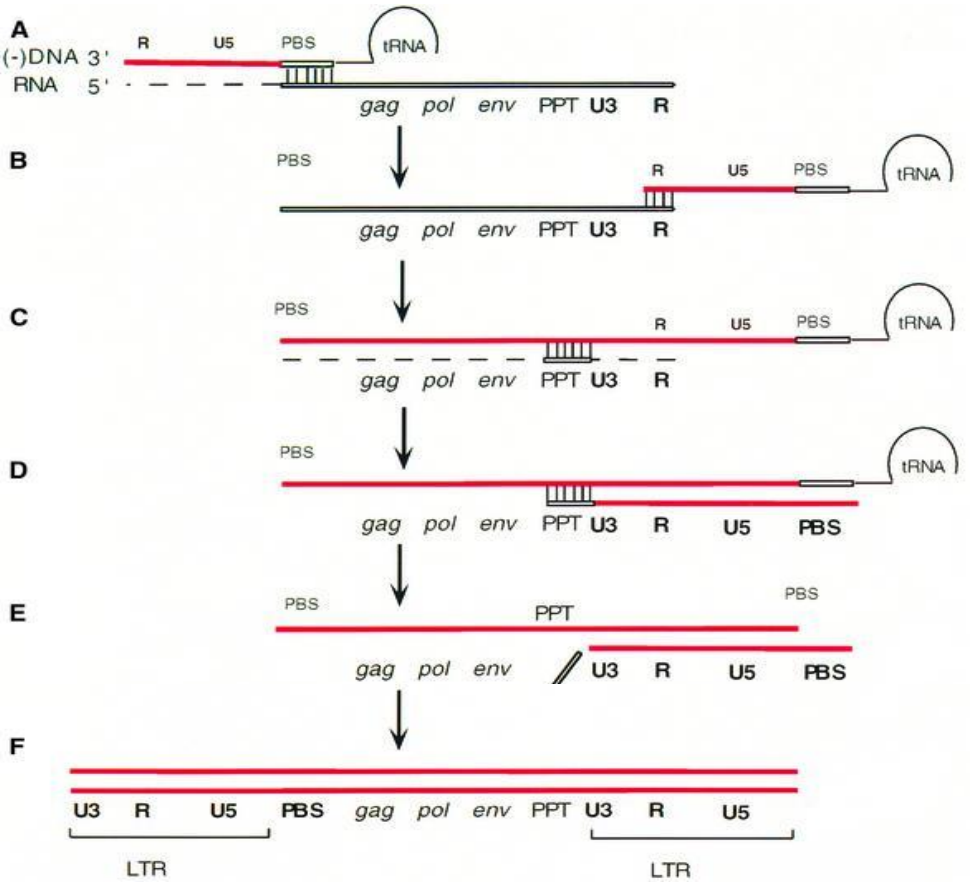

Figure 11: **A summary of the process of reverse transcription of HIV-1 (adapted from Sarafianos et al., 2001).**

Following reverse transcription, the newly synthesised viral DNA must travel to the nucleus for integration and DNA replication ensue. At this stage, the DNA is present in the cytoplasm in a high molecular weight nucleoprotein complex termed the pre-integration complex (PIC). This complex contains various viral and cellular constituents. MA but not CA are present (Farnet and Haseltine, 1991), alongside IN, RT, NC and Vpr (viral protein R) (Dismuke and Aiken, 2006). Cellular proteins include LEDGF/p75 (lens epithelium-derived growth factor) and Barrier to autointegration (BAF) (Llano et al., 2004; Vandegraaff et al., 2006).

While oncoretroviruses require nuclear envelope disintegration, which occurs during mitosis, in order to integrate their viral DNA, lentiviral PICs are able to access the nucleus through the nuclear pore complex. Small proteins may passively enter the

nucleus, however, larger proteins (>40kDa) require specific nuclear localisation signals (NLSs) for active transport (Friedrich et al., 2011). HIV has developed an active mechanism to import its viral DNA into the nucleus. Vpr is one of the main viral constituents involved in enhancing nuclear import and has evolved specific strategies that promote interactions with cellular machinery that regulate nucleo-cytoplasmic shuttling (Le Rouzic and Benichou, 2005). For example, Vpr associates with karyopherin alpha, a NLS receptor, which increases the affinity of this receptor for NLSs, including those found on HIV MA (Popov et al., 1998).

In order to traffic to the nucleus, the HIV-1 PIC travels down cellular microtubules using cytoplasmic dynein motors. Once at the nucleus, the PIC has the formidable challenge of crossing the nuclear envelope. The nuclear envelope is composed of inner and outer membranes, studded with embedded nuclear pore complexes, the lamina and associated proteins (Li and Craigie, 2006). Various proteins are known to mediate PIC entry. Soluble Karyopherin (importin) α/β heterodimers are involved in the import of proteins containing basic NLSs; the α subunit binds to the NLS of MA and the β subunit enhances affinity of this interaction and mediates the docking of this NLS/karyopherin complex to the nucleoporins (proteins constituting nuclear pore complex proteins) (Popov et al., 1998), allowing the NLS containing protein and the associated soluble import receptor to be translocated into the nucleus. The karyopherin α/β heterodimer also aids nuclear import through interactions with HIV-1 integrase in a Ran GTP dependent ATP independent manner (Hearps and Jans, 2006). Nuclear import is summarised in Figure 12.

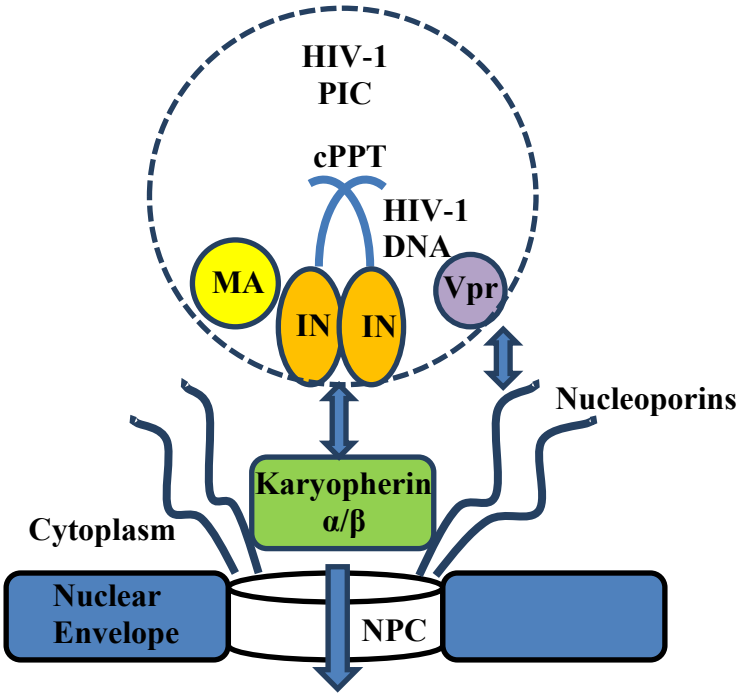

Figure 12: Viral factors within the HIV-1 PIC (central polypurine tract [cPPT], MA, IN and Vpr) involved in nuclear import. Adapted from Suzuki and Craigie, 2007.

1.4.5 Integration

Following nuclear import, integration is the next step. This is defined as the insertion of the HIV-1 cDNA into the host chromosome. If this does not occur, the cDNA circularises upon itself and forms a 2-LTR circle; a dead end for the virus as it is unable to produce any progeny (Friedrich et al., 2010). Once integrated, so called proviral DNA is replicated alongside cellular DNA during the normal cell cycle. This provirus serves as a template for the production of viral RNA; some of which is translated into viral proteins, other proviruses serving as genomic RNA to be packaged into new virions. Integration occurs precisely at the termini of the viral DNA, but many locations along the host DNA may serve as acceptor sites. Some retroviruses have preferred regions for integration, which seem to involve chromatin-associated factors that interact with IN, or kinked/distorted DNA (Frankel and Young, 1998; Craigie and Bushman, 2012).

The first stages of integration involve directing the viral DNA to host chromatin. BAF, alongside preventing autointegration of the cDNA (a suicide pathway using itself as the target) prior to integration, binds to MA and orients the PIC toward chromatin (Chen and Engelman, 1998), with assistance from lamina-associated polypeptide 2-alpha (LAP2alpha). The initial contact with chromatin is mediated by cellular emerin, which is a prerequisite to tethering. LEDGF/p75 has been demonstrated to be essential for tethering the viral DNA to chromatin (Friedrich et al., 2011).

The integration reaction is highly coordinated; 2 viral linear DNA ends, separated by around 7-10 kb, must be juxtaposed to the host target DNA in a pairwise manner (Katz and Skalka, 1994). After alignment of the DNA, the first stage is 3' end processing, whereby 2 nucleotides (nts) are removed from each 3' end of the blunt linear viral DNA, leaving overhanging conserved CA_{OH} ends. In the second step, strand transfer, the 3' ends attack a pair of phosphodiester bonds, separated by 5 nts, localised on the major groove of the opposite host DNA. This forms an integration intermediate where the 3' ends of the viral DNA become joined to the 5' ends of the host DNA. Finally, unpaired nucleotides at the 5' ends are removed, and the ends become joined to the target site 3' ends (Frankel and Young, 1998; Craigie and Bushman, 2012).

A summary of this process is shown overleaf in Figure 13.

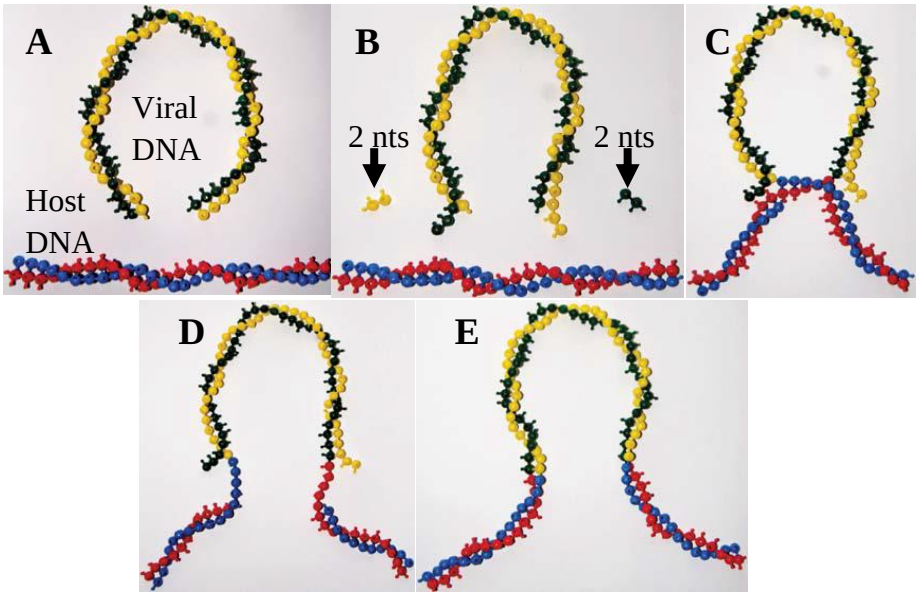

Figure 13: DNA breaking and joining reactions during Integration. A- Viral DNA is shown in yellow/green, host in red/blue. B- 3' end processing and the removal of 2 nucleotides from the 3' viral DNA. C- 3' ends attack a phosphodiester bond in target DNA. The 3' ends of the viral DNA are joined to the 5' ends of host DNA; 5' viral ends are not joined. D- Removal of unpaired bases at the 5' end of the viral DNA is required before the 5' ends are ligated to host DNA. E- The fully integrated provirus (adapted from Craigie and Bushman, 2012).

1.4.6 Transcription and Splicing

After integration, HIV-1 may either initiate transcription via cellular transcription machinery to produce progeny RNA, or alternatively enter a latency phase (Friedrich et al., 2011). Latency is defined as cells containing integrated HIV DNA that are transcriptionally silent; however, upon activation they are capable of producing infectious virions. This constitutes a latent reservoir, which creates a barrier to successful treatment. It is simple to assume that a latently infected cell would not produce viral RNA, however, it has been demonstrated that these cells do produce low levels of viral RNA (Pace et al., 2011).

The first stages of viral transcription are initiated by cellular RNA polymerase II binding to the viral 5'LTR, which contains binding sites for many transcription factors

including NF-κB, and results in low levels of full-length viral RNA. The full-length RNA may then be spliced to generate over 30 different transcripts. These RNAs can be divided into 3 groups; multiply spliced RNAs encoding Tat, Nef and Rev; singly spliced RNAs encoding Vpu, Vpr, Vif and Env; and unspliced full-length mRNA encoding Gag and Gag-Pol polyproteins (Wu, 2004). The multiply spliced RNAs are exported into the cytoplasm where Tat, Rev and Nef proteins are translated. Tat (a viral transcription activator) shuttles into the nucleus, where it acts to increase transcription of viral RNA by binding to the U-rich bulge of the TAR (trans-activation response) element, found at nucleotides +1 to +60 of the viral RNA (Lloyd et al., 2000; Sierra et al., 2005). This increase in transcriptional levels is due to a stimulation of a specific protein kinase called TAK (Tat-associated kinase), which also binds to TAR. TAK is composed of a kinase CDK9 and a cyclin, cyclin T_1. During the initiation of transcription, the kinase CDK7 of initiation factor TFIIH phosphorylates the carboxy terminal domain (CTD) of RNA polymerase II. Tat then stimulates additional phosphorylation via TAK; CDK9 hyperphosphorylates CTD of RNA polymerase II, greatly enhancing its processivity (Karn, 1999; Wu, 2004). A summary of this process is shown overleaf in Figure 14.

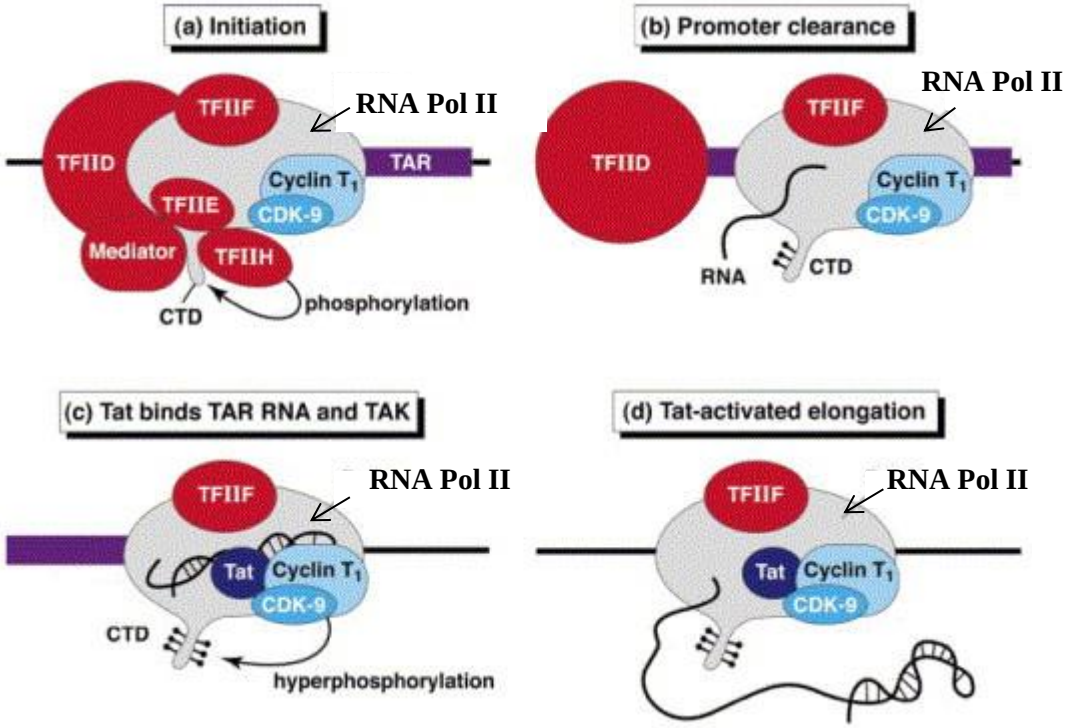

Figure 14: **Activation of RNA polymerase II by Tat and cellular cofactors. A- RNA Pol II is recruited to the viral LTR. CDK7 of TFIIH phosphorylates the CTD of RNA Pol II, clearing the promoter region and transcription of TAR ensues. B-The nascent RNA transcript corresponding to TAR folds into its characteristic stem-loop structure and binds to the RNA Pol. C- Tat is recruited to the complex and binds to the bulge of TAR. TAK kinase phosphorylates the CTD and TAR is displaced. D- The activated complex is able to transcribe the rest of the genome. (Adapted from Karn, 1999).**

The second stage of HIV-1 gene expression depends on the nuclear export of intron-containing transcripts. The multiply spliced viral RNAs use the cellular mRNA export pathway to reach the cytoplasm, but singly-spliced and unspliced viral RNAs are prevented from exiting the nucleus by this pathway, instead utilising the viral Rev protein. Once a sufficient level of Rev is translated, it shuttles into the nucleus and binds to a specific RNA structure found only on singly and non-spliced transcripts, called the RRE (Rev responsive element). Rev multimerises upon binding and stabilises the formation of a complex between Rev and cellular exportin-1 (CRM-1), targeting the mRNA to the nuclear pore complex for export. The mRNA is then

directed to polysomes for translation, preventing them for being spliced (Wu, 2004; Sierra et al., 2005).

1.4.7 Viral Translation and Viral Proteins

1.4.7i Gag and Gag-Pol

The full-length transcript of the integrated provirus serves as the mRNA for the generation of Gag and Gag-Pol polyproteins. Gag and Pol proteins are synthesised on cytosolic polysomes, using overlapping open reading frames (ORFs). The first codon of *gag* is the first AUG of the RNA, although this is not the case for many other retroviruses. Large numbers of Gag molecules are required to serve as the precursors for the structural proteins of new virions; during particle maturation (see section 1.4.9) Gag is cleaved by the viral Protease into MA, CA, NC and p6 proteins (see Figure 15). However, the enzymes encoded by *pol* (RT, IN, PR) are needed in smaller quantities; this is also essential for viral morphogenesis. HIV has developed a mechanism which allows high expression of Gag relative to the protein sequences encoded by *pol*. This is due to the usage of the same initiation codon in the same mRNA to express both *gag* and *pol*. The ratio of Gag to Gag-Pol is around 20:1; this is conserved among retroviruses (Coffin et al., 1997; Shehu-Xhilaga et al., 2001).

The domains of the Gag polypeptide each play different roles. MA is predominantly involved in membrane targeting and triggers particle assembly to occur at the correct time. The CA protein assembles into a fullerene cone which encases the viral genome, and NC binds to viral RNA, which drives genomic RNA packaging. p6 is responsible for recruiting cellular machinery involved in viral budding. The spacer peptide SP1 stabilises Gag-Gag lattice interactions which are critical for immature particle formation, whereas spacer peptide SP2 itself is indispensable, but processing of the

NC-p6 region is essential for particle morphogenesis and virion infectivity (Ganser-Pornillos et al., 2008; de Marco et al., 2012).

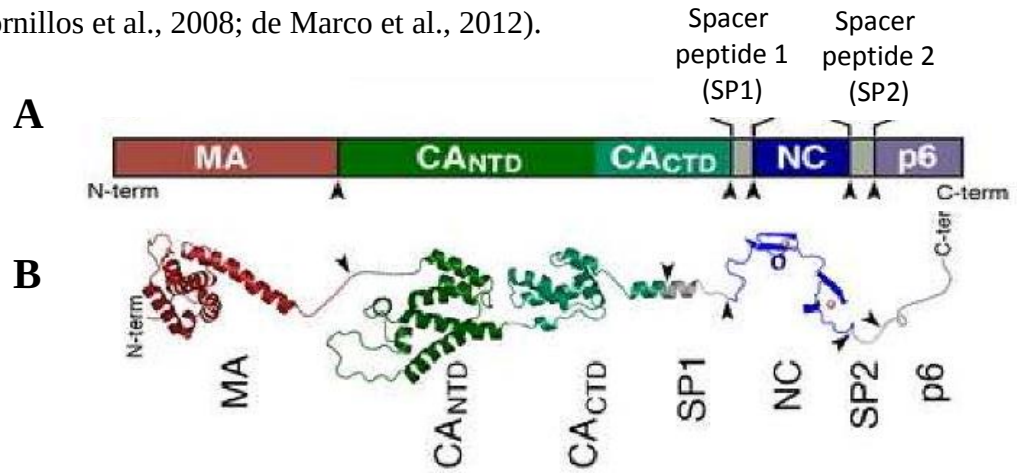

Figure 15: The HIV-1 Gag polyprotein domain structure (A) and a structural model of the extended Gag polypeptide (B). Arrowheads indicate PR cleavage sites. CA is composed of two highly helical domains; the N-terminal domain (CA_{NTD}) and the C-terminal domain (CA_{CTD}) (adapted from Ganser-Pornillos et al., 2008).

The *gag* gene is located at the 5' end of the genome, upstream to that of *pol*. Gag-Pol is generated using a strategy whereby the 3' termination codon of the *gag* ORF is bypassed, allowing translation to continue into the adjacent *pro* gene. This is achieved by a mechanism known as ribosomal frameshifting. The site of frameshifting is a heptanucleotide AU-rich sequence, also known as a "slippery sequence" found at the 3' end of the NC domain of *gag*. A stem-loop RNA structure is present 6 nt after this sequence, allowing the ribosome to stall as it scans, slipping back 1 nucleotide (-1 slippage). After this, the last codon read in the original reading frame becomes the first position nucleotide of the first codon in the new reading frame (Coffin et al., 1997; Dinman et al., 1998; Jacks et al., 1998; Shehu-Xhilaga et al., 2001; Brierley and Dos Ramos, 2006). Gag is also able to produce virus-like particles in the absence of any other viral proteins (Delchambre et al., 1989).

1.4.7ii Env

The HIV-1 Env glycoproteins play an essential role in the viral life cycle, mediating the fusion between viral and target cellular membranes during the entry process. Like other proteins destined for the plasma membrane, gp160 is synthesised on the rough endoplasmic reticulum (RER) as a polyprotein precursor, derived from a singly spliced, bicistronic *vpu/env* mRNA. gp120 contains an ER signal sequence at its N-terminus, targeting it to the RER. This signal sequence is then cotranslationally removed in the ER by signal peptidases. During gp120 translation, it is simultaneously glycosylated with *N*- and *O*-linked oligosaccharide side chains (Freed and Martin, 1995; Checkley et al., 2001).

After synthesis in the ER, gp120 oligomerises into trimers, facilitating its trafficking to the Golgi complex. Once here, it is cleaved at a highly conserved K/R-X-K/R-R motif by cellular furin into gp41 and gp120. These remain covalently attached and form a heterotrimeric spike with gp41 comprising the transmembrane domain and gp120 being fully exposed extra-cellularly. Once at the PM, this spike is rapidly endocytosed by AP-2 (see 1.5.2ii for further detail of AP-2 function) through a tyrosine YxxL motif located on the carboxy terminus of gp41. This internalisation is responsible for the relatively low levels of incorporation of Env into newly synthesised particles (Checkley et al., 2001). This also ensures that Env is retrieved unless the Gag protein is present in the same microdomains (Egan et al., 1996). This has led to the proposal that internalisation of Env can protect against immune recognition (Marsh and Pelchen-Matthews, 2000).

1.4.7iii Regulatory Proteins

HIV-1 encodes two regulatory proteins; Tat and Rev, whose primary functions in HIV gene expression have already been discussed. Tat also plays many nontranscriptional

roles within the viral life cycle. For example, Tat can influence HIV-1 RNA splicing, capping and reverse transcription, and can also modulate the expression of numerous cellular genes (Das et al., 2011). This modulation includes the upregulation of the chemokine co-receptor CCR5, used for viral entry, and the downregulation of MHC class I. Tat can also promote apoptosis by altering microtubule dynamics, and inhibit apoptosis by upregulating the anti-apoptotic protein B-cell lymphoma 2 (BCL-2); the latter is thought to be crucial to the establishment of latency (Romani et al., 2009).

In addition to nuclear export, Rev functions to enhance viral translation and facilitates the packaging of HIV-1 genomic RNA through interactions with the RRE, contributing to the selection of full-length RNAs destined for encapsidation (Groom et al., 2009).

1.4.7iv Accessory Proteins

There are 4 accessory proteins produced by HIV-1; Nef, Vif, Vpr and Vpu. These proteins function to modify the cellular environment within infected cells in order to ensure efficient viral persistence, replication, dissemination and transmission (Malim and Emerman, 2008).

Vpu (viral protein U) is an 81AA (amino acid) integral membrane phosphoprotein which mediates the degradation of CD4 within the ER. The Vpu cytosolic domain acts as an adaptor to link CD4 to an E3 ubiquitin ligase (TrCP) to facilitate CD4 ER-associated degradation. This receptor downregulation is employed by many retroviruses, including HIV, to avoid superinfection (Margottin et al., 1998; Andrew and Strebel, 2010; Strebel, 2013). Vpu, through its TM domain, also counteracts tetherin (BST-2), a cellular protein known to prevent viral release (Malim and Emerman, 2008). In these distinct ways, Vpu prevents premature CD4-Env association within the ER and enhances virion release.

The 23 kDa HIV-1 Vif (virion infectivity factor) has long been established in its role of inhibiting cellular defences which have the ability of preventing viral replication. In particular, the cellular protein APOBEC3G is fully sufficient to prevent productive infection, and in the absence of Vif is packaged into virions and consequently carried into newly infected cells, where it deaminates C residues in nascent minus strand reverse transcripts, resulting in a gross loss of genetic integrity and therefore prevents viral spread. Vif is able to antagonise this effect by recruiting a ubiquitin ligase, thereby initiating the polyubiquitination of APOBEC3G and targeting it for degradation within proteasomes (Mehle et al., 2004; Malim and Emerman, 2008).

The 14 kDa Vpr (viral protein R) has two main roles in addition to regulating the nuclear import of the PIC; arresting the infected cell cycle in G2, and facilitation of macrophage infection (Malim and Emerman, 2008). The significance of the G2 arrest is not fully understood, however, it is believed that the LTR seems to be more active in this phase, conferring a more favourable environment for efficient HIV-1 replication. Vpr is able to inactivate the cyclin dependent kinases p34/cdc2, which associate with cyclin-B during G2 during the transition from G2 to M phase (Le Rouzic and Benichou, 2005).

Nef is a 27 (HIV-1) or 34 (HIV-2) kDa myristoylated protein encoded by the 3' end of the HIV genome, and early studies suggested that it functions to attenuate viral replication, hence the name NEgative Factor. Further investigation, however, actually discovered the positive role Nef has on both replication and viral pathogenesis (Laguette et al., 2010). Nef is localised both across the cytosol and in association with cellular membranes (Sha et al., 2009). It was soon discovered that Nef plays a pivotal role in the development of AIDS following HIV infection, dramatically increasing viral particle production and therefore viral load. Long term survivors of HIV infection show

a lack of disease progression, which is commonly associated with infection of *nef* deleted strains (Peter, 1998; Fackler and Baur, 2002)

One function of Nef which has been extensively investigated is its role in avoiding super-infection by down-regulating CD4 from the plasma membrane. To do this, Nef increases the rate of CD4 internalisation through interactions with a di-leucine based motif located on the cytoplasmic tail of CD4, and subsequently targets CD4 towards lysosomal compartments for degradation (Peter, 1998; Laguette et al., 2010). Alongside interacting with the di-leucine motif, Nef also binds to the clathrin adaptor complex AP-2, coupling the Nef-CD4 complex to clathrin coated pits and facilitating endocytosis (see Figure 16 overleaf) (Oldridge and Marsh, 1998). Removal of CD4 from the surface also facilitates viral budding, as CD4 can bind to Env during budding, leading to the retention of newly formed viral particles (Horenkamp et al., 2011). Alongside CD4 receptor down-regulation, HIV Nef can also down-regulate CCR5, and to a lesser extent CXCR4, which also prevents super infection (Laguette et al., 2010).

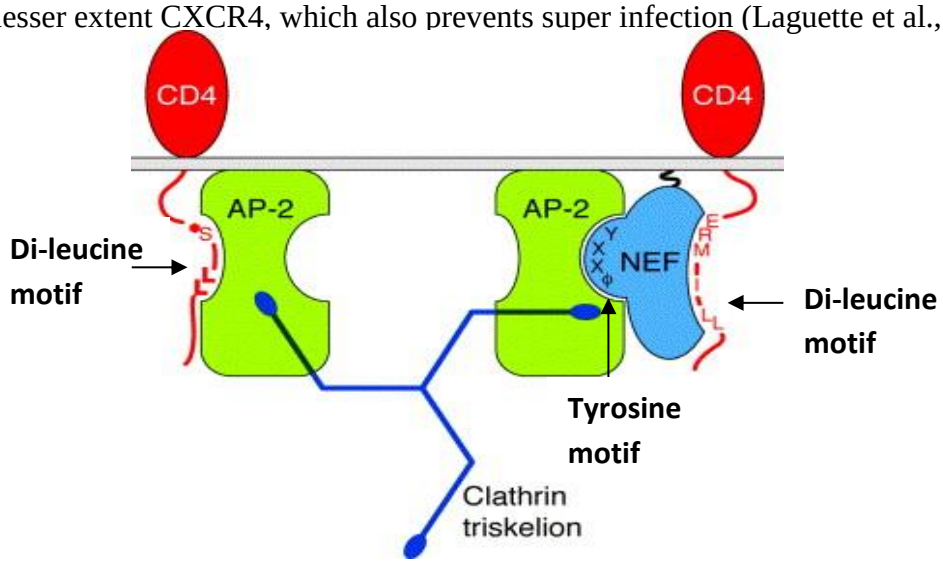

Figure 16: Model for Nef-induced endocytosis of the CD4 receptor. Nef binds CD4 through specific regions within the cytoplasmic tail; a di-leucine motif, and also glutamic acid (E), arginine (R), methionine (M) and isoleucine (I) residues at positions 405, 406, 407 and 410, respectively. Nef also binds to the clathrin adaptor AP-2 through a tyrosine motif (YXXΦ). This couples the complex into clathrin

coated pits (represented by the clathrin triskelion) (adapted from Oldridge and Marsh, 1998).

Nef is also able to modulate signal transduction machinery in order to augment the expression of its own genome and cellular genes, alongside down-modulation of various genes which could be detrimental to the HIV life cycle. Nef is able to induce transcription factors such as NFκB and c-fos, which transactivate the HIV-1 LTR promoter, and also induces the expression of cytokines and chemokines IL-2/4 and TGFβ which may assist viral replication. Nef can also down-regulate genes that are associated with antigen presentation (Arhel and Kirchoff, 2009). For example, MHC-I is downregulated by Nef by promoting binding of this protein to the clathrin adaptor protein AP-2, which directs it to endosomes and lysosomes for degradation (Roeth et al., 2004; Lubben et al., 2007).

1.4.8 Viral Protein Trafficking, Assembly and Packaging

Assembly of HIV particles is dependent on the viral Gag protein. It is well established that HIV-1 Gag budding and assembly occurs predominantly within cholesterol-enriched microdomains (detergent resistant membranes or lipid rafts) at the plasma membrane of T-cells (Ono and Freed, 2001). However, it was recently discovered that in macrophages and dendritic cells, a multivesicular late-endosome derived compartment is the site of particle assembly, prior to release from the PM (Pelchen-Matthews, 2003; Ono and Freed, 2004). These MVB-like sites of assembly in macrophages are also described as VCCs (virion containing compartmentd), which are non-acidic and linked to the PM by very narrow channels (Gaudin et al., 2013).

Live imaging of Gag by confocal microscopy and electron microscopy studies in HeLa and HEK 293 cells found the multivesicular body (MVB) was used for particle

assembly within these cell lines as well (Sherer et al., 2003). To support this, the use of a biarsenic-based imaging technique demonstrated that nascent Gag can travel through the MVB and perinuclear compartments as an intermediate, prior to arriving at the PM in HeLa cells (Perlman and Resh, 2006). This was suggestive of an involvement with endosomal pathways as trafficking routes for Gag in non-macrophage cells as well as macrophages. It has been demonstrated that Gag may form particles inside the endosomal lumen, which are then later released via fusion of the endosome-like structure with the PM by exploiting the pre-existing exosome release pathway, which was named the "Trojan exosome hypothesis" (Nguyen et al., 2003).

Consistent with this, a number of proteins involved in endosomal trafficking and recycling were found to interact with Gag. Specifically, the MA of Gag was found to interact with the clathrin adaptor proteins AP-1, AP-2 and AP-3 (see chapters 1.5.2i-iii, 3.1 and 5.1 for more detail). AP-1 and AP-3 were found to facilitate particle release, whereas AP-2 inhibits particle release (Batonick et al., 2005; Dong et al., 2005; Camus et al., 2007; Liu et al., 2012). The MA region of Gag has been found to be critical for Gag trafficking and localisation. More detail on the interaction of Gag with the adaptor protein pathways will be discussed in chapters 3 and 5.

The involvement of endosomes in the trafficking of Gag in T cells is, however, complicated by the fact that Gag present in these compartments may be derived from assembling particles which have been internalised from the PM. For example, TIRF (total internal reflection fluorescence) microscopy demonstrated that the Gag population which associated with late endosomal markers was indeed as a result of PM internalised Gag (Ivanchenko et al., 2009). Studies using a Gag-GFP construct also discovered that Gag reaches the PM prior to being found within intracellular compartments in HEK 293T cells (Jouvenet et al., 2006). Therefore, there still remains

some discrepancy over the route newly synthesised Gag adopts prior to assembly in T cells.

After trafficking to sites of assembly, Gag and Gag-Pol polyproteins sort into lipid rafts (Ono and Freed, 2001), which are rich in cholesterol and sphingolipids, with which the HIV-1 particle membrane is highly enriched (Ono, 2009). HIV-1 Gag does not extensively polymerise prior to reaching assembly sites; instead molecules are thought to arrive as soluble, monomeric proteins, folded into compact arrangements which subsequently undergo conformational changes which allow MA-membrane, NC-RNA and Gag-Gag interactions. Gag molecules arriving at assembly sites are most likely monomers/dimers, which extensively polymerise onto nucleation sites (Sundquist and Kräusslich, 2012).

Targeting of Gag to membranes requires a combination of factors; myristoylation (Gag is cotranslationally modified with the 14 carbon fatty acid myristate) (Resh, 2005), and the interaction of MA and $PI(4,5)P_2$, which is found on lipid rafts on the inner leaflet of the PM, where Gag is concentrated (Ono et al., 2004; Gousset et al., 2008; Ghanam et al., 2012). Upon MA binding to membranes, the myristoyl group becomes exposed during an event called the "myristoyl switch"; this anchors Gag to the inner leaflet of the membrane (see Figure 17). The inositol head group and unsaturated 2'-fatty acid of $PI(4,5)P_2$ bind to MA, allosterically inducing extrusion of the myristoyl group (Sundquist and Kräusslich, 2012). Once Gag has reached assembly sites, it dimerises. This process is principally driven by the C-terminus of the CA region of Gag. This, together with the N-terminus of spacer peptide p2, forms a continuous α-helix, which is critical for particle assembly (Göttlinger, 2001).

As described earlier, Env trimers travel independently of Gag to the PM. The long intracellular tail of gp41 (TM) is used to sort the Env spikes into raft-like domains and also assists specific interactions with the MA of Gag (Sundquist and Kräusslich, 2012).

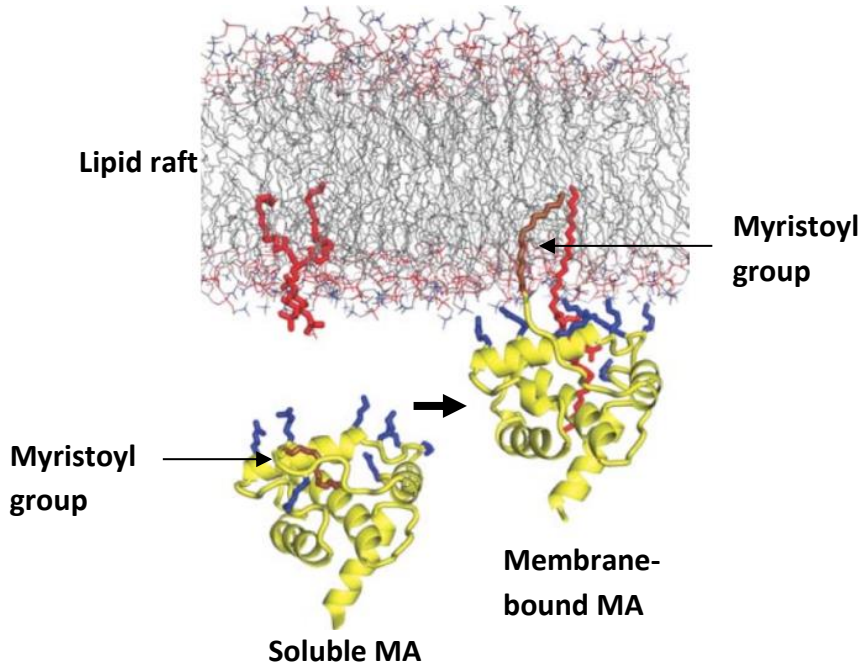

Figure 17: Myristoyl switch mechanism. MA is shown in yellow with the myristoyl (brown), sequestered within the soluble protein (left) and with the myristoyl group embedded into the membrane when bound to PI(4,5)P_2 (red) (right) (adapted from Sundquist and Kräusslich, 2012).

HIV-1, like all retroviruses, packages two copies of genomic (gRNA) RNA into each virion as a dimer, joined by non-covalent linkages at the 5' UTR. The gRNA is coated by NC at a density of roughly 1 NC molecule per 5-8 RNA bases (Johnson and Telesnitsky, 2010). Dimerisation initiates through formation of a "kissing loop" structure mediated by Watson-Crick base pairing of the self-complementary sequences found within the dimer initiation site (DIS). Efficient packaging is dependent on a packaging site (Ψ) located at the 5' end of the genome, which spans the splice donor (SD) site and the Gag initiation codon. These are part of 4 stable stem loop structures within the highly structured 5' UTR (see Figure 18 overleaf) (Sundquist and Kräusslich, 2012).

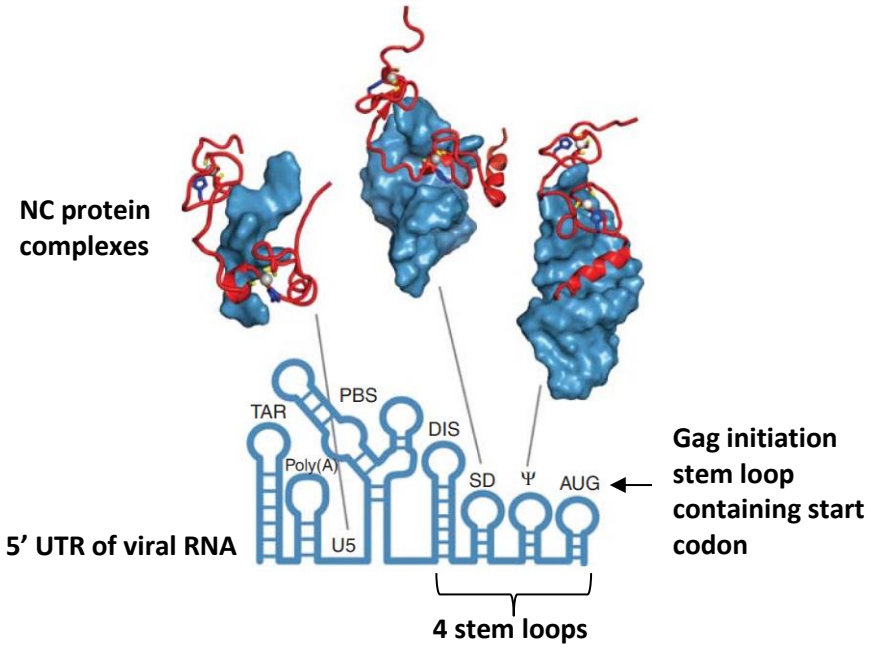

Figure 18: The 5' UTR of HIV-1 and its interactions with NC. The 4 stem loops critical to packaging are highlighted. 3 different NC/RNA complexes are shown; NC protein is shown in red, whilst viral RNA is shown in blue. TAR (Trans-activation response), PBS (primer binding site), DIS (dimer initiation site), SD (splice donor) are indicated (adapted from Sundquist and Kräusslich, 2012).

1.4.9 Particle Budding and Maturation

Assembling Gag molecules are derived from the cytoplasmic pool; they increase exponentially until a plateau is reached, and budding ensues. Initially, an immature lattice is formed, where Gag molecules are oriented radially with the amino terminus of MA still bound to the inner leaflet of the membrane, and the opposite carboxy-terminus facing the middle of the forming particle (Ivanchenko et al., 2009; Sundquist and Kräusslich, 2012). Budding of virus particles requires the host ESCRT (endosomal sorting complexes required for transport) pathway to terminate Gag polymerisation and initiate particle release, and which is recruited by the p6 domain of Gag. p6 contains a YXPL (Tyr-X[variable residue]-Pro-Leu) domain which binds the ESCRT III binding partner ALIX, and a second motif (PTAP) which binds the ESCRT-1 subunit TSG101 (Fujii et al., 2009). This interaction results in the further recruitment of ESCRT-III-like

proteins (CHMPs 2A and 4A), which polymerise into an inward spiral, forming a "dome" like structure, which closes the neck of the forming bud. The CHMPs also recruit VPS4 ATPases, which plays an active role in membrane fission, remodelling CHMP2A subunits which leads to constriction and abscission of the particle (Sundquist and Kräusslich, 2012). This process is summarised below in Figure 19.

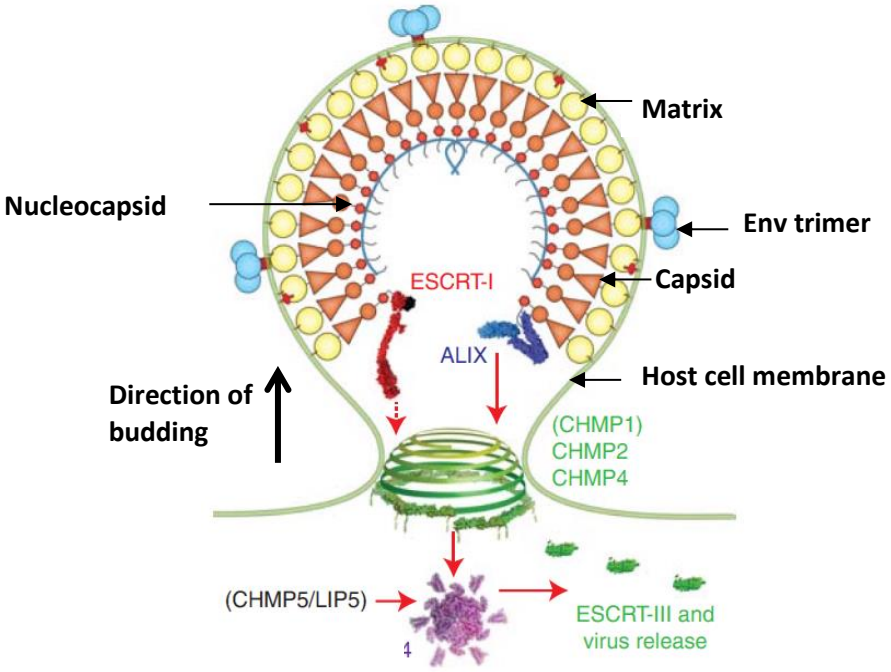

Figure 19: A summary of the ESCRT pathway utilised in HIV-1 budding. p6 interacts with ALIX (blue) and TSG101 of the ESCRT-1 heterotetramer (red), leading to the recruitment of CHMP proteins (green), which polymerise into a dome like structure, closing the neck of the bud. Recruited VPS4 ATPases (purple) complete membrane fission, releasing the ESCRT-III (adapted from Sundquist and Kräusslich, 2012).

After budding, HIV-1 viral particles are released as immature, non-infectious particles, which are proteolytically processed by viral protease to form mature, infectious particles. Viral protease is first activated by dimerization of PR in the Gag-Pol polyprotein, which is autocleaved. After this, Gag processing occurs in a stepwise fashion. First, the SP1-NC junction is cleaved, followed by cleavage of the SP2-p6 and MA-CA junctions, releasing MA and p6 together with p25 (CA-SP1) and NC-SP2

intermediates. The spacer peptides are separated from the Gag constituents to form mature p24 CA and mature NC. The cleavage of structural proteins is coupled with a morphological transition, whereby an electron dense ring of Gag is converted into a characteristic conical core, consisting of a lattice of 250 CA hexamers (Briant et al., 2011). This is shown below in Figure 20.

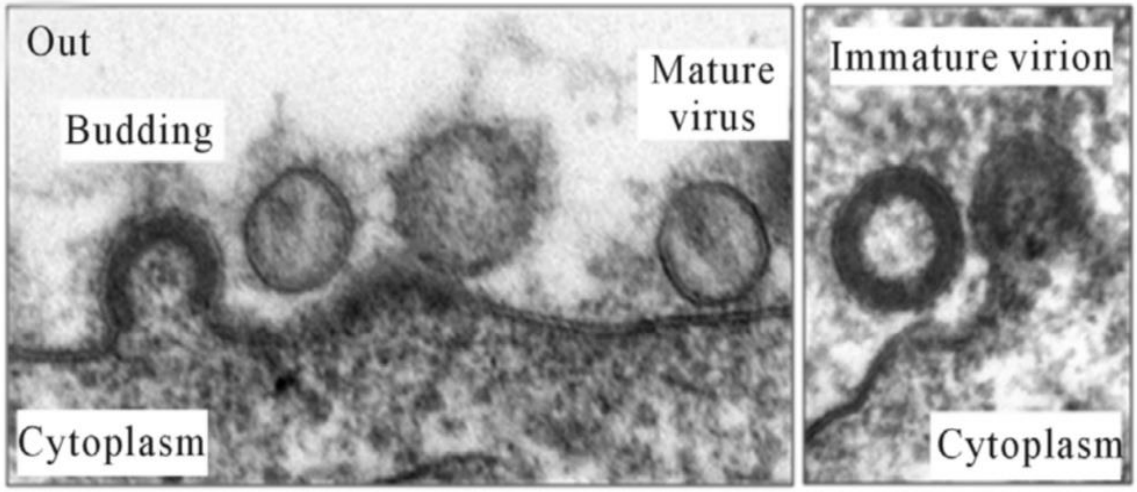

Figure 20: Morphological changes during HIV-1 maturation, demonstrated by electron microscopy (Briant et al., 2011)

1.5 Cellular Trafficking- an Overview

Within cells, the majority of proteins translated are required for use in distant locations to their site of production, such as membrane proteins or those localised to specific compartments, and are trafficked in an anterograde direction to these locations. Many extracellular proteins are also internalised, such as ligands bound to their receptors, and are trafficked in a retrograde direction to sites of modification, recycling, or destruction within the cell. All of these processes require a complex trafficking system, involving numerous pathways, molecules and chaperones. One such molecule heavily involved in the assistance of cargo trafficking is clathrin, which will be discussed in detail in the next section.

1.5.1 Clathrin

Three major classes of coat protein have now been purified which assist in cargo trafficking; clathrin, COP [coat protein complex] I and COP II. The vesicle-transport hypothesis of protein trafficking was suggested from early electron microscopy studies, whereby vesicular transport intermediates initially bud from a donor membrane, and are then transported to an acceptor organelle, where membranes fuse and cargo is deposited (McMahon and Mills, 2004).

Coated pits and vesicles used for cargo trafficking, demonstrated by these electron microscopy studies, showed membrane invaginations and vesicles with bristle-like projections in some areas of the cell, and without them in others. It was later discovered that these projections are composed of multiple molecules of a protein called clathrin, which forms around vesicles during their trafficking pathways. Clathrin is composed of a heavy chain of 180 kDa, and two light chains of 33 and 36 kDa. The heavy chain is ubiquitously expressed within cells and different species share high degrees of sequence homology between their heavy chains, whereas the light chains seem to be more polymorphic (Hirst and Robinson, 1998).

Clathrin self-polymerises into a supportive lattice, or cage-like structure which forms, when membrane bound, into a scaffold required for the deformation of these membranes into budding vesicles containing. Clathrin has limited ability to induce curvature of membranes around forming vesicles, but it gives directionality to budding since the rigid triskelions preserve inward curvature induced by other components cargo (Hirst and Robinson, 1998; Young, 2007). The structure of the clathrin unit was deduced to be a three-legged triskelion, whereby the three heavy chain legs loosely associate at the centre of the molecule, and are in close contact with three light chains

(see Figure 21A) (Kirchhausen and Harrison, 1981). The scaffold assembles by each triskelion leg extending across two neighbouring edges, resulting in each edge consisting of two proximal and two distal triskelion legs (see Figure 21B) (Crowther and Pearse, 1981; Hirst and Robinson, 1998).

Clathrin-coated vesicles are uncoated after abscission from the membrane and vesicles may then be trafficked to intracellular sites such as early endosomes, late endosomes, lysosomes and the PM by microtubules; the directionality of which is determined by the presence or absence of the motor molecule kinesin (Wacker et al., 1997; Liu et al., 2011).

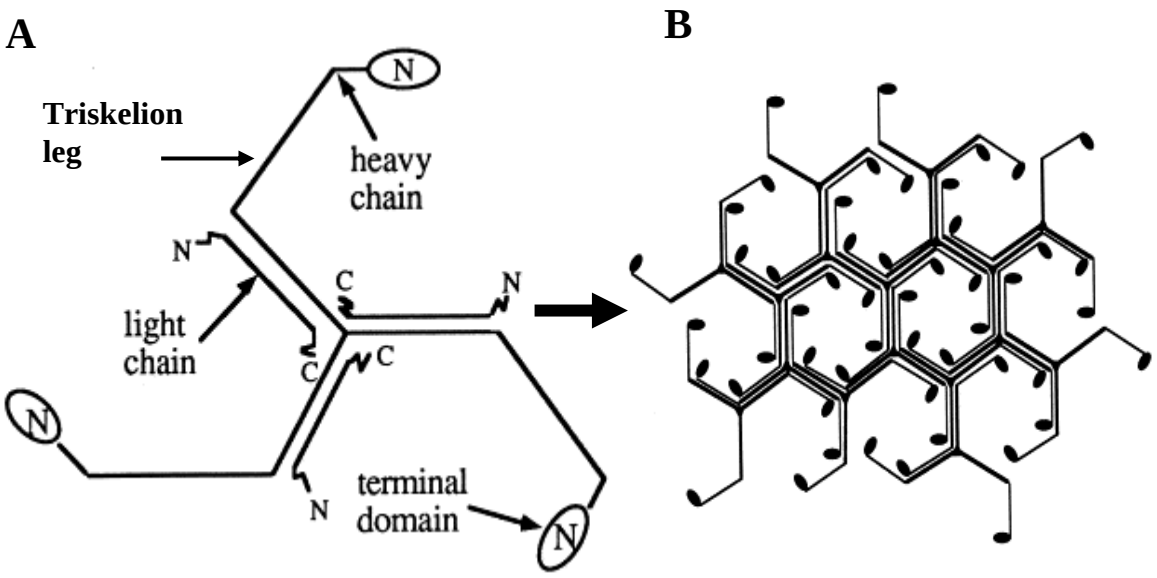

Figure 21: A- Structure of an individual clathrin triskelion molecule. B- Clathrin triskelion lattice organisation (adapted from Hirst and Robinson, 1998).

1.5.2 Clathrin Adaptor Proteins

Clathrin is a vesicle stabiliser; it is the clathrin adaptors that select cargo, which bud from 3 main areas of the cell: the plasma membrane (PM), trans-Golgi network (TGN) and endosomes (Mills, 2007). These so called adaptor proteins (APs) function within the secretory and late endocytic pathways, assisting the linkage of clathrin to the

membrane, coat formation, cargo selection, and also binding of accessory proteins that regulate clathrin assembly and disassembly, such as epsins (Robinson, 2004; Mills, 2007). Seven APs exist, AP-1 -5, with 2 isoforms of AP-1 and 3 (A and B). They are cytosolic heterotetrameric complexes, composed of two large subunits; a β subunit and one of α, γ, δ, ε or ζ, a medium subunit (μ) and a small (σ) subunit. They form a similar "Mickey Mouse" like structure, with a core 'head' composed of the amino terminals of the large subunits, the medium and small subunits, flanked by two 'ears' consisting of the carboxy terminal domains of the large subunits, bridged by flexible hinge domains (see Figure 22). The different subunits were deduced to play distinct roles within the cell. The β subunits are responsible for clathrin binding, and the α, β and presumably γ ears recruit accessory proteins where they partake in vesicle scission and uncoating (Robinson, 1994; Robinson and Bonifacino, 2001).

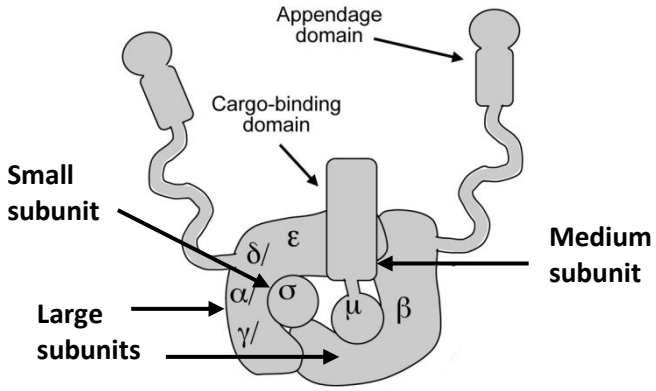

Figure 22: Structure of an AP complex, demonstrating the positions of the large, medium and small subunits comprising the adaptor (adapted from Hirst et al., 2011).

The recruitment of the APs to cellular membranes is a complicated story that has not been completely unravelled, but phosphoinositides have been shown to play a role in some circumstances. Phosphoinositide interactions were demonstrated to be crucial in the recruitment of AP-2; phosphatidylinositol(4,5)-bisphosphate (PIP_2), which is produced in the inner leaflets of the PM and where AP-2 primarily functions during endocytosis, is essential for AP-2 recruitment (Beck and Keen, 1991). AP-2 contains

PIP_2 binding sites in its μ and α subunits. AP-1 was also found to bind PtdIns(4)P which is primarily located on the TGN, where AP-1 functions. Many other adaptors have been shown to bind phosphoinositides, but this alone cannot be used to explain adaptor recruitment since their localisation is not as restricted as that of the APs (Robinson, 2004; Ohno, 2006).

Central to clathrin-mediated endocytosis is a dynamic network of AP-2 interactions with nucleation proteins, cargo and clathrin. The μ and σ subunits bind transmembrane proteins, but cargo may also be bound to the adaptor ears indirectly via accessory adaptor proteins such as β-arrestin, which recruits G-protein coupled receptors to AP-2 and clathrin (McMahon and Boucrot, 2011)

As mentioned, the APs are involved in clathrin coated cargo selection. The APs are able to recognise three distinct motifs, or sorting signals, found within specific cargos, for example in the cytoplasmic tails of certain receptors, such as the LDL (low-density lipoprotein) receptor. These motifs promote endocytosis, influence intracellular trafficking and determine steady state distributions of proteins; tyrosine based YXXØ motifs (where Ø constitutes a bulky hydrophobic residue, either leucine, isoleucine, phenylalanine, methionine or valine), dileucine motifs such as [D/E]XXXL[L/I], and the FXNPXY motifs are those currently described (Hirst and Robinson, 1998; Robinson and Bonifacino, 2001).

The μ and β subunits are involved in cargo selection; the μ subunit recognises YXXØ motifs, and this interaction is the best characterised; AAK1 (adaptor-associated kinase) can phosphorylate a specific residue, Thr156, in μ2 which induces conformational changes that unblocks the cargo binding site and ensures high affinity binding of YXXØ cargo (Ohno et al., 1998; Olusanya et al., 2001; Ricotta et al., 2002; Smythe and Ayscough, 2003). Cyclin-G-associated kinase (GAK) is also able to phosphorylate

μ2, but also μ1. The β subunit recruits clathrin through the so-called clathrin-box, a linear sequence of 5 amino acids (LØxØ[DE]) which lies within the hinge region (Owen et al., 2004). All of the AP μ subunits have been demonstrated to bind to YXXØ motifs, however, their preferences for the X and Ø residues differ; this, together with the distinct localisations of the APs, helps explain the differences in steady state distributions of proteins containing this motif (Ohno et al., 1998; Robinson, 2004).

It was originally assumed that adaptors were recruited to membranes simply by binding to proteins destined to become cargo. It was discovered, however, that ARF1, a GTPase, is critical for recruitment of AP-1, -3 and -4, which acts as a coat protein docking site. Members of the Arf family are also able to stimulate production of phosphoinositides, particularly PtdIns(4)P, and PIP_2; PIP_2 was later found to be critical for AP-2 recruitment (Robinson, 2004).

The APs have distinct localisations within the cell, and thus operate in distinct trafficking pathways. This will be described for each of the 5 APs in the sections below. The known distributions and trafficking pathways of the APs is summarised in Figure 23.

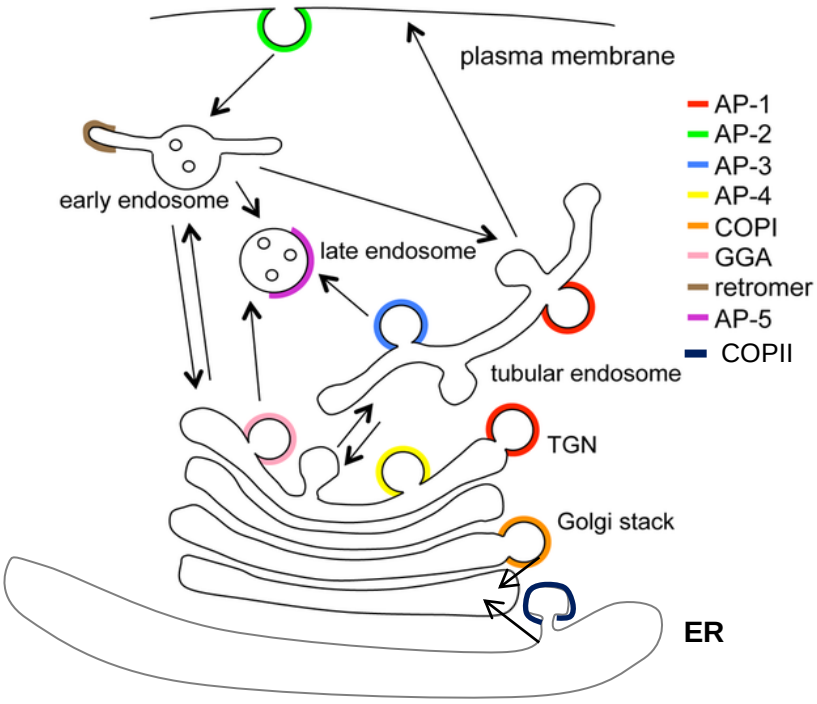

Figure 23: A summary of coat proteins and cellular trafficking pathways. AP-1 traffics between endosomes and the TGN, AP-2 assists clathrin mediated endocytosis from the PM, AP-3 is involved in endosomal trafficking, AP-4 is involved in sorting from the Golgi complex, and AP-5 is involved in endosomal sorting from late endosomes. The GGAs facilitate trafficking from the TGN to endosomes. COPI is involved in retrograde transport from the cis-Golgi to the ER, whereas COPII functions in the reverse (adapted from Hirst et al., 2011).

1.5.2i AP-1

As mentioned, there are 2 isoforms of AP-1; AP-1A and AP-1B, differing only in their μ subunits (μ1A and μ1B, respectively). Both forms do not differ in their localisation to the TGN and endosomes; however, they serve different roles. AP-1A is ubiquitously expressed and involved in TGN to endosome transport; presumably this is bidirectional, however some controversy still surrounds this. AP-1B is only expressed in epithelia and primarily functions to mediate polarised targeting of membrane proteins to the basolateral surface. Membrane sorting at the TGN and within the endocytic pathway is determined by the critical tyrosine/dileucine residues within the cytoplasmic domain of proteins, as described above (Fölsch et al., 2003). AP-1 is

thought to work in concert with, or shortly after, another class of cargo-binding adaptors; the GGAs (Golgi-localised, γ-ear-containing, Arf-binding proteins), which also function in TGN to endosome transport. AP-1 has been demonstrated to sort the 46kDa mannose-6-phosphate receptor (MPR46) to the TGN, amongst numerous other receptors (Chapuy et al., 2008).

1.5.2ii AP-2

Unlike AP-1, AP-2 is found and functions exclusively at the plasma membrane (PM), within clathrin-coated pits. AP-2 is critical for clathrin-mediated endocytosis; endocytosis is the process by which cells internalise extracellular contents and cell-surface proteins such as receptors (Lau and Chou, 2008). AP-2 holds a central role within the endocytic pathway since all proteins functioning within this pathway can, in principle, interact with it. It was found that knockdown of AP-2 μ2 or α2 by siRNA in HeLa cells results in an elimination of ~90% of endocytic clathrin-coated structures, and the disruption of functional AP-2 is lethal in mice, worms and insects (Ungewickell and Hinrichsen, 2007).

The current model proposes that endocytosis begins by the formation of a nucleation module containing FCH domain only (FCHo) proteins, EPS15, intersectins and PIP_2 at a patch of membrane (Henne et al., 2010). This region mechanically invaginates. AP-2 is then able to bind to PIP_2 and cargo directly via the μ and σ subunits, and indirectly through other adaptors, with ratcheting from the formation of the developing clathrin lattice and various accessory/regulatory proteins (Collins et al., 2002; Kelly et al., 2008). Proteins are sorted into the pit, and the mature vesicle is eventually "pinched off" in a process mediated by the GTPase dynamin which in turn is recruited by BAR-containing proteins, such as amphiphysin, that prefer the curvature of the vesicle neck

and likely assist neck formation (Wigge et al., 1997; Ferguson et al., 2009). After release from the PM, auxilin binds the terminal "leg" domains and "ankles" of clathrin, which in turn recruits the ATPase heat shock cognate 70 (HSC70) to initiate the uncoating of clathrin back to triskelia through the ATPase activity of this protein (Kirsch and Beevers, 1993; Ungewickell et al., 1995; Fotin et al., 2004; Taylor et al., 2011). AP-2 is extensively involved not only in assisting coat formation around the assembling vesicle, but also in the recruitment of the numerous accessory proteins pivotal to this process, including epsin, CALM/AP180 and dynamin (Owen and Luzio, 2000; Sorkin, 2004).

Endocytosed vesicles form part of the endosome system; at its simplest, this involves a recycling pathway, for example for membrane receptors; a degradative pathway for the degradation of certain molecules, and a connecting feeder pathway which links these two former pathways (Huotari and Helenius, 2011). Endocytic cargo is first delivered to the early endosome (EE) by fusion of the two compartments; how EEs arise is, however, unclear. EEs exchange vesicles with the TGN in a bidirectional manner. EEs have tubular and vacuolar domains; late endosomes (LEs) are derived from the vacuolar domain, and the tubular domain is lost upon formation of the LE, however again it is unclear exactly how this happens, but it is known that Rab7 recruitment to the EE precedes LE formation (Vonderheit and Helenius, 2005; Huotari and Helenius, 2011). From here, LEs undergo a number of changes, or maturation, which ultimately results in the fusion of this compartment with the lysosome. Endosomal maturation involves a Rab switch, whereby Rab5 converted to Rab7 (Rink et al., 2005), and acidification, amongst other changes (Huotari and Helenius, 2011). The pH drop is achieved by a group of vacuolar (V)-ATPases, which are proton pumps (Forgac, 2007). Acidification is critical for a number of reasons, including the sorting and routing of

cargo, and also allows the specific timed activation of various bacterial toxins, such as Diphtheria toxin (Lemichez et al., 1997; Huotari and Helenius, 2011).

1.5.2iii AP-3

AP-3 is localised generally to endosomes, but also the TGN. There is some discrepancy over whether AP-3 delivers its cargo to either late endosomes or lysosomes (Robinson, 2004). Like AP-1, there are 2 isoforms of AP-3; AP-3A and AP-3B, which also differ in their localisation. AP-3A is ubiquitously expressed, whereas AP-3B is localised to neurons only (Ohno, 2006). AP-3A generally functions *en route* to lysosomes and other related structures such as melanosomes and platelet-dense granules. AP-3B is solely involved in neuron-specific cargo sorting and vesiculation. A deficiency in AP-1 or AP-2 is embryonic lethal within mice, whereas AP-3 is not (Seong et al., 2004; Chapuy et al., 2008). AP-3 is responsible for the sorting of the lysosomal associated membrane protein 1 (LAMP1) and tyrosinase into TGN derived vesicles. Mislocalisation of tyrosinase in melanocytes is responsible for the disease Hermansky-Pudlak syndrome (a rare form of albinism) (Chapuy et al., 2008).

There was some discrepancy as to whether clathrin is involved in AP-3 containing vesicles, and that it may associate with another scaffold protein with similar morphology. It was later, however, demonstrated by Dell'Angelica et al., 1998, that clathrin does interact with AP-3 *in vitro* through the β3A subunit, and that AP-3 and clathrin colocalise on endosomal membranes (Nakatsu and Ohno, 2003). However, AP-3 is not found in pure clathrin coated vesicles (Simpson et al., 1996). Furthermore, reconstitution of vesicles from PC12 neuroendocrine cells is AP-3 dependent but clathrin-independent (Shi et al., 1998), and immunofluorescence studies have found both areas in which AP-3 and clathrin colocalise, and areas where AP-3 is present but

clathrin is absent (Simpson et al., 1997). It therefore remains uncertain as to whether the AP-3 pathway uses clathrin.

1.5.2iv AP-4

In contrast to AP-1, -2 and -3, AP-4 has not been extensively studied. One study scrutinised the cellular localisation of AP-4, and found that it has a similar localisation to that of AP-1. It is predominantly localised with clathrin coat machinery to the Golgi complex, endosomes and transport vesicles (Barois and Bakke, 2005). This adaptor protein was found to be involved in the basolateral sorting of proteins containing a tyrosine based motif in their cytoplasmic tail (Aguilar et al., 2001; Simmen et al., 2002).

1.5.2v AP-5

Recently, the existence of a fifth adaptor protein complex, AP-5, has been described. AP-5 had been previously described before under a different alias, MUDENG (Mu-2 related death-inducing gene) (Leet et al., 2008). This AP cycles on and off membranes, but is not associated with clathrin coated vesicles, but was found to play a unique role in endosome dynamics (Hirst et al., 2013). To date, this is the only AP known to localise to and associate with late endosomes and lysosomes, and is speculated to have a role in the poorly defined recycling of late endosomal membrane proteins, such as lysosomal hydrolase receptors, although this has not yet been established (Hirst et al., 2011; Hirst et al., 2013). Interestingly, this protein was also described as a putative HIV-1 infection-related protein in the UniProt entry of the mu5 subunit.

1.5.3 Vesicle Recycling Within Neuronal Cells

Vesicle recycling has been extensively studied in neurons. Neurotransmitters are contained within vesicles which are rapidly released by exocytosis events upon stimulation to transmit a signal to target cells, such as neighbouring astrocytes, which form part of the tripartite synapse. Vesicle retrieval after neurotransmitter release events is essential to prepare for future rounds of exocytosis. Although several mechanisms exist, clathrin-mediated endocytosis is one such pathway. A key player in this process is AP-2. shRNA mediated knockdown of AP-2 resulted in an impairment of vesicle endocytosis, and further investigation revealed AP-2 to be a crucial sorting adaptor at the synapse (Kim and Ryan, 2009). Further investigation revealed that in the absence of AP-2, AP-1 may behave as a functional substitute for vesicle recycling (Kim and Ryan, 2009). Furthermore, it was discovered that AP-1 deficient mice have impaired synaptic vesicle recycling and severely compromised motor coordination and long-term memory, indicating a role for this adaptor in learning and memory (Glyvuk et al., 2010). Neuronal AP-3 has also been implicated in regulating exocytosis of synaptic vesicles, and vesicle biogenesis from endosomes (Nakatsu et al., 2004; Scheuber et al., 2006; Danglot and Galli, 2007).

1.6 Project Aims

Although interactions between HIV-1 Gag, Nef and the adaptor proteins have been described, the consequences of these interactions on both HIV-1 and adaptor protein production and localisation have not been extensively investigated. The effects of these interactions on adaptor protein dependent protein trafficking has also only vaguely been described. Therefore, this project aims to further the knowledge of the complex

interactions between these distinct proteins, and how these interactions may disrupt well characterised AP dependent trafficking pathways.

Much research in this area has focussed on HIV-1, neglecting to examine possible interactions with HIV-2. Since these are similar viruses, this project also aims to scrutinise whether HIV-2, as well and HIV-1, can interact with the APs, and how these interactions may again affect the levels and localisation of HIV-2/ the APs in the presence of infection.

Another neglected field of interest is the effects of HIV-1 on protein trafficking within cells of the nervous system. This project will also investigate whether HIV infection may disrupt protein trafficking within astrocytes, in particular that of synaptic vesicles, in a similar manner to that in non-brain cells, as a possible contribution to HIV associated dementia.

CHAPTER 2: MATERIALS AND METHODS

2.1 Materials

2.1.1 Antibodies

Antibody	$1^o/2^o$	Dilution	Source
Rabbit anti-HIV-1 p24 Polyclonal	Primary	1:5000 (Western blots) 1:1000 (confocal immunofluorescence)	NIBSC
Sheep anti-HIV-1 Nef Polyclonal	Primary	1:5000 (Western blots) 1:2000 (confocal immunofluorescence)	NIBSC
Sheep anti-SIV p27 Polyclonal	Primary	1:5000 (Western blots) 1:1000 (confocal immunofluorescence)	NIBSC
Mouse anti-AP-1 γ subunit Monoclonal	Primary	1:5000 (Western blots) 1:1000 (Confocal immunofluorescence)	BD Biosciences
Mouse anti-AP-2 μ subunit Monoclonal	Primary	1:500 (Western blots) 1:500 (confocal immunofluorescence)	BD Biosciences
Mouse anti-AP-3 δ subunit Monoclonal	Primary	1:1000 (Western blots) 1:1000 (confocal immunofluorescence)	BD Biosciences
Rabbit anti-GluA1 Polyclonal	Primary	1:1000 (Western blots only)	Millipore
Mouse anti-GluA2 Monoclonal	Primary	1:1000 (Western blots only)	Zymed
Mouse anti-clathrin heavy chain (X22) Monoclonal	Primary	1:350 (Confocal immunofluorescence only)	Frances Brodsky, UCSF
Goat anti-rabbit HRP (horse radish peroxidase) conjugated	Secondary	1:5000 (Western blots only)	Santa Cruz
Rabbit anti-sheep HRP Polyclonal	Secondary	1:5000 (Western blots only)	Santa Cruz
Goat anti-mouse HRP	Secondary	1:5000 (Western blots only)	Fisher
Donkey anti-rabbit Alexa Fluor 594	Secondary	1:1000 (Confocal immunofluorescence only)	Invitrogen
Donkey anti-sheep Alexa Fluor 594	Secondary	1:1000 (Confocal immunofluorescence only)	Invitrogen
Donkey anti-mouse Alexa Fluor 488	Secondary	1:1000 (Confocal immunofluorescence only)	Invitrogen

Mouse anti γ-tubulin Monoclonal	Primary	1:10000 (Western blots only)	Sigma
Mouse anti-CD81 Monoclonal	Primary	1:500 (Confocal Immunofluorescence only)	Santa Cruz

Antibodies for Western blots were suspended in 5% Marvel/TBS-T and incubated for either 1 hour (when used at >1:2000) or overnight (when used at <1:2000) at 4^{o}C on a rotating platform to ensure even coverage. Antibodies for confocal immunofluorescence microscopy were suspended in 1% bovine serum albumin (BSA) and incubated for 1 hour at room temperature.

2.1.2 Proviruses and Plasmid Constructs

Construct	Description	Source
SVC21ΔBgl (HXB2)	Env deleted HIV-1 provirus, contains premature stop codon in Nef (missing AP binding site) (Ratner et al., 1987)	Andrew Lever, University of Cambridge
HXB2N^{+}	HXB2 with mutated premature stop codon in Nef (produces full length Nef)	Emma Anderson, University of Warwick
HXB2ΔGag	HXB2 with mutated start codon in Gag	Made (see chapter 2.2.3)
HXB2N^{+}ΔGag	HXB2N^{+} with mutated start codon in Gag	Made (see chapter 2.2.3)
HVP ΔEC PuroΔB	Control provirus, does not contain full length Gag (only part of MA) or Nef, but contains regulatory genes (Rev, Tat) and puromycin (Richardson et al., 1993)	Emma Anderson
pGag-EGFP	Expression plasmid producing full length Gag and GFP. Instability sequences have been removed so mRNA is not degraded. (Hermida-Matsumoto and Resh, 2000)	NIH AIDS Reagent Program (cat. no. 11468)
GFP pcDNA	Green Fluorescent Protein (GFP) in a pcDNA3 vector	Emma Anderson
ts045-VSV-G-EGFP (VSV-G)	Temperature sensitive vesicular stomatitis virus glycoprotein, tagged with EGFP in a pcDNA3 vector (Presley et al., 1997)	David Stephens (initial construct[University of Bristol]), further cloned in the lab
Renilla Luciferase	Renilla Luciferase (RL) in a pcDNA3	Philip Gould,

	vector	Warwick University
HIV-1 Gag C28/49S	Packaging mutant virus. HIV-1 non-envelope deleted provirus containing two amino acid substitutions (Cysteine-Serine) within the Zinc finger domain of NC (Dorfman et al., 1993)	Andrew Lever
pSVR	Full length non-envelope deleted HIV-2 provirus (McCann and Lever, 1997)	Andrew Lever
SVRΔNB	HIV-2 Env deleted provirus (Griffin et al., 2001)	Andrew Lever
SVRΔNB MA1	HIV-2 Env deleted provirus chimera with Matrix of HIV-1	Emma Anderson
SVC21ΔBgl MA2	HIV-1 Env deleted provirus chimera with Matrix of HIV-2	Emma Anderson
A4	HIV-1 non-envelope deleted provirus with a stem loop from the packaging signal removed (Miele et al., 1996)	Emma Anderson
SVCΔP1	HIV-1 non-envelope deleted provirus with packaging signal removed (Harrison et al., 1998)	Andrew Lever
pNL4-3-ΔE-EGFP (HIV-GFP)	HIV-1 provirus with Env substituted for GFP (Zhang et al., 2004)	NIH AIDS Reagent Program (cat. no. 11100)
Sy-GCaMP-mCh	Synaptophysin conjugated to mCherry tagged GCaMP	Nick Hartell, University of Leicester
KS1620	1620 bp Bgl II fragment of HIV-1 Gag in Bluescript vector (Harrison et al., 1998)	Andrew Lever

2.1.3 siRNAs

The following siRNAs, except AP-5, were purchased from Ambion (Applied Biosystems). All were stored at -80^{o}C at a concentration of 50 µM in nuclease free water provided. All were used at a concentration of 10 nM, except for AP-5 which was used at 25 nM (Hirst et al., 2011).

AP-1γ subunit (AP1G). Sequence (5'-3'): GCGCCUGUACAAAGCAAUUtt (positions 1694-1713) (Camus et al., 2007).
AP-2µ subunit (AP2M). Sequence (5'-3'): GUGGAUGCCUUUCGGGUCAtt (Motley et al., 2003)
AP-3δ subunit (AP3D). Sequence (5'-3'): CCCUGUCCUUCAUUGCCAAtt (positions 3159-3178) (Camus et al., 2007).

AP-5- SMARTpool J-015523-09 ORF (Oligo-9) (Dharmacon)

Silencer Negative Control #2 (Ambion proprietary sequence).

Doses of siRNAs were optimised previously (Emma Anderson, personal communication) except for AP-5 where 10 nM, 25 nM and 50 nM concentrations were trialled, and the optimal dose was found to be 25 nm, as described by Hirst et al. (2005).

2.2 Methods

2.2.1 Tissue culture

HeLa/ HEK 293T cells were cultured in T75 flasks (BD Biosciences) in Dulbecco's modified eagle's medium (DMEM) supplemented with 10% heat inactivated foetal calf serum (FCS) (Biosera) at 5% CO_2 37^{o}C. When 100% confluent, cells were passaged 1:10 using trypsin/EDTA incubation (5 minutes) following a phosphate buffered saline (PBS) wash. For transfection, cells were passaged and seeded into 12 or 6 well plates (BD Biosciences) and grown overnight.

U373 MG-Uppsala astrocytoma cells (European Collection of Cell Cultures [ECACC], Public Health England) were cultured also in T75 flasks in Eagles minimal essential medium (EMEM), supplemented with 10% heat inactivated FCS, 2 mM Glutamine, 1% non-essential amino acids and 1 mM Sodium Pyruvate at 5% CO_2 37^{o}C. Cells were passaged 1:4-1:6 depending on confluency, as above, when judged to be approximately 80% confluent, using only versene to prevent trypsin cleavage of external receptors. For transfection, cells were passaged and seeded into 12 or 6 well plates and grown for 48h. For lysate collection, cells were seeded into 60mm sterile tissue culture dishes (BD Biosciences).

2.2.2 Transfection

HeLa/ HEK 293T/U373 MG cells were transfected when they were judged to be >85% confluent for increased efficiency. 2.5 µl/µg DNA Lipofectamine 2000 (Invitrogen) was used, suspended in 250 µl (12 well) or 500 µl (6 well) OPTIMEM (departmental media preparation service) containing 1-2 µg plasmid DNA, and left at room temperature for 20 minutes. This was then gently added to cells by spot pipetting, following media change. Cells were then incubated for either 24, 40 or 48 hours at $37^{o}C/5\%$ CO_2.

For transfections using TransIT-2020 (Mirus) and METAFECTENE®-FluoR (Biontex), 1 µg per well of plasmid DNA was transfected per well according to the manufacturer's instructions.

2.2.3 Site Directed Mutagenesis

In order to generate mutant proviruses that would not produce Gag, it was necessary to mutate the ATG start codon in the Gag ORF. Primers were designed as follows for use in site-directed mutagenesis:

Forward primer 5'-GCTAGAAGGAGAGAGACGGGTGCGAGAGCGTC-3'

Reverse primer 5'-GACGCTCTCGCACCCGTCTCTCTCCTTCTAGC-3'

Primers (at 20 µM), alongside the dNTP mix provided, were added to HIV-1 subgenomic template (KS1620), and PCR was carried out under the following conditions: 18 cycles of $95^{o}C$ 50 sec, $60^{o}C$ 50 sec, $68^{o}C$ 7 min. Methylated, non-mutated template strands were digested using 1 µl DpnI, leaving only plasmids containing the mutation. The PCR product was then run on a 1% agarose gel to check amplification was successful. After confirmation of mutagenesis by sequencing, digestions were carried out on the mutated PCR product and 2 proviruses; HXB2 and

HXB2N^{+}, using SpeI and BssH II restriction enzymes (NEB) at 37^{o}C and 50^{o}C, respectively. The 2 digested vectors and the digested insert were then extracted from the agarose gel using a Qiagen DNA extraction kit. T4 DNA ligase (Fermentas) was then used to ligate the insert into the 2 vectors, at a molar ratio of 3:1 insert: vector, at 16^{o}C overnight in accordance with manufacturer's instructions. This produced 2 new proviral clones. Controls were also set up without the insert to confirm ligation success.

2.2.4 Transformation of *E.coli* and Purification of Bacterial DNA

Products of ligation reactions, or any other plasmid DNA requiring large-scale preparation, were used to transform 50 µl *E.coli* TG1 competent cells (5 µl ligation reaction), or 25 µl One Shot Top 10 F' chemically competent *E.coli* (Invitrogen; 1 µl plasmid DNA). Reactions were incubated on ice for 15 minutes, prior to heat-shock treatment at 42^{o}C for 30 seconds, followed by placing on ice for a further 1 minute. 200 µl SOC (super optimal broth with catabolite repression) broth (ligation) or lysogeny broth (LB) (plasmid preparation) was added to the cells, and these were incubated for one hour at either 37^{o}C (TGI) or 30^{o}C (Top 10). 100 µl of bacterial suspension was plated onto selective LB plates containing ampicillin at 100µg/ml and incubated overnight at the respective temperatures (37^{o}C or 30^{o}C).

2.2.5 DNA Miniprep

Resulting colonies from transformations were grown up overnight in a shaking incubator at 37^{o}C in 2 ml LB supplemented with 100 µg/ml ampicillin. Cultures were then decanted into 1.5 ml sterile eppendorfs and centrifuged at 13,000 RPM for 2 minutes. The supernatant was removed and the DNA was then extracted using reagents from the Plasmid Maxi Kit (Qiagen) as follows; the pellet was resuspended in 100 µl buffer P1, 100 µl P2, and 100 µl P3 (on ice) sequentially following inversion at each

step. Plasmid DNA was then extracted using phenol/chloroform and purified by ethanol precipitation.

2.2.6 Plasmid Maxiprep

For large-scale plasmid preparation, transformed colonies were grown in 2 ml LB supplemented with 100 µg/ml ampicillin (or kanamycin) for 8 hours at 30^{o}C in a shaking incubator. This culture was then transferred into 400ml LB supplemented with 100 µl/ml antibiotic, and grown overnight at 30^{o}C in a shaking incubator. Cultures were then centrifuged at 5,000 RPM for 10 minutes at 4^{o}C using a JA-10 rotor. The supernatant was removed and the plasmid DNA was extracted following the Qiagen Maxi Kit protocol. Resulting DNA was eluted using 400 µl H_2O.

2.2.7 Subcloning

Upon transfection, it was discovered that the ts045-VSV-G-EGFP (VSV-G) had extremely poor expression; only approximately 5% of cells visibly expressed the construct. In order to deduce whether there were any obvious errors in the DNA sequence, the entire insert of the plasmid was sequenced using primers which were designed as follows:

CMV Forward Primer: GTT GAC GCA AAT GGG C

VSV-G/GFP Forward Primer: GAG CGG GGT CTT CCC CAT CTC

GFP Forward Primer: GCG AGA TAC CCA GAT CAT

Following sequencing, it was deduced that a C residue was missing at the beginning of the sequence (before the AUG start site). This could possibly be a missing transcriptional start site, which would explain the poor expression. This missing residue was after the CMV promoter, and before the XhoI site; therefore removal of the insert from the vector was the simplest way to exclude this missing residue. XhoI and BamHI

sites were used to cut the VSV-G insert out of the unidentifiable vector with corresponding restriction enzymes (NEB) and buffers. This was then inserted into pcDNA3.1$^-$ (Invitrogen) using T4 DNA ligase as before. This cloning improved transfection efficiency to around 30%, therefore, 2 µg VSV-G DNA was transfected in each experiment to further increase the number of cells expressing the construct.

2.2.8 siRNA Transfection

In order to significantly reduce the levels of the cellular adaptor proteins, siRNAs directed against AP-1, AP-2, AP-3 and AP-5 were used. Negative control siRNA (#2), which does not have any known mammalian consensus sequences, was also ordered to ensure any effects seen by the above siRNAs are specific and not due to the presence of any siRNA.

siRNAs were transfected into (>85% confluent) seeded HeLa cells in either 6 or 12 well plates, and one of two methods for transfection was adopted; they were transfected 24h prior to proviral transfection, or co-transfected alongside 1 µg/well proviral DNA. 10 nM siRNA (AP-1, -2, -3, -ve) or 25nM (AP-5, -ve) was transfected using Lipofectamine 2000. Samples were harvested either 24 or 40 hours after transfection with the proviral plasmid (either 24 hours after siRNA transfection, or co-transfection with the siRNAs).

2.2.9 Cell Lysate and Viral Supernatant Collection

Viral supernatants from transfected cells were collected using a sterile 2 ml syringe. This was then passed through a 0.22 µm Minisart hydrophilic syringe filter (Sartorius Stedim Biotech) and added to half the volume filter sterilised 30% PEG/0.4 M NaCl solution for overnight precipitation at 4^{o}C. This was then centrifuged (2000 RPM, 4^{o}C, 30 mins) and the supernatant was removed, leaving a small (~0.5 ml) amount. This was

then re-centrifuged, as before, for five minutes. The remaining supernatant was removed and the pellet was re-suspended in 90 µl 1X SDS loading buffer (100 mM Tris/HCl pH 6.8, 4% w/v SDS, 20% glycerol, 0.2% w/v bromophenol Blue, supplemented with 1:20 ratio β-mercaptoethanol on the day).

To collect cell lysates of HeLa cells, cells were washed (after removal of supernatant) with ice cold PBS, and 200 µl/ well 1X Passive Lysis Buffer (Promega) was added, and vigorously shaken for 20 minutes to disturb cells. Lysates were collected and centrifuged at 13,000 RPM for two minutes, and the remaining supernatant was collected for use.

Denaturation of these lysates was carried out by adding 12 µl denaturing solution (125 mM Tris-HCl pH 6.8, 6% SDS, 10% βMe, 20% Glycerol) and boiling at 95^{o}C for 5 minutes, prior to centrifuging as above.

To collect U373 MG lysates, cells were lysed using a lysis buffer as follows: 1 mM EDTA, 1 M Tris-HCL, 1% Triton X-100, 1 mM sodium orthovanadate, 50 mM sodium fluoride, 100 mM sodium pyrophosphate, 0.27M sucrose, 20% sodium azide, 1:500 protease inhibitor cocktail (Fisher). Media was removed and cells were washed as before in ice cold PBS. 150 µl lysis buffer per 60mm was added to cells at 4^{o}C for five minutes. Cells were scraped from the plate and collected, and then left to incubate at 4^{o}C for one hour on a rotating incubator. Cells were then spun as before.

2.2.10 Western Blot Analysis

Unless stated otherwise, all cell samples that were collected were measured for total protein content using the BCA protein assay kit (Thermo Scientific) as directed in the manufacturer's protocol.

Equal amounts of protein as deduced by this method, containing an equal volume of 1X SDS-loading buffer (see above for recipe), were loaded onto a 10% SDS-PAGE gel (supernatant samples were not assayed for protein content and therefore equal volumes of sample were loaded) and run at 35 mA per gel. Gels were then trimmed and soaked in pre-cooled tris/glycine transfer buffer with 20% methanol for 20 minutes. Gels were then sandwiched in a wet transfer tank (Geneflow) with Whatman paper and a pre-soaked Nitrocellulose membrane. A magnetic stirrer was added alongside a gel cool pack, and transfer was carried out on a magnetic stirrer for 2 hours at 400 mA at 4^{o}C.

Membranes were then blocked in 5% Marvel/1 X TBS-T for either 1 hour at room temperature or overnight at 4^{o}C. Antibodies were then added as indicated at the beginning of this chapter, suspended in 5% Marvel/TBS-T either overnight at 4^{o}C or for 1 hour at room temperature. Membranes were then subjected to three 10 minute washes using 1X TBS-T, and secondary antibodies were added using the same method, and incubated for one hour at room temperature. Membranes were then washed again and ECL (enhanced chemiluminescence) Western blotting substrate was used for detection of HRP (Pierce). Densitometry analysis using ImageJ software was used as required.

2.2.11 Confocal Immunofluoresence Microscopy

A Leica SP5 confocal microscope was used with a 60X oil immersion objective. HeLa cells were seeded onto 12 mm glass coverslips within 12 well plates. Cells were transfected with various constructs, as outlined in results chapters. These were then washed with cold PBS and fixed, at 24 hours post transfection (or as indicated in results chapters), using 10% formaldehyde in PBS (Fisher) and permeabilised using 0.5% NP40 in PBS (Sigma). Cells were then blocked with 1% BSA (bovine serum albumin)

for one hour at room temperature. Cells were then labelled with antibodies as indicated in results chapters, followed by Alexa Fluor secondary antibodies (Alexa-488 and Alexa-594) suspended in 1% BSA. Cover slips were inverted and mounted on slides with Vectashield (Vector Laboratories) containing DAPI to stain the nucleus.

2.2.12 Pulse Chase Assays

HeLa cells were seeded into 6 well plates and then transfected with constructs as indicated in results chapters. Cells were then starved in pre-warmed 1.75 ml DMEM minus methionine/cysteine (-met/cys) (Invitrogen) supplemented with 4 mM L-glutamine for 40 minutes, and then pulsed with 0.25 ml of the same media supplemented with 60 µCi/well ^{35}S–Methionine EasyTag promix. Pulse only cells were harvested after 40 minutes. Chase cells were further incubated after the 40 minute pulse with 2 ml fresh complete DMEM for 2 hours after removing the radiolabelled medium.

To harvest cell lysates, radiolabelled medium was removed and cells were washed with ice cold PBS, and harvested using 400 µl/well radio-immunoprecipitation assay (RIPA) buffer (50 mM Tris-HCL, 150 mM NaCl, 0.1% SDS, 0.5% sodium deoxycholate, 1% NP40) supplemented with 1 mM protease inhibitor benzamidine (Fluka), rotating at high speed for 20 minutes to agitate cells. After harvesting, lysates were collected and left on ice for 30 minutes. Supernatants were collected after centrifuging at top speed for 10 minutes, and added to sepharose protein A beads (Sigma) overnight for immunoprecitation (see below).

Final samples were boiled at 95^{o}C for five minutes and loaded onto a 10% SDS-PAGE gel. The gel was then fixed by submerging the gel in a gel fix solution (10% acetic acid, 30% methanol, 60% dH_2O) for 15 minutes. The gel was then dried and protein bands were identified using Hypermax MR film (Kodak).

2.2.13 Immunoprecipitation

Sepharose protein A beads (Sigma) were swelled at room temperature in RIPA buffer for half an hour, followed by three 5 minute room temperature, rotating washes and brief centrifugation at 6,000 RPM for 2 minutes, removal of supernatant and addition of 0.5 ml fresh RIPA buffer. A 50% slurry was then made using RIPA buffer at a 1:3 ratio. 50 µl of this slurry was added to 100 µl fresh RIPA buffer and 2 µl primary antibody (see results sections for further details on antibodies used), which was rotated at 4^{o}C for one hour. Beads were then washed twice in fresh RIPA buffer, by briefly centrifuging at 6,000 RPM for 2 minutes, removing the supernatant and adding 200 µl RIPA and returning to rotation at 4^{o}C for five minutes.

After washing, 100 µl of cleared HeLa lysate was added to the beads (see below), which were placed on a rotating stand at 4^{o}C overnight. Following incubation, beads were washed again as before (2X RIPA washes at 4^{o}C) and after the final wash was removed, 200 µl of pulse/chase sample was added to the beads and rotated again at 4^{o}C for 4-6 hours. After incubation, samples were washed 3 times as before and 40 µl 1X SDS-loading buffer was added to samples prior to boiling and loading on a polyacrylamide gel.

2.2.13i HeLa Lysate Preparation

Confluent T75 flasks of HeLa cells were washed with ice cold PBS and incubated in trypsin to detach cells. Cells were re-suspended in 7 ml fresh DMEM to a total of 10 ml and centrifuged for 5 minutes at 4^{o}C 1500 RPM to pellet cells. The pellet was then washed twice with ice cold PBS and re-suspended in 2 ml ice cold RIPA buffer supplemented with 1 mM protease inhibitor Benzamidine per flask, and incubated on

ice for half an hour. Samples were then centrifuged for 5 minutes at 2500 RPM 4^{o}C to collect the cleared lysate, which was stored at -80^{o}C until use.

2.2.14 Subcellular Fractionation

HeLa cells were seeded into 12 well plates and transfected the following day with constructs as indicated in results sections. Cellular fractions (cytosol, membranes, nucleus and cytoskeleton) were obtained as per instruction in the Qiagen Qproteome Cell Compartment protocol. To reduce the likelihood of previous fractions remaining in the sample and contaminating the next fraction, each fraction was washed with 0.5 ml PBS and rotated at 4^{o}C prior to centrifugation as directed in the manual to remove trace protein, between each stage.

Fractions were run on a 10% SDS-PAGE gel and the transferred membranes were probed either using anti-p24 or anti-AP antibodies.

2.2.15 Cytotoxicity Assays

HeLa cells were transfected into 12 well tissue culture plates with all proviruses individually using Lipofectamine 2000. After 24 hours, cells were re-plated using trypsin incubation, into 96 well plates with fresh media for 16 hours. Decreasing 2-fold dilutions of DTx (diphtheria toxin) or RTx (ricin toxin) (50 ng/µl and 25 ng/µl starting concentrations, respectively) were then added to both transfected cells and mock cells (containing only transfection reagent) in quadruplicate and left for 4 hours. Two untreated lanes (only DMEM) were also included for comparative measures. The media was removed, and cells were then washed with PBS once and 5 µCi/well [^{35}S]-Methionine EasyTag promix in PBS was added to cells, and left for 20 minutes at 37^{o}C. The radiolabelled medium was removed, and un-incorporated [^{35}S] was then removed

by 5x washes with 1% TCA. 100 µl/well scintillant was then added to cells and a scintillation counter was used to measure [^{35}S] incorporation into proteins.

2.2.16 Time Course Assays

HeLa cells were transfected with HXB2 or mock transfected using Lipofectamine 2000 and re-plated into a 96 well plate 24 hours post-transfection as before. A fixed concentration of RTx or DTx (1 µg/ml) was added to wells every 15 minutes across the 96 well plate for 3 hours. To ensure the plate was kept at 37^{0}C at all times, this was carried out on a heat block in between incubations. Cells were then washed with PBS and 5 µCi of [^{35}S]-Methionine EasyTag promix per well was added for 20 minutes. Cells were washed 5 times with 1% TCA, scintillant was added and readings were taken from a scintillation counter as above.

2.2.17 ts045-VSV-G-EGFP Assay

HeLa cells were seeded into 12 well plates with 12 mm glass coverslips and grown overnight. Cells were then transfected with either 2 µg VSV-G DNA alone, or co-transfected with 2 µg VSV-G and 1µg HXB2 HIV-1 or SVRΔNB HIV-2 for 24 hours. Cells were initially placed in a 37^{o}C incubator for 1 hour to improve transfection efficiency, then placed at the restrictive temperature, 39.5^{o}C (see chapter 6.1 for more details), for the remaining 23 hours. After 24 hours, the first time point (t_0) cells were fixed using the same protocol as above for confocal immunofluorescence microscopy. The media on the remaining plates was replaced with pre-warmed (32^{o}C) DMEM supplemented with 5 µg/ml cycloheximide to prevent protein synthesis. Plates were then placed at the permissive temperature, 32^{o}C, until fixing at specified time points (30 mins [t_{30}], 60 mins [t_{60}], 120 mins [t_{120}]). Cells were blocked as before and stained with anti-Nef/Alexa-594 and viewed using confocal microscopy.

2.2.18 Luciferase Assays

HeLa cells were seeded into 12 well plates and grown overnight prior to transfection. The following transfection protocols were adopted; transfection of the AP siRNAs 24h prior to transfection with the RL pcDNA construct (1 µg/well); co-transfection of the siRNAs and the RL pcDNA construct, or transfection of the RL pcDNA 6 hours before transfection with the siRNAs. All samples were harvested 24h after the final transfection using the same method as stated before.

Luciferase assays were carried out using the dual luciferase reporter assay system (Promega) according to the Promega protocol, using equal protein concentrations as dictated by the BCA protein assay.

2.2.19 Lysosome Inhibition

HeLa cells were plated out into 12 well plates and grown overnight at 37^{o}C. When confluent, cells were co-transfected with the HIV-1 HXB2N^{+}, HIV-2 SVRΔNB, MA2 or MA1 proviruses, and the AP siRNAs, including the negative control siRNA. The lysosome enzyme inhibitor ammonium chloride (NH_4Cl) (FSA laboratory supplies) was added to the cell media 24h post-transfection, at a concentration of 10 mM, before harvesting at 40 hours, using the same protocol for cell and supernatant harvesting as stated in chapter 2.2.9. Samples were run on a 10% SDS-PAGE gel and Western blotted using an anti-p24/p27 antibody.

2.2.20 Proteasome Inhibition

HeLa cells were plated out into 12 well plates and grown overnight at 37^{o}C. When confluent, cells were co-transfected with the HIV-1 HXB2N^{+} or HIV-2 SVRΔNB, and the AP siRNAs, including the negative control siRNA. A DMSO only control was also

included. The proteasome inhibitor MG132 (zLLL) (Selleckchem) was added to the cell media 38h post-transfection, at a concentration of 10 µM, dissolved in DMSO, before harvesting at 40 hours (Ortiz-Lazareno et al., 2008), using the same protocol for cell and supernatant harvesting as stated in chapter 2.2.9. MG132 is a peptide aldehyde which blocks the activity of the 26S proteasome complex (Han et al., 2009). Samples were run on a 10% SDS-PAGE gel and Western blotted using an anti-p24/p27 antibody. For pulse chase analysis, the same concentration of MG132 as stated above was added to the media during the starvation period, and again during the pulse and chase period.

In experiments where the HIV protease inhibitor Saquinavir (NIBSC, Dr N Cammack) was used, a stock solution of 1 mM was added to HeLa cells seeded in 12 well plates overnight, during co-transfection of the HXB2 provirus and AP/negative control siRNAs at a final concentration of 1 µM (dose optimised by Emma Anderson, personal communication). Cells were harvested as before and cell lysates were run on an SDS-PAGE gel and analysed by Western blot using an anti p24 antibody. Saquinavir works by binding to and blocking the active site of the viral protease; this was thought to be specific, however, it was discovered that the cellular 20S proteasome cleaves the same sites; therefore, Saquinavir is also an inhibitor of the cellular proteasome (Pajonck et al., 2002).

2.2.21 Total RNA Extraction

HeLa cells were seeded into 6 well plates and transfected with 25 nM AP-5 siRNA or negative control siRNA when sub-confluent, using Lipofectamine 2000. The media was removed, and cells were then washed with ice cold PBS. Qiagen RNeasy mini kit was then used; 350 µl buffer RLT supplemented with β-mercaptoethanol as directed

was applied directly to cells to harvest cells, and RNA was then extracted according to the manufacturers protocol.

2.2.22 cDNA Production and qPCR

High Capacity RNA-to-cDNA Kit (Applied Biosystems) was used to produce cDNA from RNA. 500 ng RNA was used in a final volume of 9 µl in H_2O, plus 10 µl 2X Buffer ABI, 1 µl enzyme mix. This was heated to 37^{o}C for 60 minutes, then 95^{o}C for five minutes.

20 µl reactions were set up for qPCR using the Agilent Mx3005P qPCR system kit, which contained: 10 µl 2X mastermix, 0.3 µl Rox buffer, 0.2 µl forward primer, 0.2 µl reverse primer, 8.3 µl H_2O, 1 µl cDNA. An Agilent qPCR machine was used for the following conditions: 95^{o}C 3 min, 94^{o}C for 30 seconds, then 40 cycles of 60^{o}C for 30 seconds followed by 90^{o}C for 30 seconds.

2.2.23 Preparation of Samples for Electron Microscopy

HeLa/HEK HEK 293T cells were seeded into 60mm tissue culture dishes. Subconfluent cells were transfected using 16.25 µl Lipofectamine 2000 with 6.5 µg DNA in 1600 µl Optimem per plate. After 40 hours, cells were detached using 400 µl trypsin/EDTA per plate, and 5 ml DMEM/FCS was added. Cells were then centrifuged at 1500RPM for 5 minutes at 4^{o}C. The supernatant was discarded, and the pellet was washed twice with PBS, and then re-suspended with 1 ml PBS. Samples were then sent for overnight fixation in glutaraldehyde and staining.

2.2.24 Astrocytoma Vesicle Recycling Visualisation

2.2.24i FM1-43 Staining and Destaining

U373 MG-Uppsala astrocytoma cells (ECACC) were passaged using versene as before, and plated onto glass coverslips inside 6 well tissue culture plates and grown for 2 days at 5% CO_2/37^oC (see 2.2.1 for further details on tissue culture of this cell line). Initial studies involved using only mock transfected cells. In later studies, cells were transfected with constructs as indicated in results chapters (Gag-GFP, GFP or pNL4-3-EGFP) using Lipofectamine 2000, and were left at 37^oC for 24 hours.

Cells were equilibrated in pre-warmed 37^oC PBS for 1 hour, at 37^oC/5% CO_2, to remove serum from cells in order to prevent receptor activation, and prepare for perfusion.

In studies using mock transfected or Gag-GFP transfected cells, cells were first pre-loaded with 2.5 µM FM1-43 (Invitrogen) suspended in PBS for one hour at 37^oC. Coverslips were placed under a Leica 2 photon confocal microscope fitted with a perfusion chamber, and excited at 800-900 nm. Cells, or GFP expressing cells, were selected for analysis and then chambers were perfused with TFLLR-NH_2 (Sigma) for 5-10 minutes, followed by a wash with a hypotonic solution (130 mM NaCl, 3 mM KCl, 1 mM $MgCl_2$, 2.5 mM $CaCl_2$, 1 mM NaH_2PO_4, 22 mM $NaHCO_3$, 15 mM Glucose, pH 7.4).

In studies using GFP and pNL4-3-EGFP transfected cells, cells expressing GFP, were selected for analysis, and the coverslips were then perfused for 10-20 minutes with 5 µM FM1-43 and 10 µM UTP (Sigma). Cells were then perfused a second time with the 5 µM UTP and 10 µM TFLLR-NH_2. After each addition of agonists, cells were washed with a hypotonic solution for 5-10 minutes.

Recordings were analysed using ImageJ, measuring fluorescence intensity versus time in multiple selected regions, correcting for background fluorescence.

2.2.25 Measuring Calcium Waves

U373 MG Astrocytoma cells were passaged using versene and plated onto glass coverslips inside 6 well tissue culture plates and grown for 2 days. Cells were co-transfected with 1 µg SyPhyGCaMP-mCherry plasmid and a 2 µg of a second construct as indicated in results chapters (GFP or pNL4-3-GFP) using Lipofectamine 2000, and were left at 37^{o}C for 24 hours. A lipofectamine only control was also used.

Media was removed from cells and cells were equilibrated in pre-warmed PBS at 37^{o}C for 1 hour prior to use. Slides were placed into the perfusion chamber fitted onto the 2 photon microscope, and excited at 800-900nm. Cells co-expressing GFP and mCherry (pNL4-3-GFP or GFP), or mCherry only (lipofectamine only) were selected for analysis. Lipofectamine only slides were first perfused with Anandamide (500 nM) for 5 minutes, followed by 10 µM TFLLR-NH_2 for five minutes, and 5 µM UTP for 10 minutes. 5-10 minute washes were included between each treatment. GFP or pNL4-3-GFP transfected slides were first perfused with 10 µM TFLLR-NH_2 for 10 minutes, followed by 5 µM UTP for 10 minutes, with 5-10 minute washes in between agonist addition.

Recordings were analysed using ImageJ, measuring fluorescence intensity versus time in multiple selected regions, correcting for background fluorescence.

CHAPTER 3: DOES HIV-1 PROTEIN EXPRESSION ALTER THE LEVELS/LOCALISATION OF THE ADAPTOR PROTEINS?

3.1 Introduction

Previous work has demonstrated that HIV-1 Gag interacts with the adaptor proteins in order to mediate its own trafficking. Various studies using mutations of the adaptor proteins or siRNA knock-outs have suggested an involvement of these adaptor proteins in HIV-1 particle production (Batonick et al., 2005; Dong et al., 2005; Camus et al., 2007; Liu et al., 2012). Studies investigating the interactions between HIV-1 Gag and AP-1 found that reduction in AP-1 expression mediated by an siRNA targeted against the μ subunit of this complex was found to significantly reduce HIV-1 budding and release, delaying viral propagation; however, its overexpression enhanced HIV-1 Gag release. This effect was deduced to be due to a direct interaction with the μ subunit and a defined region of amino acids within the MA domain of Gag. It was postulated that AP-1 directly promotes Gag release by transporting it to intracellular assembly and budding sites that could involve late endosomes (Camus et al., 2007).

AP-2-Gag interactions were also found to occur, again with the MA domain of Gag; Tyr132 of the MA-CA junction was suggested to be part of an YXXΦ motif, which would explain the interaction here. Val135 was also found to be critical in this association. Gag binds specifically to AP-2 μ subunits during late phases of viral replication, and not during early phases, and colocalises with this complex. Mutations of AP-2μ caused opposing effects to mutant AP-1μ, enhancing virus release, suggesting that AP-2 normally has an inhibitory effect on viral particle release (Batonick et al., 2005).

Finally, AP-3 also interacts with Gag. siRNA depletion of AP-3 using siRNAs directed against both the μ and δ subunits in cotransfected cells reduced HIV-1 particle release by approximately 50%. Furthermore, when the experiment was repeated using only an siRNA directed against AP-3δ, and a Gag construct in which MA was deleted, the perturbation of Gag release was not observed (Dong et al., 2005). These results suggested that both the δ subunit of AP-3, and MA of Gag, are critical for this interaction. AP-3 is known to mediate the trafficking of CD63 through interactions between its cytoplasmic tail and the μ subunit of AP-3. CD63 is a component of multivesicular bodies (MVBs). Although the budding of HIV-1 occurs predominantly at the plasma membrane, research has suggested that it may also occur from these intracellular compartments. Following these observations, it was found that Gag colocalises with CD63, suggesting a role of AP-3 in directing Gag molecules to these intracellular budding sites. Specifically, it was suggested that Gag may co-traffic with CD63 to these late endosomal compartments, acquiring essential budding machinery, and then transport this to the PM ready for particle release (Dong et al., 2005).

These studies show that the HIV-1 MA domain is essential for cellular Gag trafficking.

Nef is a 27 kDa peripheral membrane protein which is known for its effects on enhancing viral pathogenicity and also replication. Nef protein also interacts with the cellular sorting machinery in order to influence cellular membrane protein trafficking. Specifically, Nef contains a 30-residue unstructured loop close to the C-terminus of the protein, which contains sequences critical for the interactions with various membrane proteins, such as ATPase. Alongside these, Nef was found to specifically interact with the μ subunit of adaptor protein complexes AP-1, -2 and -3, and colocalises with them extensively. Nef, across all primate lentiviruses, contains a conserved leucine-based motif (consensus sequence EXXXLL) found within this C-terminal region, which is

critical for the interaction with the adaptor protein complexes (Craig et al., 2000; Madrid et al., 2005).

As briefly mentioned in the introduction, HIV-1 Nef is capable of disrupting the trafficking of numerous cellular proteins in order to benefit the virus, such as that of MHC molecules. Recently, it was described that Nef is able to disturb the early/recycling compartment of the cell, and modulating the recycling of the prototypical cell surface receptor the transferrin receptor (TfR) by causing it to accumulate in an endosomal compartment and reducing its cell surface expression (Madrid et al., 2005).

The reported interactions between HIV-1 Gag/Nef and the APs prompted us to investigate whether HIV-1 infection is able to disrupt the normal functioning of these APs, which may have implications in the normal functioning of the cell. This chapter described experiments to determine whether HIV-1 alters the intracellular distribution and levels of these proteins, and if so, whether such disruptions are attributed solely to Gag or Nef, or interplay between both proteins.

3.2 Results

3.2.1 Producing Mutant Proviral Plasmids

In order to investigate whether HIV-1 Gag or Nef affect the levels of the adaptor proteins within the cell, we generated proviral plasmids (plasmids encoding proviral DNA will hereon be termed proviruses) which when used to transfect cells, make full length or truncated Gag or Nef proteins. Our parental HIV-1 proviral strain is the commonly used HXB2, which contains a premature stop codon in the 3' end of the *nef* gene; the truncated Nef produced is missing the AP binding sites. Although this HXB2

provirus is useful in deducing whether Gag alone can affect AP function, it was necessary to generate a provirus which produces full length Nef for comparative means. Therefore, the premature stop codon within *nef* was mutated to generate a provirus capable of producing full length, functional Nef; this was termed HXB2N$^+$ (work carried out by Emma Anderson). Western blotting of lysates from HeLa cells transfected with HXB2 or HXB2N$^+$ was carried out with an anti-HIV-1 Nef antibody, which recognises a C-terminal epitope of Nef (see Figure 24A). These results demonstrated that HXB2N$^+$, but not HXB2, expresses full length Nef.

Two other proviruses were subsequently generated to investigate the effects of the absence of Gag; the *gag* start codon was mutated in the two aforementioned proviruses, preventing production of Gag. These two proviruses were coined HXB2ΔGag and HXB2N$^+$ΔGag. In order to ascertain whether these proviruses were unable to produce Gag, HeLa cells were transfected with HXB2 proviruses, the Gag deleted proviruses and a control provirus; HVPΔEC PuroΔB lacking Gag and Nef (Richardson et al., 1993). HeLa cells were selected because HeLa cells were used in original papers investigating HIV-1/AP interactions (Dong et al., 2005; Batonick et al., 2005; Camus et al., 2007). The use of an antibody directed against the CA (p24) region of Gag allows detection of full-length Gag (p55), processing intermediates (p41[MA-CA]/p40[CA, NC, p6]) and fully processed CA (p24); incompletely processed CA (p25) is also detected, which is why we see two CA bands (see Figure 24B). The weaker band present between p55 and p41 is likely the result of initiation from a CUG codon that encodes leucine at amino acid 61; initiating at this codon would give a resultant protein of 48.5 kDa, which is the same size as the band observed in this blot (Emma Anderson, personal communication).

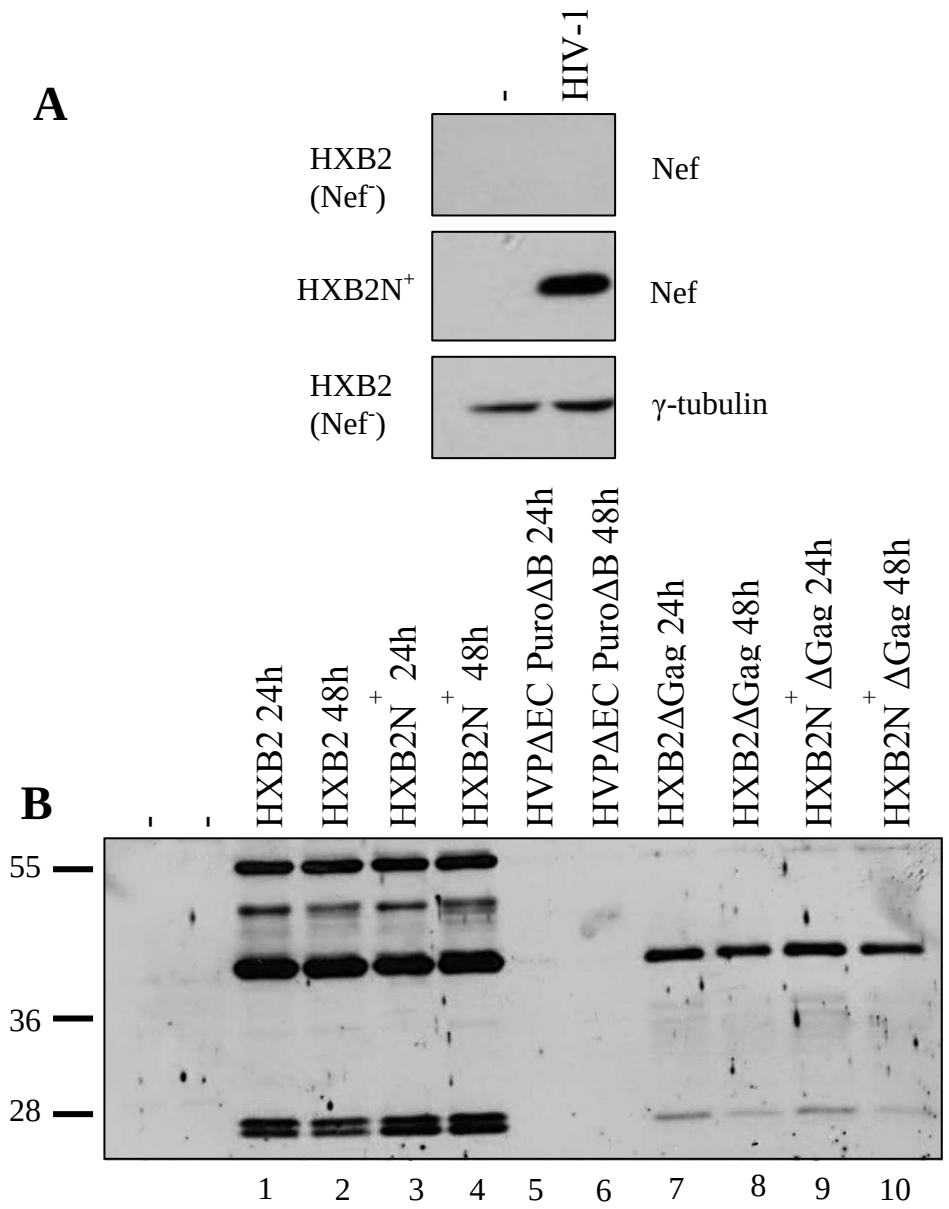

Figure 24: Gag mutant proviruses produce full-length Nef, but not full-length Gag. A- HXB2 (top panel) and HXB2N$^+$ (middle panel) proviruses were transfected into HeLa cells, and lysates were harvested 24 hours post transfection. These samples were analysed by western blot following SDS-PAGE, using an anti-Nef antibody. B- Full-length Gag (HXB2, HXB2N$^+$) and Gag deleted (HXB2ΔGag, HXB2N$^+$ΔGag, HVPΔEC PuroΔB) proviruses were transfected into HeLa cells, and lysates were harvested at 24 and 48 hours post transfection. These were then analysed by western blot following SDS-PAGE, using antibodies directed against p24 Gag (CA). Left 4 lanes; top band p55, second band likely results from initiation at a CUG codon, third band p41 MA-CA, bottom band p24 CA. Right 4 lanes; top band p40 CA-p6, bottom bands (p25 and) p24 CA. (-) lanes show mock (Lipofectamine only) samples. Western blots are representatives of 2 repeats.

Western blots of lysates, shown in Figure 24B, demonstrate that the mutants do not produce full length p55 Gag, and produce a severely depleted amount of fully processed Gag (p24 CA). They do, however, produce p40, which is not found in the Gag^+ strains (Figure 24B, lanes 7-10). This is likely produced from an internal initiation codon present within the capsid region of *gag*, which may be used in the absence of the correct initiation codon. This produces a protein containing CA, NC and p6, as opposed to the partially processed p41 (MA and CA) seen in Gag^+ strains. The blot also demonstrated an increased amount of p24 when full-length Nef was present in the HXB2 proviral strain; this supports the role for Nef in facilitating efficient viral replication. Since the AP binding sites were found to be present within MA, this mutant was sufficient to be used in subsequent experiments.

3.2.2 HIV Does Not Affect Total AP Levels, or AP Turnover

Since the APs play pivotal roles in the HIV life cycle, the effect of HIV on the expression and turnover of these proteins was investigated initially in HeLa cells.

To ascertain whether HIV-1 alters total AP protein levels within the cell, we used Western blotting of cell lysates harvested after proviral transfection. HXB2, $HXB2N^+$ and the respective Gag-deleted proviruses were used to transfect HeLa cells for either 24h or 48h. A Gag-GFP expression construct and pcDNA-GFP were also used. Different proviruses were used to give an indication of whether any observed differences in steady state levels of the APs could be potentially attributable to the presence/absence of a particular viral component, such as Gag or Nef. AP-1, AP-2, AP-3 and γ-tubulin in the cell lysates were detected with antibodies against AP-1γ, AP-2μ, AP-3δ subunits or γ-tubulin. The results from one of three repeat experiments are shown in Figure 25A.

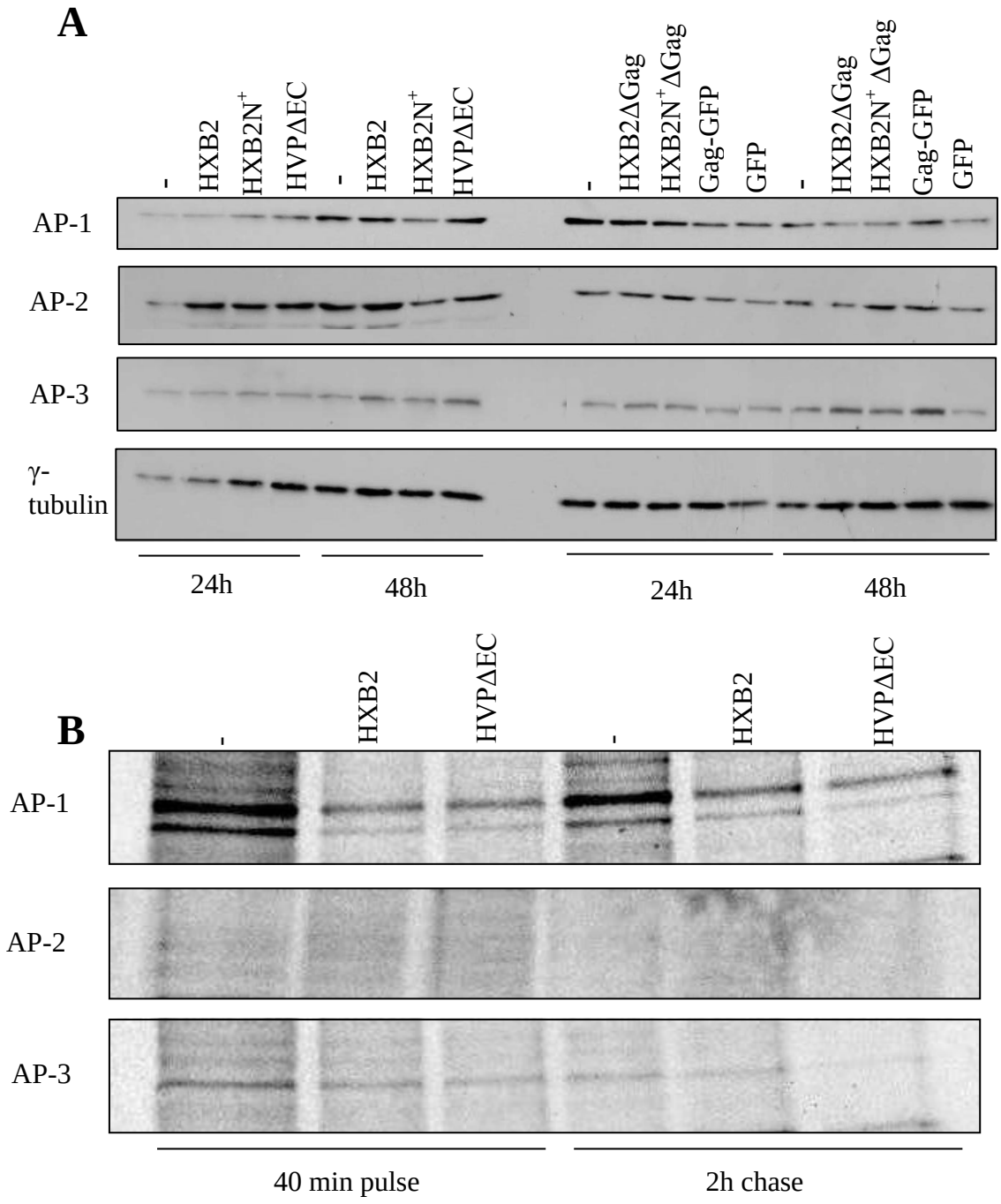

Figure 25: HIV does not affect total AP levels or turnover. A- Western blot of the APs using anti AP-1γ, -2μ and -3δ antibodies on cell lysates harvested from different HIV-1 provirus transfected HeLa cells. γ-tubulin shows endogenous proteins levels. B- Pulse chase of the APs following a 24h transfection of HeLa cells with proviral plasmids. Anti AP-1γ, -2μ and -3δ antibodies were used for immunoprecipitation. (-) lanes show mock (Lipofectamine only) samples.

Across the three repeat experiments, when compared with γ-tubulin levels, there were no consistent changes in AP levels with any of the proviral transfected cells relative to mock transfected cells.

Next, new AP synthesis and any turnover was investigated using metabolic labelling and immunoprecipitation in a pulse chase assay. This technique involved radiolabelling all proteins synthesised within transfected cells in a 40 minute "pulse" period by providing medium containing radiolabelled methionine and cysteine. Cells were then washed and provided with complete "cold" medium (without labelled methionine and cysteine) for a 2 hour "chase" period. These two stages allowed visualisation of total protein produced within the defined pulse period, and the fate of these proteins during the chase period.

Proteins were visualised following immunoprecipitation (IP), in this case with antibodies against AP-1γ, AP-2μ or AP-3δ. HXB2 was used in this experiment, alongside HVPΔEC PuroΔB as a control, which were used to transfect HeLa cells for 24 hours prior to pulse chase. A mock (Lipofectamine) only sample was also used as a negative control (-). Results of a representative experiment are shown in Figure 25B.

Many more protein bands (background) were observed in comparison to Western blot of the APs, which indicates insufficient blocking during the IP. AP-2 could not be detected via immunoprecipitation; therefore this assay was unsuitable for investigating AP-2 turnover. AP-3 showed little protein synthesis, making it difficult to interpret any turnover in the presence of HXB2, or the control provirus. Although there was a substantial decrease in synthesised AP-1 in the presence of HXB2, the same was seen for the control provirus which does not contain AP binding sites. It was also clear that far more total protein had been synthesised in the mock-transfected cells. It was therefore difficult to ascertain whether the slight decrease in newly made AP-1

observed in transfected cells was due to an interaction with HIV-1, or merely the result of cellular toxicity, which in turn caused less AP-1 to be synthesised in the 40 minute pulse following the 24 hour transfection. In an attempt to account for general cellular toxicity, densitometry of a background band on the autoradiograph was used to correct for differences in protein loading. This revealed that there were no specific differences in AP-1 synthesis in the presence of HIV-1 (data not shown). The similarity in the AP-1 levels between the pulse and chase samples suggested that the presence of HIV-1 did not affect AP-1 turnover, at least during the time course of this experiment.

3.2.3 The APs are not Incorporated into Viral Particles

Recently, it was discovered that HIV actively incorporated clathrin into viral particles (Zhang et al., 2011). This is in contrary to earlier beliefs that it is passively incorporated into virions following particle release which takes with it a small portion of the plasma membrane. Since the adaptor proteins bind clathrin and Gag, the possibility of HIV-1 also incorporating the APs into viral particles alongside clathrin was contemplated.

HeLa cells were transfected with HXB2 provirus, and cell lysates and released virions (supernatants) were harvested. Since we were primarily interested in supernatant samples, cell lysates were directly loaded onto an SDS-PAGE gel without prior equalisation with the BCA protein assay. All samples were analysed by Western blot for both Gag and the APs, and the results are shown in Figure 26.

Here, we can see that Gag was detected in both cell lysates and in released viral particles within the supernatant (processed Gag p41 [top band] and p24 [bottom band] only), whereas the APs could only be detected in cell lysates. Therefore, it can be concluded that the APs are not incorporated into viral particles. Although the APs bind

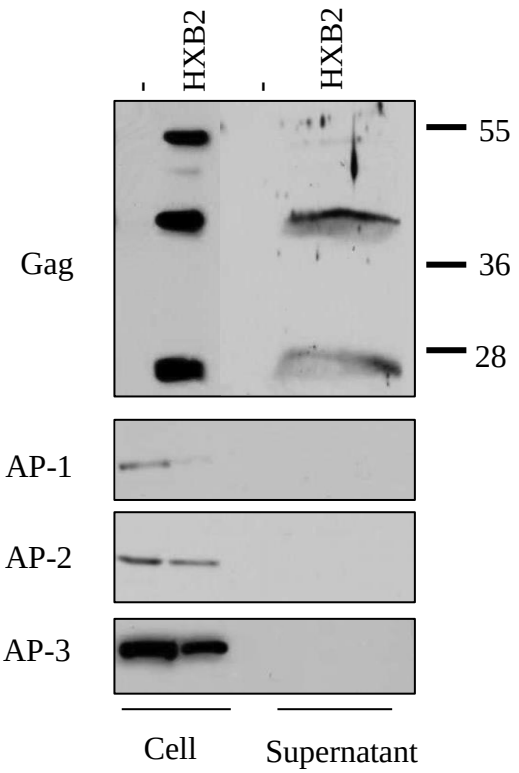

Figure 26: The APs are not incorporated into viral particles. Western blots of cell lysates and released particles (viral supernatants) harvested from HIV-1 HXB2 transfected HeLa cells at 48 hours post transfection. Membranes were probed for p24 Gag (top panel) and the APs using anti AP-1γ, -2μ and -3δ antibodies (bottom 3 panels). (-) lanes show mock (Lipofectamine only) samples.

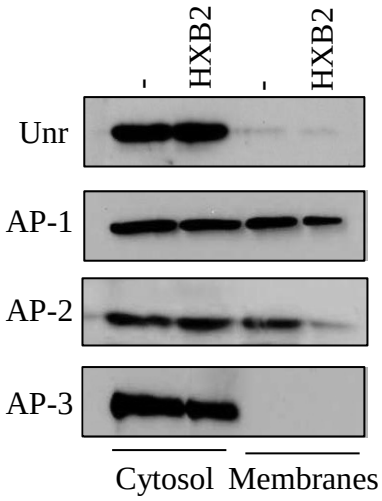

Figure 27: Subcellular Fractionation of the adaptor proteins in HIV-1 transfected cells. HeLa cells were transfected with HXB2 HIV-1 provirus, and fractions were collected using a Qiagen Q Proteome Cell Compartment kit protocol. A negative (-) Lipofectamine only control was also used. These were resolved by SDS-PAGE and analysed by western blotting for the APs and the cytosolic Unr protein as a control for endogenous protein levels.

clathrin, this may indicate that they dissociate prior to particle release. Since clathrin is actively, not passively, incorporated into virions in order to assist particle formation and infectivity, it is therefore likely that the APs have no further role in the HIV life cycle post particle egress and therefore are not required for incorporation.

3.2.4 Does HIV Alter the Intracellular Localisation of the APs?

3.2.4i Subcellular Fractionation

During the infection process, newly synthesised viral components will need to be trafficked to distant assembly sites, requiring a constant flow of the APs if they are involved in this trafficking. It was therefore postulated that HIV protein expression may re-localise the APs as a result of this. The first assay to be used was a biochemical assay, followed up by confocal immunofluorescence microscopy.

Subcellular fractionation of HeLa cells transfected with HXB2 was carried out using the Qiagen Q Proteome Cell Compartment kit. Cytosolic and membrane-bound fractions were analysed by Western blotting using antibodies directed against the APs. Results are shown in Figure 27.

This data showed that no significant differences in the intracellular location of AP-1 or AP-3 were observed in HeLa cells transfected with HXB2 compared to mock-transfected cells (-). No differences in cytosolic AP-2 were found; however, a decrease in membrane-associated AP-2 could be seen. AP-2 is known to interact with HIV-1 Gag and Nef, which may result in less membrane-bound AP-2, although no corresponding increase in cytosolic AP-2 was observed. A problem with this assay was that the fractions were not compatible with the BCA protein quantification assay. Although a control antibody against the cytosolic protein Unr (upstream of N-ras), a cytoplasmic RNA binding protein, was used to demonstrate both successful

fractionation and equal loading, this protein was not found in the membrane fraction. A control membrane protein was not available to test whether the fractionation was clean at the level of soluble versus membrane proteins, therefore, the possibility that the difference in AP-2 levels in the membrane fraction is merely a result of unequal loading cannot be excluded.

3.2.4ii Confocal Immunofluorescence Microscopy

Although subcellular fractionation allows investigation of total protein content within different compartments of the cell, it is quite a crude experiment in that it does not show whether, for example, proteins are being directed from one membrane to another. Therefore, this assay is limited in telling the full story. In order to investigate the cellular location of the adaptor proteins further, confocal immunofluorescence microscopy of transfected HeLa cells was carried out in order to observe any potential differences in AP localisation in the presence of HIV-1. This method would also give insights as to whether HIV-1 colocalises with the adaptor proteins. Preliminary experiments optimised staining of HIV-1 Gag using an anti-p24 antibody, HIV-1 Nef, AP-1γ, AP-3δ, but AP-2 could not be detected in immunofluorescence experiments. Subsequently, co-staining of cells for HIV-1 Gag or Nef, and AP-1 or AP-3 was carried out. The results are shown in Figure 28.

HIV-1 Gag (p24) was seen throughout the cytoplasm, as was AP-3 (Figure 28C). There was a small amount of colocalisation between Gag and AP-3, demonstrated by yellowing areas where pixels overlap. In order to quantify this colocalisation, ImageJ was used to calculate Pearson's Correlation Coefficient (Rr), which was found to be an average of 0.206 across 3 repeat experiments. Cut off values for this coefficient are considered as follows; 0-0.1 no colocalisation, 0.1-0.3 low colocalisation, 0.3-0.5

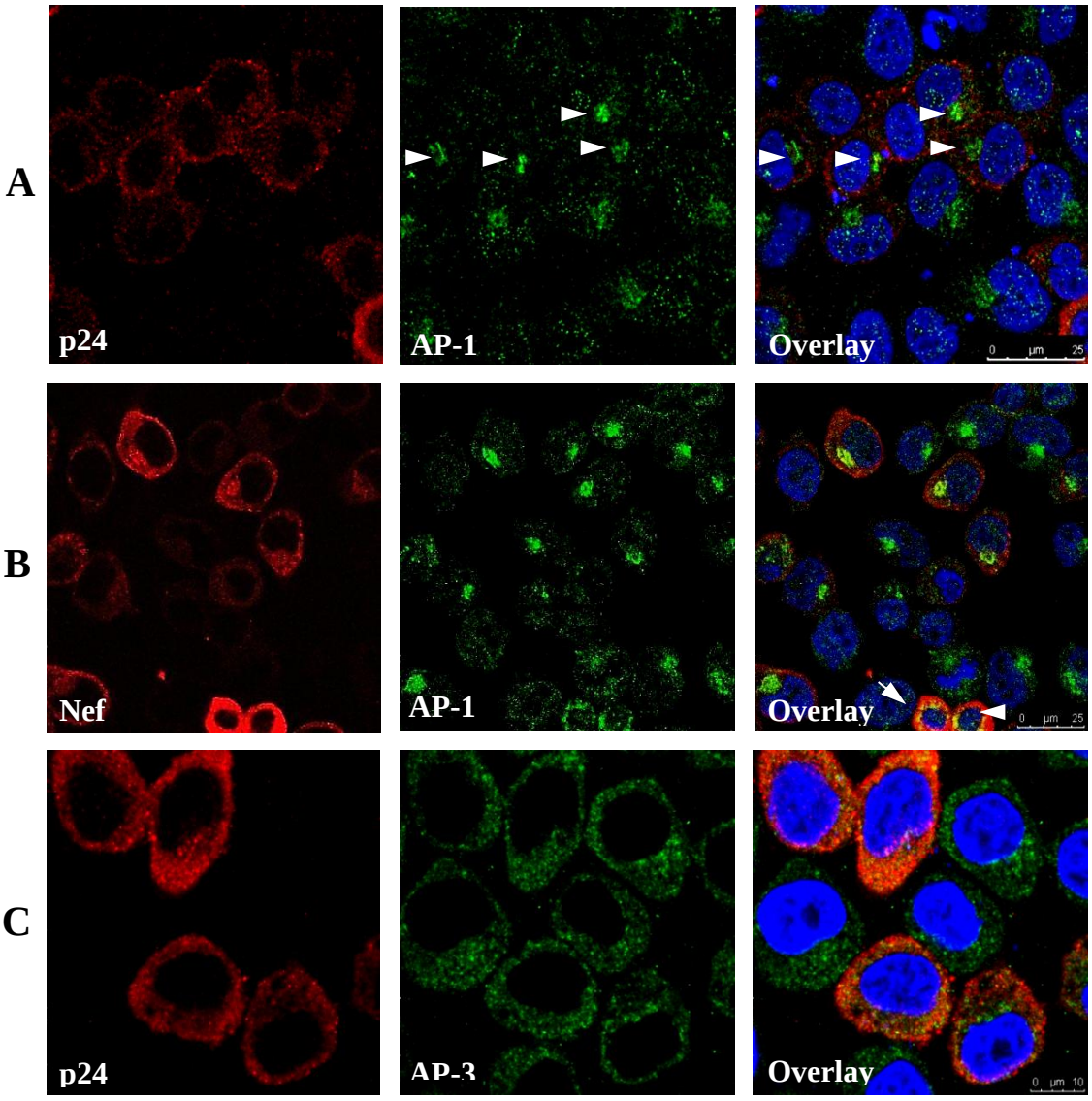

Figure 28: HIV-1 alters the intracellular localisation of AP-1. Confocal immunofluorescence microscopy images of HIV-1 transfected HeLa cells co-stained for p24/Nef and AP-1γ/-3δ. A- Cells transfected with HIV-1 HXB2 provirus, stained with anti-Gag p24 (red) and anti-AP-1γ (green). White arrows indicate changes in AP-1 localisation in HIV Gag expressing cells. B- HXB2N^{+}ΔGag transfected HeLa cells, co-stained with anti-Nef (red) and anti-AP-1γ (green). Some colocalisation could be seen, as shown by white arrows. C- Cells transfected with HXB2 and co-stained with anti-Gag p24 (red) and anti-AP-3δ (green). Colocalisation across independent repeat experiments was calculated by Pearson's Correlation Coefficient using ImageJ (Rr=0.206), which was deduced to be low.

moderate colocalisation, 0.5-1.0 high colocalisation. No obvious re-distribution of AP-3 in cells expressing HIV-1 Gag could be observed.

The opposite could be seen for AP-1; HIV-1 Gag did not colocalise with AP-1, but AP-1 did show a somewhat altered localisation (Figure 28A). In HXB2 transfected cells, AP-1 appeared in a tighter juxtanuclear position as compared to untransfected cells in the same field shown. In order to investigate whether this effect was mediated by Gag, the HXB2N^{+}ΔGag provirus was used to transfect HeLa cells (Figure 28B) and staining of Nef and AP-1 analysed. Although less obvious differences between transfected and un-transfected cells in the same field were observed, all cells in this experiment seemed to have tight juxtanuclear AP-1 staining, in contrast to the experiment described above whereby un-transfected cells displayed a more diffuse juxtanuclear AP-1 staining. However, some cells did show colocalisation between Nef and AP-1 in juxtanuclear regions, as indicated by the white arrows, which supports the current literature described on these protein interactions (Craig et al., 2000; Roeth et al., 2004; Lubben et al., 2007).

3.3 Discussion

Although the interactions between HIV-1 and the adaptor proteins have been researched recently, these studies did not to characterise the effects that HIV has on the functioning of the APs; namely, their levels and localisation. This chapter aimed to fill in gaps of current research and shed light on the consequences of HIV-1 infection on the APs.

The first aim of this chapter was to investigate whether, as a consequence of HIV-1 infection, expression or turnover of the APs was altered. It was that diversion of the APs from their normal cellular functions by HIV-1 Gag and/or Nef may result in their

increased turnover, or possibly increased expression of the APs via homeostatic mechanisms.

Western blot analysis of cell lysates collected in the presence of various HIV-1 proviruses demonstrated that the total levels of the APs were unaltered under these conditions.

Although no change in total protein levels was found, a simple Western blot cannot provide information on what happens to the APs over defined periods of time. This is where pulse chase analysis is particularly useful, allowing information to be divulged on protein synthesis and turnover. Since HIV will be constantly and rapidly producing progeny viral proteins which all require the APs to traffic to assembly sites, it may be that a consequence of HIV-1 infection is a transient up or down-regulation of AP expression or turnover. Pulse chase analysis, however, failed to demonstrate this for AP-1 and -3. AP-2 was unable to be investigated since the antibody was not suitable for immunoprecipitation. We can therefore conclude that despite the strains imposed on the AP trafficking pathway by HIV protein expression, the host cell does not up-regulate AP-1 or -3 expression in order to ensure normal functioning of these pathways.

It has been demonstrated that HIV-1 actively incorporates clathrin into particles (Zhang et al., 2011). Since the APs bind clathrin alongside cargo, it was postulated that the APs may also be incorporated into particles. Analysis of viral particles through Western blot of collected viral supernatants, however, could not find evidence of any presence of the APs. This could be for several reasons. Firstly, since clathrin is actively recruited into viral particles to assist virion morphogenesis, it may be that HIV does not require the APs post viral egress and therefore has no reason to actively incorporate them into assembling virions. Second, it may be that the APs dissociate from clathrin prior to its incorporation into virions. It may well also be that very small amounts of the APs are

incorporated, for example AP-2 which would be present in the plasma membrane from which HIV buds, but that they are in too small quantities to be detected by Western blot. More sensitive methods, for example mass spectrometry, may shed more light on this.

Finally, the ability of HIV-1 to alter the cellular location of the APs was investigated using two different techniques; a biochemical assay, and immunofluorescence microscopy. Although subcellular fractionation is a crude assay, it can divulge information on whether proteins are shifted from one total fraction to another, i.e. from membranes to the cytosol or vice versa. Subcellular fractionation here, however, could not provide any evidence for any change in the localisation of AP-1 or -3. A small decrease in membrane associated AP-2 was observed. Since a protein assay was not compatible with this kit, equal amounts of protein could not be loaded onto gels for investigation. Therefore, the possibility that this is a result of unequal loading cannot be excluded. If this is a real effect, it may be a result of HIV-1 Nef recruiting AP-2 for internalisation CD4 molecules (Chaudhuri et al., 2007).

More information was gained from confocal immunofluorescence microscopy with regards to AP-1 and -3 localisation in the presence of HIV-1. Although the interactions between HIV-1 and these APs have been described, the intracellular localisation of these with respect to Gag has not been investigated, although studies have elucidated distributions with respect to various endosomal/Golgi markers (Liu et al., 2012). Colocalisation between Gag and AP-1 could not be observed, as Gag and AP-1 appeared to have very separate intracellular locations, which was surprising since AP-1 facilitates Gag trafficking. AP-1 was observed in a tight juxtanuclear location, whereas Gag was diffuse throughout the cytoplasm or at the plasma membrane. What could be seen, however, was that in the presence of HIV-1, AP-1 staining appeared more

condensed than in un-transfected cells within the same field. When compared with a Gag-deleted mutant (Figure 28B), the differences in AP-1 staining between Gag expressing and non-Gag expressing cells within the same field were not as obvious, which could suggest a Gag mediated effect. It may be that through disrupting the AP-1 trafficking pathway, the trans-Golgi network becomes compromised, resulting in an altered appearance of this compartment. This in turn may have other effects on the cell, indirectly affecting the trafficking of host cellular proteins.

With regards to AP-3, little colocalisation between Gag and AP-3 could be observed. Conflicting results have been obtained as to whether HIV-1 Gag can directly bind AP-3δ. Data collected by Dong et al., (2005) showed a direct interaction, whereas later data collected in 2012 by Kyere at al., in a different cell line suggest that there is no direct interaction. This may explain why limited colocalisation can be seen. Alternatively, this data may also support the fact that we do not see AP-3 in the supernatant samples; interactions with AP-3 may be transient.

3.4 Future Work

One limitation of this section was that a suitable AP-2 antibody for immunoprecipitation and immunofluorescence microscopy was not available. Future experiments should consider utilising a more appropriate antibody that can fill in the gaps in this chapter.

Another crucial set of experiments to be considered are further confocal immunofluorescence studies. This is because, although results gathered in this chapter suggest that AP-1 is relocalised in the presence of HIV-1 Gag, the area which AP-1 is relocalised to was not investigated. Therefore, appropriate studies may include the use of TGN markers, such as TGN38 (Bos et al., 1993), which could indicate whether more

AP-1 is present in the TGN area in the presence of HIV-1 Gag, as compared with cells not expressing Gag.

CHAPTER 4: DO THE ADAPTOR PROTEINS AFFECT HIV-1 GENE EXPRESSION?

4.1 Introduction

The clathrin adaptor proteins play pivotal roles in cargo trafficking within the cell. They function in various different well characterised pathways, including clathrin mediated endocytosis (AP-2), and secretory/endocytic pathways (AP-1/-3). HIV has evolved ways to utilise these proteins in order to assist the viral life cycle. The interactions of HIV-1 Gag, Nef and Env with these adaptor proteins have recently been characterised, indicating roles within the later stages of the life cycle. Specifically, AP-1 and -3 facilitate particle release (Dong et al., 2005; Camus et al., 2007), whereas AP-2 inhibits particle release (Batonick et al., 2005). Much still, however, remains unknown about their precise involvement within the viral life cycle.

Previous results gathered in this lab indicated a role for AP-1 in HIV-1 Gag expression; siRNA mediated knockdown of AP-1 was found to reduce protein expression from a transfected viral plasmid (Gemma Watkins, personal communication). This opened up the possibility that a role for the adaptor proteins in protein synthesis or turnover had been overlooked, suggesting a potential role for these adaptor proteins in other stages of the viral life cycle besides viral egress.

This chapter describes work carried out to investigate the role of the clathrin adaptor proteins -1, -2 and -3 in earlier stages of the viral life cycle through characterising effects mediated by siRNA knockdown of these proteins.

4.2 Results

4.2.1 siRNA Knockdown of AP-1 or AP-3 Prior to Proviral Transfection Reduces HIV-1 Protein Expression, but not Endogenous Protein Expression

In order to deduce whether our custom designed siRNAs against the gamma subunit of AP-1, the mu subunit of AP-3, and the delta subunit of AP-3, achieved a significant and specific reduction of the APs, Western blots and confocal microscopy were performed on siRNA treated HeLa cells. Figure 29A shows Western blots of 24h HeLa cell lysates collected in the presence of the same siRNAs, including AP-2. A negative control siRNA was included to ensure specificity of the siRNAs. Samples were compared to siRNA untreated cells. As can be seen, these siRNAs cause efficient and specific (knockdown not observed in negative control siRNA samples) knockdown of these adaptor proteins over 40 hours. Figure 29B shows confocal immunofluorescence images of the adaptor proteins with and without siRNA treatment, using antibodies directed against the APs. As can be seen in Figure 29Bi and ii, AP-1 presents a diffuse staining throughout the cytoplasm, coupled with strong juxtanuclear Golgi staining, and AP-3 presents a combination of diffuse and punctuate cytoplasmic staining. Punctae may represent endosomal compartments, but without colocalisation studies it is not possible to identify them. Figure 29Biii and iv demonstrate 40h siRNA mediated knockdown of AP-1 and AP-3, respectively. Quantification of the average number of cells which did not appear to express these proteins by counting fluorescent cells in siRNA treated samples across multiple fields of cells deduced these siRNAs to reduce expression in >90% of cells (data not shown). AP-2 was found unsuitable for immunofluorescence, as staining appeared highly non-specific due to showing the same level of fluorescence in extracellular areas as within cells, therefore true staining could

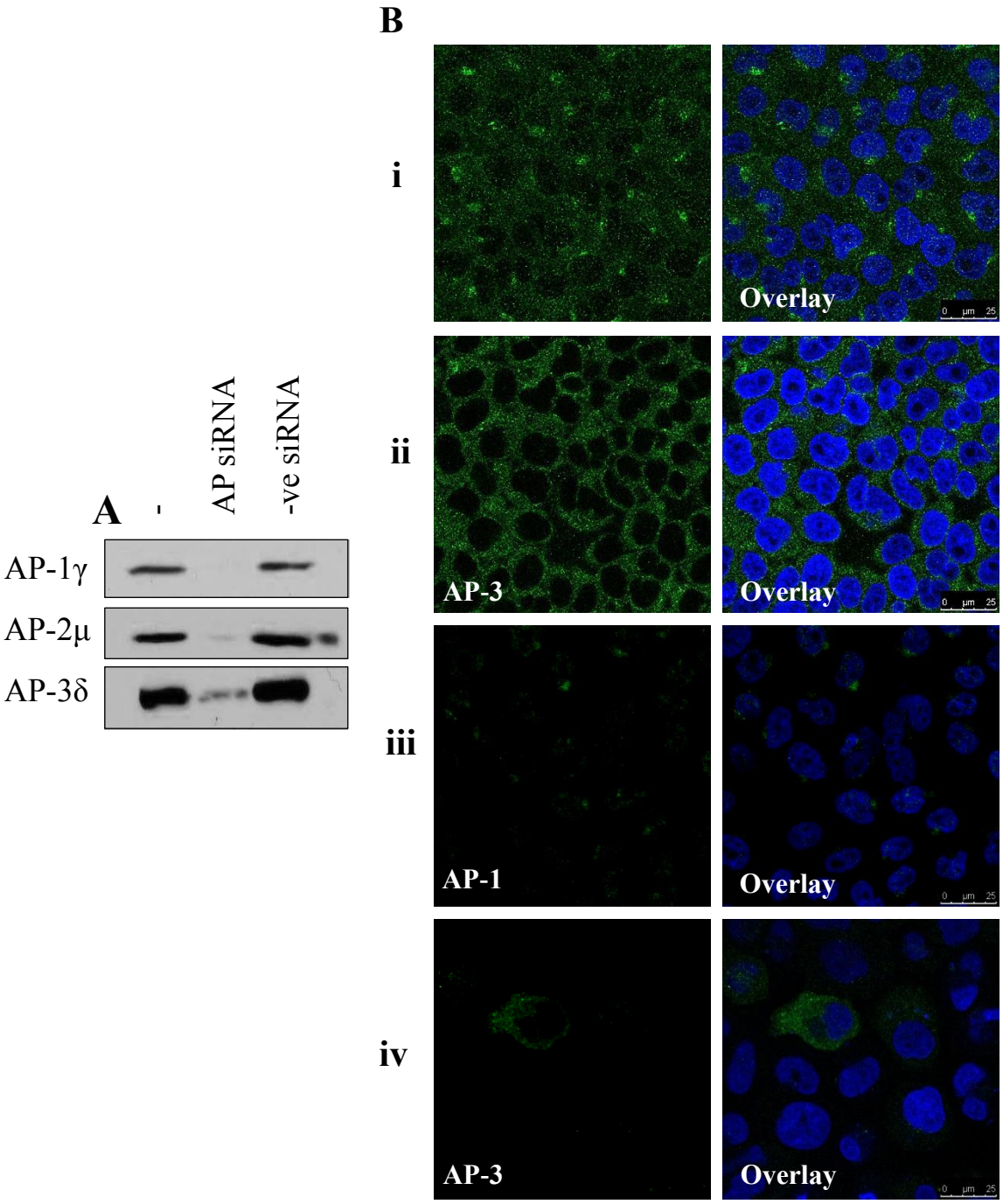

Figure 29: siRNA mediated knockdown of APs. A- Western blot of HeLa cell lysates treated with no siRNA (-), an siRNA against AP-1γ, AP-2μ, AP-3δ (AP siRNA) or a negative control siRNA (-ve siRNA), using antibodies against AP-1γ, AP-2μ or AP-3δ. B- Confocal immunofluorescence microscopy of HeLa cells using antibodies against AP-1γ (i and iii) and AP-3δ (ii and iv) in the absence of siRNAs (I and ii) or after treatment with siRNAs against AP-1γ (iii) or AP-3δ (iv). Blue stain=DAPI (included in overlay of individual channels).

not be deduced from background despite attempting numerous concentrations of antibody (data not shown).

In order to investigate the effects of reducing the adaptor proteins on HIV-1 Gag expression, siRNAs directed against AP-1, -2 and -3 were transfected into HeLa cells 24 hours prior to HIV-1 proviral transfection, in order to achieve a significant reduction in these proteins. Cells were harvested 24 h and 48 h post proviral transfection, and samples analysed by Western blot using antibodies directed against HIV-1 p24 and γ-tubulin. Figure 30A shows representative blot, revealing a reduction in the level of full length Gag protein (p55), the processing intermediate MA-CA (p41), and fully processed CA (p24) at both 24h and 48h in the presence of AP-1 and -3 siRNAs, but endogenous protein levels remained the same as shown by γ-tubulin levels. AP-2 siRNA and the negative control siRNA were found to have no effect on Gag levels. Densitometry was used to quantify autoradiograph bands corresponding to p55, p41 and p24 from 3 independent experiments, and the results are shown in Figure 30B. Student's t-test deduced Gag to be significantly lower in the presence of AP-1 and AP-3 siRNAs, but not AP-2 ($p>0.05$), as shown by asterisks.

In order to visualise this effect, HeLa cells plated onto coverslips were again siRNA treated 24h prior to HIV-1 proviral transfection, and 24h later were fixed, permeabilised and stained for the adaptor proteins and Gag p24. These slides were then analysed by confocal immunofluorescence microscopy. Figure 31 demonstrates a significant reduction in p24 expressing cells in the presence of AP-1 and AP-3 siRNAs, but not the negative control siRNA. In order to quantify this data, five randomly selected fields of cells were chosen, and cells expressing p24 were counted. This was repeated across three independent experiments. Figure 32 shows these results graphically; there was a clear reduction in Gag expressing cells in the presence of AP-1

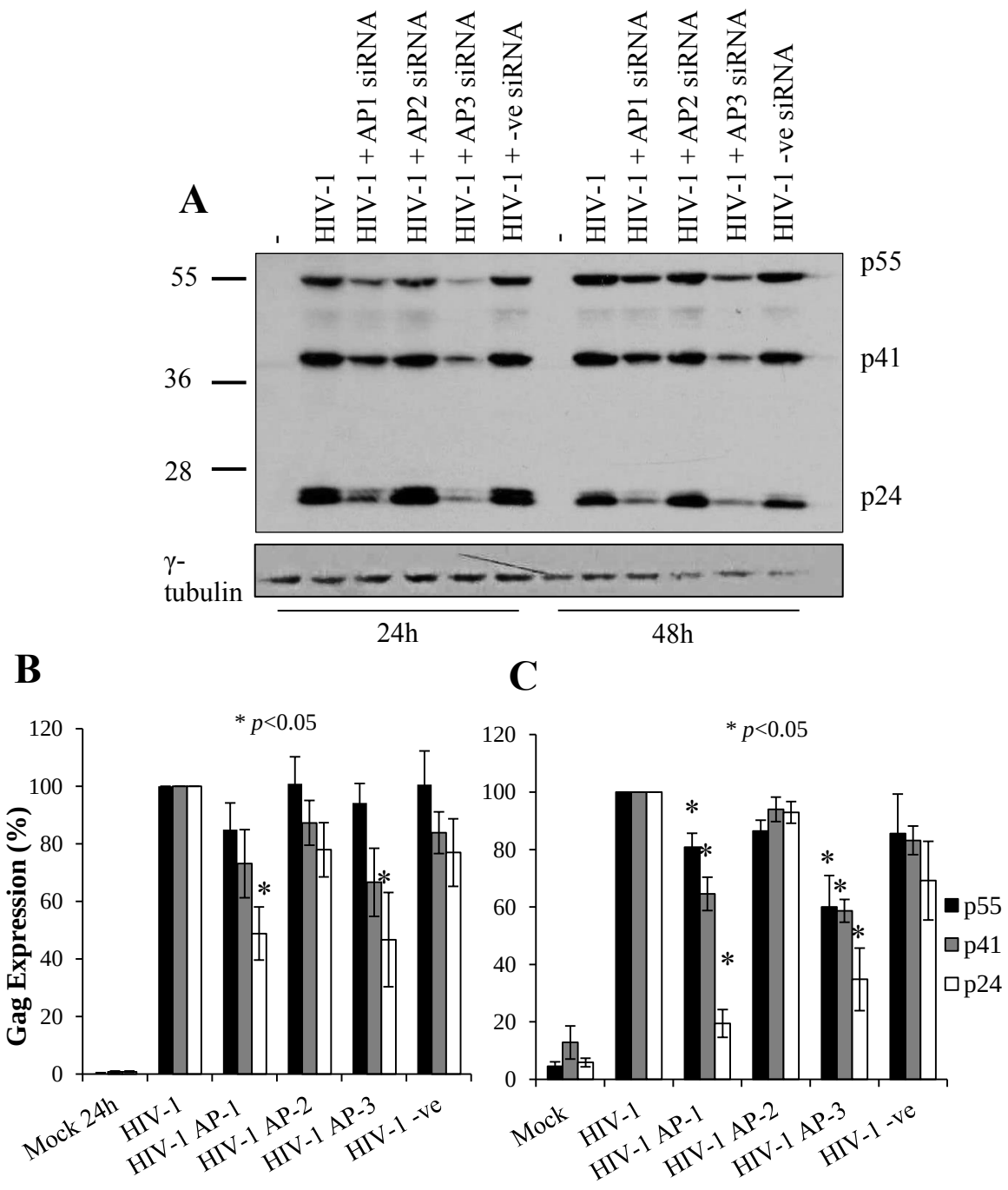

Figure 30: HIV-1 Gag expression in HeLa cells after siRNA treatment. A- Western blot analysis of cellular HIV-1 Gag with and without AP/control siRNAs at 24 and 48 hours. The same lysates were probed with γ-tubulin antibody to ensure loading was equal. Densitometry was carried out across 3 independent repeat experiments using ImageJ, with numbers expressed as percentages of no siRNA treated samples (B and C). B shows 24 hour Gag expression, C shows 48 hour Gag expression. Statistically significant (p<0.05) values are indicated with asterisks.

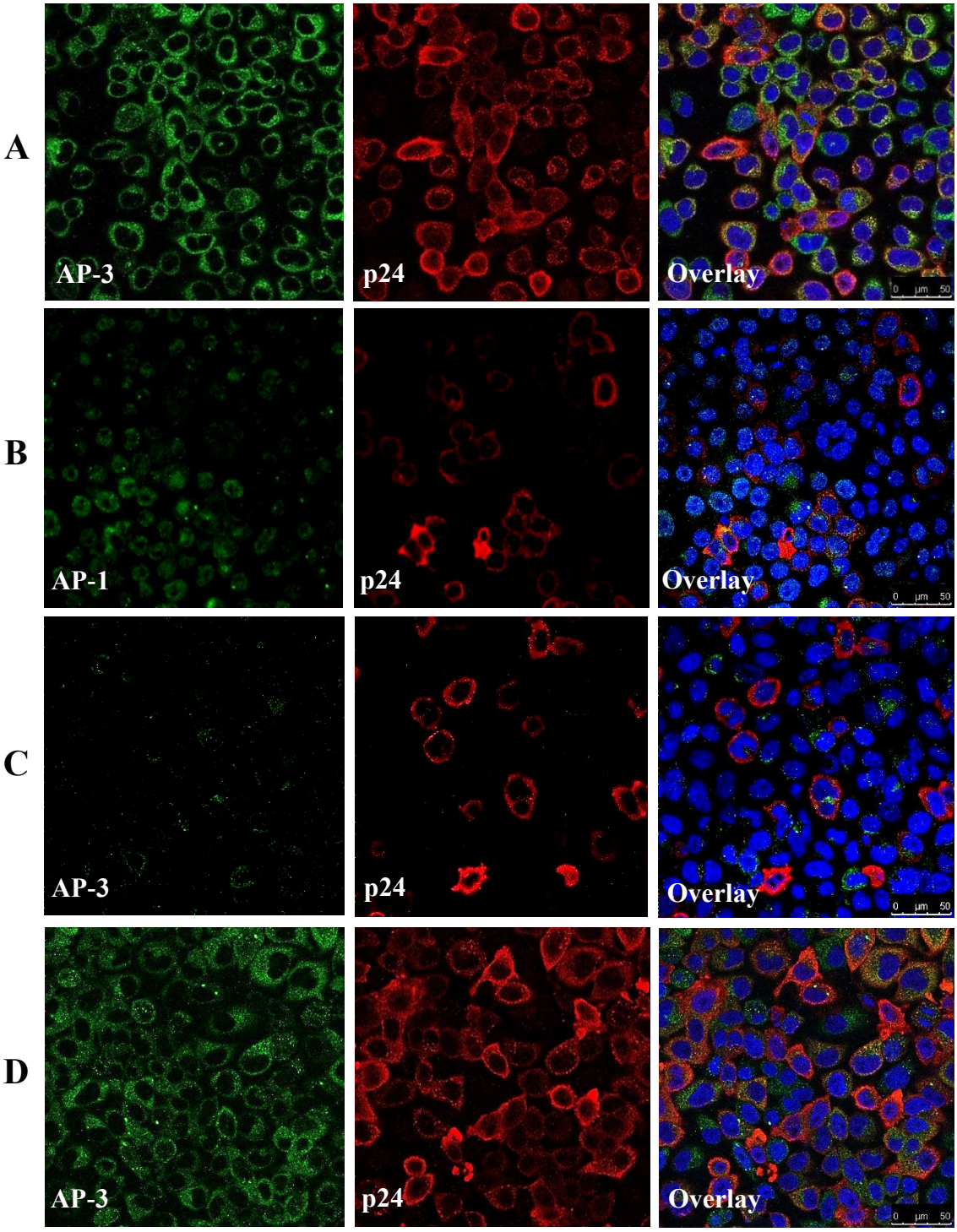

Figure 31: AP-1 and -3 knockdown appears to reduce HIV-1 Gag expression. Confocal immunofluorescence images of HIV-1 Gag following no/AP siRNA treatment. Panel A shows AP-3 (green) and Gag p24 (red) with no siRNA treatment. B shows AP-1 (green) and Gag p24 (red) in the presence of AP-1 siRNA, C shows AP-3 and Gag p24 in the presence of AP-3 siRNA and D shows AP-3 and Gag p24 in the presence of a negative control siRNA. Blue stain= DAPI.

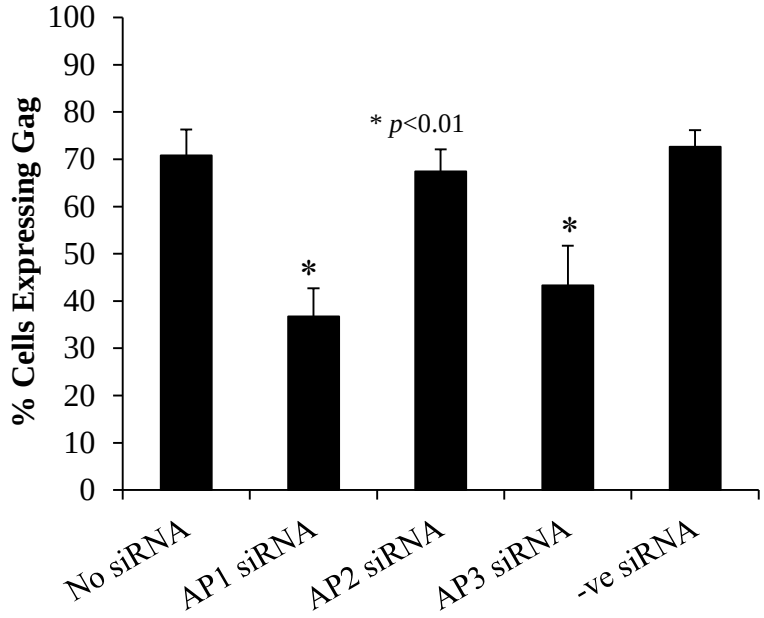

Figure 32: Quantification of HIV-1 Gag expressing cells in siRNA treated and untreated HeLa cells, as visualised by confocal immunofluorescence microscopy. Average counts of Gag expressing cells from 5 randomly selected fields of cells from each of 3 independent experiments were plotted and analysed by Student's t-test for significance. Significant results are highlighted by asterisks (p<0.01).

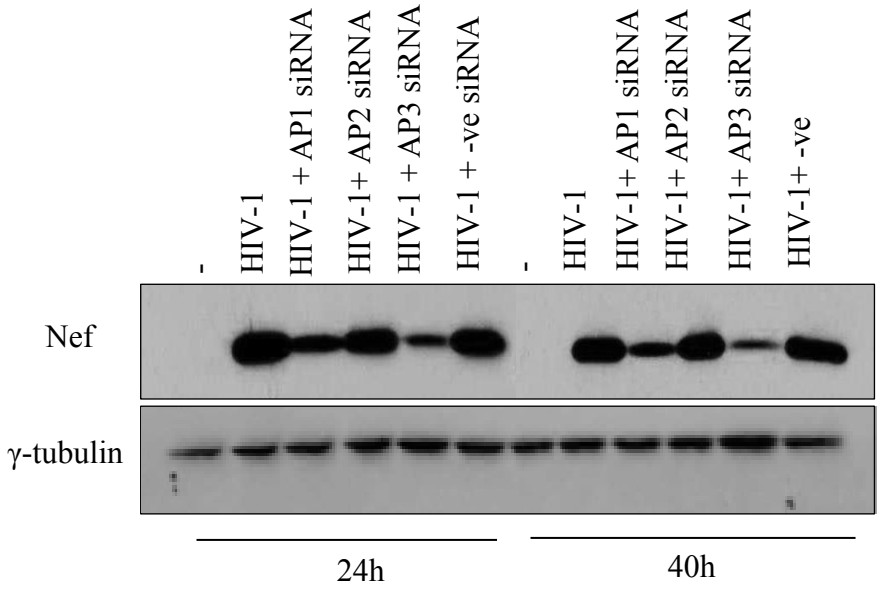

Figure 33: AP-1 and -3 knockdown reduces the level of HIV-1 Nef. Nef levels (top panel) are demonstrated by western blot of 24 and 48h cell lysates harvested from HeLa cells transfected with HXB2N^{+} provirus 24 hours after siRNA treatment. The same lysates were probed with γ-tubulin antibody to ensure that loading was equal (bottom panel).

and -3 siRNAs, but not AP-2 or the negative control. These results were deduced to be significantly different to siRNA untreated cells ($p<0.01$).

To investigate whether this effect was specific to Gag, Western blots were also performed on independently collected lysates following the same protocol, using anti-Nef antibodies. Figure 33 demonstrates that Nef is clearly reduced in the presence of AP-1 and AP-3 siRNAs, but not AP-2 or the negative control. Again, endogenous proteins were unaffected as shown by constant γ-tubulin levels.

It has been demonstrated previously (Dong et al., 2005; Camus et al., 2007) and in this thesis that knockdown of AP-1 or AP-3 inhibits viral particle release (see chapter 5.5.2). One explanation of the decreased cellular levels of Gag and Nef when these APs are knocked down may be that prevention of viral particle release increases turnover of the viral proteins within cells, although there is no evidence in the literature for this.

4.2.2 Reduction in Exogenous Protein Expression is not specific to HIV

In order to investigate whether reducing AP-1 or AP-3 specifically reduces HIV gene expression, expression of two other exogenous proteins were tested; *Renilla* luciferase (RL) and GFP. HeLa cells were transfected with either pcDNA RL or pcDNA GFP, 24 hours after AP siRNA transfection, and analysed either by quantifying relative luminescence, or by confocal immunofluorescence microscopy, respectively.

Figure 34A shows data collected from *Renilla* luciferase experiments. The graph demonstrates that *Renilla* luciferase expression is also significantly reduced when AP-1 and AP-3 siRNAs were transfected prior to the luciferase expression plasmid, but not AP-2 or the negative control siRNAs. Analysis of Variance (ANOVA) was performed, which deduced AP-1 and AP-3 to be extremely significantly different ($p<0.001$) from

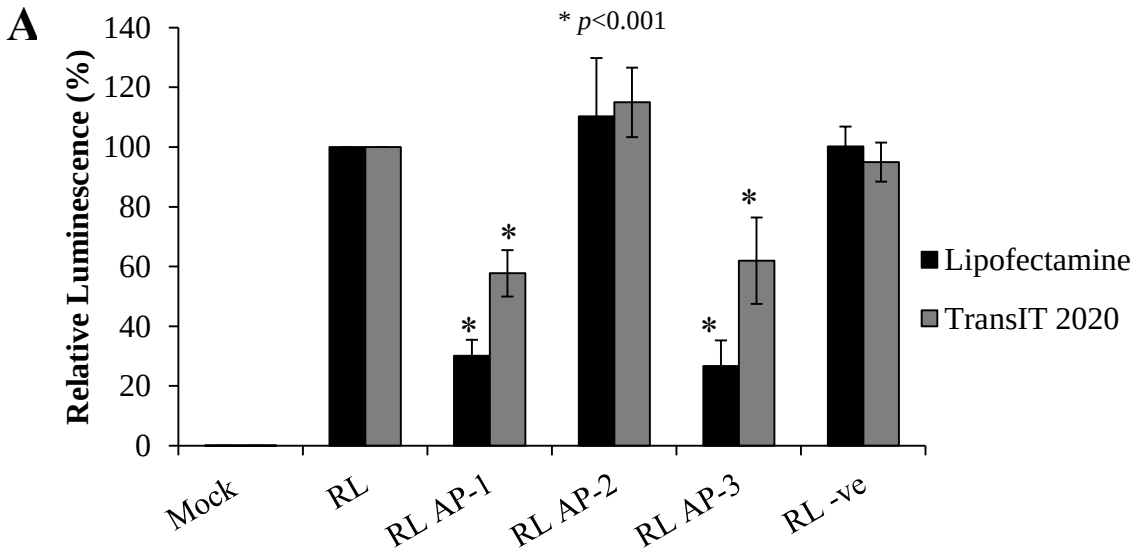

B

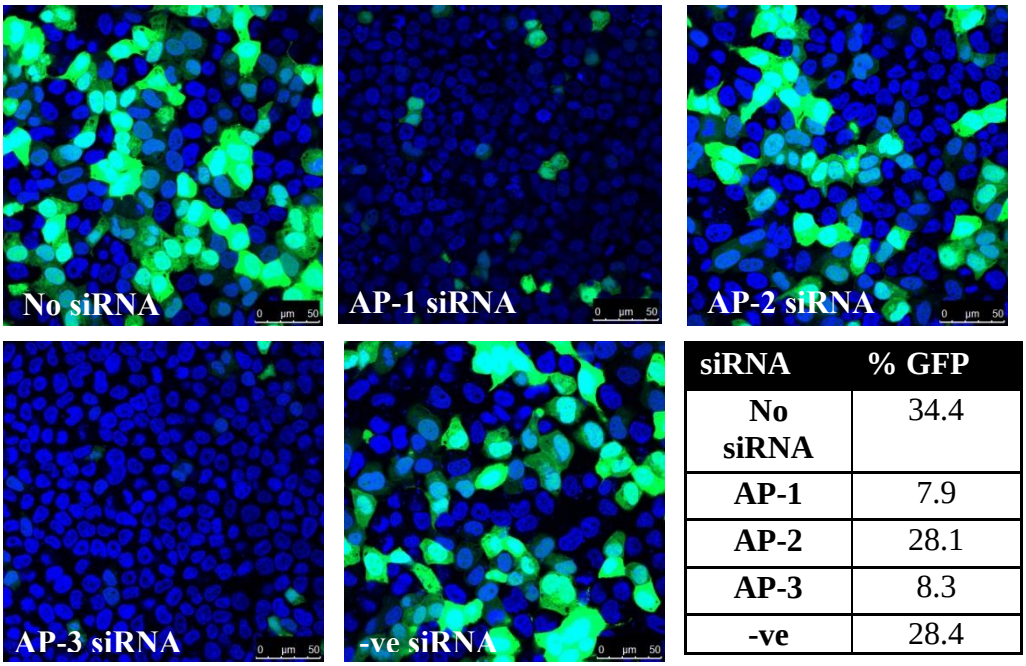

siRNA	% GFP
No siRNA	34.4
AP-1	7.9
AP-2	28.1
AP-3	8.3
-ve	28.4

Figure 34: siRNA reduction in AP-1 or -3 reduces expression of other exogenous proteins. A demonstrates 24 hour *Renilla* luciferase (RL) expression using two different transfection reagents, in AP/negative control siRNA treated cells. Values are relative luminescence, expressed as percentages of siRNA untreated samples (RL), from 3 independent repeat experiments. Statistically significant values are highlighted by an asterisk ($p<0.001$). B- Confocal immunofluorescence images of GFP expression in untreated/siRNA treated cells. Average percentages of cells expressing GFP across independent repeat experiments are shown in the table. (*Trans*-IT 2020 and GFP data collected by Jade Gumbs).

siRNA untreated samples. To deduce whether this effect was specific to the transfection reagent used (Lipofectamine 2000), a different reagent was tested; *Trans*IT-2020. Figure 34 also clearly shows that when AP-1 and AP-3 are reduced prior to transfection with this transfection reagent, we see the same result as with Lipofectamine 2000; a significant reduction in expression as deduced by ANOVA ($p<0.001$). Again, AP-2 and the negative control siRNAs were seen to have no effect.

Confocal immunofluorescence microscopy revealed the same pattern of results when pcDNA GFP was transfected, with both Lipofectamine 2000 (data not shown) and *Trans*IT-2020 (Figure 34B).

Collectively, these data suggest that reducing the levels of AP-1 or -3 has a non-specific inhibitory effect on protein expression from transfected plasmid DNA introduced into cells by lipofection, which is non-specific. This therefore excludes a role for AP-1 and -3 in specifically assisting viral gene expression, but indicates a more general role for these adaptor proteins in expression from transfected plasmids.

4.2.3 Co-Transfection of AP siRNAs with HIV-1 Provirus Does Not Affect HIV-1 Protein Expression

To deduce whether the same reduction in exogenous protein expression could be observed when the siRNAs were not transfected prior to proviral transfection, the AP siRNAs (10 µM) were co-transfected alongside the HIV-1 provirus. To investigate total Gag protein levels, this was carried out in the presence of the HIV-1 Protease inhibitor Saquinavir (1 µM). Cell lysates were again collected 24h and 48h post transfection and analysed by Western blot using antibodies directed against p24 and Nef. Figure 35A shows that both Gag and Nef protein levels now appeared to be unaffected by knockdown of AP-1 or AP-3. Densitometry was then carried out on 3 independent

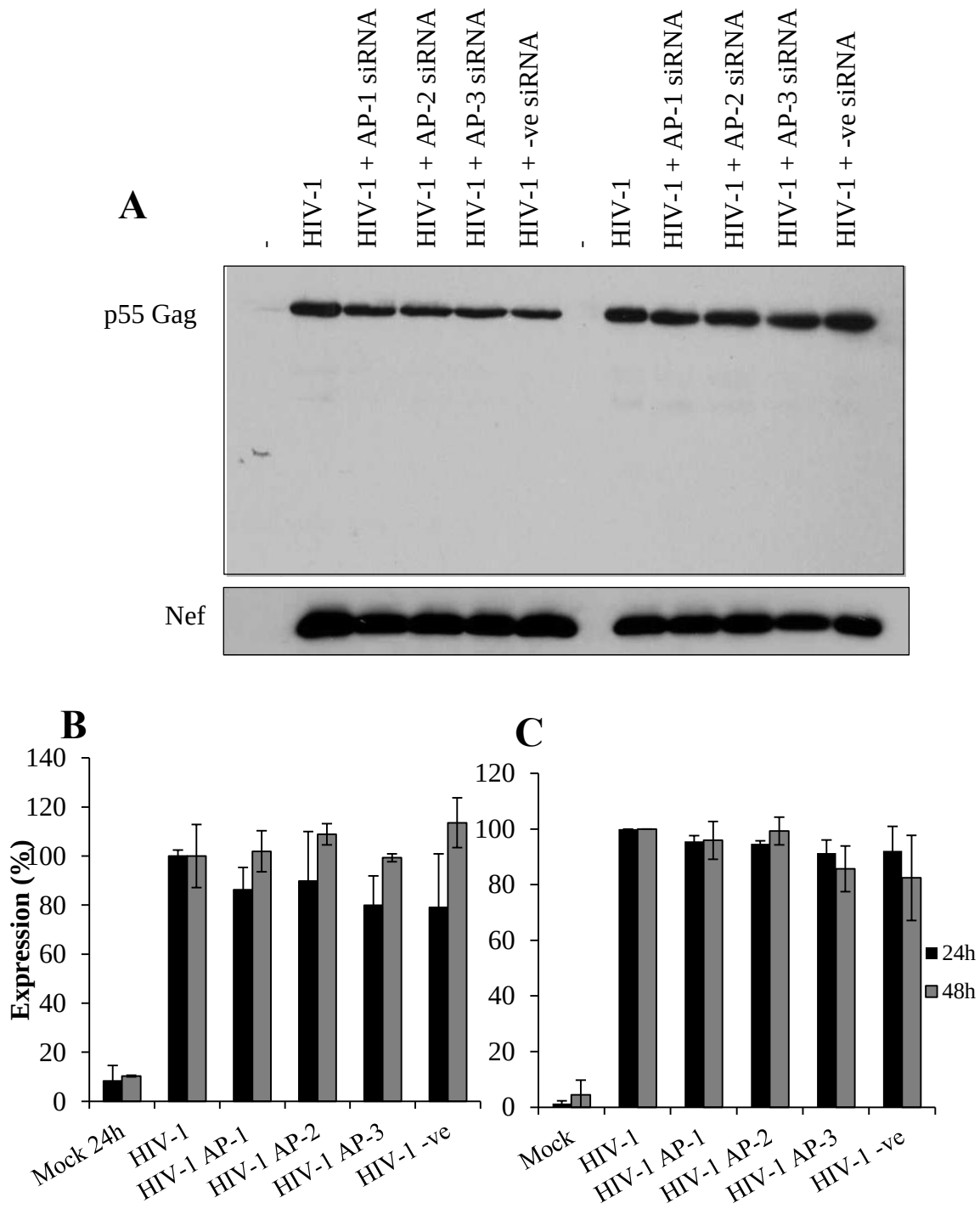

Figure 35: HIV expression in proviral plasmid and siRNA co-transfected cells. A- Western blots of cell lysates harvested 24 and 48 hours post siRNA/provirus co-transfection; the top panel shows total Gag (p55) protein in the presence of the protease inhibitor Saquinavir, the bottom panel shows total Nef levels. These were quantified in ImageJ using densitometry, normalising to siRNA untreated samples. B and C show these values for Gag and Nef, respectively. No differences were found to be statistically significant (p>0.05).

experiments, and the results are shown in Figures 35B and C. Student's t-test deduced none of the results to be significantly different to the siRNA untreated control (p>0.05). To ensure that the siRNAs were effective when transfected in this way, Western blots were carried out using these lysates, and it was found that they were still able to significantly reduce AP expression (Jade Gumbs, personal communication).

Again, in order to investigate whether this was specific to HIV, the same protocol was repeated but using pcDNA RL. This also found that when siRNAs were co-transfected, protein expression was unaffected when AP-1 or AP-3 were reduced (p>0.05) (data not shown).

These results suggest that the effects of reducing AP-1 and AP-3 can be bypassed if plasmids are transfected alongside the siRNAs. However, since a pool of pre-existing APs will exist for some time after the co-transfection, this may reduce any potential effects of the AP knockdown.

4.2.4 Reduction in Exogenous Protein Expression Does not Occur when mRNA is Transfected

Results obtained so far infer a non-specific reduction in gene expression from transfected plasmids, only when levels of AP-1 and -3 subunits are reduced prior to transfection. In order to investigate the stage of transfection which is affected by knocking down AP-1 or -3, mRNAs were used in transfection as opposed to DNA. This is because mRNA can be directly translated in the cytoplasm, and does not require nuclear entry, as plasmids do for transcription.

Renilla luciferase (RL) and GFP mRNAs were *in vitro* transcribed, capped and polyadenylated, and used to transfect cells 24 h post-siRNA transfection. Cell lysates or

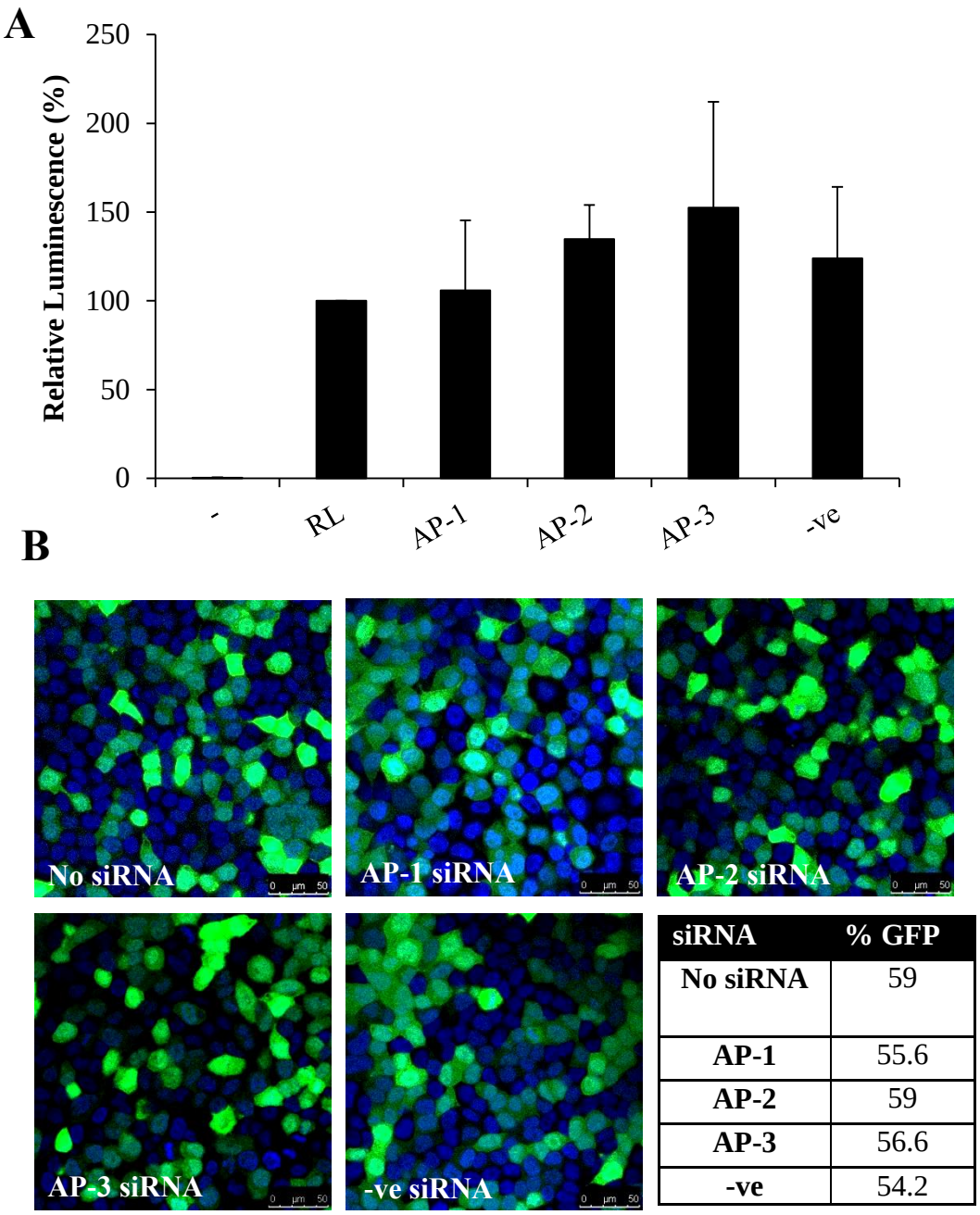

siRNA	% GFP
No siRNA	59
AP-1	55.6
AP-2	59
AP-3	56.6
-ve	54.2

Figure 36: Protein expression from transfected mRNA is not decreased by AP-1/-3 knockdown. A- *Renilla* luciferase (RL) expression after RL mRNA transfection into AP siRNA treated cells. Relative luminescence units are expressed as percentages of siRNA untreated samples. B- Confocal immunofluorescence microscopy images of GFP (green) mRNA transfected into AP siRNA treated cells. The table shows counts of average percentage of GFP expressing cells from repeat experiments. None of the differences were found to be statistically significant (p >0.05). Blue stain = DAPI.

fixed cells were analysed for relative luminescence or by confocal immunofluorescence, respectively.

Luciferase results from transfected RL mRNA (shown in Figure 36A) showed that although differences in protein expression could be observed in the presence of the AP siRNAs, Student's t-test revealed that none of the results were significantly different ($p>0.05$); furthermore, no reduction in RL expression in AP-1 or AP-3 treated cells was observed.

Confocal immunofluorescence microscopy of GFP mRNA-transfected cells also showed no differences in the presence of the AP siRNAs (Figure 36B). Together, these results infer that AP-1 and AP-3 depletion likely affects DNA trafficking to the nucleus, rather than lipoplex entry or escape from endosomes.

4.3 Discussion

This chapter aimed to investigate a potential role of the adaptor proteins in facilitating viral protein expression. Previous results obtained in this lab suggested a potential role of AP-1 in viral Gag expression, therefore this chapter focussed on investigating this effect, extending it to include the other adaptor proteins with which HIV-1 is known to associate.

Initial results obtained supported previous results, indicating that AP-1 does indeed play a role in facilitating viral protein expression (Figures 30-33). This was found to not be specific to AP-1 only, but AP-3 also. AP-2 was deduced to have no effect. Investigation of endogenous protein expression levels (γ-tubulin) revealed that this effect is specific to exogenous proteins. Since experiments were performed using transfected envelope deleted proviral constructs, we know that the effect observed is

not via obstruction of viral entry, since this is bypassed in transfection. Progeny particles produced by infected cells are also uninfectious since they do not possess Env, which is absolutely required for viral entry into cells. Therefore, we can also conclude that we were not affecting re-entry into uninfected cells. The fact that AP-1 and -3 knockdown inhibits viral egress (Dong et al., 2005; Camus et al., 2007; chapter 5.2.2) also rules out that the effect on cellular Gag is due to an increase in particle release.

GFP and RL expression studies revealed that the effect of AP-1/-3 reduction was not in fact specific to HIV proteins, but rather a general effect on protein expression from transfected plasmids (Figure 34). Co-transfection of plasmids and siRNAs also revealed that this effect can be bypassed if the siRNAs are not transfected prior to plasmid transfections (Figure 35), which has implications on appropriate methodology for future experiments in which AP knockdown is required. This also narrowed down the effect we were seeing to exclude the possibility that reducing AP-1/-3 affected protein turnover.

As mentioned earlier, AP-2 was deduced to have no effect on plasmid protein expression. It has been suggested that lipoplexes may enter the cell by 2 mechanisms; coated pit/ clathrin mediated endocytosis (Friend et al., 1996; Zuhorn et al., 2002), or non-coated pit endocytosis (Simões et al., 2000), and that this may be due, at least in part, to cell type (Elouahabi and Ruysschaert, 2005). Since AP-2 plays a pivotal role in the former process, we can infer that this is not the mechanism by which the plasmids are entering the cell, or at least within HeLa cells.

mRNA studies were critical in narrowing down the stage in the lipoplex trafficking that is affected by reducing AP-1/-3 expression. Protein expression from transfected mRNAs was unaffected under conditions in which expression from transfected

plasmids was reduced (Figure 36). Firstly, this suggested that cell entry of lipoplexes was not inhibited by AP-1/-3 depletion (unless mRNA-liposome complexes have very different properties to DNA-liposome complexes). Secondly, these results suggested that escape of lipoplexes from endosomes is not dependent on the APs, as mRNA would need to enter the cytosol for translation. Thirdly, this suggested that trafficking of DNA to the nucleus requires AP-1 and AP-3. Since we transfected dividing cells in which plasmid nuclear entry can occur during nuclear membrane breakdown, it is more likely that AP-1/-3 depletion affected trafficking of DNA to the perinuclear region rather than translocation of the nuclear membrane.

Since a major pathway of lipoplex entry was found to be endocytosis, a subsequent stage of endosomal escape is necessary to facilitate cytosolic entry of DNA destined for the nucleus (Elouahabi and Ruysschaert, 2005). Whether after this stage DNA enters the nucleus still in lipoplex complexes, or dissociated as naked DNA, is disputed.

Further studies in our laboratory using a fluorescent transfection reagent (Metafectene-fluoR, data not shown) have found that DNA enters the nucleus in a lipid complex, since a strong nuclear signal from the Metafectene-fluoR was observed in cells expressing GFP from a plasmid (Jade Gumbs, personal communication). Therefore, the APs may facilitate the trafficking of lipid/DNA complexes, rather than naked DNA. However, it seems unlikely that the APs can bind lipoplexes directly since they bind specific peptide motifs found on cargo. That being said, it is not implausible that their ability to bind other molecules has been overlooked. Another interesting discovery through the use of Metafectene-fluoR (data not shown) was that, although 6 hours post transfection, Metafectene-fluoR fluorescence seemed relatively even in siRNA treated and untreated samples, at 24 hours, there was a dramatic reduction in Metafectene-fluoR fluorescence in cells. Since it is unlikely that rhodamine, the dye used in

Metafectene-fluoR, would be degraded as a result of instability, there must be a specific reason for the reduction in signal observed at this time point. It is possible that since Metafectene-fluoR, and other transfection reagents, are toxic, that if they are unable to enter the nucleus as a result of AP-1/-3 knockdown, that they are degraded in lysosomes or recycled out of the cell in order to prevent cell death.

Recent studies have shown that the molecular motor kinesin KIFC1 is involved in the intracellular trafficking of naked DNA (Farina et al., 2013). It cannot be ruled out that these APs might therefore play a role in the delivery of kinesin KIFC1 to DNA/lipoplexes, or vice versa, prior to trafficking along cytoskeletal filaments towards the nucleus. Although most kinesins are plus end directed, KIFC1 moves towards the minus end (Farina et al., 2013), which would fit in with this theory.

Together, these results demonstrate a novel and surprising role for adaptor proteins 1 and 3 in the trafficking of lipoplexes to the nucleus, but not earlier stages of the lipoplex trafficking pathway.

4.4 Future Work

This chapter has shed some light on the mechanisms underlying lipoplex trafficking. The finding that AP-1 and -3 are required for efficient nuclear delivery of lipoplexes was surprising, as was the apparent observation that AP-2 is not involved in lipoplex entry. Much more work is needed on this topic to divulge the precise action of the APs in lipoplex delivery. For example- are the APs the only players in this process? Since these APs generally function in concert with other proteins, such as clathrin, one could assume that they are likely not the only players. If so- which other molecules work as chaperones to collectively deliver lipoplexes to the nucleus? Kinesin KIFC1 is one such possibility that could be investigated.

Another crucial set of experiments which may shed light on what happens to lipoplexes if they are unable to enter the nucleus would be to repeat Metafectene-fluoR experiments, but at different time points. For example, 6 hours, 12 hours, 18 hours and 24 hours post transfection. We may then be able to see where the complexes go, and at what time point they disappear.

It is also necessary to investigate whether it is indeed the APs which directly bind to the lipoplexes, or whether they act as a linker molecule between the lipoplex and another chaperone/molecule.

CHAPTER 5: WHAT IS THE EFFECT OF ADAPTOR PROTEIN DEPLETION ON HIV-1 GAG TRAFFICKING?

5.1 Introduction

Progeny virion formation is a complex multi-step process which is driven by HIV Gag. Preceding this stage of the life cycle are trafficking events which bring together both the full-length Gag precursor polypeptides and the viral RNA to discrete assembly domains within the cell. As mentioned earlier in chapter 1, HIV Env trafficking follows a distinct pathway to that of Gag, but ultimately becomes inserted within the cellular membranes at the site of viral budding. Gag trafficking has come under scrutiny over the past few years due to the presence of an incomplete story; how precisely is Gag targeted to assembly sites, and what factors determine these areas as sites of assembly?

HIV-1 has been observed through electron microscopy (EM) to bud from 2 different areas; the plasma membrane (PM) and late endosomes/multivesicular bodies (LEs/MVBs), and preferences for these sites differs in two natural host cell types; in T cells HIV-1 preferentially buds from the PM, whereas in macrophages budding preferentially occurs into MVBs. Gag has also been observed at both sites in certain cell lines, suggesting that the endosomal pathway may serve as a route for both the trafficking of Gag and assembled particles (Ono, 2009).

Consistent with the notion of an endosomal trafficking pathway, various cellular factors which are involved in endosomal trafficking have been found to associate with HIV-1. As mentioned in chapter 3.1, AP-1 and AP-3 are thought to facilitate particle release by directing Gag through its MA region to intracellular assembly and budding sites (Dong et al., 2005; Camus et al., 2007). In contrast, AP-2 has an inhibitory effect on particle release, also through direct binding of the MA region (Batonick et al., 2005).

After the discovery of interactions between Gag and various cellular trafficking pathway components such as these adaptor protein complexes, we began to postulate exactly the route which Gag takes to reach assembly sites via these cellular proteins. A summary of some potential pathways is given below in Figure 37.

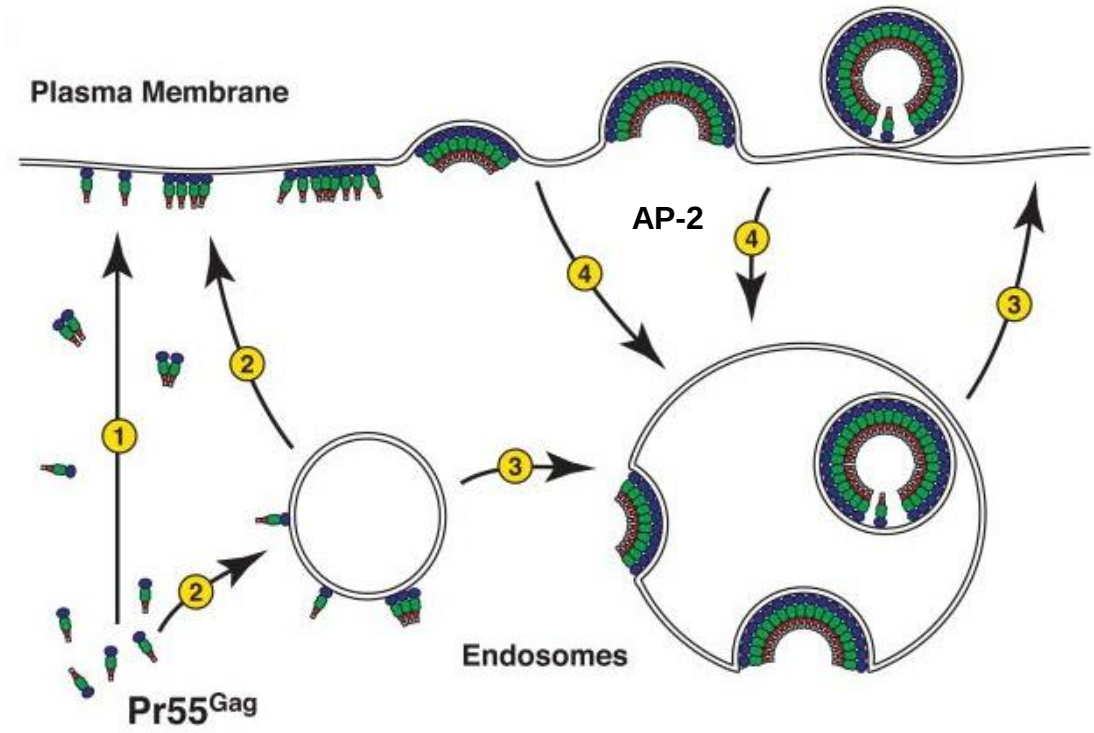

Figure 37: Possible trafficking pathways of HIV-1 Gag to intracellular assembly sites. 1- Gag may be directly targeted to the PM. 2- Gag may be targeted to the PM by travelling first through an endosomal intermediate. 3- During trafficking through endosomes, Gag may form particles in the endosomal lumen which become released extracellularly through endosome/PM fusion. 4- Gag particles present in endosomes may alternatively have formed through the internalisation of particles at the PM, assisted at least in part by AP-2, which will then be released extracellularly (adapted from Ono, 2009).

As this image suggests, there exists some controversy over the precise route which Gag takes in order to bud from cells. It is clear that particles must be released from the PM in order for infection to be productive, but also evident that Gag may use an endosomal

route prior to reaching the PM; but whether this is a separate pathway, a detrimental consequence or an intermediate step is unknown.

Despite the fact that differing budding sites have been observed in T cells and macrophages, it has been postulated that regardless of cell type, Gag traffics to the PM via endosomes, forming particles within the endosomal lumen which will be released extracellularly through fusion of the endosomal and plasma membranes (Sherer et al., 2003; Perlman and Resh, 2006). This theory, however, was complicated by the fact that Gag presence in endosomes could be explained by internalised particles which first formed at the PM. Long-term monitoring studies of GFP tagged virus concluded that the majority of endosomal Gag was indeed derived from internalised particles that had initially reached the PM first. However, they did not rule out the idea that Gag could indeed traffic via endosomes in a minority of cases (Jouvenet et al., 2006; Ono, 2009).

The purpose of this chapter, therefore, is to gain some more insight into the trafficking of HIV-1 Gag, through its use of the clathrin adaptor proteins. Do AP-1 and AP-3 have the same consequences on Gag localisation? Does AP-2 also affect Gag localisation? Is it likely that Gag simply diffuses through the cytoplasm without an intermediate step, and then arrives at the PM for budding? Are localisation and budding the only effects that the APs exert on Gag?

5.2 Results

5.2.1 AP-1 and -3 knockdown Affects Gag localisation

It was recently shown that cells deficient of AP-3 caused an accumulation of HIV-1 Gag in an intermediate endosomal compartment (Lui et al., 2012). Dong et al. (2005), using a different cell line, also found that addition of a dominant negative AP-3 decreased plasma membrane localisation of Gag, however, it also resulted in an

increase in diffusely stained Gag, which is in contrast to the more punctate appearance observed by Liu et al., (2012). In order to investigate the effects of AP knockdown on Gag localisation, confocal microscopy of transfected HeLa cells was carried out, for consistency with the previous chapters. Results are shown in Figure 38.

Experiments carried out using siRNAs within this chapter were performed using siRNA/provirus co-transfection; thus siRNAs were used for the time period stated when the time samples were taken (see chapters 2.1.3 and 2.2.8 for a more detailed description of the siRNAs and transfection protocol).

Images shown in A, B and C show the 3 typical Gag localisations observed by p24 staining in a population of cells. As can be seen, HIV-1 Gag either displays a punctate intracellular localisation, a predominantly plasma membrane (PM) localisation, or a diffuse cytoplasmic localisation. The relative abundances of these 3 different localisations is demonstrated in G, whereby cells expressing Gag were counted across repeat experiments and assessed for Gag localisation. As can be seen, HIV-1 Gag predominantly displays diffuse cytoplasmic staining when no siRNA is present; PM and punctate have roughly similar abundances; this is in contrast to Dong et al. (2005) who found HIV-1 Gag to be predominantly punctate. Figures D, E and F demonstrate typical Gag staining observed in the presence of AP-1, -2 and -3 siRNAs, respectively (see figure 39A for confirmation of siRNA efficacy). As can be seen, when AP-1 is knocked down Gag appears very diffuse, more so than in untreated samples. AP-2 knockdown visually had no effect on Gag localisation, as cells were still a mixture of punctate, diffuse and PM localised. AP-3 siRNA resulted in cells appearing more punctate, which would support data collected by Liu et al. (2012), as described above, but is in contrast to Dong et al. (2005) who found a shift towards a diffusely stained cytoplasmic Gag. A likely explanation for the differences observed here is that a more

aggressive knockdown of AP-3 was adopted by Dong et al., who transfected the AP-3 siRNAs twice prior to further co-transfection alongside the provirus. As results gathered in the previous chapter demonstrate that knocking down the APs prior to plasmid transfection decreases transfection efficiency and therefore protein expression, it is possible that differences in Gag levels could contribute to the apparent visual differences observed in Gag patterns.

To quantify this data, counts of Gag expressing cells across 3 repeat experiments were also taken as before. Average Gag localisations in the presence of AP siRNAs are also shown in Figure 38G. As can be seen, a significant decrease in PM Gag is observed in the presence of AP-1 siRNA. When AP-3 siRNA is used, PM localisation is significantly reduced, and punctate staining is significantly increased. AP-2 and –ve siRNAs had no significant effect.

These results suggest that both AP-1 and AP-3 are required for HIV-1 Gag to reach the plasma membrane, but that they may function at different points in the pathway. AP-3 is implicated in directing Gag from endosomal compartments to the plasma membrane, in an indirect manner, for example by facilitating delivery from an early endosome/intermediate compartment to a late endosome, which may then be recycled back to the PM (Dong et al., 2005; Liu et al., 2012), whereas AP-1 may be involved prior to this stage of trafficking; likely facilitating trafficking from the TGN to either the PM or endosomes, since Gag trafficking has been found to be positively affected by the TGN associated ubiquitin ligase hPOSH (Alroy et al., 2005). This would agree with published cellular roles of AP-1 in TGN-endosome trafficking, and AP-3 in endosome-lysosome trafficking.

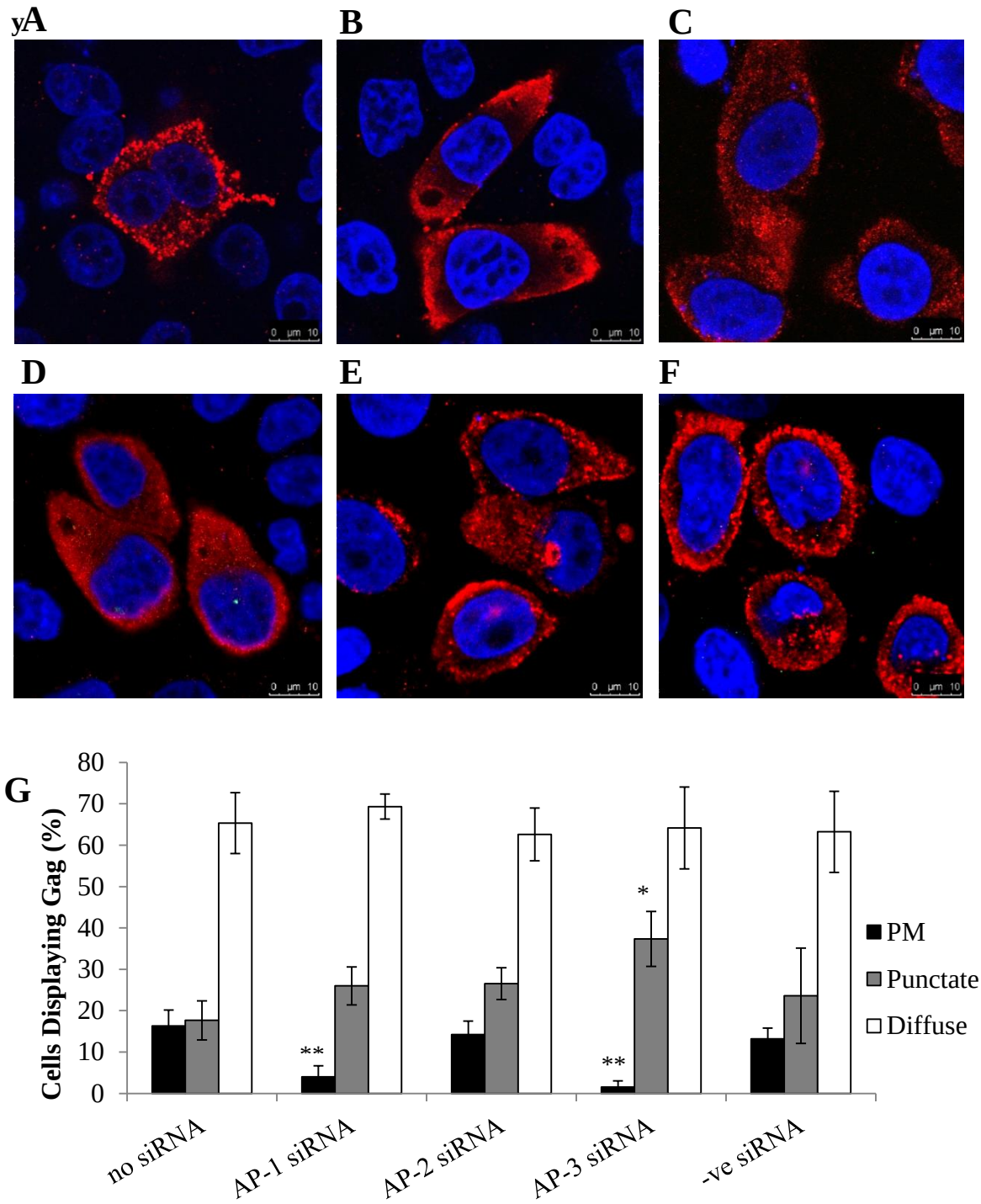

Figure 38: AP-1 and -3 knockdown affects Gag localisation in HeLa cells. A-C- Confocal immunofluorescence microscopy images of the 3 typical Gag (p24) localisations observed in HIV-1 transfected cells; punctate intracellular, plasma membrane (PM), and diffuse cytoplasmic, respectively. D-F- Typical Gag staining in the presence of AP-1, -2 and -3 siRNAs, respectively. G- Quantification of Gag expressing cells from 3 repeat experiments. Statistically significant results are highlighted by asterisks (*=p<0.05, **=p<0.01).

5.2.2 AP-1 and -3 Assist Gag Processing and Viral Particle Release

Although previous studies have inferred a link between AP-1 and -3 and viral assembly (Dong et al., 2005; Camus et al., 2007), this link has only been suggested through the observation that particle release is severely retarded in the absence of these proteins. We investigated the effects of siRNA mediated knockdown of the APs on both cellular Gag and released Gag by Western blot of harvested HIV-1 and AP siRNA co-transfected HeLa cells. By using an antibody against the capsid region of Gag, we could detect full length Gag (p55), processing intermediates (p41) and fully processed CA (p24). Gag processing depends on the activity of the HIV-1 Protease, which is only activated when GagPol proteins dimerise during the assembly process (see chapter 1). Consequently, changes in the ratio of p55, p41 and p24 suggest changes in the ability of virus particles to assemble.

Figure 39A shows a Western blot of AP siRNA treated cells (1 of 3 repeats), confirming that when both AP-1 and AP-3 siRNAs were added, significant knockdown of both APs occurred. AP-2 appeared to have no effect on any Gag fractions. As shown by the γ-tubulin Western of the cell lysates, endogenous protein levels were unaffected and differences observed could not be attributed to uneven protein loading.

Figure 39B shows that in the presence of AP-1 or -3 siRNAs, little change was observed at 24 hours, however there was a decrease in the amount of viral p24 produced in cells at 40 hours post transfection, but p55 remained unchanged. This is in contrast to results gathered in chapter 4 (see figure 30A) whereby a significant decrease in all Gag fractions were observed at both 24 and 40 hours post-transfection; however, the siRNAs were co-transfected in this chapter, as oppose to transfection 24h prior to proviral transfection in chapter 4.

Figure 39B also demonstrated a modest decrease in p41 could be observed when AP-1 or -3 siRNAs were used, 40 hours post transfection. When AP-1 and -3 siRNAs were transfected together, however, it could be seen that the effect on viral p24 was increased at both 24 and 40 hours post transfection; this additive effect of dual knockdown suggests that there may be some redundancy between AP-1 and AP-3 function. Western blot of viral supernatant samples also confirmed that AP-1 and -3 siRNA co-transfections had an additive effect (middle panel, Figure 39A, 1 of 3 repeats); inhibiting viral particle release (middle strong band = p41, bottom faint band = p24). AP-2 knockdown also confirmed an increase in particle release as per the literature (Batonick et al., 2005).

In order to quantify this data, densitometry using ImageJ was carried out across repeat experiments. Results are shown in Figure 40. At 24 hours post transfection (Figure 40A), no effect was seen on p55, however, p41 was reduced by 18% when AP-1 and -3 siRNAs were used together, which was found to be significantly lower than when no siRNA was present ($p<0.001$). p24 was also found to be significantly lower at 24 hours post transfection when AP-1 and -3 siRNAs were added in combination, reducing this fraction by 44%. AP-1 alone was also found to significantly reduce p24 at 24 hours, but only by 15%. By 40 hours (Figure 40B), AP-1 and -3 siRNAs alone significantly reduced the p24 band by 40 and 38%, respectively. AP-1 and -3 in combination was found to significantly reduce all 3 Gag fractions (15, 20 and 64%, respectively).

With regards to viral release, p41 and p24 levels were investigated. AP-1 and -3 knockdown in combination reduced p41 release by 94%, and p24 by 75%. AP-1 and -3 knockdown individually was found to also significantly reduce particle release, as is described in current literature (Dong et al., 2005; Camus et al., 2007). Knockdown of AP-2 was found to facilitate particle release, also as per the current literature (Batonick

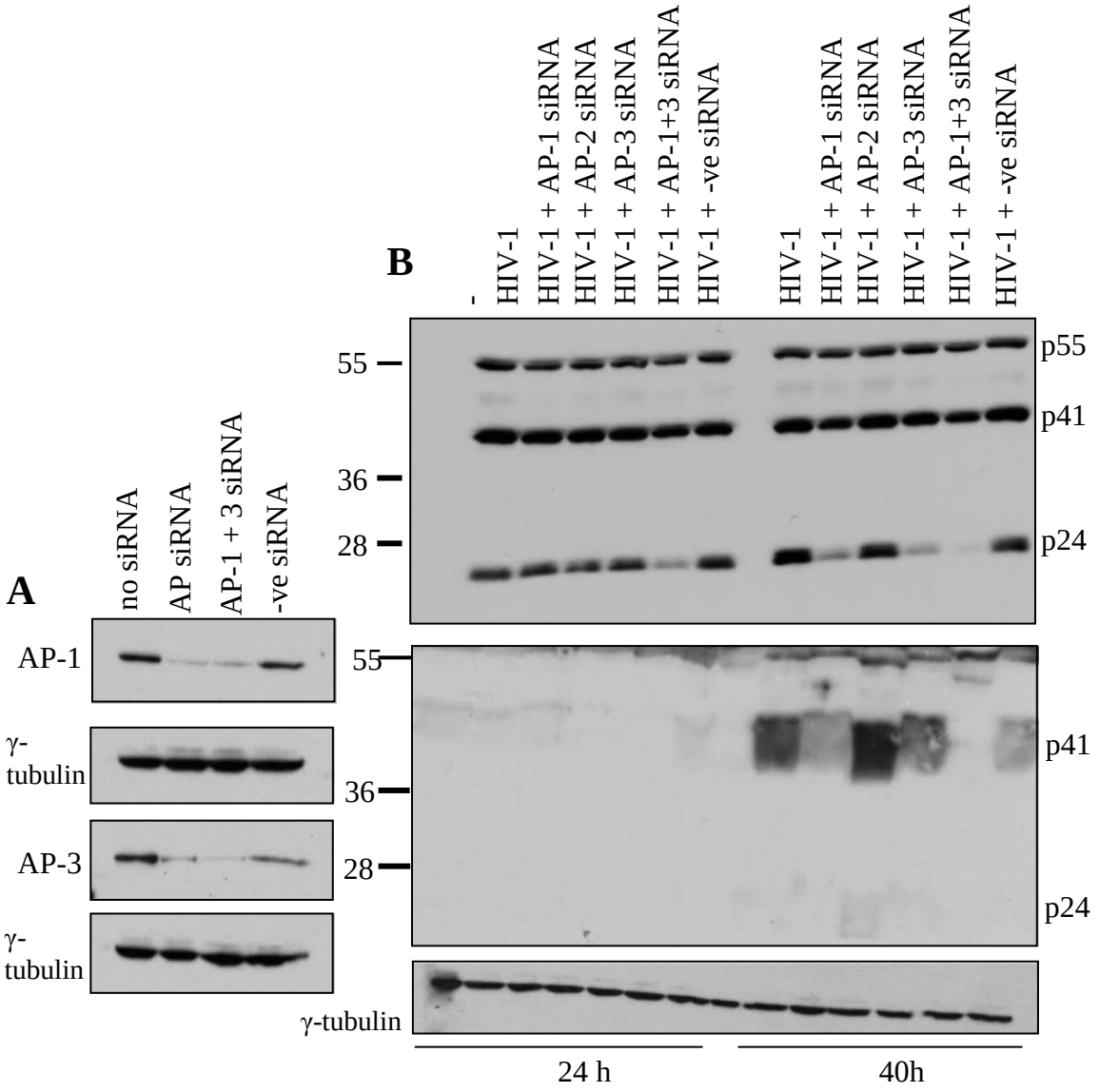

Figure 39: AP-1 and -3 knockdown affects HIV-1 Gag processing and particle release. A- Western blot of HeLa cell samples harvested 40 hours post-transfection with AP or negative control siRNAs, using anti AP-1γ (upper panel) and anti AP-3δ (middle panel) or anti γ-tubulin (lower panel, control) antibodies. B- Western blots of cell (upper and lower) or supernatant (middle panel) samples collected at 24 or 40h post co-transfection of HeLa cells with HIV-1 HXB2 proviral plasmid and AP or negative control siRNAs. Proteins were detected with an anti-Gag p24 antibody (upper and middle panel) or anti γ-tubulin control antibody (lower panel).

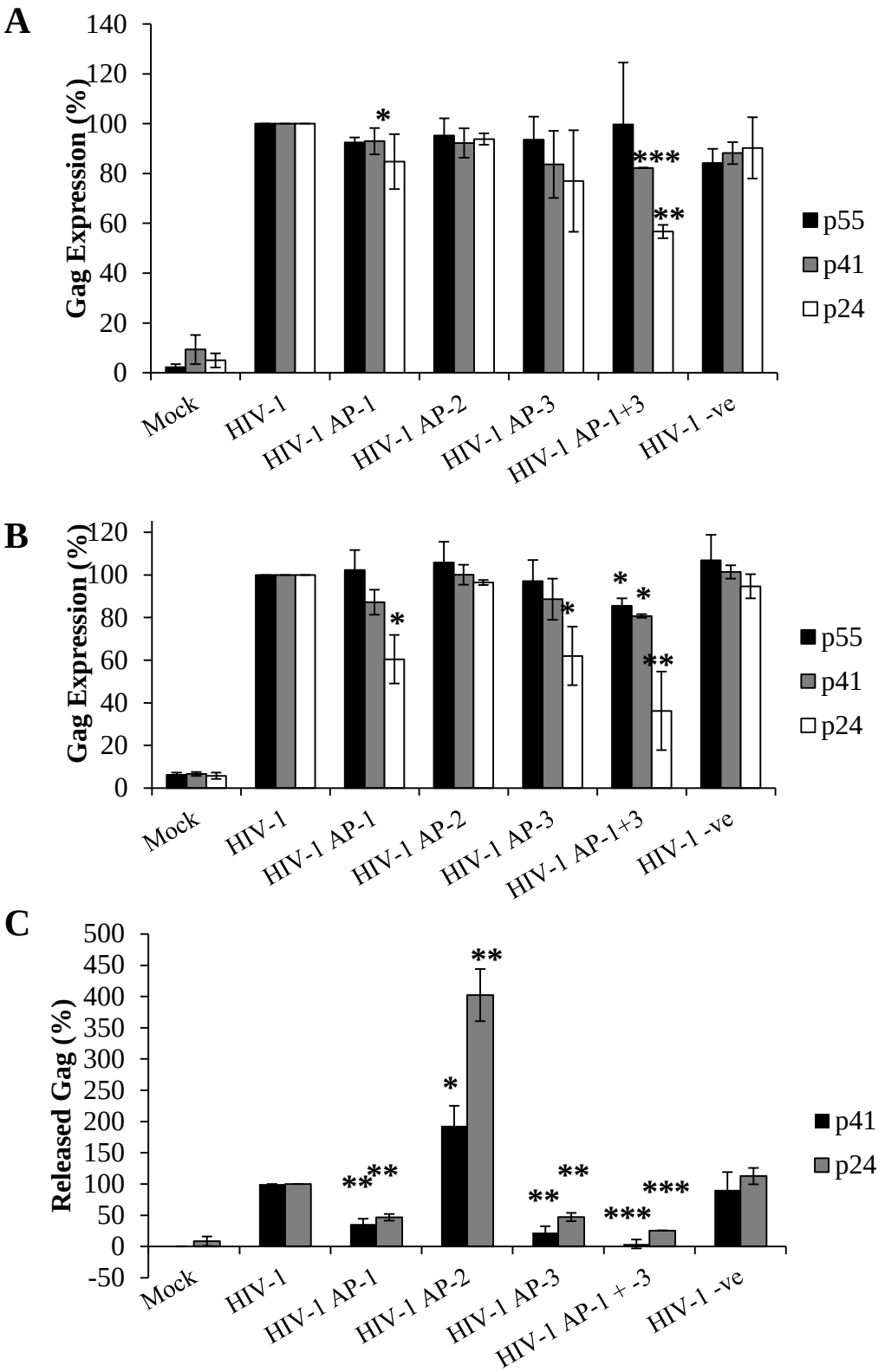

Figure 40: Co-transfection of AP-1 and -3 siRNAs has an additive effect on HIV-1 Gag processing and release. Densitometry was carried out on cell (A, 24h; B, 40h) and supernatant (C) western blots from repeat experiments. Results are expressed as percentages of siRNA untreated samples. Statistically significant results are highlighted by asterisks (Key: *=p<0.05, **p<0.01, ***p<0.001).

et al., 2005). This is likely due to prevention of AP-2/clathrin-mediated endocytosis of budding viral particles.

Another observation to note from this data is that, when AP-1 and -3 were knocked down individually, a corresponding increase in unprocessed p55 was not seen to co-occur with the reduction in processed Gag. AP-1 and -3 siRNAs in combination also reduced all 3 Gag fractions by 40 hours. Since there was also less Gag being released from cells, this suggested that Gag is disappearing when it cannot be assembled. Three hypotheses were made to account for this, and tested below.

5.2.3 AP-1 and -3 Knockdown does not Increase Gag Translation Inhibition

Anderson and Lever (2006), found that at high levels, Gag modulates its own translation. This was found to be through interactions between zinc fingers present in Gag NC and the packaging signal present on viral RNA. At high levels, Gag bound to this signal, sterically obstructing the ribosome from scanning through the RNA, and therefore preventing Gag synthesis. It seemed a plausible idea that, if Gag is unable to traffic to intracellular assembly sites in the absence of AP-1 or -3, that Gag may accumulate at its site of synthesis and therefore reduce translation by this mechanism. We hypothesised that by using mutant viruses in which the interaction between NC and the packaging signal is inhibited, Gag translation would be able to continue in the absence of AP-1 or AP-3. The first mutant virus, C2849S, contains point mutations of the first cysteine residue of each zinc finger (C28 and C49 of NC) to serine, and consequently RNA binding is inhibited (Dorfman et al., 1993). The second, SVCΔP1 has the packaging signal removed (Harrison et al., 1998). The third, A4, has a stem loop from the packaging signal removed, but also results in an in-frame AUG codon upstream of the Gag start codon. As a consequence, this N-terminally extended Gag is

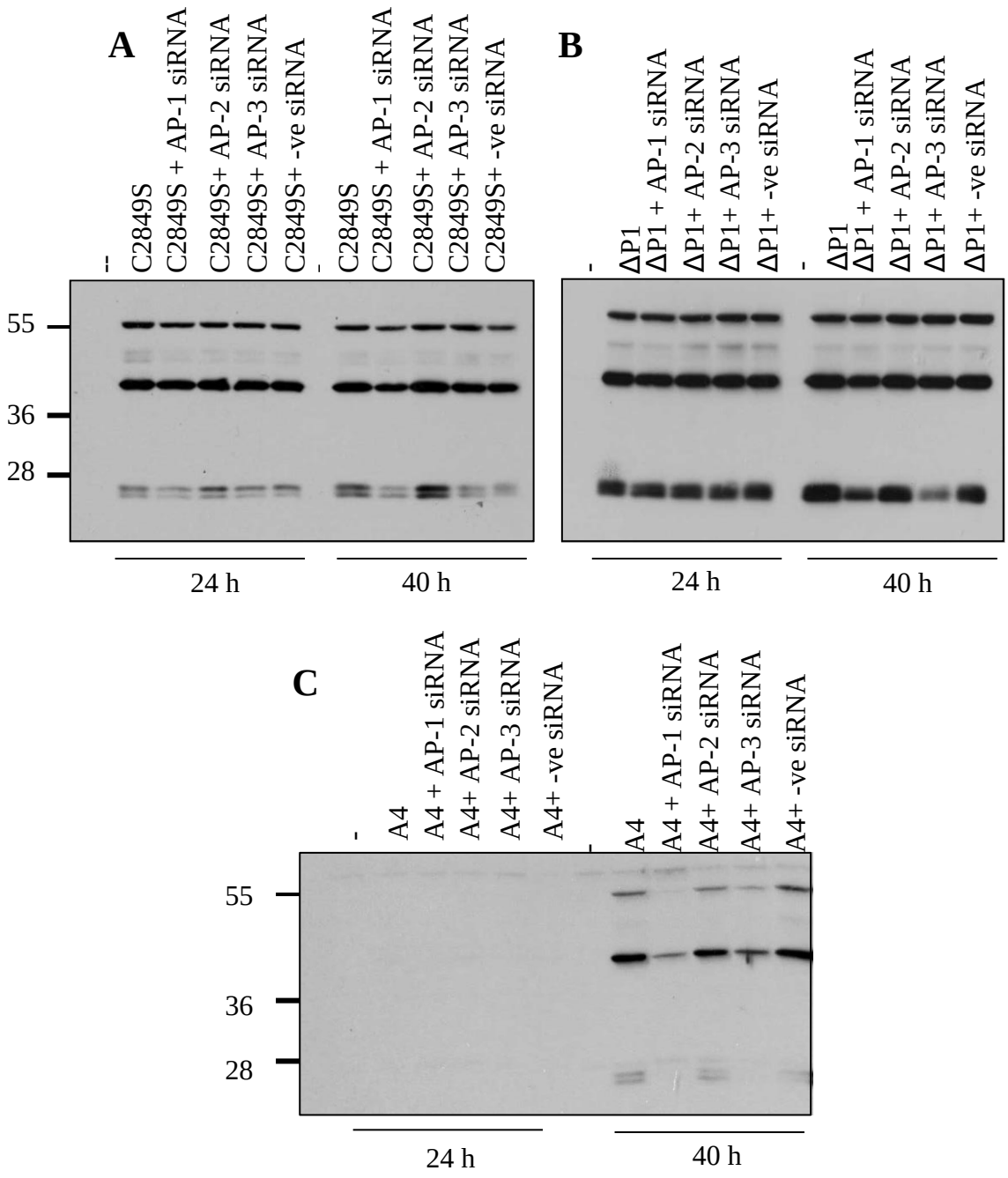

Figure 41: The effect of AP knockdown on Gag processing of packaging mutants. Western blots of cell samples 24 and 40h post co-transfection with AP siRNAs and C2849S (A), ΔP1 (B) and A4 (C) proviruses detected with anti-Gag p24 antibody.

not myristoylated (Miele et al., 1996). These 3 proviruses were co-transfected with the siRNAs, and collected cell lysates were analysed by Western blot. The results are shown in Figure 41.

These blots show that in the presence of AP-1 or -3 siRNA, despite still observing a decrease in processed p24, we did not see a corresponding increase in unprocessed p55 when the AP siRNA lanes were compared with the no siRNA lanes in each experiment (Figure 41A-C). This would indicate that negative feedback inhibition of Gag synthesis is not increased when AP-1 and -3 are absent. These results suggest that the absence of AP-1 or AP-3 does not result in increased accumulation of Gag at its site of synthesis. This is not attributable to an increase in viral egress since particle release is severely impeded/absent in these mutants (Dorfman et al., 1993; Miele et al., 1996; Harrison et al., 1998), which was confirmed by Western blot of viral supernatants (data not shown). One observation, however, is that when the myristoylation signal is absent in A4, Gag levels were very low (detectable only at 40 hours) and the absence of AP-1 or -3 further depleted the amount of Gag present within the cell. This would indicate a role of the myristoylation domain in Gag stabilisation.

5.2.4 Knockdown of AP-1 and -3 does not Increase Lysosomal/Proteasomal Gag Degradation

Another possible explanation for the disappearance of Gag in the presence of AP-1 and -3 siRNAs is that Gag may be being degraded as a result of a failure to be released. This hypothesis was tested using proteasome and lysosome inhibitors MG132 and ammonium chloride (NH_4Cl), respectively, on siRNA and HIV-1 co-transfected samples. The results are shown in Figure 42.

As this Figure shows, inhibiting either the proteasome (Figure 42A) or lysosomes (Figure 42C) did not increase the amount of Gag present when AP-1 or -3 were

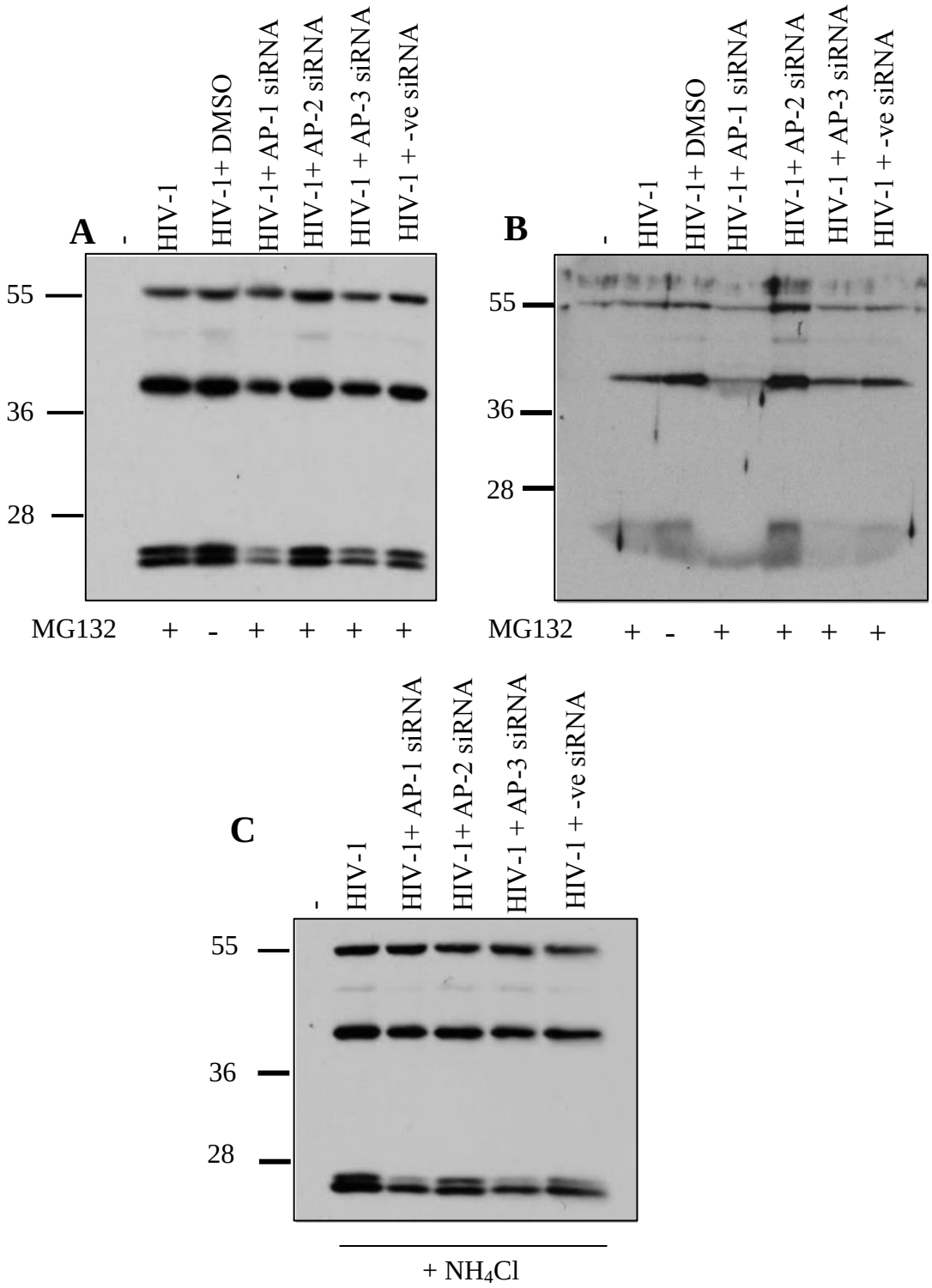

Figure 42: Absence of AP-1 or -3 does not cause an increase of Gag degradation by lysosomes or the proteasome. A- Western blot of cellular Gag levels after 2 hour MG132 treatment 40hours post siRNA and HIV-1 provirus co-transfection. B- Western blot of supernatant samples collected under the same conditions as A. C- Western blot of cellular Gag levels after 16 hour NH_4Cl treatment 40 hours post siRNA and HIV-1 provirus co-transfection.

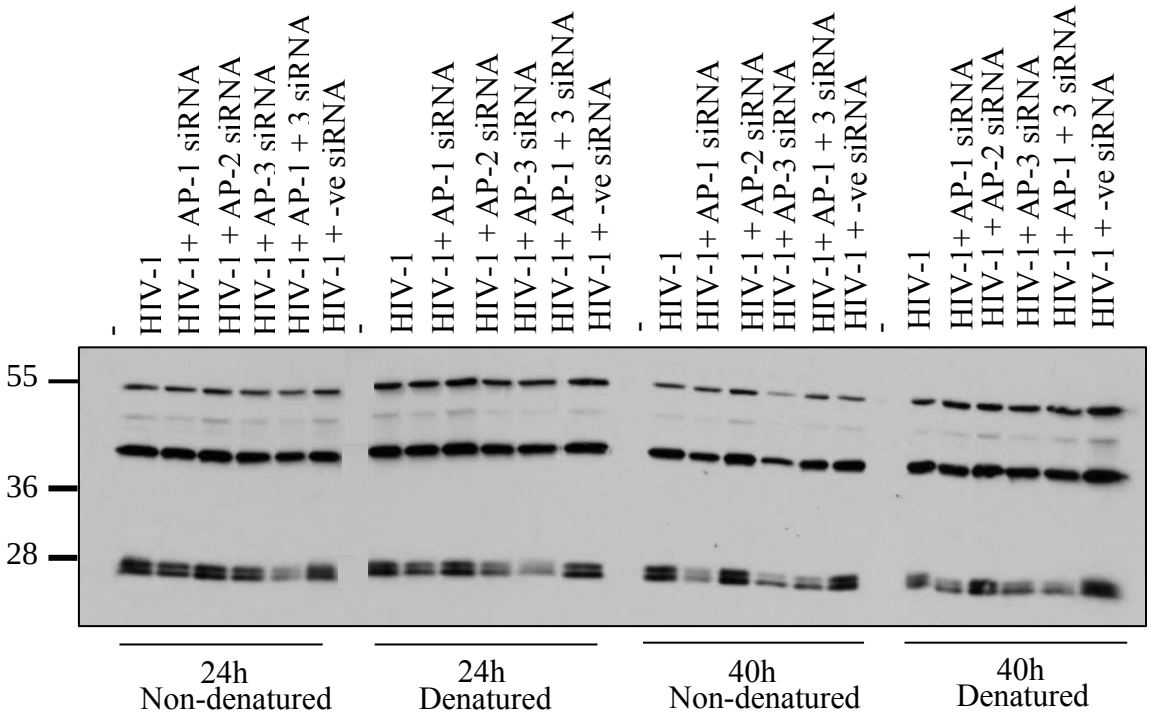

Figure 43: Absence of AP-1 or AP-3 does not cause Gag to aggregate in a way that cannot be recovered by passive lysis. Western blot of samples collected 24 and 40 hours post HIV-1 provirus and AP or negative control siRNA co-transfection in HeLa cells. Samples were either collected using only a passive lysis buffer (non-denatured) which excluded cellular debris, or using a passive lysis buffer followed by denaturation of the total sample including the cellular debris (denatured). Gag proteins were detected using an anti-Gag p24 antibody.

knocked down. Although controls were not used to ensure that either inhibitor were working, the supernatant samples collected from MG132 treated cells (Figure 42B) demonstrate that in the presence of MG132 (lane 1), viral release is decreased, as compared with the DMSO only control (lane 2). This would agree with the published results that the proteasome is required for viral release, and indicates that the inhibitor is exerting an effect and therefore is functioning (Schubert et al., 2000). Lysosomal and proteasomal degradation are, however, not the only forms of degradation found in the cell, so it still remains a possibility that Gag is degraded when it is unable to be released.

Another hypothesis that could explain the disappearance of Gag is that when AP-1 or -3 are knocked down, Gag may aggregate in such a way that it is not recovered by the method of lysis used, since only centrifuged supernatants are included, which excludes cellular debris such as membranes. Therefore, HeLa cells were co-transfected with the HIV-1 provirus and the AP siRNAs in duplicate; half of the samples were lysed as normal, whereas the other half were lysed followed by denaturation of the whole sample, including the cellular debris, using a "denaturing solution" (see chapter 2.2.9 for more details). The results are shown in Figure 43. As can be seen, no significant increase in p55 occurred in the denatured samples when AP-1 and -3 were knocked down, as compared with the non-denatured samples. While more total protein was harvested in the denatured samples, the pattern of p55, p41 and p24 Gag products in siRNA-treated cells was similar between denatured and non-denatured samples.

5.2.5 AP-5 Does Not Affect HIV-1 Assembly, Release or Localisation

A fifth adaptor protein complex has recently been discovered (Hirst et al., 2011). Intriguingly, the UniProt entry of the mu5 subunit lists "Putative HIV-1 interacting

protein" as an alternative name. The only related reference given, however, is a 1998 nucleotide entry of the partial mRNA sequence under the title "HIV-1 induced gene expression", author Li. F. Although we were unable to find any further published data to back this up, we decided to investigate whether AP-5 may play a role in HIV-1 Gag trafficking. We used siRNA mediated knockdown of the mu5 subunit of AP-5 as recently described (Hirst et al., 2011). Although a commercial antibody was available for this protein, it was unable to detect anything in HeLa cells, even at high protein concentrations (data not shown). Therefore, to investigate whether the siRNA did indeed reduce AP-5 levels, RT-qPCR was carried out of AP-5µ mRNA. Figure 44A demonstrates cDNA copies from non-quantitative RT-PCR run on an agarose gel, showing that visually AP-5µ mRNA is reduced in the presence of the siRNA. Results from qPCR are demonstrated in Figure 44B, which shows that the siRNA significantly reduces AP-5µ mRNA levels by 70%.

To investigate the effect of AP-5 on cellular and released Gag, 25 nM AP-5/-ve siRNA was co-transfected with HIV-1 provirus, and harvested cell and supernatant samples were analysed by Western blot. These are shown in Figures 45A and B. Visually, AP-5 had no effect on either Gag assembly or release. Repeat experiments were analysed by ImageJ, which revealed AP-5 had no significant effect on cellular or released Gag (data not shown).

Next, the effect of AP-5 knockdown on Gag localisation was investigated by confocal immunofluorescence microscopy. Figures 45 C, D and E show HIV-1 Gag in untreated, AP-5 treated, and –ve siRNA treated HeLa cells, respectively. Visually, no effect of AP-5 on Gag localisation could be observed. To quantify this, counts of Gag expressing cells were analysed for Gag localisation across repeat experiments. As Figure 45F shows, AP-5 knockdown did not significantly alter the localisation of HIV-1 Gag.

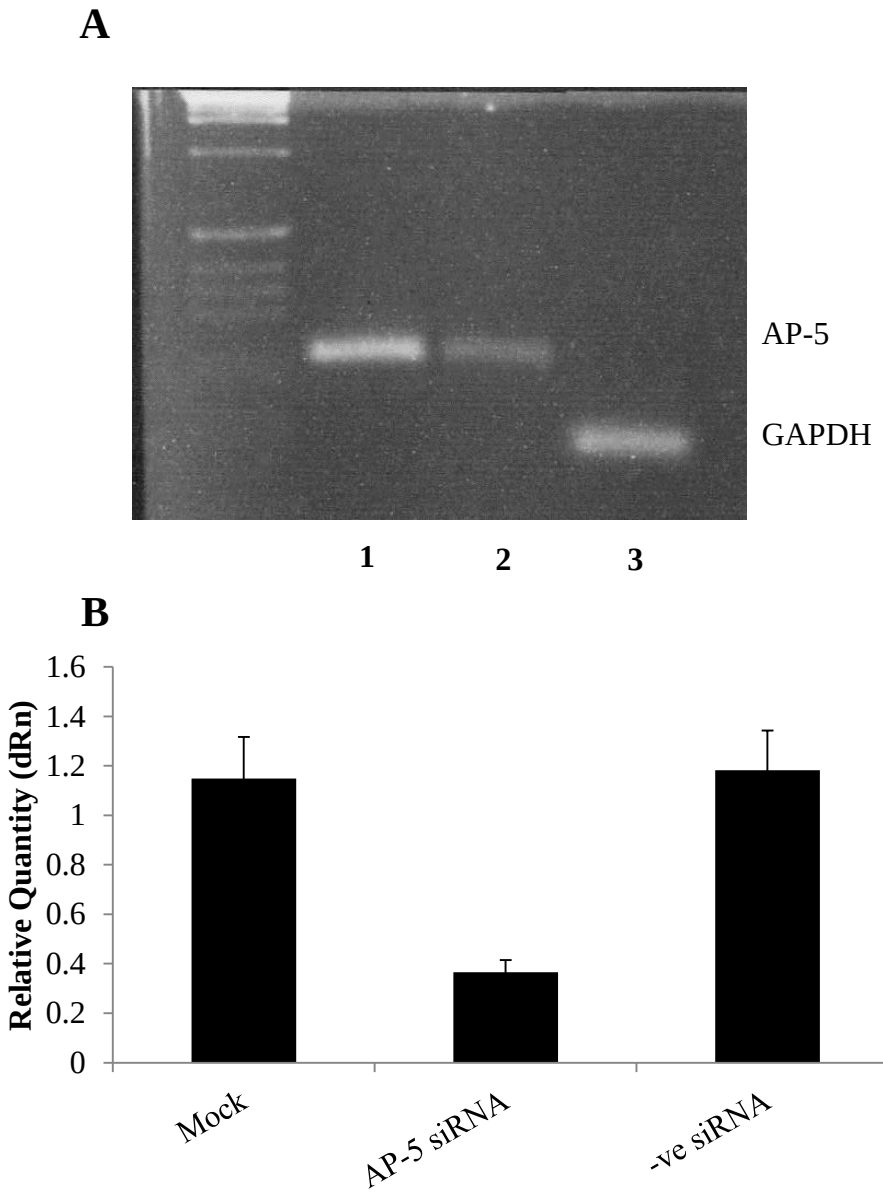

Figure 44: AP-5 knockdown by AP-5 siRNA. A shows an agarose gel of RT-PCR products. AP-5μ PCR product in the absence (lane 1) or presence (lane 2) of 24 nM AP-5μ siRNA. GAPDH PCR product in the presence of 25 nm AP-5μ siRNA. B- Relative quantity of AP-5μ RNA in HeLa cells transfected with no siRNA, AP-5μ siRNA, or negative control siRNA, as determined by RT-qPCR.

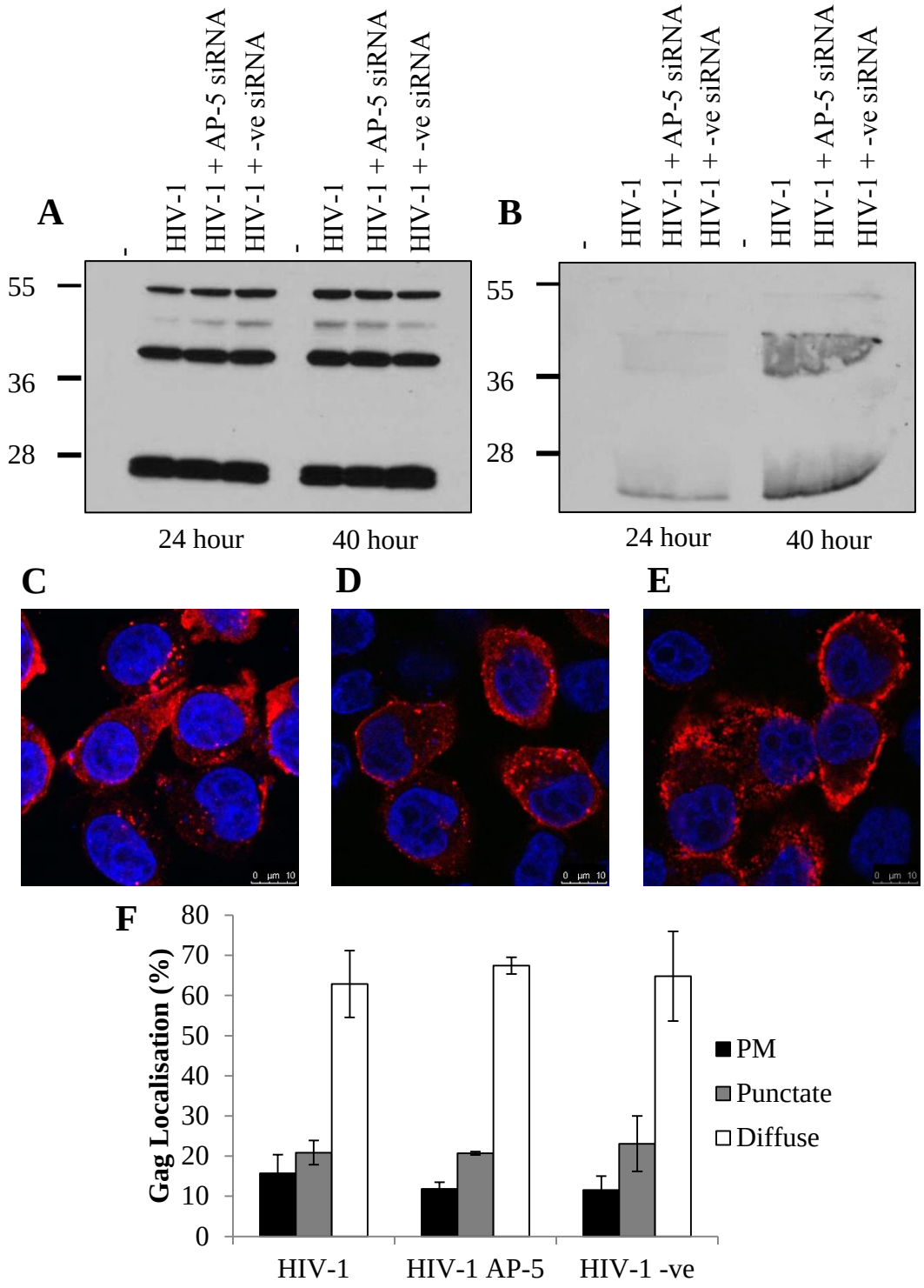

Figure 45: AP-5 does not affect HIV-1 Gag processing, release or localisation. A and B- Western blots of Gag from no siRNA, or AP-5/control siRNA and HIV-1 proviral co-transfections 24 and 40 hours post-transfection; cell (A) and supernatant (B) samples, respectively. C, D and E show confocal immunofluorescence images of HIV-1 Gag in untreated (C), AP-5 siRNA (D) and control siRNA (E) transfected HeLa cells. Gag localisation from 2 repeat experiments was quantified, and the data is shown graphically in F.

5.3 Discussion

This chapter aimed to investigate the roles of the APs in HIV-1 Gag trafficking and assembly further, and to investigate a potential role for the newly discovered fifth adaptor protein complex.

Evidence reported recently (Liu et al., 2012) and in this chapter support the hypothesis that HIV-1 Gag can traffic via endosomes to the PM. This is because when AP-3 is knocked down, we see a concomitant decrease in PM Gag staining, and an increase in punctate intracellular staining (Figure 38). This is suggestive of Gag becoming stuck in endosomal compartments in the absence of AP-3. One could postulate that this is because AP-3 is required for Gag to subsequently traffic from these compartments to the PM, which could involve directing Gag from early endosomal compartments to late endosomal compartments, which would then be recycled to the PM. This would also support a decrease in viral assembly/Gag processing (Figure 39), since if Gag is not arriving at the correct assembly sites, particles are unlikely to be able to form efficiently. It is possible that AP-3 may assist in the trafficking of Gag to the PM in a similar manner to how AP-3 was found to assist in the trafficking of VSV-G (Nishimura et al., 2002).

Although there remains some discrepancy over the exact trafficking pathway that AP-3 facilitates, studies using naturally occurring AP-3 mutants have shown that AP-3 does indeed facilitate the trafficking of cargo toward the LE/lysosome, because lysosomes and lysosome-related organelles such as melanosomes are affected. It was found that the AP-3 pathway begins from EE-associated tubules (Peden et al., 2004). However, these studies have also shown that AP-3 is not absolutely required for this pathway to function, because AP-3 mutants are not embryonic lethal, and some lysosomal cargo

can still reach lysosomes/lysosome-related organelles in the absence of AP-3. What is also interesting is that in an absence of AP-3, alongside a fraction of cargo still being able to reach melanosomes, there was a concomitant increase in endosomal-associated AP-1. This indicates that AP-1 and AP-3 may function in partially redundant pathways (Theos et al., 2005). Therefore, it is evident that compensatory pathways may be adopted in the absence of AP-3; this could explain why not all Gag becomes punctate when AP-3 is knocked down, and why AP-3 knockdown does not entirely abolish Gag release. While the results gathered in this chapter with respect to AP-3 in Gag trafficking contradict those gathered by Dong et al. (2005), who found that AP-3 knockdown caused an increase in diffuse (cytosolic) Gag in the same cell line (HeLa), our results do make sense in that when AP-3 is knocked down, Gag accumulates upstream of AP-3 function, perhaps in early endosomes. This could explain the punctate appearance of Gag observed. The harsher knockdown of AP-3 utilised by Dong et al. (2005) may explain differences with our results.

AP-1 knockdown presented an interesting Gag phenotype. Although PM staining was decreased significantly, unlike when AP-3 was knocked down, an increase in punctate Gag was not observed (Figure 38). This would infer the possibility that AP-1 and -3 function in different stages of Gag trafficking, which would make sense since they function in different cellular pathways, although there is some overlap. We could envisage an earlier role for AP-1 in driving newly synthesised Gag into endosomal compartments, likely from the TGN, followed by the delivery of Gag from these compartments to the PM by AP-3 in an indirect manner. This is because the human ubiquitin ligase POSH, which functions at the TGN, was found to positively affect Gag release (Alroy et al., 2005); therefore it may be that after Gag ubiquitination at the TGN, Gag is directed to endosomes by AP-1. It is also possible, however, that in

instances whereby endosomal trafficking is bypassed, AP-1 delivers Gag straight to the PM and assists particle assembly here. This would explain the lack of PM staining observed, but also the very diffuse phenotype.

Interestingly, it was discovered that AP-2 has no effect on Gag localisation (Figure 38). AP-2 is thought to assist in the clathrin-mediated endocytosis of plasma membrane associated particles, and its knockdown results in an increase in viral particle release. But our data suggest that AP-2 plays no role in intracellular Gag trafficking or particle assembly.

Data gathered in this chapter from Western blot of cellular protein samples revealed that when AP-1 and -3 were reduced, less processed p24 Gag was also present (Figure 39). This would infer that these APs facilitate particle assembly, since you would not expect to see processed Gag until particle assembly begins. This is because GagPol multimerisation at assembly sites is a pre requisite for Protease activity. It could be assumed that the decrease in p24 is merely a result of a perturbation of Gag trafficking, whereby particles do not reach assembly sites and therefore cannot begin to assemble. However, if this were the case, we would expect to see a corresponding increase in unprocessed p55.

Three hypotheses were postulated as an explanation for Gag disappearance in the absence of AP-1/-3; Gag accumulation results in an increase in Gag translation inhibition, Gag is degraded by the proteasome/lysosomes, Gag may aggregate in such a way that cannot be recovered by passive lysis.

To investigate the first hypothesis, 3 mutants were used which are unable to package RNA, and therefore are unable to inhibit Gag translation by obstructing ribosomal scanning. It was found that in the presence of AP-1/3 siRNAs, unprocessed Gag was

not increased, despite still seeing a reduction in processed Gag (Figure 41). Therefore, it is apparent that when Gag is unable to traffic to assembly sites in the absence of AP-1/3, Gag does not likely accumulate at translation sites and therefore switch off its own translation. A possible explanation for this is that Gag may initially accumulate when it cannot be trafficked, but that it is rapidly degraded by the cell, and therefore does not build up around translation sites. Therefore, no effect will be seen.

The second hypothesis to be tested was that Gag may be being degraded when it cannot be assembled and processed into viral particles. This would support previous suggestions that clathrin may stabilise Gag processing products (Zhang et al., 2011); in the absence of AP-1/3 we could propose that clathrin is unable to be recruited to assembly sites and therefore assist in the formation of viral particles. Two potential degradation pathways were tested; lysosomes and proteasomes. Some conflicting results exist for the role of the proteasome in the viral life cycle; it has been suggested that both lysosomes and the proteasome are capable of destroying HIV and therefore decrease viral infectivity (Wei et al., 2005), however another group suggest that the proteasome is required for processing, release and maturation (Schubert et al., 2000).

Results gathered in this chapter, although supporting a role for the proteasome in viral release, did not suggest that degradation by these pathways is increased when particles cannot assemble (Figure 42). This was particularly surprising since this seemed the most logical explanation for the disappearance of Gag. It must be pointed out, however, that MG132 (and indeed all proteasome inhibitors) is only functional for up to 2 hours, before cellular compensatory mechanisms prevent its efficacy. Therefore, it is entirely possible that the Gag had already been degraded prior to MG132 addition, meaning we saw no effect of the inhibitor. This is may not be the most appropriate assay to investigate proteasomal degradation, and so it remains possible that proteasomal

degradation of HIV-1 may indeed increase upon cellular accumulation when viral release is prevented by AP knockdown. A pulse chase assay could be considered in future experiments, as this is a more effective way of investigating protein stability, rather than only looking at steady-state levels.

To investigate whether the disappearance of Gag could be attributed to Gag aggregates that are not recovered by the method of lysis used, cellular debris including membranes was included and denatured in samples which were then analysed by Western blot. Unfortunately, since no increase in Gag was seen in these samples in the presence of AP-1 or -3 siRNAs when compared to non-denatured controls (Figure 43), we can rule out the likelihood of this hypothesis.

Some evidence gathered by other groups which may explain the disappearance of Gag relate to the role of clathrin in the HIV life cycle. Zhang et al. (2011) suggested that clathrin is responsible for regulating the activity of protease, or alternatively stabilises the products of Gag proteolysis during particle morphogenesis. In the absence of AP-1/-3, we would expect the recruitment of clathrin to be compromised. Therefore, this could explain why we see less processed Gag, and why we do not see a corresponding increase in p55 when these proteins are knocked down. How precisely Gag is degraded, or rendered undetectable, however, remains unsolved.

A reasonable model that can be drawn from our data and that of others is that the APs assist particle assembly, likely by first directing Gag towards appropriate membranes, which may involve an endosomal intermediate, and then directly facilitating particle assembly. This may be by binding to and facilitating clathrin formation around membrane-bound Gag and promoting particle formation via recruitment of further proteins required for clathrin scaffold formation and disassembly, such as epsins.

AP-5 has been recently characterised as an adaptor protein complex associating with late endosomes; however, it does not associate with clathrin. Although AP-5µ had been suggested to have role in the HIV-1 life cycle, no evidence for this is published, and we found no influence of AP-5 on HIV-1 trafficking (Figure 45). This would suggest that HIV-1 does not require late endosomes in its trafficking pathway. Since AP-5 does also not associate with clathrin, it makes sense that reducing AP-5 does not affect Gag assembly, since we can assume that this will not affect clathrin function.

5.4 Future Work

Although the most likely explanation for the disappearance of Gag in the absence of AP-1/-3 seems degradation, this could not be ascertained. Limitations imposed by the short window of efficacy of MG132 may be the reason that we did not see an increase in Gag; therefore a pulse chase assay whereby protein synthesis and turnover in the presence/absence of MG132 would be a more appropriate assay for future experiments. The use of proteasome inhibitors, however, is not the only method which can be applied to inhibit proteasomal degradation. Therefore, an appropriate way to take this section further would be to inhibit ubiquitination, for example via the use of ubiquitin ligase inhibitors such as SMER 3, which inhibits E3 ubiquitin ligase.

Another interesting set of experiments which could follow on from this data would be to use a clathrin siRNA. Gag phenotypes across AP and clathrin knockdown could be compared, which may give further insight into whether it is likely clathrin destabilisation which causes both a disappearance of unprocessed and processed Gag. However knockdown of clathrin may have a severe effect on cell function.

CHAPTER 6: INVESTIGATING HIV-2 TRAFFICKING AND THE ROLE OF THE MATRIX DOMAIN IN HIV-1 AND HIV-2 TRAFFICKING

6.1 Introduction

As mentioned in Chapter 1, multiple interspecies introductions from simian species gave rise to two genetically distinct HIV viruses; HIV-1 and HIV-2. Genomic analysis deduced that HIV-2 is closely related to the simian immunodeficiency virus (SIV) of sooty mangabeys (SIVsm), inferring this is the species responsible for the introduction of HIV-2 into the human population (Lemey et al., 2003). Although the HIV-1 groups are distributed globally, albeit different clades dominate in different geographical regions, HIV-2 is almost exclusively found in Western Africa, although infections have been described in Europe and America (Campbell-Yesufu and Gandhi, 2011). HIV-2 is categorised by either epidemic subtypes (A and B) or non-epidemic subtypes (C-H) (Lemey et al., 2003). All HIV-1 subtypes and HIV-2 A and B have established human-human transmission chains (Wertheim and Worobey, 2009). The non-epidemic subtypes have only been isolated from single individuals, and are "dead-end" viruses; they are weakly pathogenic, replicate poorly and are not transmissible to other humans. They are also exclusively found within the range of the sooty mangabey, for example HIV-2 subtype F was found in one individual among over 9,000 living in the same area of Sierra Leone, where SIVsm is found naturally within the sooty mangabey population (Marx et al., 2001).

Although these two viruses are closely related, HIV-2 is less pathogenic than HIV-1. Heterosexual transmission is less efficient in HIV-2, and vertical transmission rarely occurs. HIV-2 infected individuals progress to AIDS at a slower rate than those infected with HIV-1; around 95% of HIV-2 infected individuals are classified as long-

term non-progressors 8 years after infection. It was initially assumed that this may be related to proviral levels, which were assumed to be lower in individuals infected with HIV-2; interestingly, this was found not to be the case, and proviral levels are in fact similar in both HIV-1 and HIV-2 infected individuals. It was discovered, however, that the viral load remains relatively stable even years after initial infection, which is consistent with a lack of disease progression, and similar to the trends seen in long-term nonprogressors (Popper et al., 1999; de Silva et al., 2013).

Although similar proviral levels have been observed in HIV-1 and HIV-2 infected patients, it was discovered that plasma viraemia, or plasma RNA, levels were much lower in HIV-2 patients (Simon et al., 1993). Furthermore, in a study carried out on HIV-2 infected patients in Portugal, it was found that plasma viral load also correlated with $CD4^+$ cell levels (Soriano et al., 2000). It was also discovered that plasma viral load levels were correlated with disease progression, whether the patient was infected with either HIV-1 or HIV-2 (Gottleib et al., 2002). In a study investigating both HIV-1 and HIV-2 infected AIDS patients in a West African clinic, it was found that HIV-2 AIDS patients had higher CD4 levels, even at the time of death, suggesting that a loss of CD4 cells does not provide a complete story for the immune pathology in infected individuals (Martinez-Steele et al., 2007; Nyamweya et al., 2013).

Therefore, a scenario has emerged whereby there are two distinct groups of HIV-2 infected individuals; the first is individuals with low plasma viral load, who have mortality rates similar to that of the background rate of the population. This is highlighted by a cohort study of HIV-2 infected individuals in Caio, Guinea Bissau, where low and stable plasma viraemia levels were present in the population, and 37% had less than 100 RNA copies per ml, with a concomitant high percentage of $CD4^+$ cells. Infected individuals also had the same mortality rate as the uninfected control

group (Berry et al., 2002; Nyamweya et al., 2013). A similar study found that HIV-2 infected patients with undetectable viral load also had normal survival rate, indicating this could be a predictor for survival (Schim van der Loeff et al., 2012). The second group contains HIV-2 infected individuals who have a high viral load (>10,000 copies per ml), and consequently progress to AIDS at a similar rate to HIV-1 infected individuals (Martinez-Steele et al., 2007).

Several possible explanations have emerged for the lower levels of plasma viraemia in HIV-2 patients, including tighter transcriptional control and a weaker ability to evade immune responses. For example, a study found that HIV-1 and HIV-2 had similar levels of integration, but that HIV-2 produced lower amounts of mRNA, which is consistent with lower plasma viraemia levels observed (MacNeil et al., 2007). Differences in the LTRs between HIV-1 and HIV-2 have also been observed, which could contribute to lower levels of mRNA expression (Guyader et al., 1987; de Silva et al., 2008). With regards to the immune system. it has been suggested that HIV-2 may be more susceptible to broadly neutralising antibodies than HIV-1, perhaps due to a more open V3 domain in the envelope (Shi et al., 2005). It was also discovered that HIV-2 is controlled by the restriction factor tripartite motif protein isoform 5 alpha (TRIM5α) to a greater extent than HIV-1 (Ylinen et al., 2005).

Since they are closely related, HIV-1 and HIV-2 have a similar genome composition and organisation, although differences can be observed. See Figure 46 overleaf for a schematic of the HIV-1 and -2 genomes.

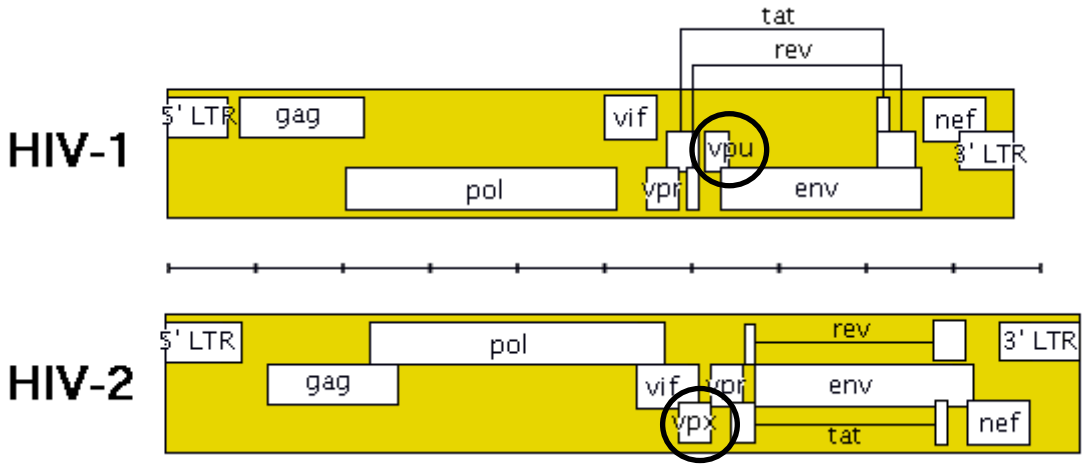

Figure 46: HIV-1 and HIV-2 genome organisation. Note the presence of *vpu* in HIV-1, and *vpx* in HIV-2.

(Source: adapted from http://www.mcld.co.uk/hiv/?q=HIV%20genome, accessed June 2013)

As this figure shows, HIV-2 does not possess *vpu*, but instead has a *vpx* gene. The Vpx protein encoded by this gene was found to antagonise the restriction factor SAMHD1 by enhancing its proteasomal degradation. SAMHD1 is expressed in myeloid and dendritic cells; HIV-1 is unable to counteract SAMHD1, rendering HIV-1 replication in dendritic cells severely impaired (Laguette et al., 2011). SAMHD1 was found to deplete the pool of dNTPs to levels lower than those required for DNA synthesis during reverse transcription (Laguette et al., 2011).

Like HIV-1, HIV-2 Gag is synthesised as a polyprotein which is later cleaved during maturation. HIV-2 Gag is, however, 57 kDa, as oppose to 55 kDa in HIV-1 (Luo et al., 1990), but is still cleaved into the same constituent mature structural proteins of MA, CA, NC and p6. Despite their similarity, only ~60% amino acid sequence identity has been found between HIV-1 and -2 Gag, and only 40% genome nucleotide identity (Dilley et al., 2011). It has been established that HIV-2 is more closely related to the simian immunodeficiency viruses than HIV-1; *gag*, *pol* and *env* proteins of SIV and HIV-2 were found to be antigenically cross reactive, whereas cross reactivity to the

corresponding HIV-1 proteins are restricted to only certain antigens (Guyader et al., 1987).

As mentioned in the previous chapter; the current theories surrounding HIV Gag trafficking are incomplete. More specifically, it is assumed that HIV-1 and -2 Gag follow similar trafficking pathways, although this has never been established.

Early electron microscope images of HIV-1 found that assembly differs in two natural host cell types; T cells and macrophages. It was found that in the former, HIV-1 is found predominantly budding from the plasma membrane (PM), where Gag recruits ESCRT proteins away from multivesicular bodies (MVBs), whereas in the latter, abundant ESCRT components at MVBs can permit budding within these intracellular compartments, or MVB-like organelles rich in tetraspanins such as CD81 that are continuous with the PM (Raposo et al., 2002; Deneka et al., 2007; Welsch et al., 2007). Amino acid substitutions in the basic region of MA were found to retarget Gag from the PM to MVBs in HeLa cells and COS cells, but did not affect the localisation to MVBs in macrophages. These MA mutations were also found to lead to less efficient particle release from HeLa cells, but not from macrophages; together these results were suggestive of the presence of an alternative pathway whereby Gag was directed to MVBs. Further evidence also ruled out the possibility that the presence of Gag in MVBs was merely a result of internalisation of released virions (Ono and Freed, 2004).

The purpose of this chapter is to further investigate the role of the MA domain in Gag trafficking and localisation, since it is this region which was found to both contain the AP binding sites, and also determine preference for intracellular budding sites of HIV-2. Does HIV-2 follow the same trafficking pathway as HIV-1? Are the same interactions with the APs present in HIV-2 Gag? Does the MA region of Gag determine the localisation of both HIV-1 and HIV-2?

6.2 Results

6.2.1 Adaptor Proteins 1 and 3 Affect HIV-2 Particle Assembly and Release

Throughout this chapter, when siRNAs have been used with proviral constructs, they have been co-transfected at the same time. To investigate whether HIV-2 interacts with the APs in the same manner as HIV-1, HeLa cells were co-transfected with the AP siRNAs and a HIV-2 proviral construct (SVRΔNB); this provirus is once again *env* deleted. Cell lysates were harvested at both 24 and 40 hours post transfection, and analysed by Western blot with anti-SIV p27 antibody (which recognises HIV-2 CA). Viral supernatants were not harvested for this provirus since in the absence of Env, HIV-2 particle release is inefficient. Therefore, wild-type (WT) HIV-2 (SVR) was also utilised to analyse viral supernatant samples; cellular samples were also taken for comparative measures. Results are shown in Figure 47.

As can be seen, in a similar manner to HIV-1, at 24 hours, little effect was seen on both cellular HIV-2 Gag samples, except when AP-1 and -3 siRNAs were used together. At 40 hours, however, a slight decrease in p57 (full-length unprocessed HIV-2 Gag) and p27 (fully processed CA) could be seen in the presence of AP-1 siRNA. When AP-3 siRNA, or AP-1 and -3 siRNAs together were used, p57 was reduced to a greater extent than in the presence of AP-1 siRNA. AP-2 siRNA had no observed effect on HIV-2 cell samples, as with HIV-1. The third panel demonstrates that the effect was not due to a decrease in total protein, or errors in loading, since the endogenous protein γ-tubulin remained even.

Interestingly, viral supernatant samples presented a slightly different story to that of HIV-1. As the bottom panel in Figure 47 clearly shows, AP-2 knockdown did not cause an increase in HIV-2 particle release. AP-1 siRNA had a slight effect on particle

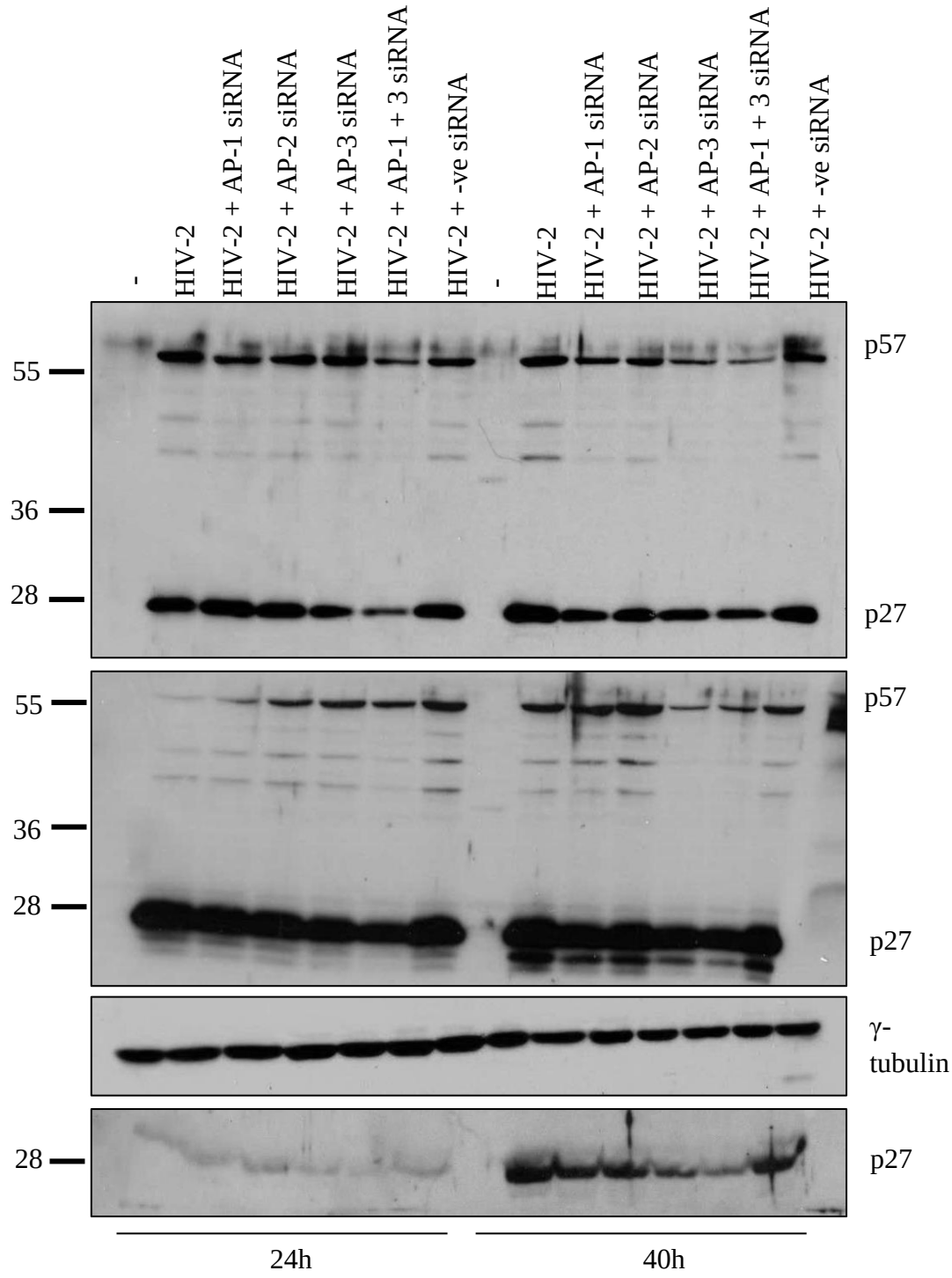

Figure 47: The adaptor proteins affect HIV-2 Gag processing and release. Western blots of cell lysate (top and second panel) and viral supernatant (bottom panel) samples using an anti-SIV p27 antibody, harvested following 24 and 40 hour transfection of HeLa cells with HIV-2 provirus and AP or control. *env* deleted HIV-2 (SVRΔNB) was used for the top panel, WT HIV-2 (SVR) was used for second panel and viral supernatant (bottom) samples. The third panel shows SVRΔNB cell lysate samples detected with an anti-γ-tubulin antibody.

release, causing a modest decrease in p27. AP-3 siRNA, or AP-1 and -3 in combination, caused a larger decrease in particle release.

In order to quantify this data, densitometry was carried out using ImageJ on three repeat SVRΔNB experiments only, and the results are shown in Figure 48. Figures 48A and B show data from 24 and 40 hour cell samples, respectively. Similar to HIV-1, the only significant effect seen at 24 hours was when AP-1 and -3 were used together, however, it was unprocessed Gag (p57) which was significantly reduced, rather than processed Gag (p27), which was the case for HIV-1. At 40 hours, AP-1 siRNA significantly reduced both p57 and p27 by 25% ($p<0.05$). AP-3 siRNA treatment, however, had a larger effect than AP-1, and significantly reduced p57 and p27 by 50% and 35%, respectively ($p<0.005$). When AP-1 and -3 siRNAs were used in combination, an even bigger effect was seen on p57 and p27; a 68% and 46% reduction, respectively ($p<0.001$). These results would indicate that although both AP-1 and AP-3 play a role in the HIV-2 life cycle, that AP-3 likely plays a more important role, perhaps in facilitating particle assembly. Alternatively, it may mean that AP-1 and AP-3 play roles at different stages of the HIV-2 life cycle.

Figure 48C shows densitometry results from 40 hour viral supernatant samples. Although particles could be sometimes observed at 24 hours, bands were inadequate to analyse and were therefore excluded. This Figure shows a similar story to that of the cell samples; AP-1 had a small but significant impact in facilitating particle release, whereas AP-3 plays a larger role. AP-1 siRNA treatment resulted in a modest (25%) reduction in p27 release ($p<0.05$). Although AP-2 siRNA treatment caused a 22% reduction in particle release, this was found to not be statistically significant ($p>0.05$). AP-3 siRNA treatment resulted in a much larger reduction in particle release; 77% less than when no siRNA was used ($p<0.005$). Again, when AP-1 and -3 siRNAs were

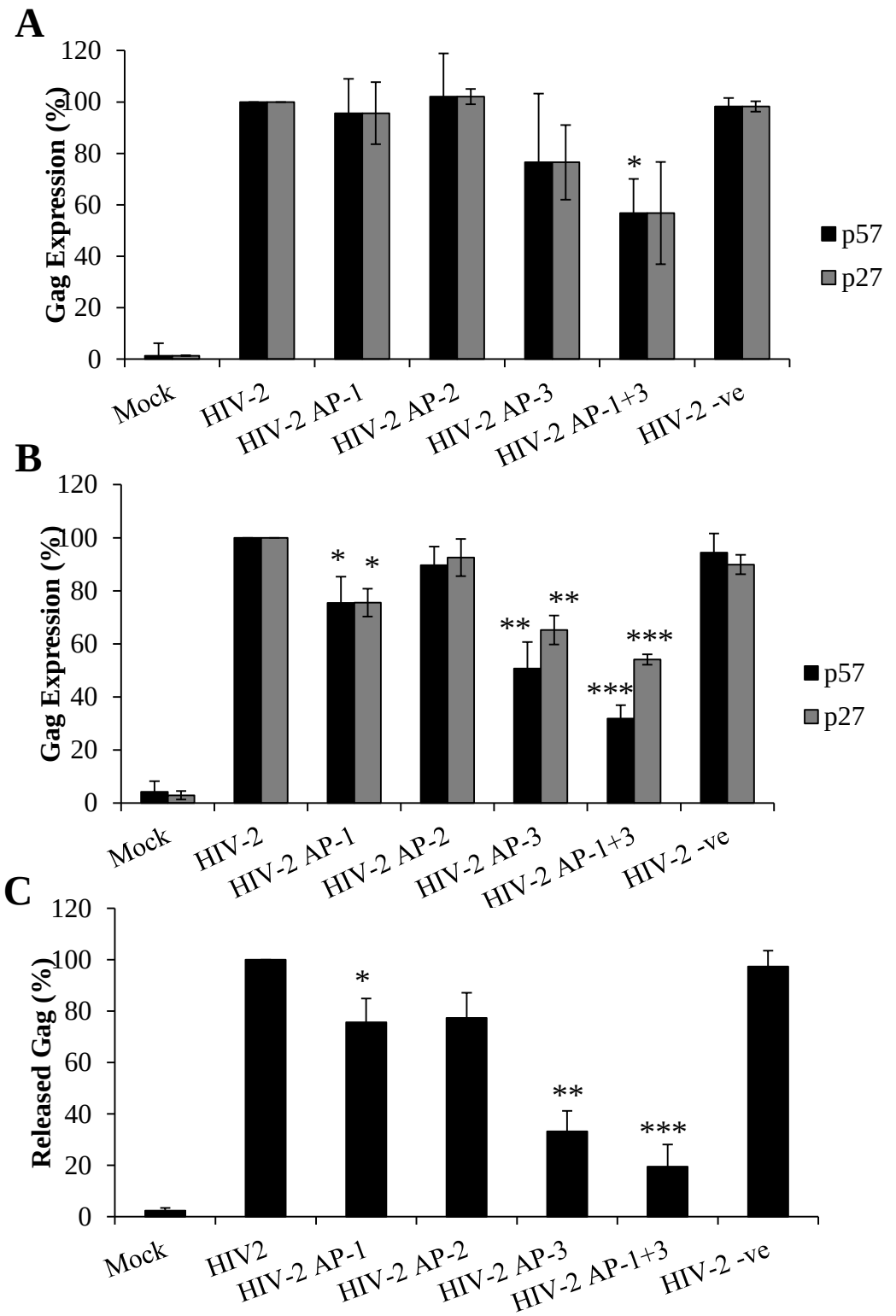

Figure 48: AP-1 and -3 assist HIV-2 particle processing and release. Densitometry was performed on bands from western blots using ImageJ, to calculate Gag levels obtained from independent repeat experiments. A and B- Gag p57 and p27 levels from 24 and 40 hour post-transfection cell lysate samples, respectively. C- p27 levels from 40 hour post-transfection viral supernatant samples. Results shown are percentages of Gag expression with no siRNA treatment. (Key: *=p<0.05, **=p<0.005, ***=p<0.001).

added together, a larger effect was seen than when the siRNAs were used alone; an 81% decrease in particle release was observed ($p<0.001$).

Together these results suggest that although AP-1 clearly plays a role in the HIV-2 life cycle, AP-3 likely plays a more essential role. Since AP-3 functions along the endosomal pathway, this may indicate that HIV-2 traffics via endosomes to reach intracellular assembly or release sites.

6.2.2 Absence of AP-1 or -3 does not Increase Lysosomal/Proteasomal HIV-2 Degradation

Since it is evident that knockdown of AP-1, and particularly AP-3, caused a decrease in total HIV-2 Gag, one possible explanation for this seemed degradation. Although HIV-1 was found not to be degraded by lysosomes/proteasomes when AP-1/-3 were absent, the effect observed on HIV-1 was less dramatic than with HIV-2. Therefore, the same protocol as before was followed whereby the lysomotropic NH_4Cl or the proteasome inhibitor MG132 were added to AP siRNA/HIV-2 co-transfected HeLa cells for either 16 or 2 hours, respectively. Cell samples were harvested at 40 hours and were analysed by Western blot. The results are shown in Figures 49 A and B.

As both of these Figures demonstrate, no significant increase in HIV-2 Gag steady state levels was observed in the presence of these inhibitors, when AP-1/-3 were knocked down. This would again indicate that the reduction in Gag observed is not mediated by these degradation pathways. However, no controls were performed to confirm these treatments were effective under the conditions used.

Since MG132 was only used for 2 hours, the experimental design of checking steady state levels is flawed. To get around this, a pulse chase immunoprecipitation was carried out on AP-1/-3 siRNA and HIV-2 provirus co-transfected HeLa cells. MG132

was added to the cells during the methionine starvation period prior to the pulse, during a 40 minute pulse with ^{35}S-methionine, and again during a 2 hour chase with cold methionine. HIV-2 Gag was then immunoprecipitated from the cell lysates, run on SDS-PAGE and exposed to a film to visualise the fate of HIV-2 Gag synthesised during the pulse period. Figure 49C shows the results of the pulse chase.

This Figure demonstrated that the proteasome may degrade HIV-2 Gag, as there was more HIV-2 Gag present in lanes where MG132 was added, as compared with the DMSO control. As is also evident, the proteasome is essential for Gag proteolytic processing, as lanes containing MG132 showed much less p27 than the DMSO only lanes. This supports the current literature on the roles of the proteasome on the HIV-2 life cycle (Schubert et al., 2000). When pulse and chase lanes are compared, it is evident that the signal in all of the chase lanes is weaker than in the pulse lanes; this would infer that the inhibitor only has a weakly stabilising effect. What was also once again clear was that in the presence of AP-1/-3 siRNAs, the level of HIV-2 Gag was still less than in the untreated or negative control siRNA treated cells. Therefore, it is currently not clear as to what happens to Gag when AP-1 and AP-3 levels are reduced. A time course with more chase points would likely give more clear-cut results.

In chapter 5.2.4, it was suggested that in the presence of AP-1 or -3 siRNAs, HIV-1 Gag may form aggregates that are not recovered by passive lysis, for example because they are collected as cellular debris which is excluded from samples used for Western blot analysis. To investigate this in HIV-2 transfected cells, the same protocol was followed as for HIV-1 but using the HIV-2 provirus, but once again no more Gag was recovered in samples which included denatured cellular debris (data not shown).

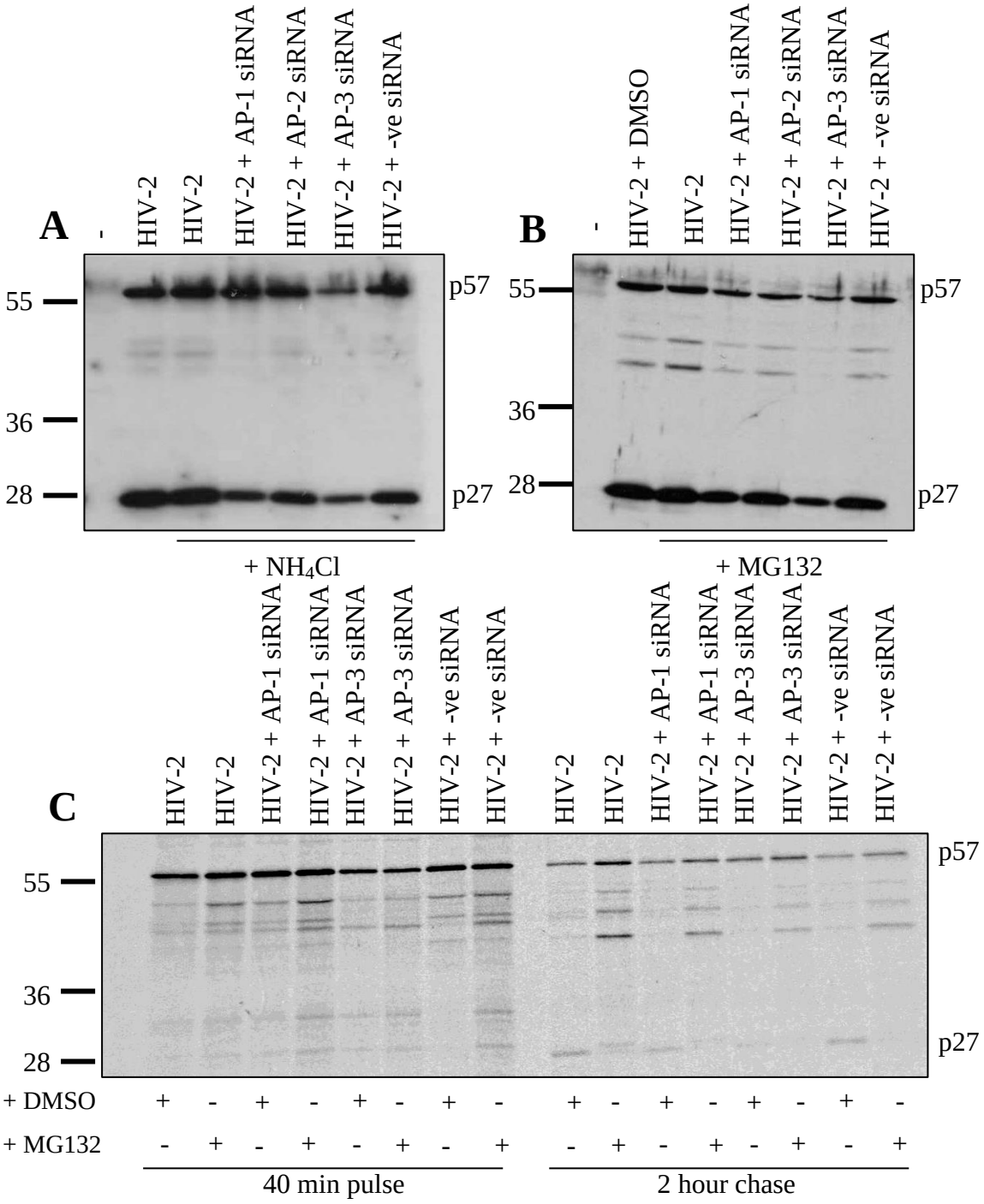

Figure 49: HIV-2 Gag processing in the presence of lysosome and proteasome inhibitors. Western blots of cellular HIV-2 Gag levels in HeLa cells co-transfected with HIV-2 provirus and the AP or negative control siRNAs, after 16 hour treatment with a lysosome inhibitor (NH_4Cl) (A) or after 2 hour treatment with the proteasome inhibitor MG132 (B), harvested at 40 hours, using an anti-SIV p27 antibody. C- HIV-2 Gag levels during a pulse chase assay in transfected HeLa cells, whereby MG132/DMSO control was added during the pulse, and again during the chase. IP was carried out using anti-SIV p27.

6.2.3 The Effect of AP-1 and -3 on HIV-2 Gag Localisation

As mentioned in chapter 5, HIV-1 Gag displays 3 typical cellular distributions; diffuse, punctate intracellular, and plasma membrane (PM), with diffuse being the most abundant. To investigate whether HIV-2 Gag follows the same pattern, envelope deleted HIV-2 (SVRΔNB) transfected HeLa cells were stained with anti-SIV p27 antibody and viewed under the confocal microscope. Figures 50A and B demonstrate the 2 typical Gag localisations found in HIV-2 transfected cells. As can be seen, HIV-2 Gag was either very punctate or localised strongly to the PM. HIV-2 Gag was never found to be diffuse, unlike HIV-1. Gag localisation was recorded in cells across 3 repeat experiments, and the average localisation is shown graphically, shown in Figure 50C. As can be seen, HIV-2 Gag had a very different localisation to that of HIV-1; instead of diffuse being the predominant pattern observed, HIV-2 Gag was mainly punctate (74%). HIV-1 and -2 have fairly similar percentages of PM Gag, although HIV-2 has a slightly higher percentage (24% vs. 16%).

This very punctate distribution would support the results previously obtained by Western blot, which indicate a role of AP-3 in the HIV-2 life cycle. Since we would expect that if Gag was accumulating in endosomes, or endosomal structures, we would see aggregates of Gag, therefore explaining the punctate staining.

To investigate whether AP knockdown affects HIV-2 localisation, siRNA and HIV-2 provirus co-transfected HeLa cells were investigated by confocal immunofluorescence microscopy as before. The results are shown in Figure 51.

AP-2 siRNA had no visual effect on HIV-2 Gag. This means that the punctate appearance of Gag is likely not a result of clathrin-mediated endocytosis budding or membrane-linked viral particles, which would be assisted by AP-2. Some PM staining

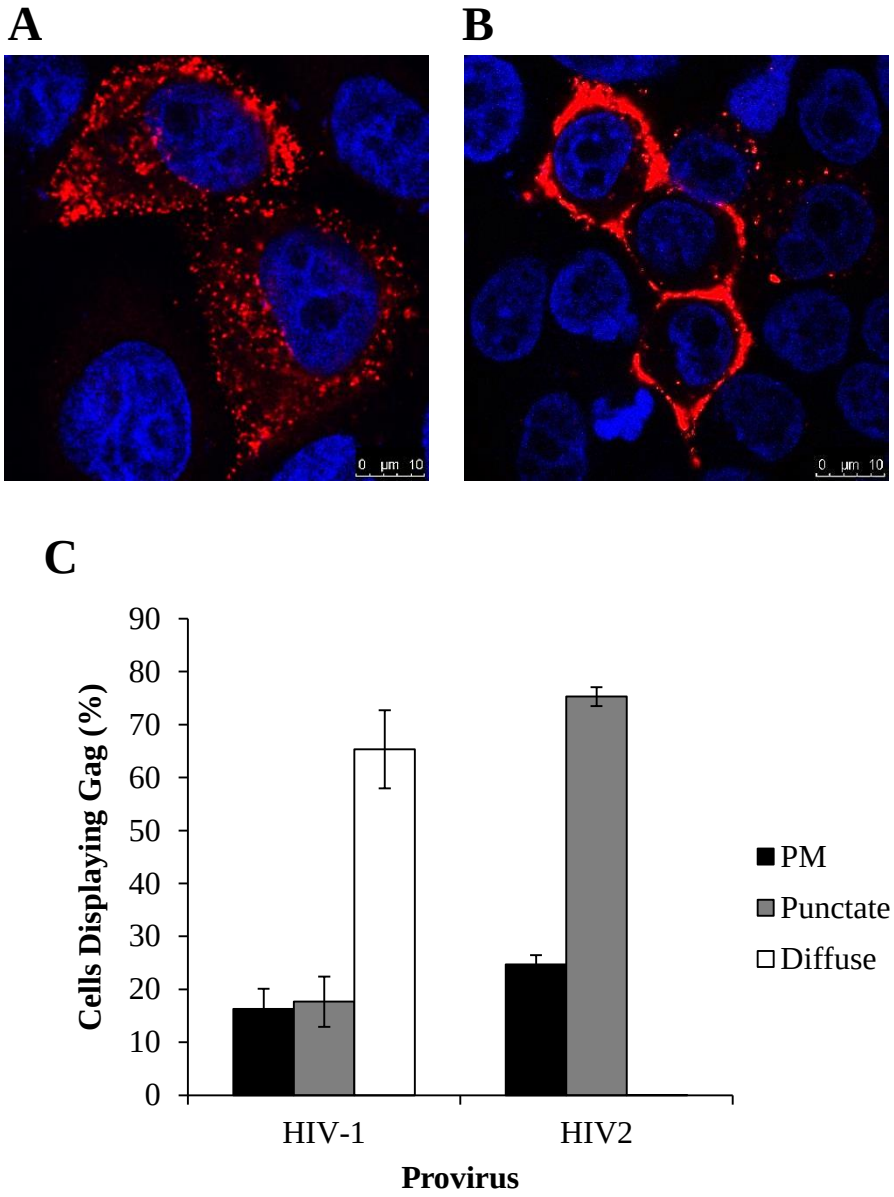

Figure 50: HIV-2 Gag displays a different intracellular localisation to HIV-1. A and B- Confocal immunofluorescence images of 24 hour HIV-2 provirus transfected HeLa cells, demonstrating the TWO typical staining patterns observed by using an anti-SIV p27 antibody (red). These are punctate intracellular (A) and plasma membrane (PM) (B). Blue stain = DAPI. C- Average percentages of Gag distributions in HIV-1 and HIV-2 provirus transfected HeLa cells taken from cell counts from 3 independent experiments.

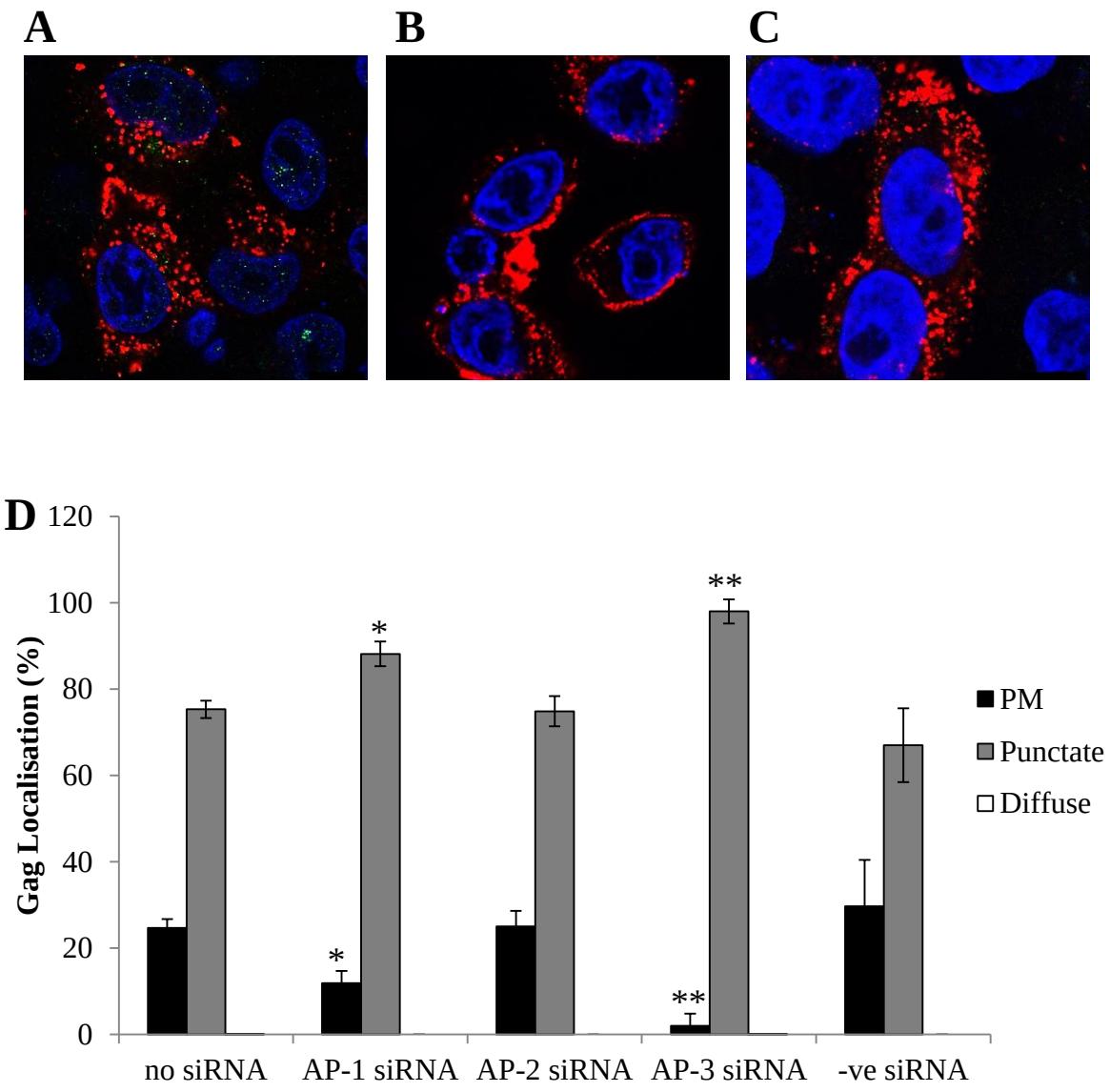

Figure 51: AP-1 and -3 affect HIV-2 Gag localisation. A-C- Confocal immunofluorescence images of 24 hour anti-SIV p27 (red) staining in HIV-2 co-transfected HeLa cells with either AP-1, -2 or -3 siRNAs, respectively. Blue stain= DAPI. Experiments were quantified by counting Gag localisation in cells from 3 independent experiments (D). (Key *=p<0.05, **=p<0.01).

could be observed in the presence of AP-1 siRNA, however, when AP-3 siRNA was used, PM Gag was almost totally abolished. No diffusely stained Gag appeared in any condition. When these results were quantified by counting Gag localisation in cells across repeat 3 experiments (shown in 51D), a similar story emerged. AP-1 siRNA had a significant effect on reducing PM HIV-2 Gag by approximately 50% ($p<0.05$), whereas AP-3 had a larger effect, reducing PM Gag by around 90% ($p<0.005$). Since diffuse Gag was not observed in HIV-2 transfected cells, a decrease in PM staining resulted in a significant increase in punctate intracellular staining also. AP-2 was found to have no significant effect, as with HIV-1, indicating that the punctate appearance of HIV-2 Gag is not due to clathrin-mediated endocytosis of assembled particles at the PM.

The likely explanation for the increase in punctate HIV-2 Gag in the presence of AP-3 siRNA is that, if HIV-2 also uses an endosomal trafficking pathway to reach assembly sites, it stands to reason that AP-3, like in the case of HIV-1, assists in the transport of Gag through endosomal compartments, thereby indirectly facilitating PM trafficking of Gag. Therefore, knocking down AP-3 causes an accumulation in endosomal compartments upstream of the AP-3 pathway.

6.2.4 AP-5 Affects HIV-2 Assembly, Release and Localisation

As mentioned in the introductory chapter, the newly discovered fifth adaptor protein complex (AP-5) is the only AP to date known to associate with late endosomes/lysosomes, although the precise location and function of AP-5 is currently unclear; however it is likely important in late endosome dynamics (Hirst et al., 2011; Hirst et al., 2013). Although results gathered in the previous chapter found no role for AP-5 in HIV-1 assembly or localisation, since it seems that HIV-2 may adopt a

different trafficking route to HIV-1, it seemed plausible that this protein may affect HIV-2. This seemed especially likely due to the strong involvement of AP-3 found in the HIV-2 life cycle in this chapter.

The first experiment carried out with AP-5 was to investigate the effects on cellular Gag. AP-5 siRNA was co-transfected with the HIV-2 SVRΔNB provirus, and samples were harvested at 24 and 40 hours. Equal amounts of protein were run on an SDS-PAGE gel, and Western blotted using anti-SIV p27 antibody. The results are shown in Figure 52.

As can be seen in Figure 52A, at both 24 and 40 hours, a decrease in p57 and p27 was observed. Again, endogenous protein levels were unaffected. To quantify this, densitometry was carried out across 3 repeat experiments, and the results are shown in Figures 52B and C. As can be seen, a significant decrease (68%) in p57 was observed at 24 hours in the presence of AP-5 siRNA ($p<0.05$), however p27 was not significantly reduced. At 40 hours, both p57 and p27 were significantly reduced; 42% and 38%, respectively. Although the negative control reduced p57 by 25% at 40 hours, this was found not to be significant ($p>0.05$), suggesting that although a small non-specific effect of using 25 nM siRNA may be exerted, the effect seen with AP-5 is specific. This would possibly indicate a role for AP-5 in HIV-2 assembly, and further supports the hypothesis that HIV-2 traffics at least via endosomes.

To investigate the role of AP-5 on particle release, WT HIV-2 was used as before, and viral supernatant samples were again analysed by Western blot. The results are shown in Figure 53. As can be seen in Figure 53A, AP-5 siRNA qualitatively reduced HIV-2 Gag release, further indicating a role of AP-5 in the HIV-2 life cycle. Cell samples obtained from WT HIV-2 also displayed the same pattern to that of *env* deleted HIV-2. Densitometry (Figure 53B) indicated that an absence of AP-5 caused decrease in Gag

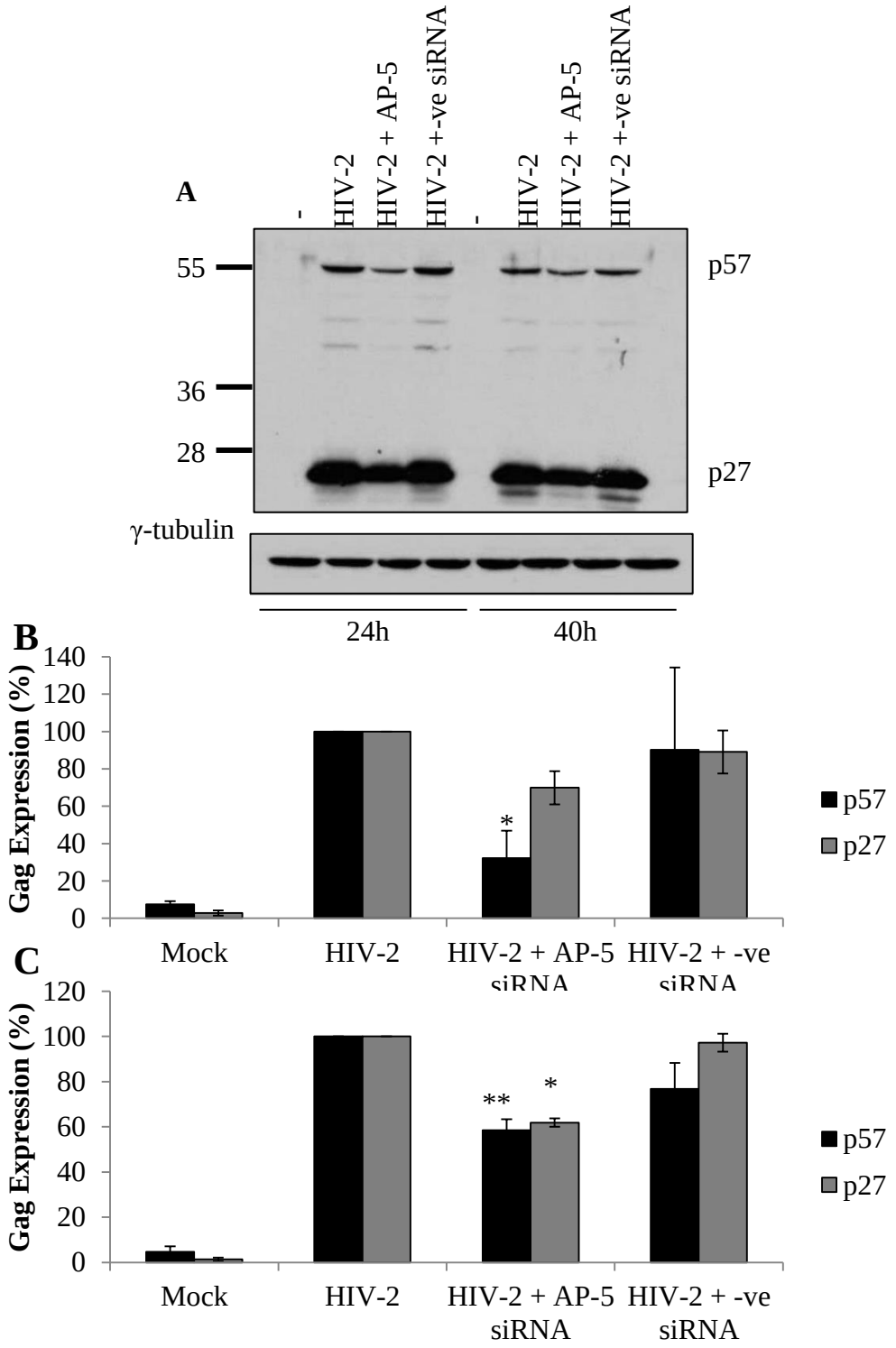

Figure 52: The effect of AP-5 on HIV-2 Gag processing. A- Western blot of cell samples from 24 and 40 hour HIV-2 provirus and AP-5 siRNA co-transfections, using an anti-SIV p27 antibody. B and C- Quantification of cellular Gag levels from 2 independent experiments using densitometry at 24 (B) and 40 hours (C). Values are expressed as percentages of Gag in siRNA untreated samples. (Key: *p<0.05, **p<0.01).

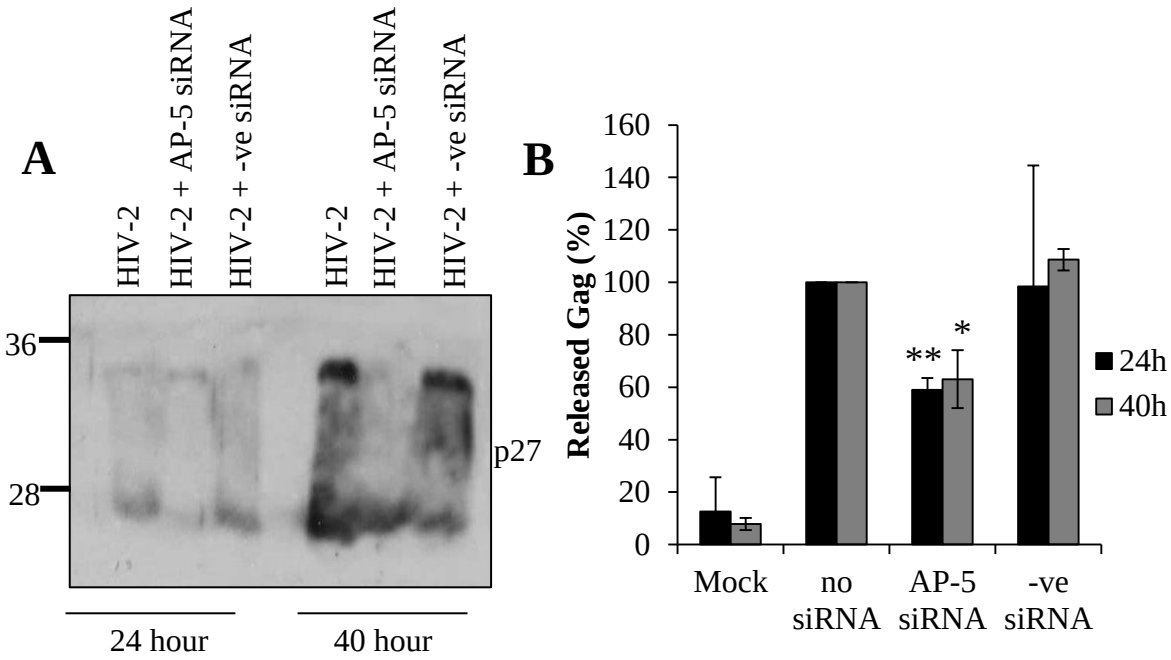

Figure 53: The effect of AP-5 on HIV-2 release. A- Western blot viral supernatants taken from untreated, AP-5 or negative control siRNA treated HeLa cells 24 and 40 h post-transfection. B- HIV-2 Gag (p27) release was quantified from 3 repeat experiments using ImageJ. (Key: *=*p*<0.05, ***p*<0.01).

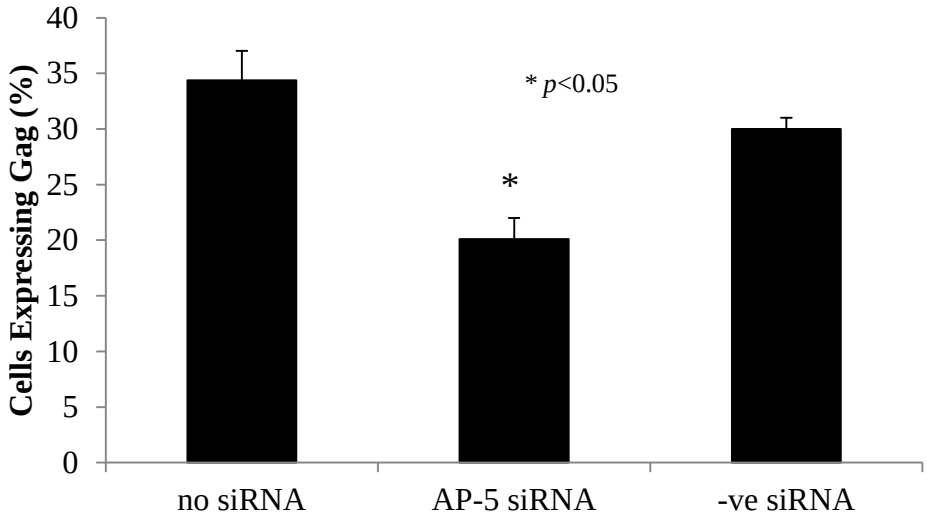

Figure 54: AP-5 knockdown causes a slight reduction in Gag expressing cells. HeLa cells were transfected with HIV-2 provirus, with or without the AP-5 or negative control siRNA. Confocal immunofluorescence microscopy was used to identify Gag expressing cells using an anti-SIV p27 antibody. This was quantified from 2 repeat experiments, and represented graphically. Statistically significant differences from untreated cells are highlighted by an asterisk (*p*<0.05).

release at both 24 and 40 hours, although it is difficult to ascertain quality data from smeared bands.

Since AP-5 knockdown seemed to be reducing total Gag at both 24 and 40 hours, it seemed plausible that the number of HIV-2 Gag expressing cells would also be reduced. To investigate this, AP-5 siRNA and HIV-2 provirus co-transfected cells were investigated by confocal microscopy. The results are shown graphically in Figure 54. As can be seen, the presence of AP-5 siRNA caused a significant (40%), reduction in HIV-2 Gag expressing cells ($p<0.05$). The negative control siRNA also reduced Gag expressing cells by 12%, but this was found not to be significant ($p>0.05$). This again indicates that although there is some non-specific effect of using siRNAs at this concentration, AP-5 siRNA also exerts a specific effect on HIV-2 Gag.

The final investigation of the role of AP-5 on the HIV-2 life cycle was to investigate whether it affected HIV-2 Gag localisation. The same protocol was followed as before for the other siRNAs, and cells were viewed under the confocal microscope. Results are shown in Figure 55.

Figures 55A-C demonstrate typical Gag staining observed with no siRNA, AP-5 siRNA, and the negative control siRNA, respectively. As can be seen, in the presence of AP-5 siRNA, some slightly more diffusely stained cells appeared, as indicated by the white arrow, in comparison to the usual appearance of HIV-2 Gag (Figure 55A). To quantify whether this was significant, counts of Gag localisation in cells across repeat experiments were plotted, and the results are shown in Figure 55D. As can be seen, when AP-5 was knocked down, there was an increase in cells displaying a diffuse Gag stain from 0% to 7%. This was, however, not found to be significant ($p>0.05$). What was found, however, was that AP-5 siRNA caused a significant decrease the percentage of PM localised Gag (from 22% to 7%) ($p<0.05$), with a concomitant significant 9%

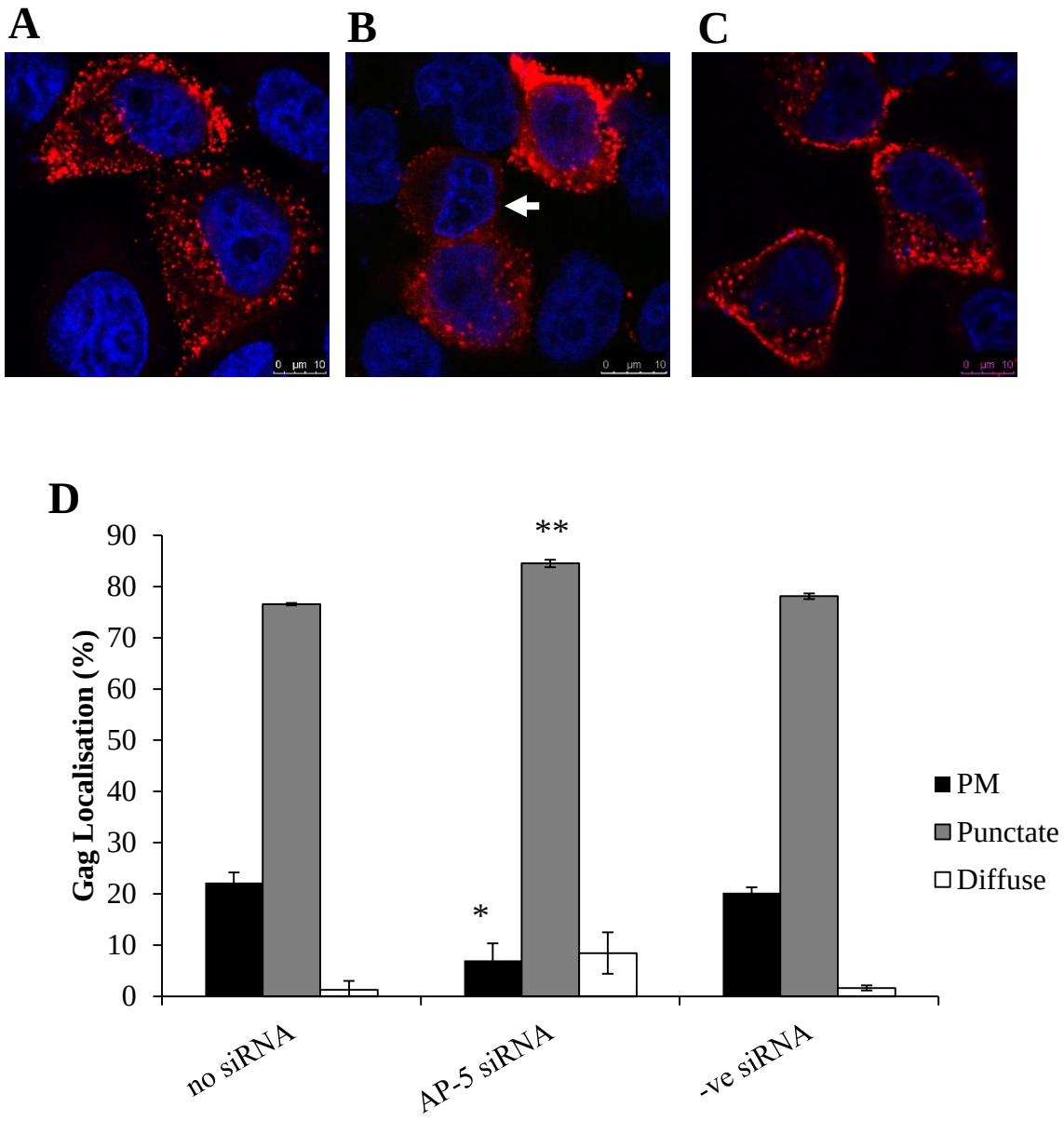

Figure 55: The effect of AP-5 on HIV-2 localisation. A-C- Confocal immunofluorescence images of HIV-2 Gag in HeLa cells using an anti-SIV p27 antibody (red), in untreated, AP-5 siRNA treated and negative control siRNA treated cells, respectively. A diffusely stained cell is indicated by the white arrow. Blue stain= DAPI. Gag localisation was quantified across 2 repeat experiments, and the results are shown in D. Statistically significant differences from untreated cells are highlighted by an asterisk. (Key *=p<0.05, **p<0.005).

increase in the percentage of punctate Gag (p<0.005). This would again suggest a role for AP-5 in the trafficking and localisation of HIV-2 Gag, unlike HIV-1 where it was found to play no role.

Together these results, alongside the role found for AP-3, indicate that HIV-2 Gag transport likely involves intracellular compartments as a route to release sites. Whether this is transient, or Gag actually begins to assemble within these intracellular organelles is unclear

6.2.5 The Effect of the Adaptor Proteins on MA2 Assembly and Release

In order to investigate the role of the matrix (MA) domain on HIV trafficking, 2 chimeric viruses were used; MA1 and MA2. MA1 has the HIV-2 pSVRΔNB backbone, but with HIV-2 MA replaced by HIV-1 MA. MA2 has the HIV-1 pSVC21ΔBgl (HxB2) backbone, but with HIV-1 MA replaced with HIV-2 MA (E.C. Anderson and M. Marongiu, unpublished results). The MA domain of HIV-1 has been reported to contain the AP binding sites (Dong et al., 2005; Batonick et al., 2005; Camus et al., 2007), although Kyere et al. (2012) have since reported that MA does not interact directly with AP-3. Through the use of these chimeric viruses, we should be able to deduce whether it is solely MA which is responsible for the trafficking/assembly phenotypes of HIV. At present, the AP binding sites of HIV-2 Gag have not been identified in the literature.

To investigate the effects of AP siRNA treatment on MA2 assembly and release, HeLa cells were co-transfected with MA2 and the AP siRNAs as before, and cell and supernatant samples were analysed via Western blot using an anti-HIV-1 p24 antibody, after loading equal amounts of (cell) lysate onto an SDS-PAGE gel. The results are shown in Figure 56.

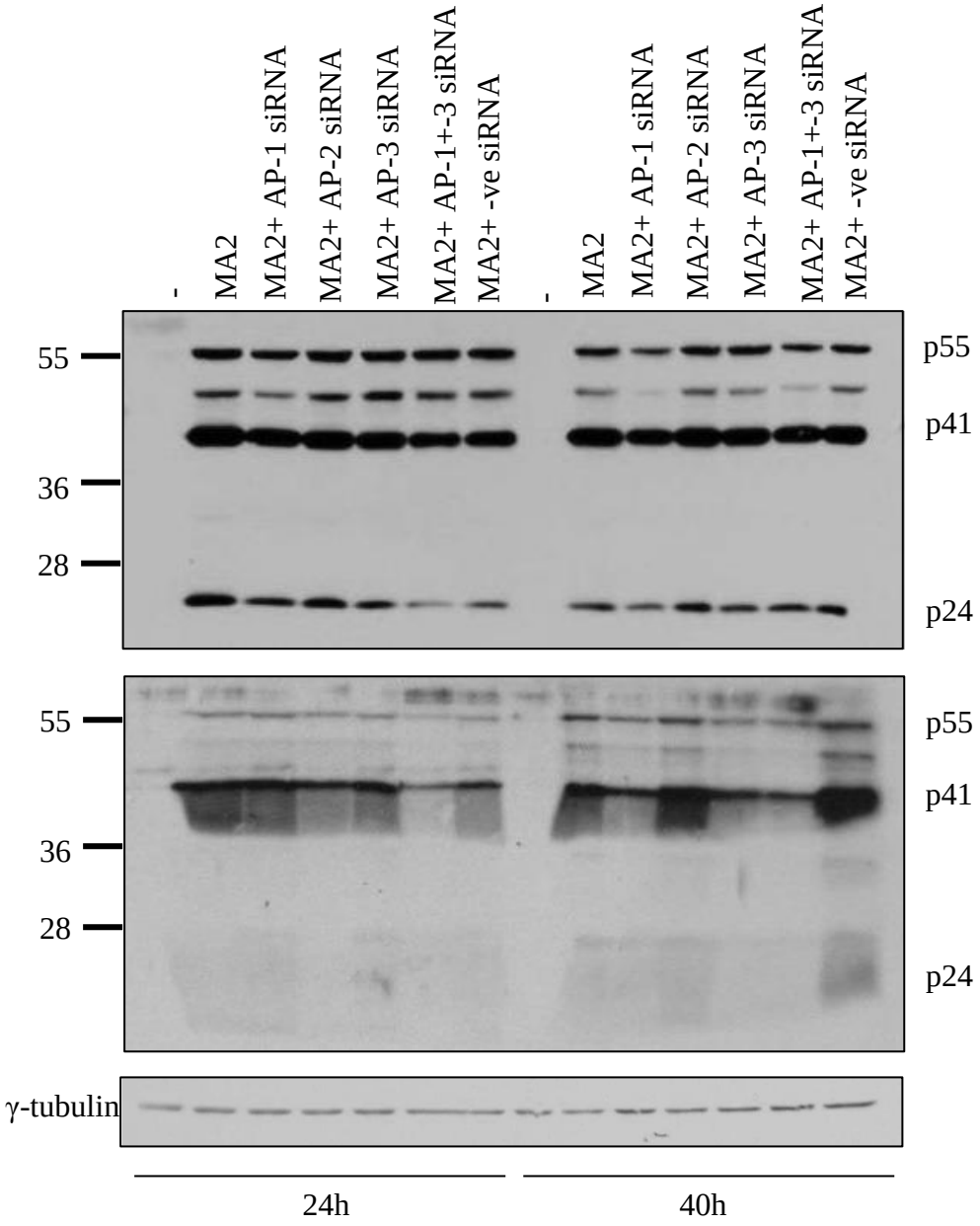

Figure 56: The effect of the adaptor proteins on MA2 processing and release. The top panel shows a western blot of cell lysate samples from MA2 and AP or negative control siRNA co-transfected HeLa cells 24 and 40h post-transfection, using an anti-HIV-1 p24 antibody. The middle panel shows a western blot of viral supernatants collected at the same time points. The same cell samples were probed with an anti-γ-tubulin antibody (bottom panel).

As this Figure demonstrates, small decreases in cellular Gag (top panel) were observed in the presence of AP-1 or -3 siRNAs. Once again, when used in combination, a larger effect was exerted. AP-2 also again had no visible effect on cellular Gag. When 3 repeat experiments were analysed by densitometry (Figures 57A and B), it was revealed that AP-1 and -3 siRNAs caused a significant ($p<0.005$) decrease in processed Gag at both 24 and 40 hours post transfection, however, AP-1 had a larger (approximately 10%) effect in both instances. When AP-1 and -3 siRNAs were used together, a significant ($p<0.05$) decrease in both processed Gag fractions (p41 and p24) was observed at 24 hours, whereas at 40 hours, a significant decrease in all Gag fractions (p55, p41 and p24) was seen.

The middle panel of Figure 56 shows MA2 viral supernatant samples. As can be seen, little effect was seen at 24 hours, except when AP-1 and -3 were used in combination. At 40 hours, however, AP-1 and -3 siRNAs caused a decrease in Gag release, and AP-1 and -3 siRNAs together once again exerted a larger effect. AP-2 knockdown increased particle release, as for HIV-1. When 3 repeat experiments were analysed by densitometry (Figure 57C), it was found that AP-1 and -3 siRNAs had a similar effect, reducing particle release by approximately 60% ($p<0.05$), whereas AP-1 and -3 siRNAs in combination reduced particle release by 74% ($p<0.05$). AP-2 siRNA indeed was found to significantly increase particle release by 30% ($p<0.05$).

These results were slightly surprising; although the AP binding sites have not been reported in HIV-2, it could be assumed that due to sharing 60% amino acid sequence identity in Gag (Dilley et al., 2011), they exist in a similar position to HIV-1. Since we know that the APs do indeed effect HIV-2 trafficking and assembly, it was assumed that MA2 would behave in a similar manner to HIV-2. These results, however, suggest something different. AP-2 was found to have an inhibitory effect on MA2 particle

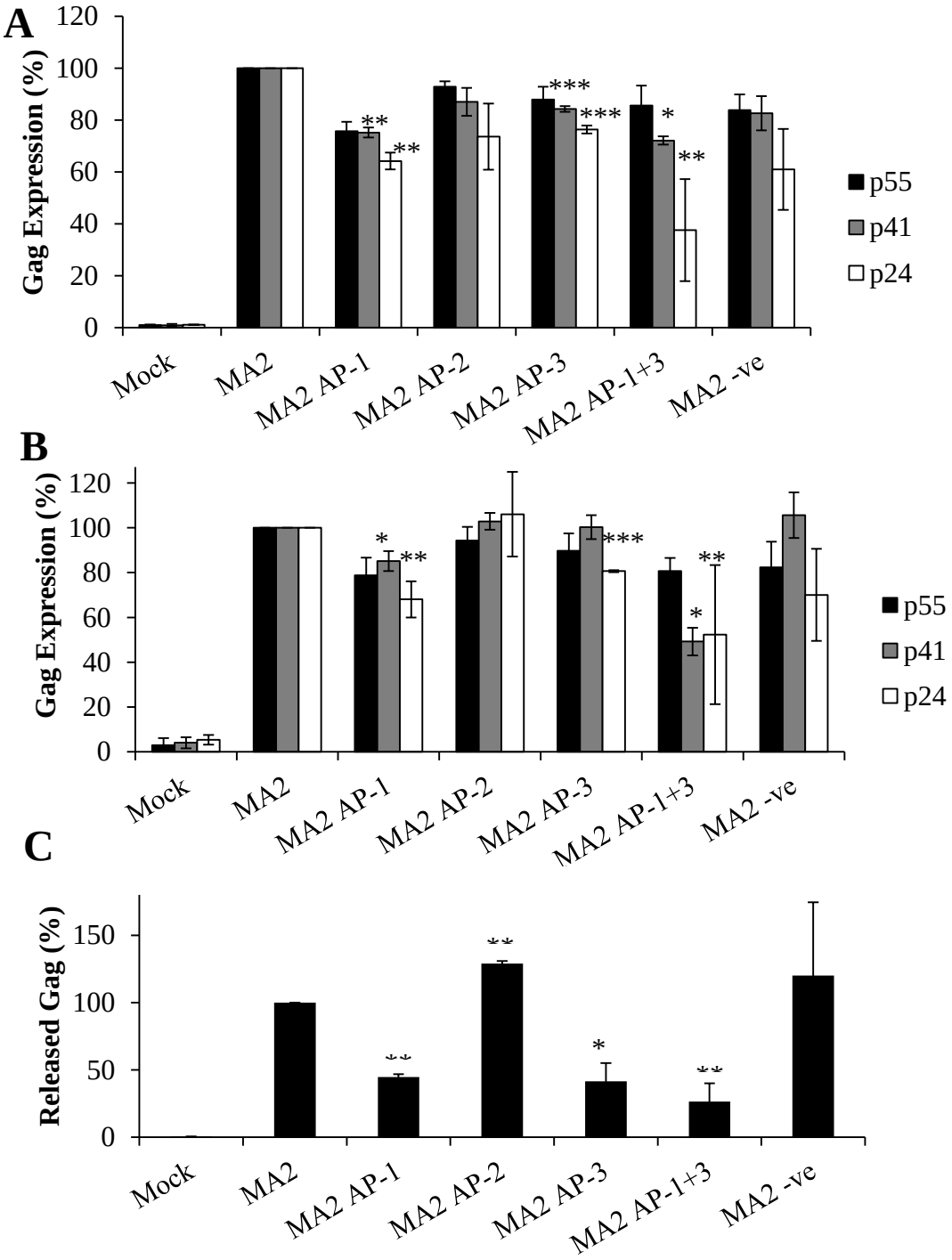

Figure 57: The effect of the adaptor proteins on MA2 assembly and release. Densitometry was performed on bands from 3 western blots using ImageJ, to calculate Gag levels obtained from independent repeat experiments. A and B- 24 and 40 hour cell samples, respectively. Supernatants (C) represent 40 hour p41 values only. Results shown are percentages of Gag expression from no siRNA treatment. (Key: *=p<0.05, **=p<0.005, ***=p<0.001).

release, similar to that of HIV-1; however, this was not observed for HIV-2. Furthermore, AP-1 only had a modest effect on HIV-2 assembly and release, whereas the effect was found to be slightly larger than AP-3 on MA2. Together, these results suggest that the MA domain is likely not the only area containing AP binding sites, and that MA2 has a similar trafficking phenotype to that of HIV-1, as opposed to HIV-2.

6.2.6 The Effect of the Adaptor Proteins on MA1 Assembly

To investigate the effects of the APs on MA1, the same protocol for MA2 was repeated, except that an anti-SIV p27 antibody was used in Western blots. Viral supernatant samples were not collected, however, since data collected previously in this lab found that MA1 is unable to egress (Michela Marongiu, unpublished data). The results for MA1 cell samples are shown in Figures 58 and 59.

The Western blot (Figure 58) presents a similar story to that of HIV-2; AP-1 siRNA caused a moderate effect on Gag, causing a decrease in Gag at both 24 and 40 hours. AP-3 siRNA, however, once again exerted a larger effect than AP-1; densitometry of 3 repeat experiments revealed that p27 was reduced by 12% more in the presence of AP-3 siRNA at 24 hours, and 19% more at 40 hours (see Figure 59A and B). Interestingly, however, p57 was significantly reduced by both AP-1 and AP-3 at 24 hours, but not at 40 hours, whereas little effect was seen at 24 hours when HIV-2 was used. Currently, it is unclear as to why this is occurring. AP-2 was again found to have no significant effect. This data suggests that, despite containing the known AP binding sites of HIV-1, this provirus adopts a similar phenotype to that of HIV-2, again inferring that perhaps the MA domain is not the only region to contain AP binding sites.

As mentioned, MA1 is incapable of releasing viral particles. It was not discovered, however, why this is. One possibility for this that seemed plausible was that the virus is incapable of antagonising tetherin. Tetherin is a restriction factor expressed on the

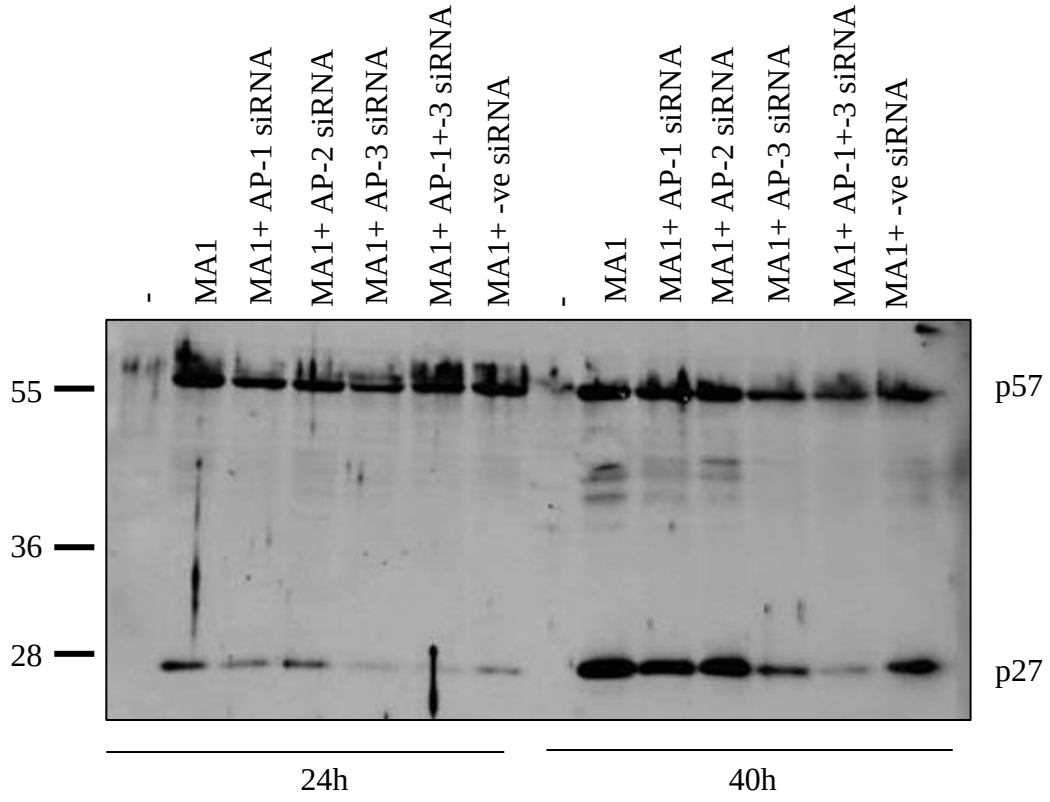

Figure 58: The effect of the adaptor proteins on MA1 Gag processing. Western blot of cell lysate samples taken from MA1 and AP or negative control siRNA co-transfected HeLa cells, 24 or 40h post-transfection, using an anti-SIV p27 antibody.

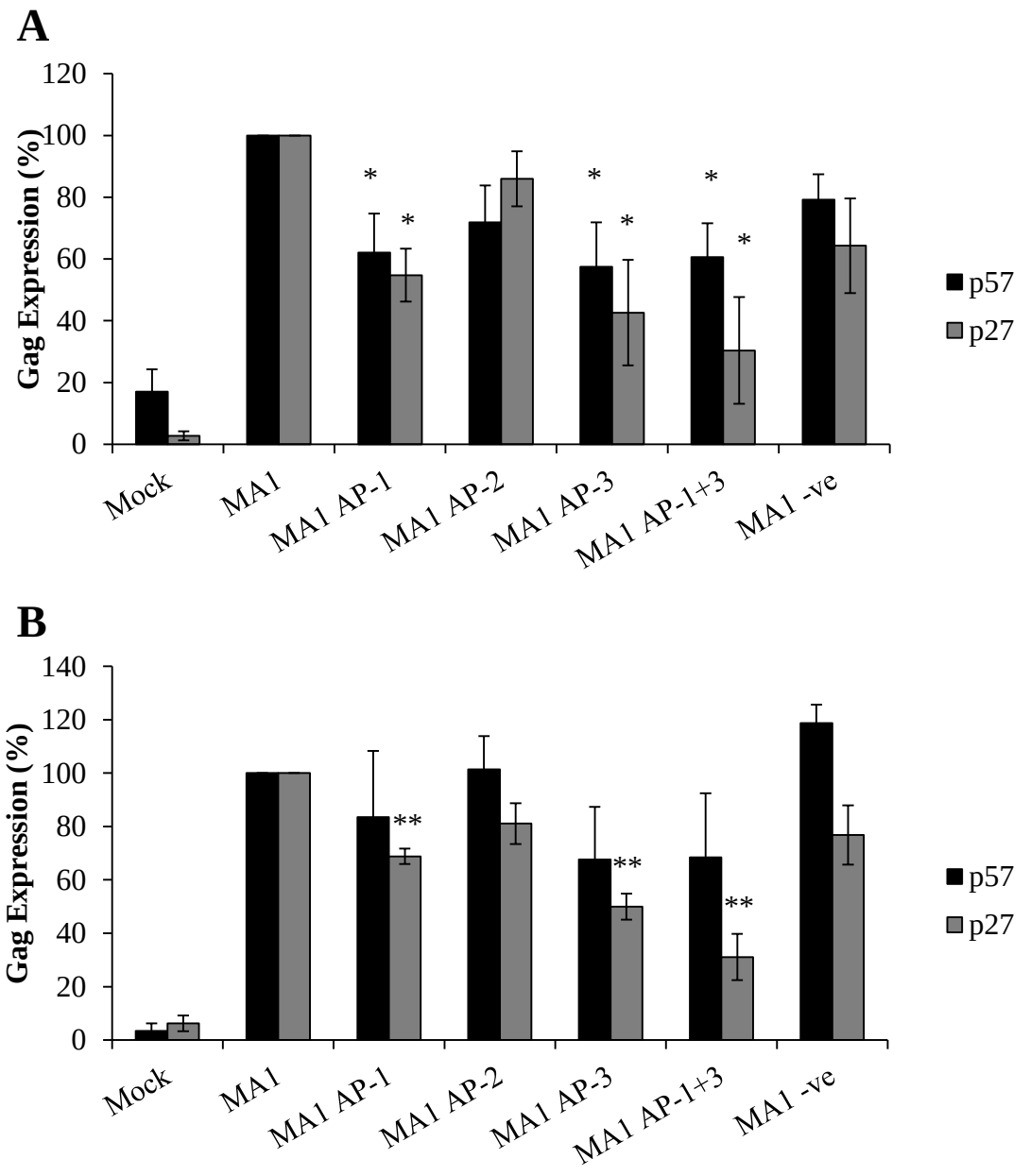

Figure 59: The effect of the adaptor proteins on MA1 Gag processing. Densitometry was performed on bands from western blots using ImageJ, to calculate Gag levels obtained from 3 independent repeat experiments. A- 24 hour cell samples, B- 40 hour cell samples. Results shown are percentages of Gag expression from no siRNA treatment. (Key: *=p<0.05, **=p<0.005).

surface of some cells, including HeLa cells, which prevents release of budding particles. HIV-2 Env is a tetherin antagonist, but is absent in the *env*-deleted HIV-2 provirus SVRΔNB, which was also the backbone of MA1. It therefore seemed a possibility that tetherin restriction is the reason for the inability of MA1 to egress.

To test this theory, a cell line which does not express tetherin was utilised; HEK 293T cells. HIV-2 and MA1 proviruses were transfected into these cells, and supernatant samples were harvested at 24 and 40 hours. The results are shown in Figure 60.

As can be seen *env* deleted HIV-2 was able to egress in this tetherin-deficient cell line; MA1, however, was still unable to escape HEK 293T cells. This tells us that there are other factors at play resulting in the ability of MA1 to egress, other than the inability to antagonise tetherin.

6.2.7 The Effect of the Adaptor Proteins on MA1 and MA2 Localisation

Previous studies (Ono et al., 2000) have demonstrated that the MA domain of Gag directs the trafficking and targeting of HIV-1 to assembly sites. Since it is apparent from Western blot analysis that these chimeras have different to expected phenotypes with regards to interactions with the APs, Gag localisation was analysed by confocal immunofluorescence microscopy, to see whether MA does indeed direct Gag localisation. HeLa cells were transfected with the chimeric proviruses, and compared with HIV-1 and -2 proviruses. The results are shown in Figure 61.

Figures 61 A-D demonstrate the typical Gag distributions observed for HIV-1, MA2, HIV-2 and MA1, respectively. As can be seen, MA2 Gag clearly adopted a more punctate staining, which is reminiscent of HIV-2 Gag. MA1 Gag also remained more diffusely stained, similar to that of HIV-1 Gag. This is intriguing since with regards to

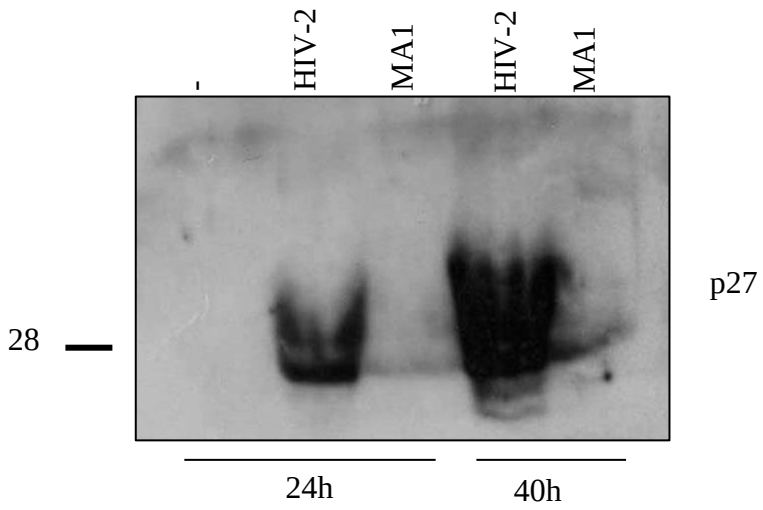

Figure 60: Viral egress from HEK 293T cells. This figure shows a western blot of viral supernatant samples from HIV-2 and MA1 transfected HEK 293T cells, 24 and 40h post-transfection, using an anti-SIV p27 antibody.

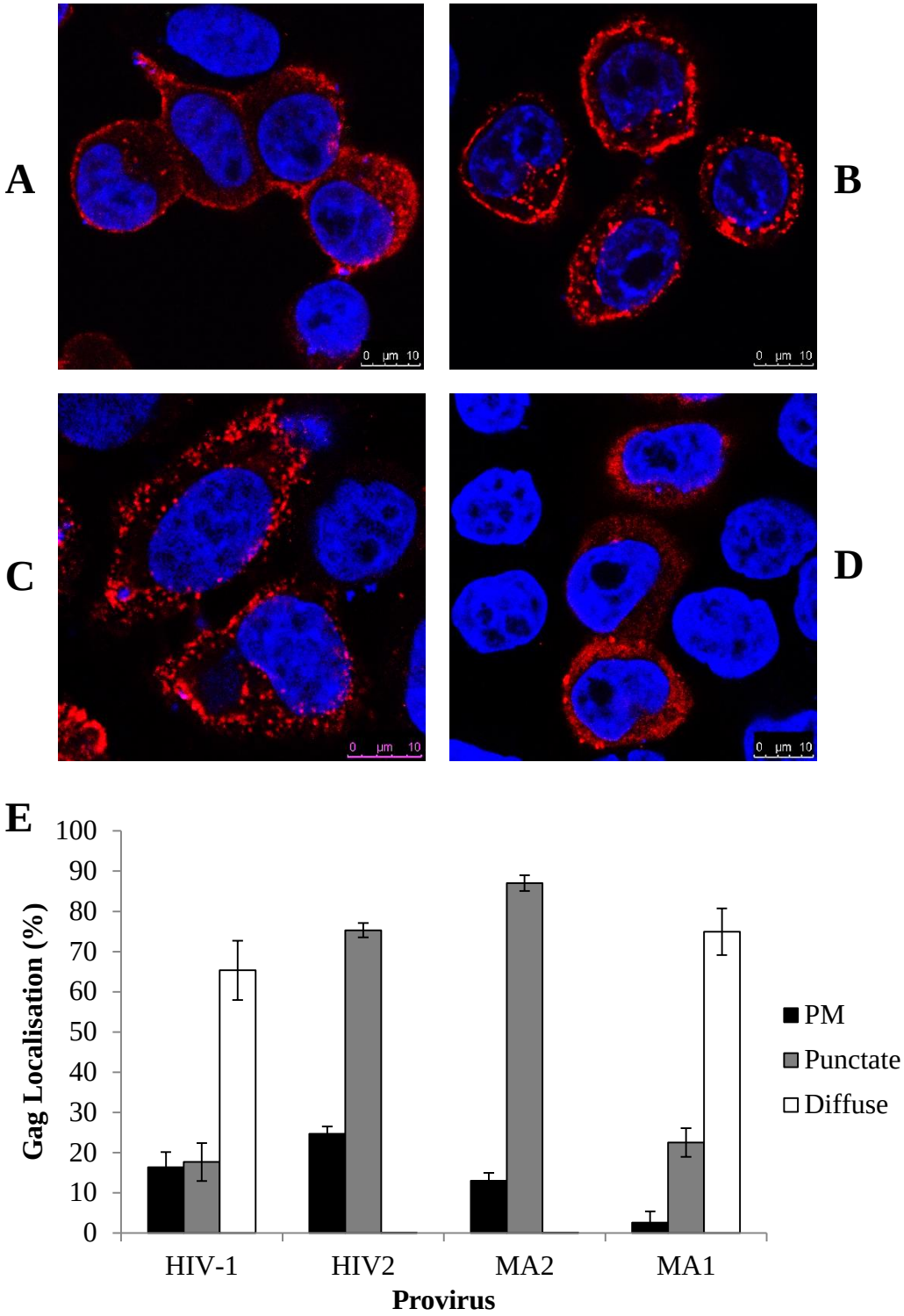

Figure 61: The effect of HIV Matrix on Gag localisation. A-D- Confocal immunofluorescence images of HIV-1, MA2, HIV-2 and MA1 transfected HeLa cells, respectively. Anti-HIV-1 p24 (HIV-1, MA2) and anti-SIV p27 (HIV-2, MA1) antibodies were used (red). Gag localisation was quantified from 3 independent experiments, and the results are shown graphically in E. Blue stain= DAPI.

the interactions with the APs, MA2 typically behaved like HIV-1, and MA1 like HIV-2. It was surprising therefore to find the Gag localisation phenotype was the opposite way around. When this data was quantified across repeat experiments (Figure 61E), a similar story was observed. MA2 was predominantly punctate and rarely diffuse, whereas MA1 was predominantly diffuse. PM Gag staining was rarely observed for MA1; this would support the observation that MA1 is inefficient at release, and perhaps suggests a trafficking/membrane localisation defect of this virus.

Since MA1 and MA2 have differing phenotypes with regards to Gag localisation, it seems plausible that it is a function other than the APs which is directing Gag to assembly sites. One such possibility is that myristoylation plays an essential role in directing Gag to assembly sites. Myristoylation of Gag is a two-step process; first, a free myristate is activated to myristoyl-CoA, then this myristoyl residue is transferred to the N-terminal glycine of Gag (Morikawa et al., 1996). The myristate group on Gag exists in two conformations, exposed (which is required for membrane binding) and sequestered within the protein. The HIV-1 Gag myristate group is in a dynamic equilibrium between exposed and sequestered conformation whereas the HIV-2 Gag myristate is more tightly sequestered (Saad et al., 2008). Insertion of the HIV-1 myristate into the PM is important in stabilising the association of Gag with the PM (Saad et al., 2006). If the HIV-2 Gag myristate is sequestered it may not be able to stabilise an association with the PM; it is possible that association with internal membranes occurs instead.

To investigate the effects the APs exert on MA1/MA2 Gag localisation, HeLa cells were co-transfected with these proviruses and the AP siRNAs, and viewed under the confocal microscope after staining for Gag. The results from 3 repeat experiments are summarised in Figure 62.

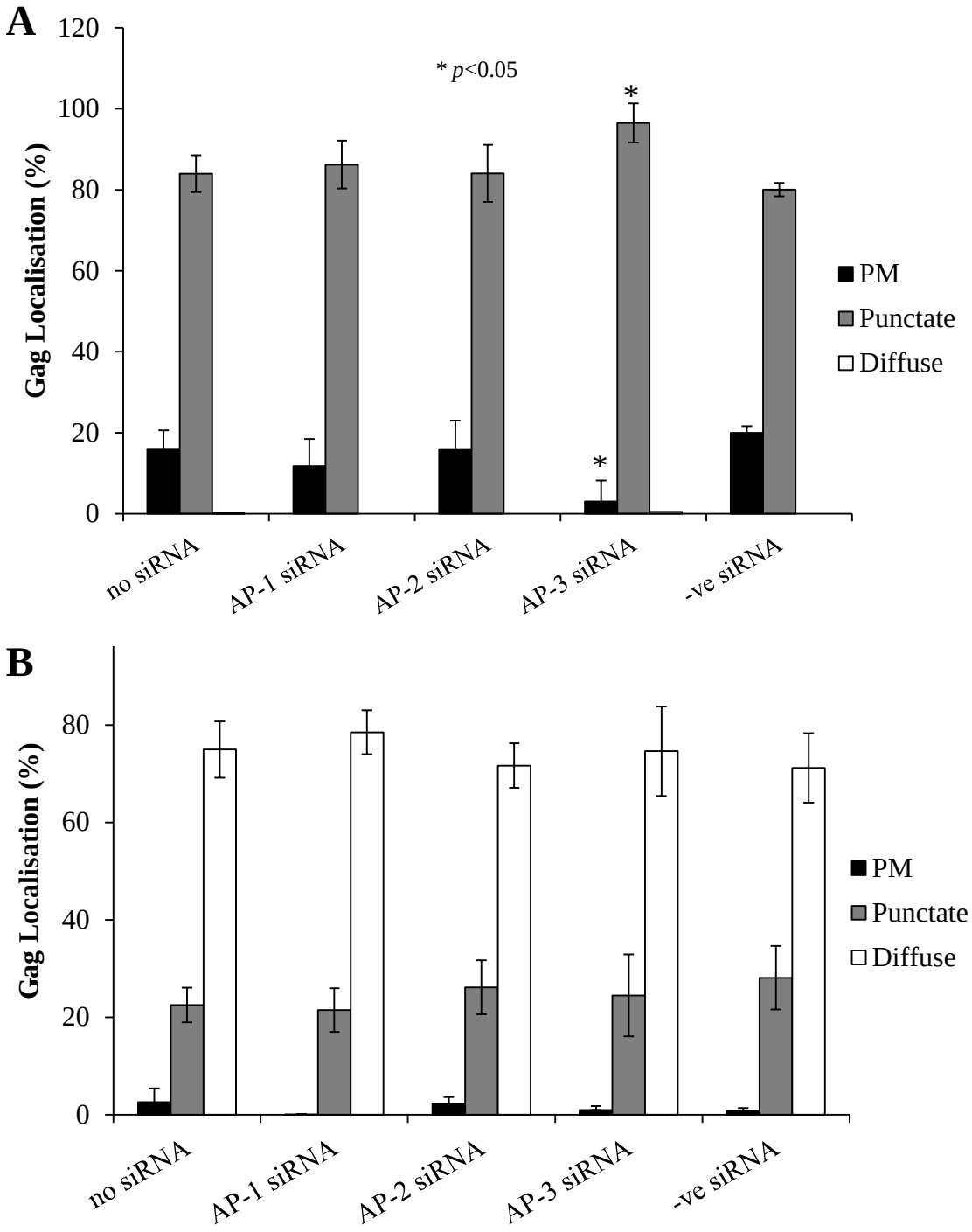

Figure 62: The effect of the AP siRNAs on MA2 and MA1 Gag localisation. Percentages of Gag distributions from 3 independent experiments seen in AP or negative control siRNA and HIV provirus co-transfected HeLa cells 24h post-transfection, viewed under a confocal microscope. A- Gag localisation in MA2 transfected HeLa cells. B- MA1 Gag localisation under the same conditions. Significant differences from untreated cells are highlighted with an asterisk (*p*<0.05).

As shown in figure 62, the AP siRNAs actually had little effect on the localisation of Gag from these proviruses. The only result that was significant was a reduction in PM Gag localisation of MA2 when AP-3 siRNA was used (see Figure 62A). AP-1 knockdown did slightly reduce MA2 PM Gag localisation, but this was not found to be statistically significant ($p>0.05$). Interestingly, no siRNA treatment significantly affected the localisation of MA1 Gag. Although AP-1 and -3 siRNAs did reduce PM localised MA1 Gag, since so few cells express Gag at this location, the reduction was not significant. Once again, AP-2 was found to have no effect. This also means that the very punctate staining observed for MA2 is likely not a result of the clathrin mediated endocytosis of budding viral particles. The fact that AP-3 had a larger effect than AP-1 on reducing PM localised Gag in MA2 supports the notion that this virus presents a similar phenotype to HIV-2 in regards to the trafficking pathway adopted to reach assembly sites.

A summary of the results gathered so far for HIV-1, HIV-2, MA1 and MA2 with regards to adaptor protein interactions is shown in Table 3.

	HIV-1	HIV-2	MA2	MA1
Assembly	AP-1 and AP-3 KD exerted similar effects on decreasing Gag processing. AP-2 and AP-5 KD no effect.	AP-3 KD exerted greater effect on decreasing Gag processing than AP-1. AP-5 KD inhibited processing. AP-2 KD no effect.	AP-1 and AP-3 KD exerted similar effects on decreasing Gag processing. AP-2 KD no effect.	AP-3 KD exerted greater effect on decreasing Gag processing than AP-1. AP-2 KD no effect.
Gag Release	AP-1 and AP-3 KD exerted similar effects on inhibiting Gag release. AP-2 KD enhanced Gag release. AP-5 KD had no effect.	AP-3 KD inhibited Gag release to a greater extent than AP-1. AP-2 did not inhibit release. AP-5 KD inhibited release.	AP-1 and AP-3 KD exerted similar effects on inhibiting Gag release. AP-2 KD enhanced Gag release.	N/A- inefficient at particle release.
Gag Localisation	AP-1 and AP-3 KD decreased PM localised Gag. AP-3 KD increased punctate Gag appearance. AP-1 KD made Gag appear more diffuse. AP-5 KD had no effect.	AP-3 KD decreased PM localised Gag to a greater extent than AP-1. AP-2 KD no effect. AP-5 KD decreased PM Gag and slightly increased diffuse Gag.	AP-3 only reduced PM Gag.	No effect.

Table 3: A summary of the effect of AP knockdown (KD) on Gag assembly, release and localisation of the 4 proviruses tested.

6.2.8 The Effect of HIV Gag on AP-3 Localisation

In chapter 3, it was found that HIV-1 Gag had no effect on the localisation of AP-3, and also only displayed minimal colocalisation with this protein, despite it being required for efficient particle release and assembly. Since Gag of HIV-2 and MA2 was localised predominantly to intracellular compartments, and both of these viruses require AP-3 as part of their life cycle, it was predicted that colocalisation with AP-3 would be higher than HIV-1. To investigate this, HeLa cells were transfected with HIV-2, MA2 and

MA1 proviruses for 24 hours, and co-stained for AP-3 and Gag, prior to viewing under the confocal microscope. The results are shown in Figure 63.

Figure 63A shows that HIV-2 could be seen to not only strongly colocalise with AP-3 (Pearson's correlation coefficient Rr=0.736), but also relocalised it. When cells expressing Gag were compared with surrounding untransfected cells, the localisation of AP-3 was dramatically different; it was concentrated into areas where Gag was present. This provides further evidence for the hypothesis that HIV-2 utilises AP-3 to traffic to or from intracellular compartments, either for particle assembly, or for delivery to the PM via endosomal/PM fusion. It could be speculated that AP-3 works in concert with ESCRT proteins and clathrin to drive Gag into endosomal compartments. Since clathrin is known to form scaffolds around cargo containing membranes in order to form vesicles, it could be that these two proteins work together with, for example Tsg101 to direct HIV-2 to intracellular sites of assembly, and assist in the formation of viral particles through cargo concentration and membrane deformation. Presumably, an absence of AP-3 would affect clathrin recruitment, which is reported to stabilise Gag in SIV and HIV-1 (Zhang et al., 2011), which could explain why an absence of AP-3 causes a decrease in Gag levels; if Gag is unable to assemble it seems likely that it would be degraded. However, the results gathered so far do not convincingly show that Gag is being degraded under the conditions tested.

Surprisingly, when MA2 was investigated, the same pattern was not observed. AP-3 was not relocalised to Gag containing areas, and only a small amount of colocalisation could be seen (see Figure 63B). Pearson's correlation coefficient was calculated across repeat experiments, and deduced the colocalisation to be moderate (Rr=0.455). When MA1 was investigated (Figure 63C), a similar observation was made. A small amount

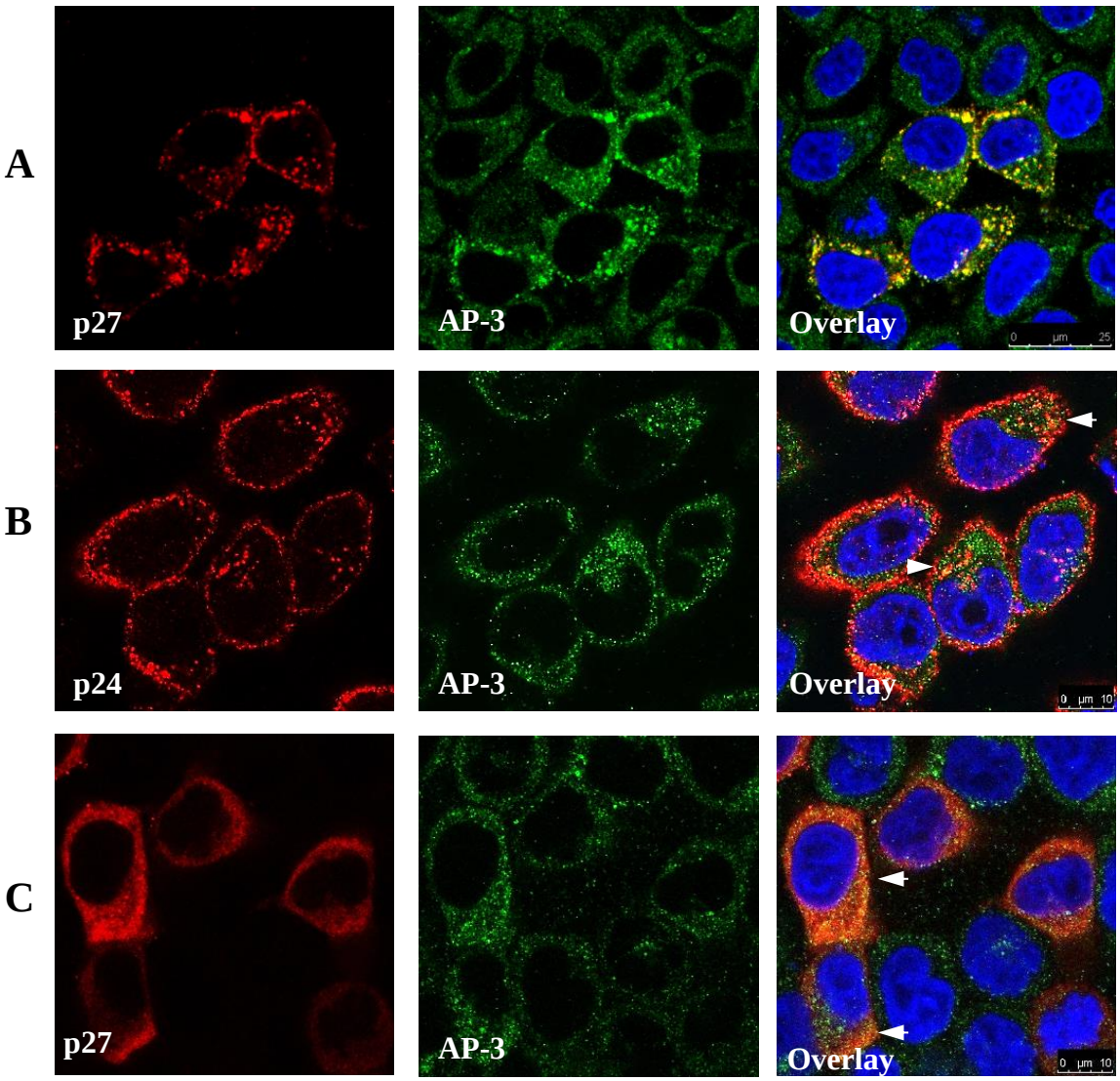

Figure 63: The effect of HIV Gag on AP-3 localisation. Confocal immunofluorescence images of transfected HeLa cells co-stained for Gag (red) and AP-3δ (green), in the presence of HIV-2 (A), MA2 (B), and MA1 (C). Blue stain= DAPI. HIV-2 Gag and AP-3 colocalisation was calculated by Pearson's correlation coefficient (average Rr=0.736), which was found to be high. MA2 shows a small amount of colocalisation, as indicated by the white arrows, which was found to be moderate by Pearson's correlation coefficient (average Rr=0.455). MA1 also displays colocalisation with AP-3, as demonstrated by white arrows, which was also found to be moderate (average Rr = 0.434).

of colocalisation was observed (Rr=0.434), but no relocalisation. This was similar to what was seen in HIV-1 transfected cells.

It was predicted that since MA2 displayed a similar Gag localisation to HIV-2, that we would also see a strong colocalisation with AP-3. Why this was not observed is unclear. It remains a possibility that since there potentially exists ulterior AP binding sites other than in MA, that MA2 is efficient at using the APs interchangeably. Therefore, a reliance on one AP would not exist, and this virus may not solely be dependent on AP-3 to reach assembly sites.

Interestingly, it was discovered that the cytoplasmic tail of HIV-2 Env contains a GYxxΦ (where Φ is a bulky hydrophobic residue) motif which binds AP-2; this was found to direct Env to a particular cellular location that is critical for the ability of Env to enhance viral release. Exchanging this tail with that of MLV (murine leukaemia virus), however, provided a functional substitute that did not require this GYxxΦ motif, or AP-2 (Noble et al., 2006). This could potentially suggest an ability of HIV constituents to alter usual trafficking pathways taken when, for example, the availability of or interactions between certain proteins are changed. Therefore, an absence of a particular AP could cause HIV to adopt a different trafficking route, in order to overcome something that could potentially inhibit efficient viral replication.

6.2.9 The Effect of HIV Gag on AP-1 Localisation

HIV-1 was found to slightly alter the localisation of AP-1 in transfected HeLa cells (Figure 28); when HIV-1 was present, AP-1 was present in a smaller, more concentrated juxtanuclear position (see chapter 3.2.4ii for more details). This experiment was repeated for HIV-2, MA2 and MA1 to see if the same pattern was observed. Since AP-1 siRNA was found to only have a moderate effect on HIV-2 Gag

as compared with HIV-1 Gag, it was predicted that HIV-2 would likely not exert the same effects. The results are shown in Figure 64 for HIV-2 and MA1.

As can be seen, surprisingly, both HIV-2 and MA1 had a dramatic effect on the localisation of AP-1. In cells expressing Gag, AP-1 was present not only in the usual juxtanuclear area, but also appeared to be localised to long, tubular structures, which was not observed in cells that were not transfected. This was also different to the effect exerted by HIV-1, and suggested that it is not a MA mediated effect, but rather a result of another HIV-2 encoded protein. It is unclear as to what these structures are that HIV-2/MA1 is relocalising AP-1 to, but possibilities include tubular endosomes or cytoskeletal elements.

Next, to investigate whether MA2 exerted a similar effect to HIV-1 or HIV-2, the experiment was repeated using the MA2 provirus. The results are shown in Figure 65. As is indicated by the white arrows, AP-1 in MA2 Gag expressing cells appeared once again in a tighter juxtanuclear position, as compared with untransfected cells. This is a similar observation to AP-1 in HIV-1 transfected cells, as is shown in Figure 65B, although the relocalisation was slightly less obvious in MA2 transfected cells.

It is clear from these results that HIV Gag expression can alter the cellular distribution of AP-1; however, it is also evident that HIV-1 and HIV-2 exert different effects on this protein, and that these are not mediated by the MA domain. This could be because these viruses utilise AP-1 at different cellular locations, and at slightly different stages of the virus life cycle. This also suggests that the relocalisation is not merely a result of interactions between MA and AP-1, whereby AP-1 is directing the intracellular trafficking of HIV, and therefore becomes localised to Gag containing areas. This is also unlikely since although redistribution is seen, we did not see colocalisation between these proteins.

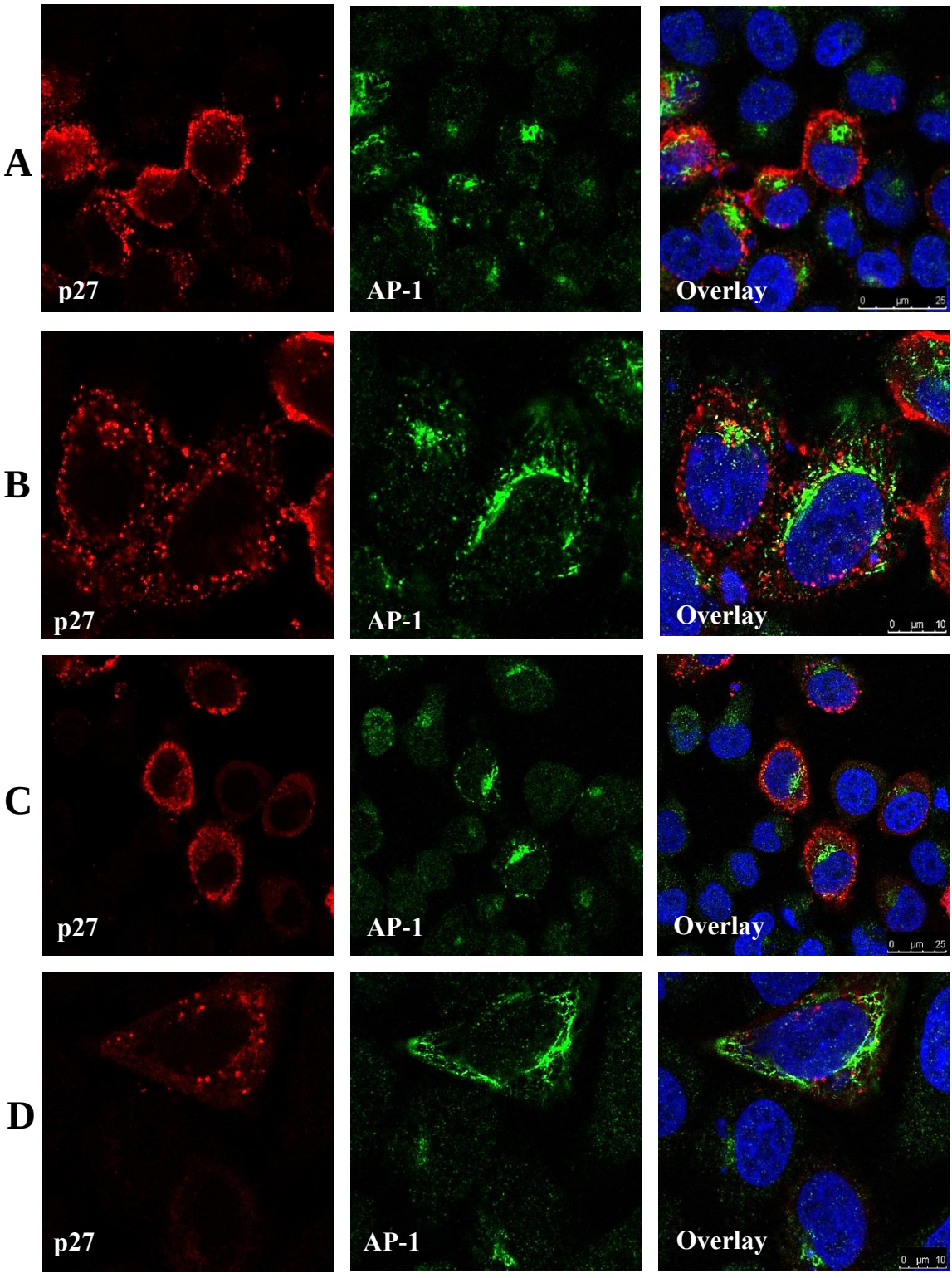

Figure 64: The effect of HIV-2 and MA1 on AP-1 localisation. Confocal immunofluorescence images of HeLa cells transfected with HIV proviruses co-stained with anti-SIV Gag (p27, red) and anti-AP-1γ antibodies (green). A and B- HIV-2 at 2X and 4X zoom, respectively. C and D- Repeat conditions for MA1 transfected cells. Scale bars are shown in the bottom right of overlay images.

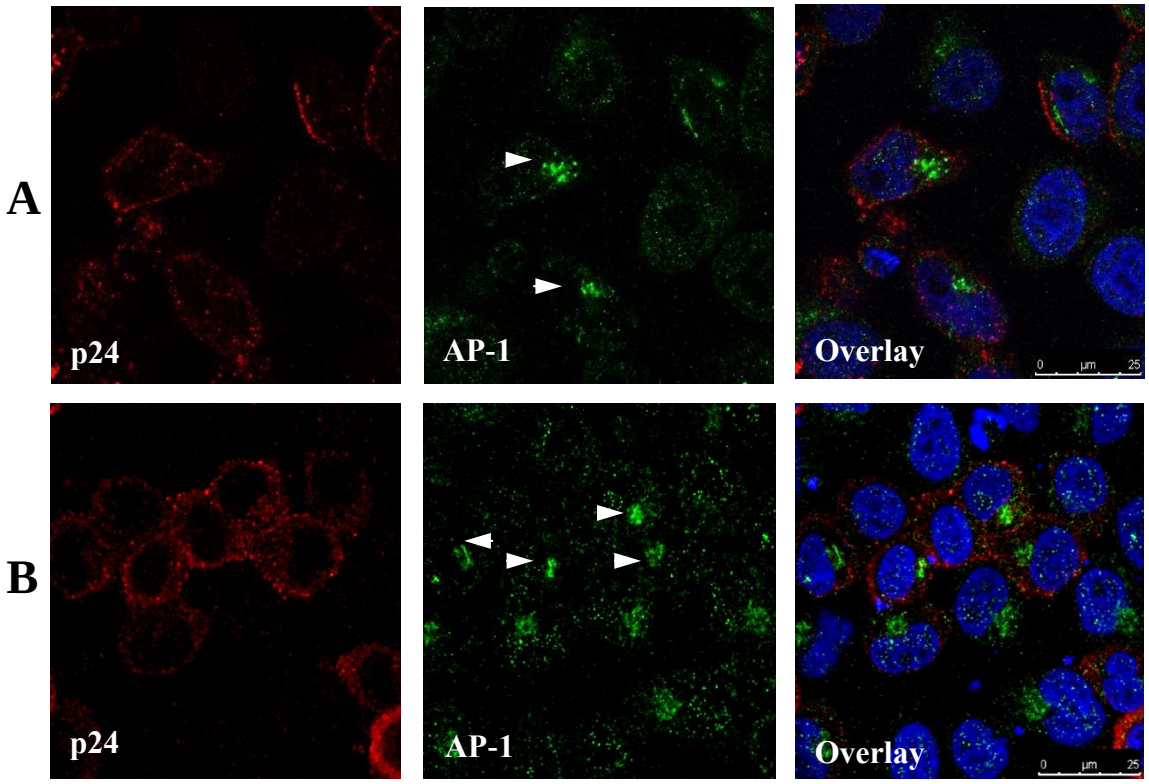

Figure 65: The effect of MA2 on AP-1 localisation. Confocal immunofluorescence images of HIV provirus transfected HeLa cells co-stained with anti-HIV-1 Gag p24 (red) and anti-AP-1γ antibodies (green). A- MA2 transfected cells, B- HIV-1 transfected cells. White arrows indicate changes in AP-1 localisation. Blue stain= DAPI.

6.2.10 The Interactions Between HIV Gag and Clathrin

It was recently reported that clathrin facilitates the morphogenesis of retrovirus particles through interactions with GagPol (Zhang et al., 2011); although HIV-2 was not investigated, its simian homologue SIV_{sm} was investigated, alongside HIV-1. Since results gathered in this chapter suggest a strong role for the APs, in particular AP-3 in the HIV-2 life cycle, it seemed plausible that clathrin may be recruited to intracellular budding areas via AP-3. To investigate the localisations of HIV-1 and HIV-2 Gag with respect to clathrin, HeLa cells were transfected with the HIV-1 and HIV-2 proviruses (HXB2 and SVRΔNB) and co-stained with anti-Gag p24/p27 and anti-clathrin heavy chain antibodies, and viewed under the confocal microscope. Results for HIV-1 and HIV-2 are demonstrated in Figure 66.

Figure 66A shows the typical distribution of clathrin in untransfected HeLa cells. Although a diffuse cytoplasmic localisation was observed, more clathrin staining was seen in a juxtanuclear position. This likely represents the TGN area. When cells were transfected with HIV-1 (Figure 66B), we saw some colocalisation with clathrin, and also a slight redistribution of clathrin to Gag containing areas such as the PM. We would expect this as per the current literature (Zhang et al., 2011). Colocalisation was analysed using ImageJ across 2 independent repeat experiments, and Pearson's correlation coefficient deduced the colocalisation with clathrin to be moderate (Rr=0.435). When cells were transfected with HIV-2 (Figure 66C), the colocalisation was observed to be much stronger (Rr=0.671). We also saw a more obvious redistribution of clathrin to Gag containing areas. This supports the current literature described for SIV_{sm} (Zhang et al., 2011), and also supports the hypothesis that AP-3 and clathrin function in concert to facilitate HIV-2 assembly; since clathrin is critical to Gag stabilisation and the morphogenesis of viral particles (Zhang et al., 2011), it

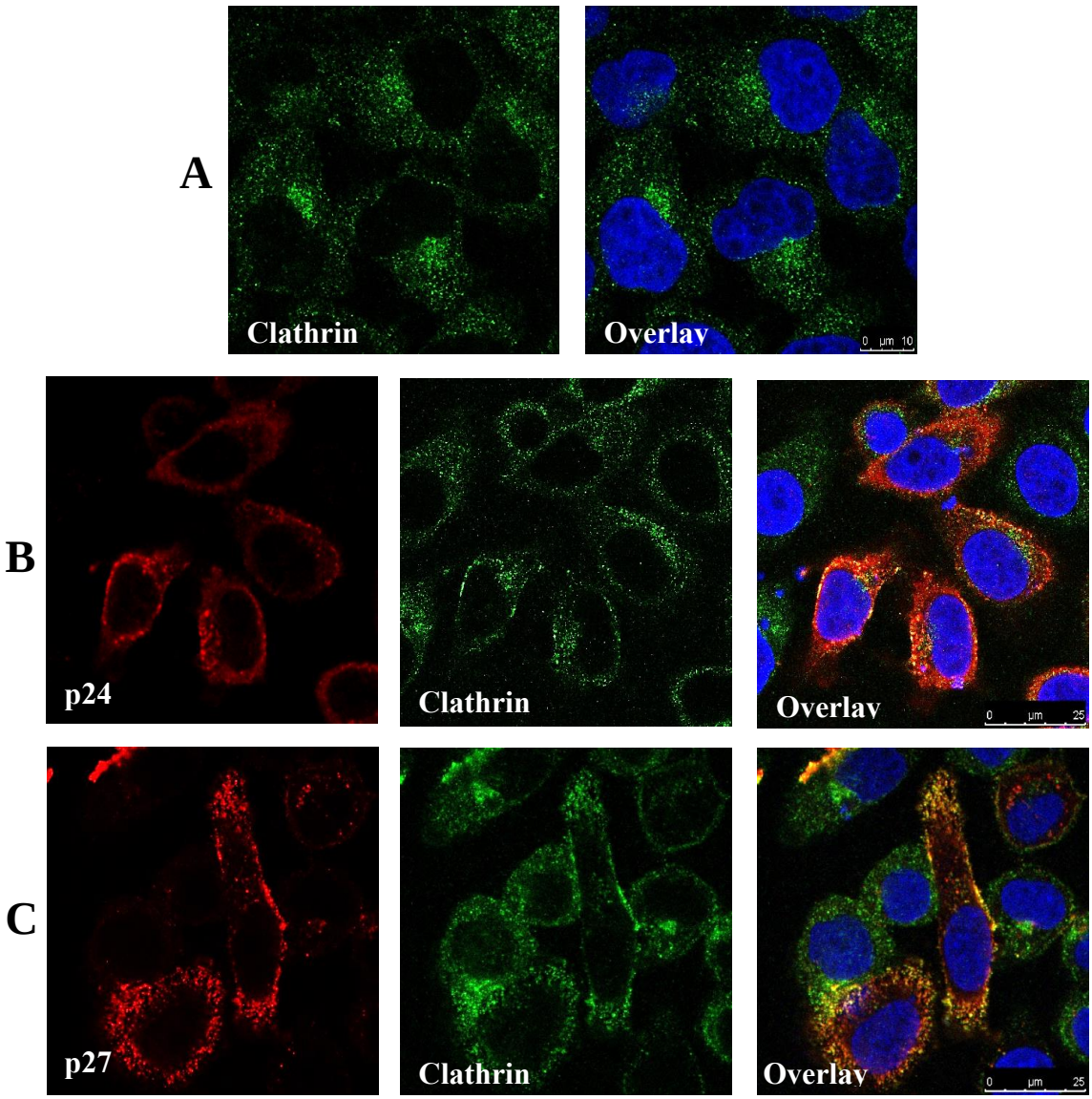

Figure 66: The effect of HIV-1 and HIV-2 on clathrin localisation. Confocal immunofluorescence images of HeLa cells with or without HIV-1/2 proviruses, stained with an anti-clathrin heavy chain antibody (green), and in transfected cells, anti-Gag antibodies were also used (red). A- Clathrin distribution in untransfected cells. B- HIV-1 transfected cells; colocalisation observed was deduced to be moderate across independent repeat experiments by Pearson's correlation coefficient (Rr=0.435). C- HIV-2 transfected cells. Pearson's correlation coefficient demonstrated this colocalisation to be high (Rr=0.671). Blue stain= DAPI.

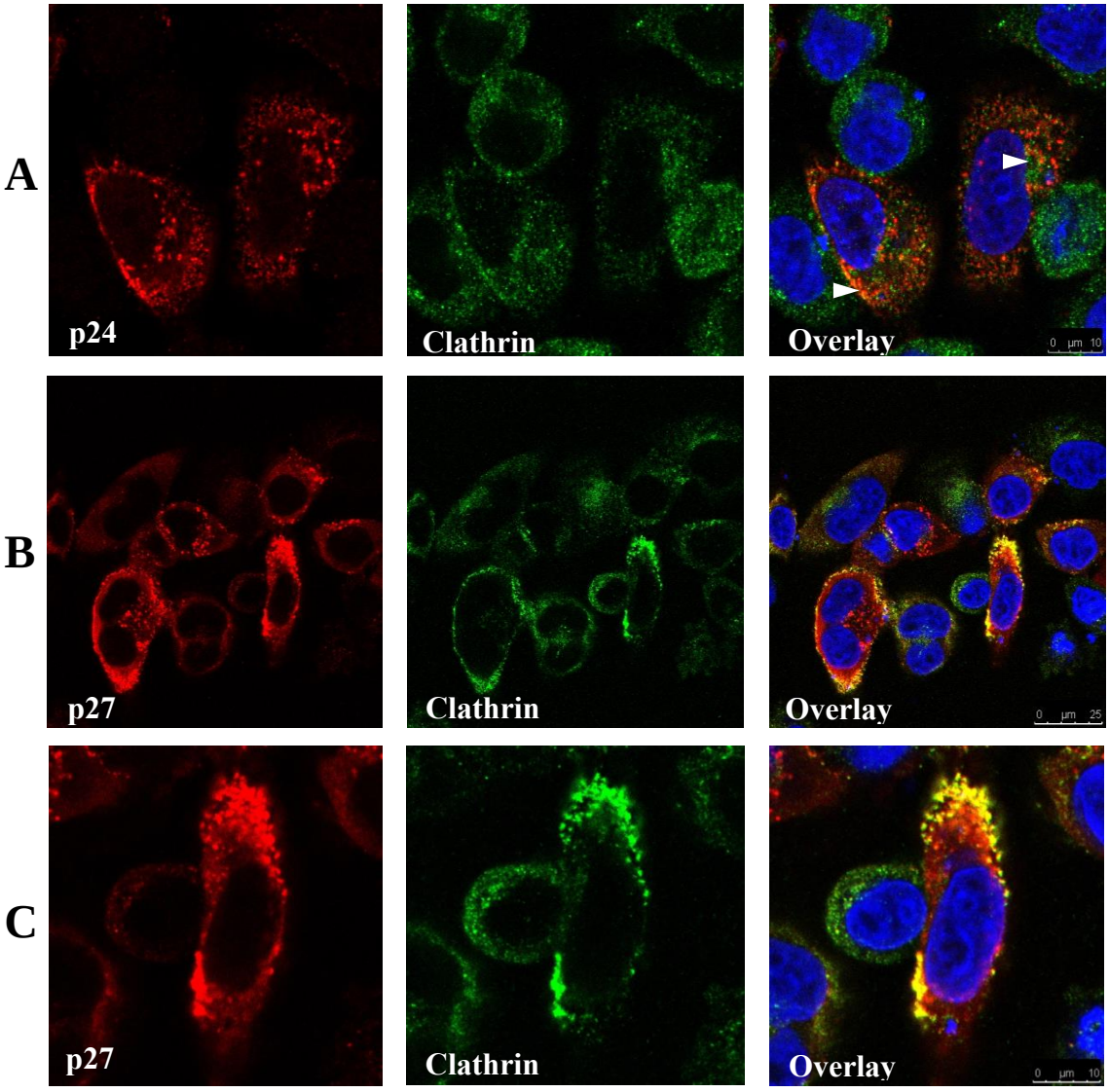

Figure 67: The effect of MA2 and MA1 on clathrin localisation. Confocal immunofluorescence images of provirus transfected HeLa cells, co-stained for Gag (p24/p27, red) and clathrin heavy chain (green). A- MA2 transfected cells. White arrows indicate areas of colocalisation; colocalisation was deduced to be moderate by Pearson's colocalisation coefficient (Rr=0.483) across independent experiments. B and C- MA1 transfected cells, at 2X and 4X zoom, respectively. Pearson's correlation coefficient deduced this colocalisation to be high (Rr=0.709). Blue stain= DAPI.

seems plausible that AP-3 assists in this by recruiting clathrin to Gag assembly sites. Since HIV-2 Gag strongly colocalises with both of these proteins, this makes sense.

When MA2 and MA1 were investigated (Figure 67), slightly different observations were made. MA2 demonstrated little colocalisation with clathrin, reminiscent of the lack of colocalisation observed with AP-3 (Figure 63B). This was deduced to be moderate from independent repeat experiments, by Pearson's correlation coefficient (Rr=0.483). MA1, however, showed very strong colocalisation with clathrin (Rr=0.709), which was seen mostly around the PM. This may represent assembling particles which have become stuck intracellularly, unable to egress, concentrated in areas where clathrin is abundant (the PM).

6.2.11 The Effect of Tetherin on HIV Gag

As mentioned, tetherin is a restriction factor present on the surface of HeLa cells, capable of trapping released virions, preventing their efficient release. HIV-1 Vpu is a tetherin antagonist, as are HIV-2 Env and Nef. HIV-1 Vpu and HIV-2 Env are non-functional in proviral strains utilised in previous experiments (HXB2, SVRΔNB). It was therefore hypothesised that the punctate appearance of both MA2 (lacking Vpu) and HIV-2 (lacking Env) could be due to re-internalisation of tethered particles, causing accumulation in endosomes. Therefore, HEK 293T cells which do not express tetherin, and full-length wild type (WT) HIV-2 (pSVR) which produces Env, were used to investigate the role of tetherin in Gag localisation in the proviruses through confocal immunofluorescence microscopy. The results for HIV-2 are shown in Figure 68.

Figure 68A shows the typical Gag localisation observed in HIV-2 (SVRΔNB) transfected HeLa cells, demonstrating a very punctate appearance. Figure 68B shows Gag localisation from HeLa cells transfected with WT HIV-2 (pSVR). Once again,

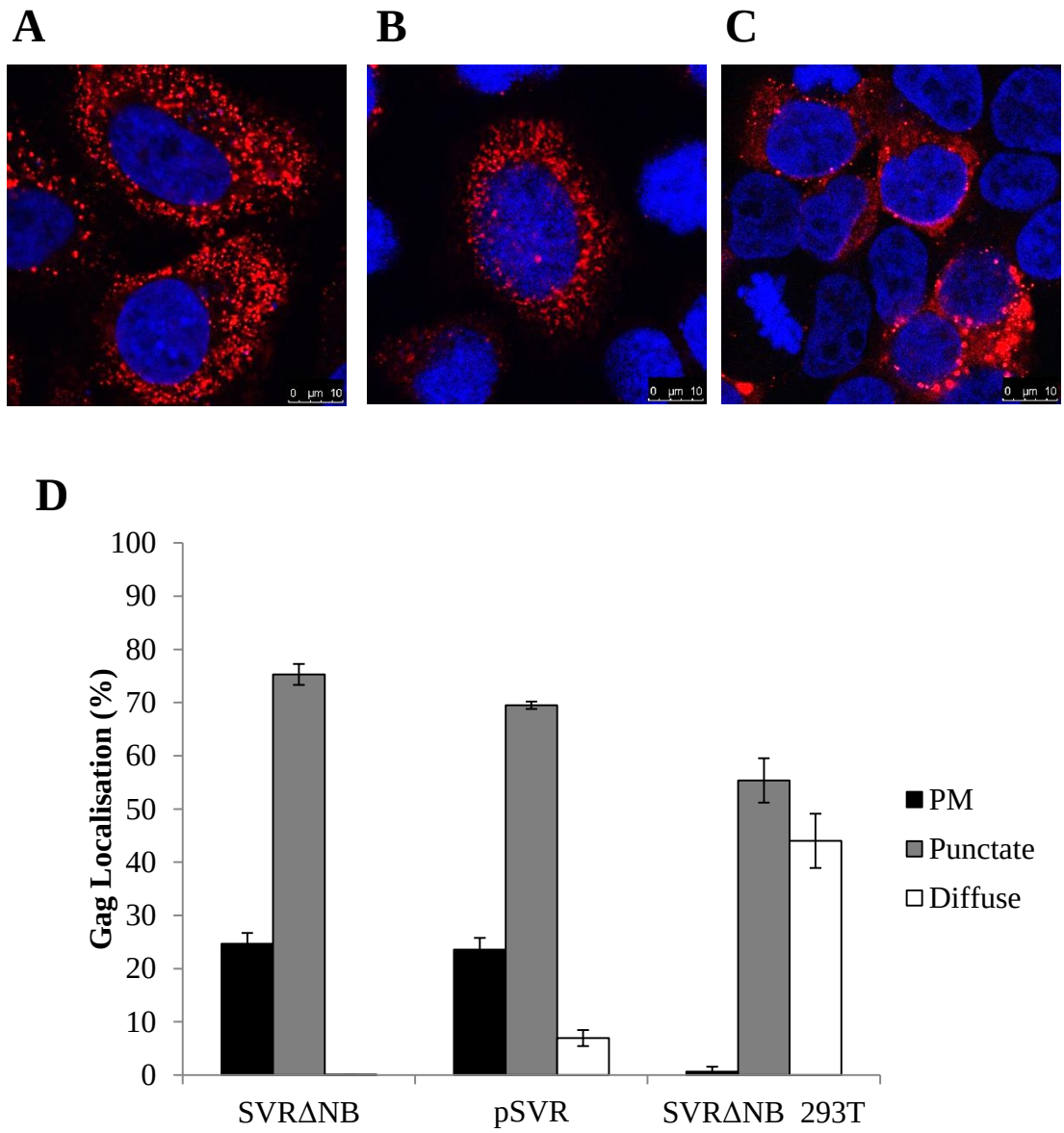

Figure 68: HIV-2 localisation using different HIV-2 proviruses and cell lines. A-C- Confocal immunofluorescence images of Gag in HIV-2 transfected cells using an anti-SIV p27 antibody (red). Gag distribution when HeLa cells are transfected with *env* deleted HIV-2 provirus (SVRΔNB, A) or wild-type HIV-2 (pSVR, B). C- Gag distribution when HEK 293T cells are transfected with SVRΔNB. Blue stain= DAPI. D- Percentages of Gag distribution quantified from 2 independent experiments.

similar observations were made; a very punctate appearance of Gag. When HIV-2 was transfected into HEK 293T cells (Figure 68C), however, we see a slightly different image. Although we do still see some very large puncta, we also now see some diffusely staining cells, which were never seen in HeLa cells. When Gag localisation was quantified in these conditions across 2 independent repeat experiments (Figure 68D), we see that HIV-2 and WT HIV-2 had similar Gag localisations, albeit WT HIV-2 does display some diffusely stained cells unlike HIV-2. HIV-2 Gag in HEK 293T cells, however, had a different phenotype. Not only was there virtually no PM localised Gag, but we also saw similar levels of diffuse and punctate Gag; punctate Gag still remained the most abundant form, however. This suggests that although tetherin clearly plays a part in determining the localisation of Gag, it is not the sole reason for the punctate pattern observed.

When MA2 was investigated, the cell type was significant. Figure 69A shows the typical Gag localisation observed in MA2 transfected HeLa cells; similar to HIV-2 it had a very punctate appearance. When MA2 was transfected into HEK 293T cells (Figure 69B), however, we saw a dramatically different localisation pattern. Although we still saw some puncta, it was more reminiscent of the staining observed in HIV-1 transfected cells. When Gag localisation was quantified across independent repeat experiments (Figure 69C), we saw a complete reversion of the Gag localisation phenotype; from HIV-2 like to HIV-1 like. This suggested that the MA domain is not solely responsible for Gag localisation, and that tetherin is a factor in causing the punctate appearance of MA2 Gag through re-internalisation of tethered particles.

When MA1 was investigated (Figure 69D), the localisation of Gag remained essentially unchanged, except for a slight reduction in punctate staining. Since MA1 is unable to

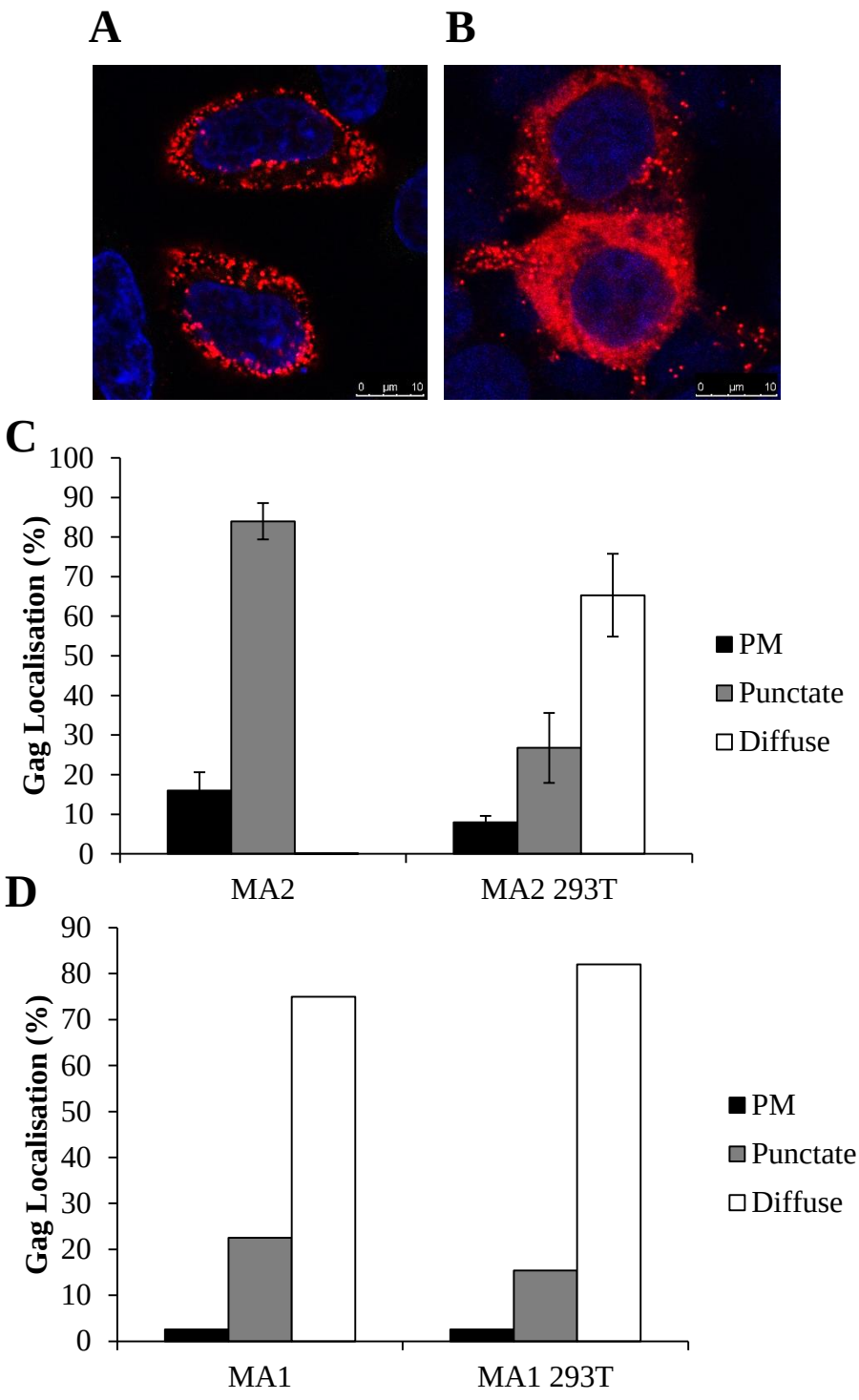

Figure 69: MA2 and MA1 Gag localisation in different cell types. A and B- Confocal immunofluorescence images of MA2 using an anti-HIV-1 p24 antibody (red) in MA2 transfected HeLa and HEK 293T cells, respectively. Blue stain= DAPI. C and D- Quantification of Gag localisation in HeLa and HEK 293T cells transfected with MA2 or MA1, respectively, from 2 independent repeat experiments.

egress, we would not expect the absence of tetherin to have much of an effect on this virus. HIV-1 Gag also remained unchanged in HEK 293T cells (data not shown).

To see if tetherin could also explain the strong colocalisation observed with both clathrin and AP-3 in HIV-2 transfected cells, WT HIV-2 (pSVR) was transfected into HeLa cells, and these were co-stained for both proteins under scrutiny. Figure 70 shows results from confocal immunofluorescence microscopy.

Figure 70A shows that WT HIV-2 still colocalised with clathrin, and was capable of re-distributing clathrin to areas concentrated with Gag. Figure 70B, however, demonstrates that although WT HIV-2 still strongly colocalised with AP-3, the re-distribution of this protein was not observed as before. In the presence of HIV-2, AP-3 still remained evenly distributed throughout the cytoplasm, albeit it seemed to be slightly more concentrated in the areas containing Gag. This suggests that tetherin plays a role in the strong colocalisation of AP-3 with Gag, and the redistribution of AP-3 observed previously (Figure 63A).

When HIV-2 (SVRΔNB) was transfected into HEK 293T cells (Figure 71), we saw a similar story with regards to AP-3 and clathrin. Once again, we saw colocalisation with AP-3 (Figure 71A) but without an obvious re-distribution. Clathrin (Figure 71B), however, was once again relocalised to Gag containing areas, and strong colocalisation within these areas was seen. Interestingly, however, when MA1 was transfected into HEK 293T cells, we no longer saw the extreme clathrin-Gag colocalisation. This was suggestive of tetherin restriction possibly causing an entanglement of assembling MA1 particles with clathrin, which was absent therefore when tetherin was not expressed. As previously deduced in this chapter, however, tetherin is not the sole factor in preventing MA1 egress.

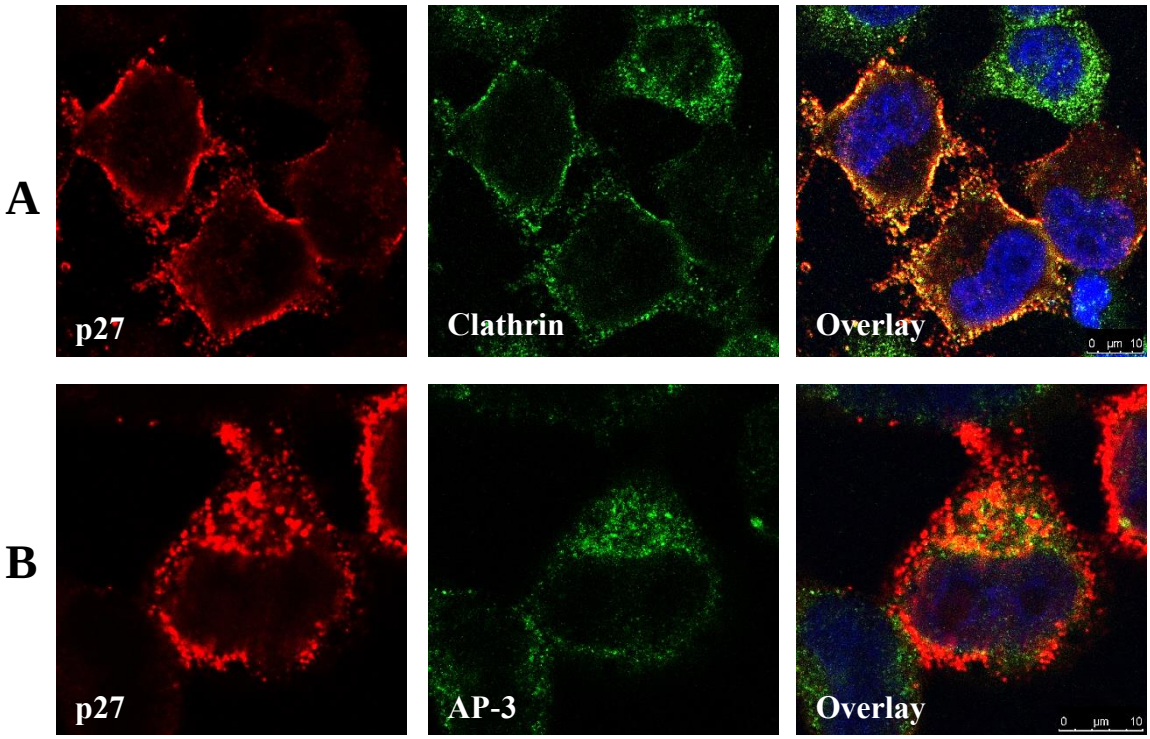

Figure 70: Wild-type HIV-2 strongly colocalises with and redistributes clathrin. Confocal immunofluorescence images of WT HIV-2 transfected HeLa cells. A- HeLa cells stained with anti-SIV p27 (red) and anti-clathrin heavy chain (green) antibodies. Colocalisation between Gag and clathrin was deduced to be strong by Pearson's correlation coefficient (average Rr= 0.681). B- HeLa cells co-stained for AP-3δ (green) and Gag p27 (red). Pearson's correlation coefficient deduced the colocalisation to be moderate (average Rr=0.43), however, Mander's overlap coefficient deduced the colocalisation to be strong (average R=0.645). Blue stain= DAPI.

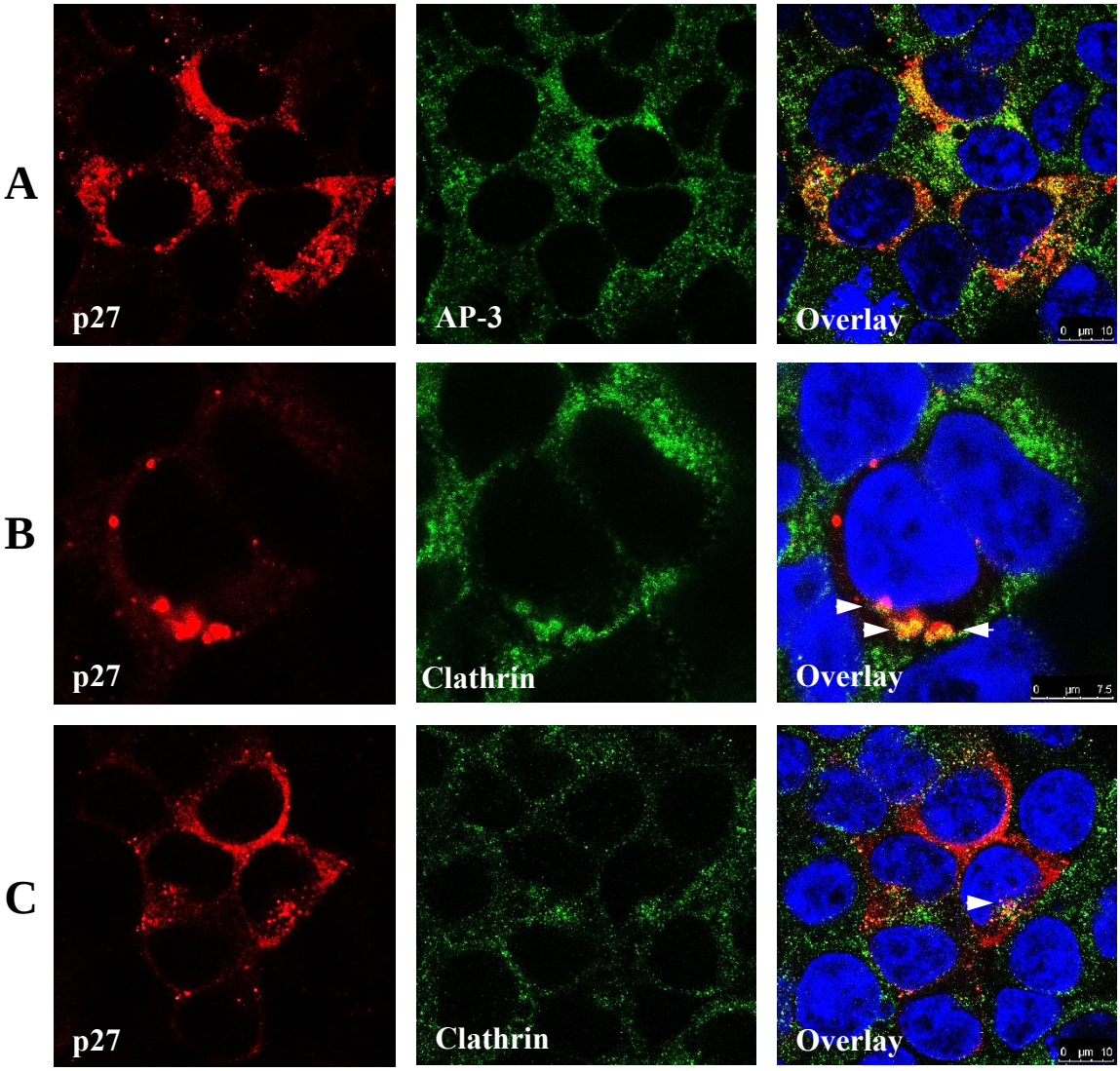

Figure 71: HIV-2 Gag colocalises with AP-3 and clathrin in HEK 293T cells. Confocal immunofluorescence images of HEK 293T cells transfected with HIV-2 or MA1. A- HIV-2 transfected cells co-stained with anti-SIV p27 (red) and anti-AP-3δ (green) antibodies. Strong colocalisation is seen (average Rr= 0.541). B- HIV-2 transfected cells co-stained with anti-SIV p27 (red) and anti-clathrin heavy chain (green) antibodies. White arrow indicates areas of colocalisation with clathrin (average Rr= 0.675). C- MA1 transfected cells co-stained with anti-SIV p27 and clathrin. The white arrow indicates small areas displaying colocalisation. Blue stain= DAPI.

To determine the intracellular compartment to which HIV-2 Gag is localising, endosomal markers were used. CD81 is a member of the tetraspanin family, and is enriched in LE/MVBs (Escola et al., 1998); if HIV Gag is localising to this compartment, we would expect to see colocalisation between these two proteins. Therefore, the HIV-2 provirus (SVRΔNB), and HIV-1 HXB2 for comparative measures, were transfected into both HeLa and HEK 293T cells for 24 hours, followed by preparation of samples for confocal immunofluorescence using anti-Gag and anti-CD81 antibodies. The results are shown in Figure 72.

As can be seen, HIV-1 displayed no/little colocalisation with CD81 in both HEK 293T (Figure 72A) and HeLa cells (Figure 72B). The average Pearson's correlation coefficient, calculated from multiple cells across 2 repeat experiments, confirmed low colocalisation (Rr=0.21 and 0.18, respectively). HIV-2, however, displayed colocalisation in both HEK 293T and HeLa cells (average Rr= 0.62 and 0.491, respectively). This demonstrates that HIV-2 Gag, but not HIV-1, is localised to CD81 positive compartments.

Previous results also gathered in this lab demonstrated that HIV-2 Gag, but not HIV-1, was localised to CD63 positive compartments (M. Marongiu and E.C. Anderson, unpublished results); CD63 is another member of the tetraspanin family and is also enriched in the LE/MVB (Escola et al., 1998). Therefore, HIV-2 Gag is localised to CD81 and CD63 positive compartments; this therefore indicates that HIV-2 uses the LE/MVB in Gag trafficking to a greater extent than HIV-1. This suggests that although results gathered in chapter 5 indicate that at least some HIV-1 Gag is directed to endosomal compartments in the normal trafficking pathway, this likely represents a small population of total Gag. HIV-2 Gag, however, is likely either beginning to assemble in these compartments, or uses an endosomal trafficking route to reach the

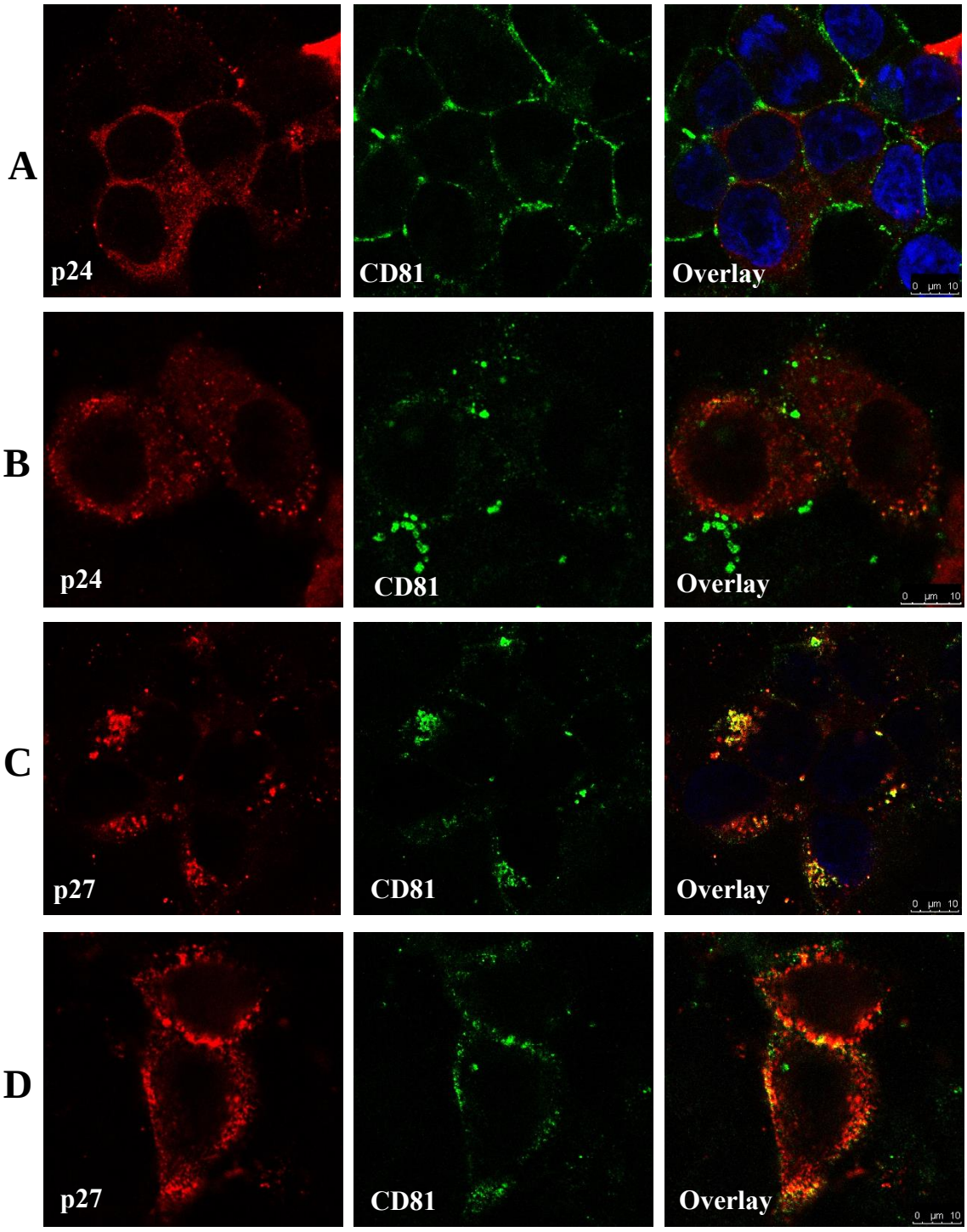

Figure 72: HIV-2, but not HIV-1, colocalises with CD81 in HeLa and HEK 293T cells. Confocal immunofluorescence images of HEK 293T cells transfected with a HIV-1 provirus (A) or HIV-2 provirus (C), co-stained with anti-p24 (HIV-1, red) or anti-p27 (HIV-2, red) and anti-CD81 (green). Pearson's correlation coefficient calculated across 2 repeat experiments deduced colocalisation to be low for HIV-1 (average Rr=0.21) but high for HIV-2 (0.62). B and D show HIV-1 and HIV-2 proviruses transfected into HeLa cells, staining for the same proteins. Pearson's correlation coefficient deduced colocalisation to be low for HIV-1 (average Rr=0.18) but borderline moderate/high for HIV-2 (average Rr=0.491). Blue stain=DAPI.

PM assembly site; direct trafficking of newly synthesised Gag to the PM is not supported by these results.

In order to ascertain whether HIV-2 Gag is indeed capable of assembling in intracellular compartments, electron microscopy studies were carried out. Results gathered previously in this lab found, through cryo-electron microscopy (EM), both immature and mature HIV-2 particles within intracellular compartments of HeLa cells (M. Marongiu, I. Portman and E.C. Anderson, unpublished results). HIV-1, in contrast, was found predominantly at the PM. Since these particles may have been a result of tetherin restriction, EM was carried out on HIV-2 transfected HEK 293T cells. Results are shown in Figure 73.

Although mature particles could not be seen intracellularly, immature particles were observed within a clear intracellular compartment distant from the PM. This indicates the possibility that HIV-2 is capable of assembling within intracellular compartments, destined for extracellular release by PM fusion. Particles were also seen, however, budding from the PM (data not shown). Therefore, it is possible that HIV-2 may adopt two intracellular assembly sites in both HeLa and HEK 293T cells; intracellular compartments or the PM.

6.2.12 Inhibition of Endocytosis Does Not Affect HIV-2 Gag Localisation

Although knockdown of AP-2, which would impair clathrin mediated endocytosis, did not alter the punctate phenotype of HIV-2 Gag, and HIV-2 Gag is still predominantly punctate in tetherin deficient (HEK 293T) cell lines, it was necessary to investigate the possibility of clathrin-independent endocytosis playing a role in the phenotype of HIV-2 Gag. Rab5 is localised to early endosomes (EE), and has been demonstrated to

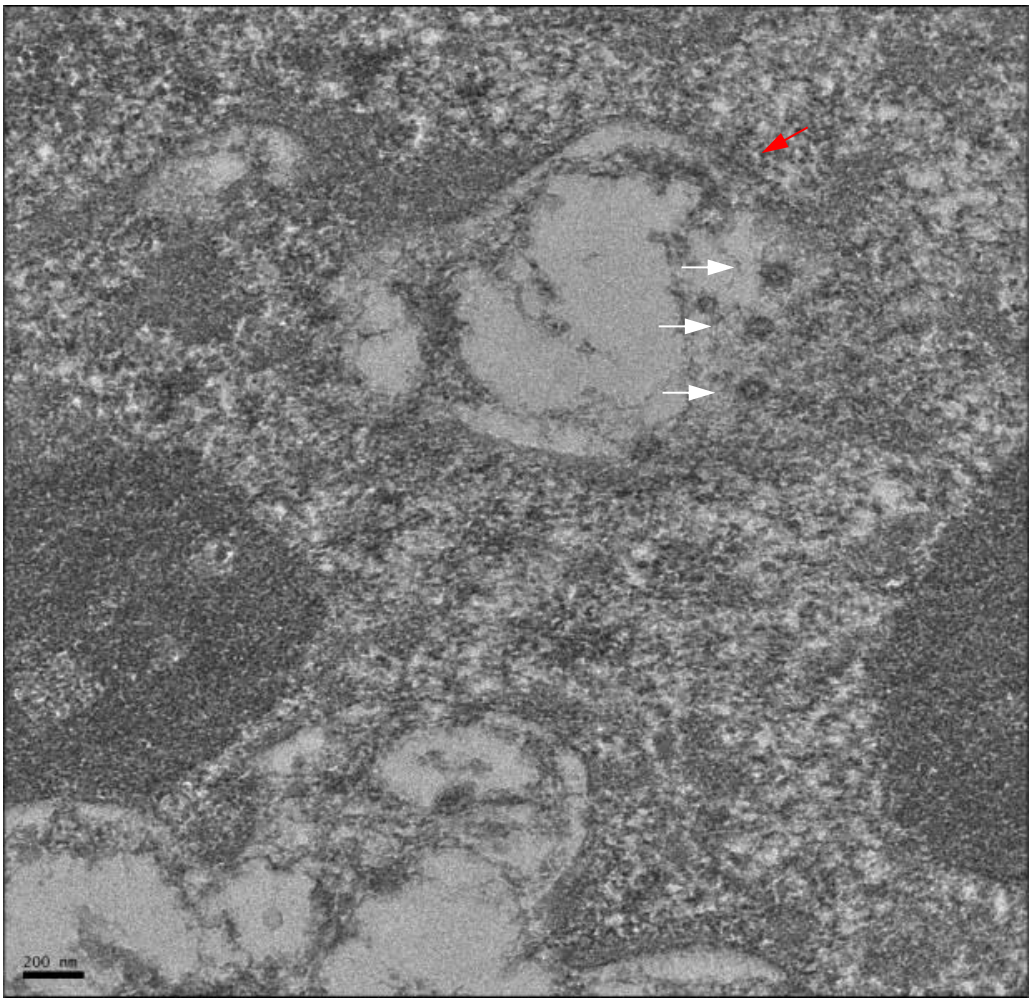

Figure 73: Localisation of HIV-2 particles in HEK 293T cells. HEK 293T cells were transfected with HIV-2 pSVRΔNB proviral plasmid for 40 hours prior to formaldehyde fixation and viewing with a cryo-transmission electron microscope. Assembled HIV-2 particles can be observed within an intracellular compartment. White arrows indicate immature viral particles approximately 100nm in diameter, red arrow indicates intracellular compartment membrane.

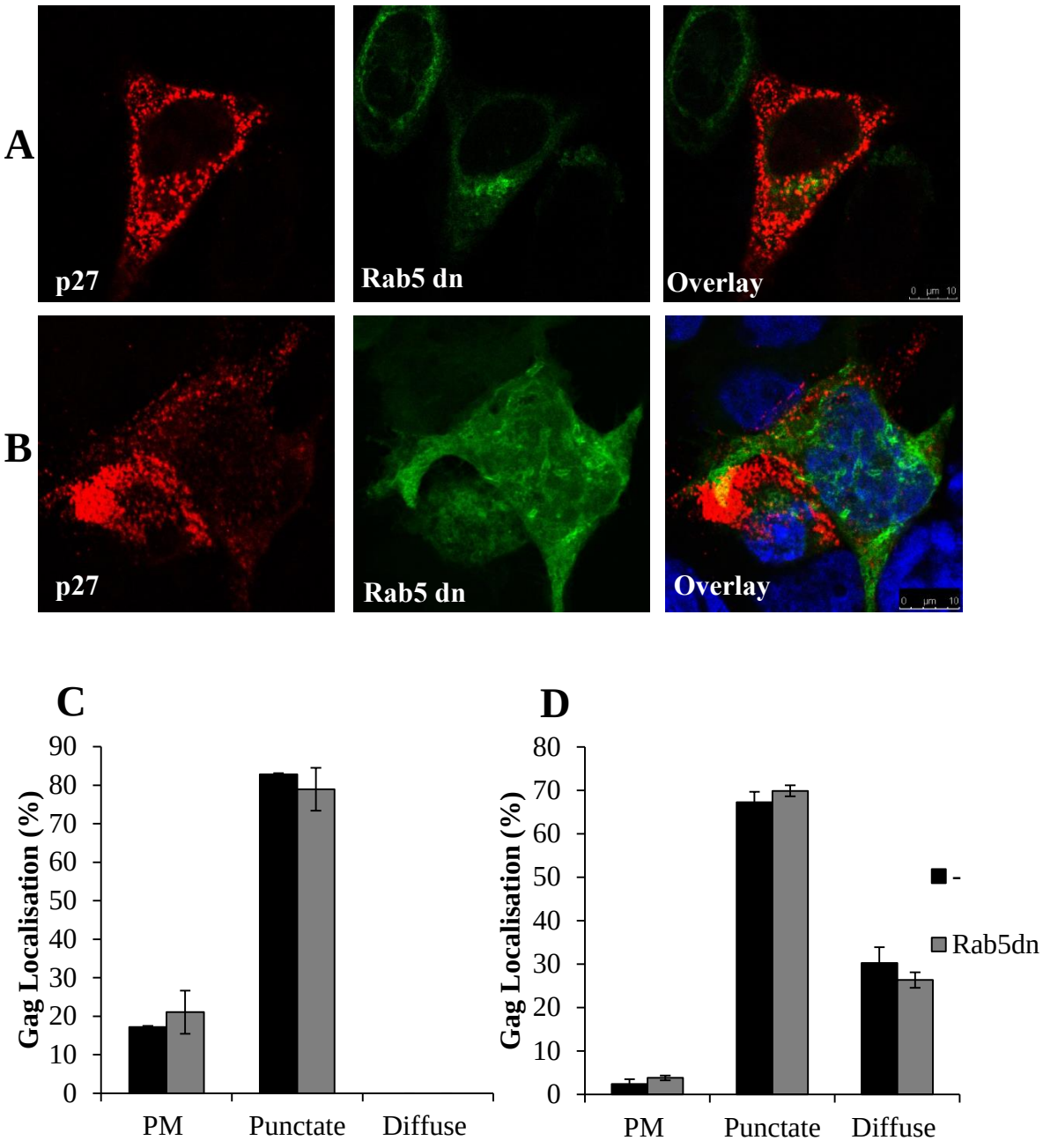

Figure 74: Dominant negative Rab5 does not alter the localisation of HIV-2 Gag. A and B show confocal immunofluorescence images of HeLa and HEK 293T cells, respectively, co-transfected with a HIV-2 provirus and a Rab5dn (green) construct. Anti-p27 was used to stain Gag (red). Blue stain=DAPI. C and D show average percentages of Gag localisations taken from counts of cells expressing Gag, with and without Rab5dn, across 2 repeat experiments in HeLa and HEK 293T cells, respectively.

regulate endosome biogenesis (Zeigerer et al., 2012) and regulates the fusion of incoming endocytic vesicles from the PM to the EE (Barbieri et al., 1996). A dominant negative Rab5 construct has been developed, which blocks both clathrin-dependent and clathrin-independent endocytosis events (Dinneen and Ceresa, 2004; Zeigerer et al., 2012). This is because the Rab5dn is unable to facilitate fusion of the endocytic vesicle with the EE, and cannot promote the recycling of factors necessary to internalisation (Li et al., 1995). To investigate the localisation of HIV-2 Gag in the presence of this construct, HeLa and HEK 293T cells were co-transfected with the HIV-2 SVRΔNB provirus and Rab5dn for 24 hours. Samples were prepared for confocal immunofluorescence microscopy, and stained for anti-p27 Gag. The results are demonstrated in Figure 74.

As can be seen, visually the presence of Rab5dn did not reduce the punctate appearance of HIV-2 Gag. In order to quantify the localisation of HIV-2 Gag in these two cell lines, with and without the Rab5dn, cells expressing Gag were counted across 2 repeat experiments, and Gag localisation was recorded. The results are shown graphically in Figures 74C and D. As can be seen, Rab5dn did not significantly alter the HIV-2 Gag localisation in either cell line. This again indicates that the presence of HIV-2 in punctae is not a result of internalisation of particles from the PM, further supporting a role for endosomal compartments in the trafficking of HIV-2 Gag.

6.3 Discussion

HIV-2 is certainly less prevalent worldwide in comparison to HIV-1, however it is still an important feature of the AIDS epidemic. Although the epidemic of HIV-2 has been limited in comparison to HIV-1, with the majority of HIV-2 infections reported in West Africa and countries with colonial links to this region, HIV-2 infections have been

documented globally, for example in Europe, America and India (Remy, 1998; McCutchan, 2006; de Silva and Weiss, 2010). Fewer HIV-2 patients progress to AIDS than HIV-1; however, in HIV-2 patients that have reached this stage, the clinical manifestations are very similar (Nyamweya et al., 2013). The interactions between HIV-1 and the adaptor proteins have been described, however, no such studies existed for HIV-2. HIV-1 and HIV-2 Gag share 60% amino acid similarity in their Gag proteins (Dilley et al., 2011), it was assumed that they likely follow similar pathways. This chapter aimed to shed light on the trafficking pathways of newly synthesised HIV-2 Gag proteins, and how HIV-2 interacts with the clathrin adaptor proteins.

Initial experiments indicated that HIV-1 and HIV-2 were not identical with regards to interactions with the APs; the effects on HIV-1 viral assembly and egress when AP-1/-3 were knocked down were similar (Figure 39), whereas AP-3 siRNA had a markedly larger effect than AP-1 siRNA on HIV-2 (Figure 47). AP-2 knockdown had no effect on HIV-2 release, whereas AP-2 is known to inhibit HIV-1 particle release. HIV-2 also colocalised extensively with AP-3, redirecting it to Gag concentrated intracellular areas. The late endosome adaptor AP-5 also played a prominent role in HIV-2 assembly and release (Figures 52 and 53), unlike HIV-1 (Figure 45). This, taken together with the very punctate intracellular appearance of HIV-2 Gag, seemed to draw an obvious conclusion that HIV-2 trafficking is heavily dependent on internal compartments, most probably endosomes.

Two possible non-exclusive hypotheses emerged; HIV-2 Gag traffics to the PM via endosomes and assembles at the PM, or HIV-2 particles predominantly assemble within intracellular compartments, in a similar manner to that of HIV-1 within macrophages. Both of these could explain the heavy co-staining with AP-3; if AP-3 is facilitating the delivery of Gag to or from intracellular compartments, we would expect

to see these proteins together in discrete colocalised areas. Since AP-3 is involved in endosomal trafficking, this would also explain the prominent effects of AP-3 knockdown on Gag. A severe depletion in total Gag levels was observed upon AP siRNA treatment, particularly when AP-3 was knocked down. A plausible explanation for this is that in the absence of AP-3, Gag filled or coated endosomes are unable to efficiently traffic to the PM for assembly and release of particles. Therefore, we could envisage that they instead become fused with lysosomes or are targeted to the proteasome, and Gag is ultimately degraded. Experiments involving lysosome/proteasome inhibitors (Figure 49) would however suggest that this is not the case. A more likely explanation therefore is that AP-3 indeed facilitates the entry of HIV-2 Gag into endosomal compartments, working in concert with clathrin to deform endosomal membranes and concentrate Gag into virus-like particles. In the absence of AP-3, therefore, we might expect unbound cytoplasmic Gag to be readily degraded by cellular systems.

This theory would support the evidence gathered by Zhang et al. (2011), who found that clathrin stabilised SIV Gag proteolysis products. Since the adaptors are crucial to clathrin function, we could assume that in their absence, clathrin would be unable to be recruited efficiently, therefore explaining the disappearance of HIV-2 Gag when AP-1/-3 are knocked down. AP-5, however, was discovered not to interact with clathrin, and when AP-5 was knocked down, we saw a decrease in HIV-2 Gag levels only. This suggested that clathrin stabilisation, although playing a role in preventing Gag degradation is not the sole reason for the disappearance of Gag when AP-1/-3 were knocked down.

Where does AP-1 come in? Clearly AP-1 is involved in HIV-2 trafficking, since in its absence we see a slight decrease in both cellular and released Gag (Figure 47), however

its role is certainly superseded by AP-3, given that AP-3 knockdown caused significantly larger effects. Although these proteins function in different cellular pathways, there is some overlap. Indeed, AP-1 is involved in facilitating cargo delivery to endosomes. Therefore we cannot exclude the possibility that AP-1 is actually involved in the direction of Gag to endosomes, and that the role of AP-3 is instead in ensuring maturation/delivery of endosomes; perhaps HIV-2 is unable to bud into early endosomes, and therefore the requirement of AP-3 is to facilitate the trafficking to mature, late intracellular compartments for budding. What seems a more likely explanation, however, is there is some redundancy in AP-1 and AP-3 function, but that in the case of HIV-2, AP-3 plays the greater role; thus when AP-1 is knocked down, AP-3 compensates for this loss, but when AP-3 is knocked down, AP-1 is unable to fully compensate.

This model of HIV-2 trafficking was, however, complicated by confocal immunofluorescence results gathered in HEK 293T cells. Although Gag expressed in HEK 293T cells was still predominantly punctate, we saw a large increase in the amount of diffusely stained cells. This suggested that tetherin played a role in the punctate appearance of HIV-2 Gag. There may also be other differences between these cell types. Although a tetherin antagonist, Env was evidently unable to antagonise tetherin entirely since WT HIV-2 and *env* deleted HIV-2 exhibited almost identical Gag appearances. We also know that AP-2/clathrin mediated endocytosis of newly released particles is not the reason for the punctate Gag pattern, since AP-2 knockdown exerted no effect on Gag localisation. The use of a dominant negative Rab5 construct, in both HeLa and HEK 293T cells, demonstrated that the Gag phenotype we observed was not due to endocytosis of released particles (Figure 74). Tetherin was also, however, found to be responsible for the relocalisation of AP-3 to Gag concentrated areas; this is likely

because re-internalised particles would aggregate into endosomal-like compartments, around which AP-3 would be relatively abundant. Electron microscopy, however, found immature particles within clear intracellular compartments in HEK 293T cells; this supports the theory that HIV-2 may indeed begin assembling within these compartments. Confocal immunofluorescence microscopy found that the compartments HIV-2 Gag localises to are enriched in CD81, a late endosome marker (Figure 72), and CD63, another late endosome marker (M. Marongiu and E. C. Anderson, unpublished data), further supporting the role of late endosomes in HIV-2 assembly.

It therefore remains a possibility that HIV-2 Gag is capable of adopting two independent trafficking pathways for viral egress; HIV-2 traffics directly/via an endosomal intermediate to the PM where assembly begins, or HIV-2 traffics to the PM after assembling within intracellular compartments. Why HIV-2 adopts a different pathway to HIV-1 is so far unclear. The presence of Vpx, which allows HIV-2 to evade restriction by SAMHD1 in myeloid cells may have given rise to evolutionary pressures to adopt different cellular pathways to HIV-1(Laguette et al., 2011).

The MA domain of HIV-1 Gag was discovered to not only contain AP binding sites, but may also contribute to the intracellular trafficking and localisation of newly synthesised Gag. MA chimeras were used to investigate whether the possession of an alternate MA domain may confer a Gag phenotype similar to that of the donor virus. Initial results suggested the contrary; MA2 in fact behaved more like HIV-1 with regards to interactions with the APs, particularly since AP-2 was found to affect particle release (Figure 56). MA1 also had assembly characteristics reminiscent of HIV-2 (Figure 58). Intriguingly, however, when these viruses were investigated by confocal microscopy, MA2 Gag behaved more like HIV-2, and MA1 Gag like HIV-1 (Figure 61). Taken together, these do indeed support a role for MA in the Gag

targeting, but also suggest that AP binding sites may exist outside of MA. Although HIV-1 Nef binds AP-1, -2 and -3, Nef and Gag traffic independently, therefore this cannot be the explanation for the effects seen on Gag.

Initial results suggested that possession of HIV-2 MA was solely able to confer the localisation of Gag, and the ability of HIV-1 to assemble within intracellular compartments, since a very punctate Gag appearance was observed, reminiscent of HIV-2 Gag (Figure 61). The same could be said for MA1; cells transfected with this provirus displayed a Gag localisation phenotype more similar to HIV-1 than HIV-2 (Figure 61). MA2 was also observed in immature and mature forms within intracellular compartments through the use of EM, suggesting an ability of this virus to also assemble within such compartments (M. Marongiu, I. Portman and E.C. Anderson, unpublished results). Since we know MA is responsible for Gag targeting, this made sense. The story was complicated, however, by the reversal of the Gag phenotype when MA2 was transfected into HEK 293T cells, where Gag localisation became reminiscent of observations typically found in HIV-1 transfected cells. It could therefore be concluded that the punctate appearance of MA2 was not due to assembly within intracellular compartments, but by re-internalisation of tetherin-restricted virus particles. This also means that although MA targets Gag to assembly sites, it is unable to solely confer Gag localisation and assembly within the context of the virus.

The story emerging for MA1 is also complex. MA1 is unable to egress, but this was not solely due to tetherin restriction as released particles could not be observed when MA1 was transfected into HEK 293T cells (Figure 60). However, the strong colocalisation seen between MA1 Gag and clathrin in HeLa cells was not observed in HEK 293T cells (Figure 71). It may be that MA1 only colocalises with clathrin after it has been re-internalised into vesicles from the PM (Figure 67). Therefore, tetherin may be

responsible in part for MA1's inability to egress, but another feature of the virus makes it unable to release even in the absence of tetherin. The lack of PM Gag staining seen by confocal microscopy using this virus may hint that it is unable to engage efficiently with the PM; very few particles could be observed at the PM via EM (M. Marongiu, I. Portman and E.C. Anderson, unpublished results).

MA1 and HIV-2 also exerted interesting effects on AP-1 localisation, which were not observed in MA2 or HIV-1 transfected cells. The localisation of AP-1 appeared dramatically different in transfected HeLa cells, yet colocalisation was not seen with MA1 or HIV-2 Gag. AP-1 appeared less diffuse, and in some cells could be observed in long filamentous structures, which was never observed in un-transfected cells. Three potential explanations for this surfaced.

The first was from previous observations that HIV-1 Gag, in particular the NC domain, interacts directly with the cytoskeletal element actin. Although some controversy exists as to the exact role actin plays within the retroviral life cycle, it was proposed to be involved in assembly and budding (Rey et al., 1996; Liu et al., 1999; Gladnikoff et al., 2009). Although Gag may reach the PM via cytosolic diffusion, it remains a possibility that cytoskeletal elements may indeed actively transport Gag to the PM (Stolp and Fackler, 2011). Although the same interactions have not been elucidated for HIV-2, it is possible that actin plays a role in facilitating Gag trafficking to either the PM or intracellular compartments, and that this is AP-1 driven. AP-1 may recruit Gag to cytoskeletal elements for active trafficking through the cytosol, which would explain the filamentous appearance of AP-1 in HIV-2 transfected cells. Since the interacting domain was deduced to be NC within HIV-1 Gag, it may be that this is the same for HIV-2, explaining why we see the same AP-1 distribution in HIV-2 and MA1 transfected cells. HIV-1 may rely on actin in later stages only, for example assembly

and budding, explaining why we do not see the same AP-1 distribution in HIV-1 transfected cells.

The second possibility comes from a similar observation in HIV-1 transfected cells. KIF4, a microtubule motor and member of the kinesin family, was found to play a role in increasing the efficiency of HIV-1 Gag trafficking and assembly (Martinez et al., 2008). Once again, although this has not been studied in HIV-2, it remains a possibility that similar mechanisms exist to promote HIV-2 trafficking through the cytoplasm. It seems plausible that AP-1 may either direct KIF4 towards Gag molecules for microtubule associated trafficking, or vice versa. This would not only explain the tubular appearance of AP-1, but also support the comments made in results chapter 2 with regards to kinesin assisting lipoplex trafficking, possibly mediated by AP-1. The same group also found that an absence of KIF4 resulted in Gag instability and subsequent degradation, which could explain the decrease in Gag observed in AP-1 siRNA treated cells. This hypothesis is, however, complicated by the fact that we would expect similar AP-1 observations in HIV-1 transfected cells, which we do not.

The third possibility is that AP-1 is recruited to tubular endosomes by Gag, from which HIV-2 may pass through as an intermediate step to late endosomes or the PM. Since we know that HIV-1 does not require AP-5 for assembly and release but HIV-2 does, this also seemed a plausible explanation for the alteration in AP-1 localisation.

6.4 Future Work

Although the work in this chapter has characterised the phenotypes of MA1 and MA2 with regards likely trafficking pathways utilised and AP interactions, little is still known about why these viruses have striking differences in their ability to be able to

egress. Therefore, more work is needed to elucidate the reasons behind these characteristics.

More work needs to be continued on HIV-2 to also further characterise the trafficking pathway adopted by this virus. It would be interesting to see if an absence of AP-3, or indeed AP-1 also, decreased expression/functionality of viral protease, thus explaining the decrease in processed Gag observed when these proteins are absent. It would also be interesting to see if the same is seen when clathrin is knocked down. Yeast two-hybrid screening on HIV-2 MA mutants would also be a good assay to ascertain where the AP binding sites lie within Gag. Since results in this chapter also suggest that there may be further AP interacting domains outside of MA, further research is critical to determine whether this is indeed true, and where these potential interactions occur.

Future work on this project would also benefit from the construction of a GFP-tagged HIV-2 provirus could be used to directly visualise Gag trafficking in live cells.

CHAPTER 7: CAN HIV DISTURB WELL CHARACTERISED TRAFFICKING PATHWAYS?

7.1 Introduction

Diphtheria toxin (DTx), produced by toxigenic strains of the bacterium *Corynebacterium diphtheriae*, is one of the most extensively studied bacterial toxins and is widely utilised in scientific research. This is because of its many properties which include its cytotoxicity, the ability to cause a cessation in protein synthesis through the ADP-ribosylation of elongation factor 2 (EF-2) and capability of crossing membranes (Collier, 2001, Murphy, 2011). DTx is a single-chain member of the A-B toxin family, where the A and B chains are linked by a disulphide bridge (Watson and Spooner, 2006). The DTx mode of action and its trafficking pathway is well known, making it an ideal candidate for investigating trafficking.

Ricin, from the seeds of the castor oil plant *Ricinus communis* (Sandvig and van Deurs, 1999), is a heterodimeric ribosome inactivating protein composed of a catalytic A and galactose binding B chain, both of which are around 30 kDa and are also linked by a disulphide bridge (Sandvig et al., 2010). Enzymatically active ricin is able to specifically cleave 28S rRNA, and one active ricin molecule is capable of inactivating around 2000 ribosomes per minute, making it an extremely potent toxin (Schep et al., 2009). Ricin is also widely used today as a valuable marker for the study of endocytosis and intracellular transport steps (Sandvig and van Deurs, 1999).

Diphtheria toxin is synthesised in a single-chain precursor form that is processed by cellular furin upon uptake into 2 fragments; the catalytic A fragment, and fragment B which is composed of the translocation and receptor binding domains (Drazin et al., 1971; Choe et al., 1992; Lemichez et al., 1997; Murphy 2011). DTx enters the cell via clathrin-mediated receptor endocytosis of the bound toxin to the heparin-binding

epidermal growth factor (HB-EGF) precursor receptor, which is mediated by the receptor binding domain of the toxin (Naglich et al., 1992). This results in clathrin-coated vesicles containing the toxin which is enzymatically inactive. From an endosomal compartment, the B fragment of the toxin must assist in the translocation across the endosomal membrane to facilitate the transport of the catalytic domain into the cytosol, which is a pH sensitive step (Lemichez et al., 1997). The clathrin coat on these vesicles becomes replaced by Arf1 and COPI, and the proton pump vacuolar (v)ATPase lowers the pH of these endosomal vesicles (Murphy, 2011). This acidification triggers the transmembrane domain to unfold and consequently become inserted in the endosomal membrane, forming a transmembrane channel, or pore, which results in the translocation of the catalytic domain into the cytosol (Boquet et al., 1976; Donovan et al., 1981). There has been some controversy over the endosomal compartment from which DTx translocates into the cytosol; some suggested this may occur in compartments as late as lysosomes (Donovan et al., 1981), whereas others report that it occurs in a compartment upstream of late endosomes, which is the general consensus (Papini et al., 1993; Lemichez et al., 1997).

Once in the cytosol, the catalytic domain catalyses the NAD^+-dependent ADP-ribosylation of elongation factor 2 (EF-2) (Spooner et al., 2006; Murphy, 2011). EF-2 facilitates the movement of the peptidyl tRNA-mRNA complex from the A site of the ribosome to the P site during protein synthesis, and its ADP-ribosylation inhibits its translocation activity, and therefore prevents protein synthesis, resulting in cell death (Mateyak and Kinsy, 2013).

Ricin enters cells via galactose containing receptors (Sandvig and van Deurs, 1999; Li et al., 2010), and can utilise both clathrin-dependent and clathrin-independent endocytic pathways (Sandvig et al., 2010; Sandvig et al., 2013). From here, a large portion of

endocytosed ricin is actually recycled back to the cell surface (Sandvig and van Deurs, 1996), but the rest traffics to the Golgi directly from early endosomes in a clathrin-independent manner (Iversen et al., 2001; Sandvig et al., 2013). From here, ricin travels to the endoplasmic reticulum (ER) in a COPI independent manner (Llorente et al., 2003). In the ER, ricin is reduced to its RTA (ricin A chain) and RTB subunits (ricin B chain) before RTA is dislocated and enters the cytoplasm by exploiting the ERAD (ER-associated protein degradation) pathway (Watson and Spooner, 2006; Spooner et al., 2008; Li et al., 2010). From here, ricin acts in a different to way to DTx by directly modifying the EF-2 binding site within the large subunit of eukaryotic ribosomes. RTA is an RNA *N*-glycosidase that removes an adenine residue from 28s rRNA which forms part of a motif that interacts with EF-2 (Endo and Tsurugi, 1988).

Since HIV-1 Gag and Nef are known to bind to and interact with the adaptor proteins, we hypothesised that HIV-1 might cause disruption of cellular trafficking pathways; to test this hypothesis, we carried out DTx cytotoxicity assays and tested whether HIV-1 could interfere with this pathway via (reducing the cytotoxic effect of DTx). Ricin (RTx) was chosen as the control in these experiments since it is capable of trafficking in a clathrin-independent manner.

ts045-VSV-G-EGFP (VSV-G) is a temperature-sensitive mutant of the vesicular stomatitis virus glycoprotein, fused with EGFP (enhanced GFP) for visualisation. This glycoprotein has a well characterised secretory trafficking pathway and due to its strict temperature sensitivity it is a useful tool in determining interference with protein trafficking. At the restrictive temperature (39.5^{o}C) the protein is co-translationally synthesised and imported into the endoplasmic reticulum where it becomes glycosylated. However, it cannot traffic further than the ER (Schnitzer et al., 1979). Upon transition to the permissive temperature (32^{o}C) the glycoprotein follows a

particular route to its final destination; the plasma membrane, via the Golgi. This trafficking takes approximately 2 hours after the temperature shift; therefore it is possible to fix cells at predetermined points and visualise the localisation of the GFP-tagged glycoprotein. At t_0 (39.5^{o}C) VSV-G appears at the ER, at t_{30} (30 minutes post temperature shift) VSV-G is present in the Golgi, at t_{60} the construct begins to shift towards the PM, presenting a diffuse localisation with some presence at the PM, and at t_{120} the construct is almost entirely present at the PM with some remaining Golgi/diffuse localisation.

It was reported that VSV-G requires the delta subunit of AP-3 in order to traffic efficiently from the ER to the PM (Nishimura et al., 2002). This is the same subunit which HIV-1 Gag has been reported to interact with, directly or indirectly, and is required for efficient viral egress. It was therefore hypothesised that HIV-1 may interfere with VSV-G trafficking to the PM through competition for the AP-3δ subunit.

7.2 Results

7.2.1 HIV-1 Protects against Diphtheria Toxin

Diphtheria toxin (DTx) traffics down the endosomal pathway, requiring clathrin for cell entry and therefore most likely AP-2 also. Although a role for AP-3 in DTx trafficking has never been formally defined, we propose to investigate a possible role for AP-3 in DTx trafficking. Since HIV-1 Gag may traffic at least some of the time via endosomal compartments in an AP-3 dependent manner, we speculated whether HIV-1 transfection could therefore interfere with the trafficking of DTx. Although ricin (RTx) may involve clathrin in its trafficking, it can also traffic in a clathrin-independent manner. Since inhibition of protein synthesis by DTx and RTx can be quantified by measuring the effect of the toxins on incorporation of 35S-methionine, we used these assays to test whether HIV-1 perturbs cellular trafficking of DTx and RTx.

HeLa cells, which express the DTx receptor on their surface, were transfected with one of a number of different proviral plasmids. 40 hours post-transfection the cells were challenged with increasing concentrations of DTx or RTx. 4 hours after toxin challenge, cellular ^{35}S-methionine incorporation was measured to determine cytotoxicity by IC_{50} values (the amount of a substance required to inhibit a biological process by 50%). All assays were carried out in quadruplicate on at least 3 independent occasions. Cytotoxicity curves from one representative experiment, used to calculate IC_{50} values, are shown in Figures 75 A-G. A change in IC_{50} values in the presence of provirus was used to calculate the protective effect of the provirus on DTx or RTx toxicity, shown in Figure 75H.

$HXB2N^+$ (see chapter 3) was the first provirus tested; this is the envelope-deleted HXB2 HIV-1 provirus, with full length Nef. Figure 73A shows a large difference between the DTx cytotoxicity curves of the mock (no DNA, Lipofectamine only) transfected cells, and the proviral transfected cells, and consequently a large difference between the IC_{50}s. As can be seen, a higher concentration of toxin was required to cause a 50% cessation in protein synthesis. The calculated protective effect of HIV-1 $HXB2N^+$ against DTx across repeat experiments was 3.5 fold (Figure 75H). Although the effect on RTx was minor (Figure 75Ai), as seen by little change in the IC_{50} values and cytotoxicity curves, the opposite effect could be seen; a slight sensitisation, as a lower concentration of toxin was required to cause a cessation in protein synthesis. This was calculated to be 1.6 fold (Figure 75H). These results demonstrate the ability of HIV-1 to interfere with a stage of the DTx trafficking pathway, but also a surprising slight effect on the RTx pathway.

Since both Gag and Nef are able to interact with the APs, it was next investigated whether the presence of Nef is necessary for this protective effect against DTx. To ascertain this, the HXB2 provirus was used, has a truncated Nef protein. The results are shown in Figures 75B, Bi and H. The average protective effect against DTx was calculated to be 3.2 fold, and a 1.7 fold sensitisation to RTx. To determine whether this slight difference in protection was significant, *p* values were calculated. This test deduced that the results are not significantly different ($p>0.05$). This would indicate that Nef is not required for the protective effect observed against DTx cytotoxicity.

To ascertain whether the protective effect observed was specific to the presence of HIV-1 proteins, and not transfecting cells with any provirus, HVPΔEC was used (Richardson et al., 1993). Although this provirus has the backbone of HIV-1, it does not produce Env, most of Gag, or the accessory genes (including Nef). The results are shown in Figures 75C, Ci and H. As can be seen, this provirus has little effect on both DTx and RTx cytotoxicity. The observed effects against DTx and RTx were found to be a 1.9 fold protection, and a 1.3 fold sensitisation, respectively. Student's t-test deduced the protective effect to DTx to be very significantly different from the results obtained from HXB2N$^+$ ($p<0.01$), whereas once again the sensitisation to RTx was not significantly different ($p>0.05$). This indicated that the presence of HIV-1 are required to increase protection against DTx. It is possible that this slight effect observed is due to an interruption of plasma membrane function caused by transfection, which could possibly interfere with DTx internalisation.

Next, to investigate whether Gag was necessary to produce the protective effect against DTx, the two Gag mutant proviruses were used; HXB2N$^+$ΔGag and HXB2ΔGag. The use of these two proviruses would also demonstrate whether the presence of Nef can

A

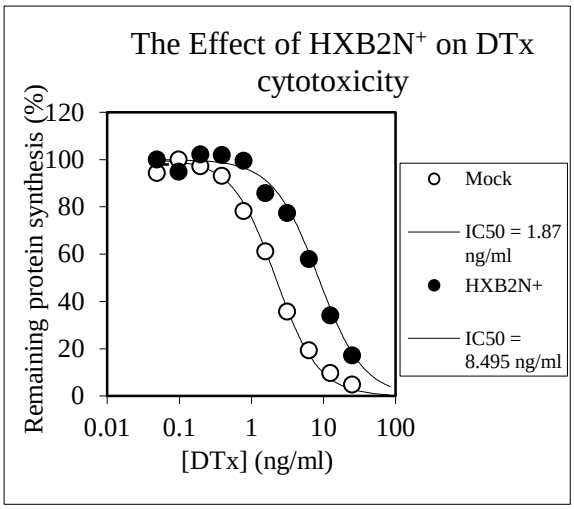
The Effect of HXB2N+ on DTx cytotoxicity
Remaining protein synthesis (%)
120
100
80
60
40
20
0
0.01
0.1
1
10
100
[DTx] (ng/ml)
Mock
IC50 = 1.87 ng/ml
HXB2N+
IC50 = 8.495 ng/ml

Ai

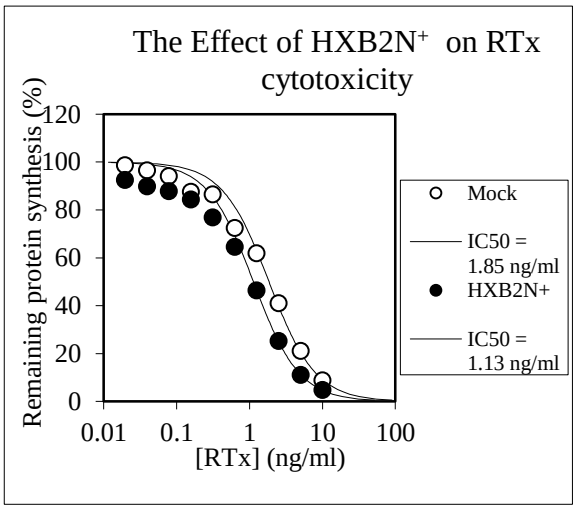
The Effect of HXB2N+ on RTx cytotoxicity
Remaining protein synthesis (%)
120
100
80
60
40
20
0
0.01
0.1
1
10
100
[RTx] (ng/ml)
Mock
IC50 = 1.85 ng/ml
HXB2N+
IC50 = 1.13 ng/ml

B

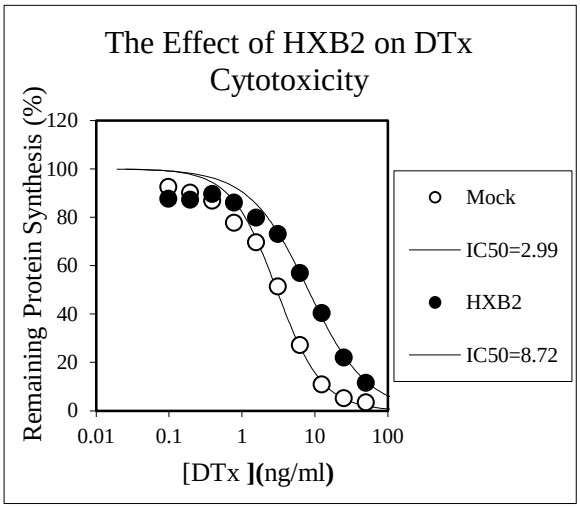
The Effect of HXB2 on DTx Cytotoxicity
Remaining Protein Synthesis (%)
120
100
80
60
40
20
0
0.01
0.1
1
10
100
[DTx](ng/ml)
Mock
IC50=2.99
HXB2
IC50=8.72

Bi

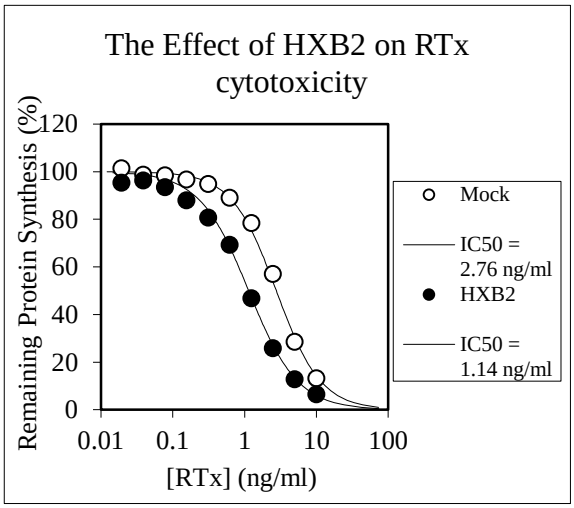
The Effect of HXB2 on RTx cytotoxicity
Remaining Protein Synthesis (%)
120
100
80
60
40
20
0
0.01
0.1
1
10
100
[RTx] (ng/ml)
Mock
IC50 = 2.76 ng/ml
HXB2
IC50 = 1.14 ng/ml

C

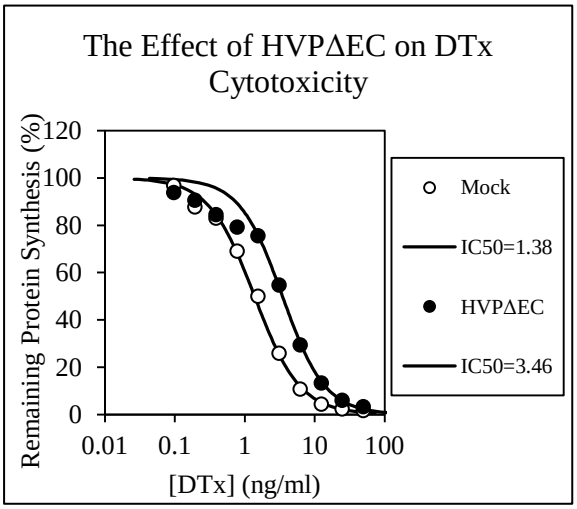
The Effect of HVPΔEC on DTx Cytotoxicity
Remaining Protein Synthesis (%)
120
100
80
60
40
20
0
0.01
0.1
1
10
100
[DTx] (ng/ml)
Mock
IC50=1.38
HVPΔEC
IC50=3.46

Ci

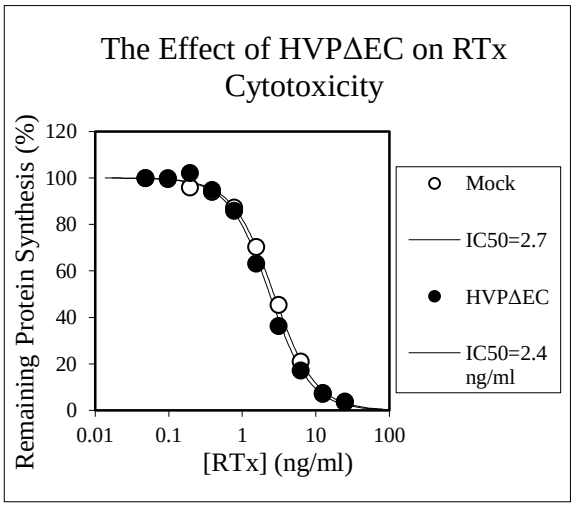
The Effect of HVPΔEC on RTx Cytotoxicity
Remaining Protein Synthesis (%)
120
100
80
60
40
20
0
0.01
0.1
1
10
100
[RTx] (ng/ml)
Mock
IC50=2.7
HVPΔEC
IC50=2.4 ng/ml

compensate for the absence of Gag. The results are shown in Figures 75D, E and H. Small protective effects against DTx were observed for these proviruses; 1.9 fold for $HXB2N^{+}\Delta Gag$ and 2.3 fold for HXB2ΔGag. These were deduced not to be significantly different from HVPΔEC ($p>0.05$), but very significantly different from $HXB2N^{+}$ ($p<0.01$). Together, these results indicate that Gag is likely necessary for the protective effect. Once again, slight sensitisations to RTx were observed (Figures 75Di, Ei and H); 1.6 fold for $HXB2N^{+}\Delta Gag$, and 1.5 fold for HXB2ΔGag, which were also not significantly different from $HXB2N^{+}$.

Since it was clear that Gag is required to protect against the cytotoxic effects of DTx, the next logical step was to ascertain whether Gag alone could produce the same effect as the provirus. A Gag-GFP pcDNA construct was used, alongside a GFP only control. The results are shown in Figures 75F, G and H. Although Gag-GFP produced a larger 2.4 fold protection against DTx, compared with only 1.75 fold for GFP, t-test deduced these results to be not significantly different from each other ($p>0.05$). Both of these results, however, were once again very significantly different from $HXB2N^{+}$ ($p<0.01$). Both of these plasmids also produced a slight sensitisation to RTx (Figures 75Fi, Gi and H); 1.1 fold for Gag-GFP and 1.6 fold for GFP, which were not significantly different from $HXB2N^{+}$. Together, these results indicate that Gag is necessary, but not sufficient, to protect against DTx. The fact that GFP also produces a slight sensitisation to RTx also indicates that this is a non-specific effect of transfecting in DNA or overexpressing exogenous protein, rather than a HIV mediated effect. The compiled protective effects observed are summarised in Figure 75H, which also highlights significant differences in values by asterisks, as compared with $HXB2N^{+}$.

D

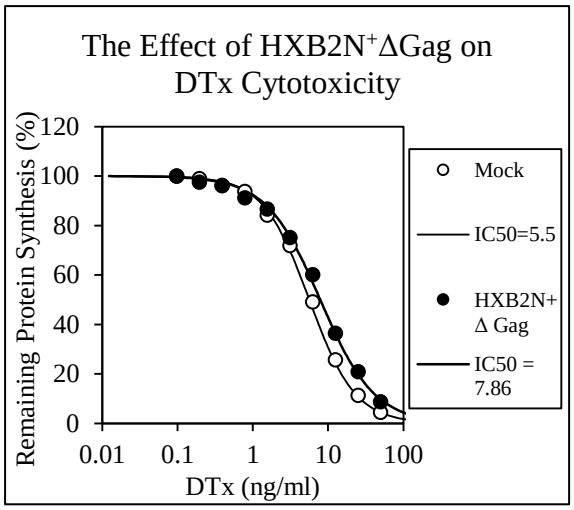
The Effect of HXB2N+ΔGag on DTx Cytotoxicity
Remaining Protein Synthesis (%)
120
100
80
60
40
20
0
0.01
0.1
1
10
100
DTx (ng/ml)
Mock
IC50=5.5
HXB2N+ Δ Gag
IC50 = 7.86

Di

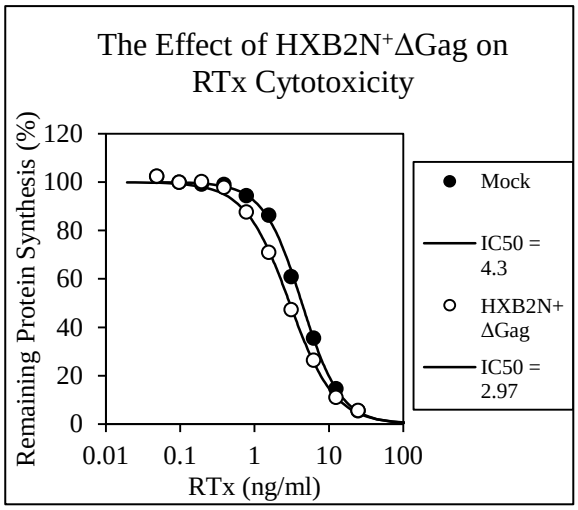
The Effect of HXB2N+ΔGag on RTx Cytotoxicity
Remaining Protein Synthesis (%)
120
100
80
60
40
20
0
0.01
0.1
1
10
100
RTx (ng/ml)
Mock
IC50 = 4.3
HXB2N+ ΔGag
IC50 = 2.97

E

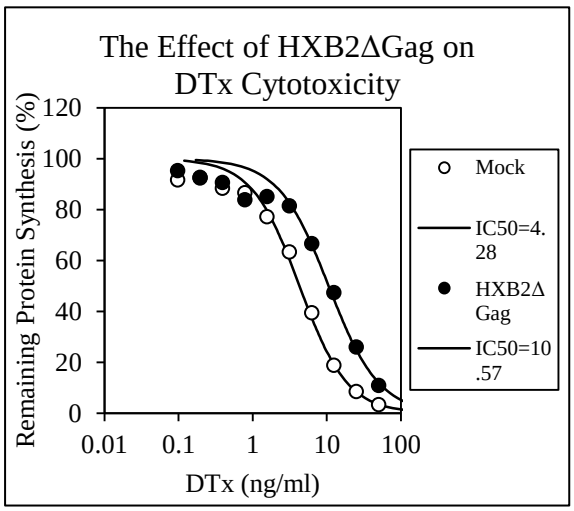
The Effect of HXB2ΔGag on DTx Cytotoxicity
Remaining Protein Synthesis (%)
120
100
80
60
40
20
0
0.01
0.1
1
10
100
DTx (ng/ml)
Mock
IC50=4.28
HXB2Δ Gag
IC50=10.57

Ei

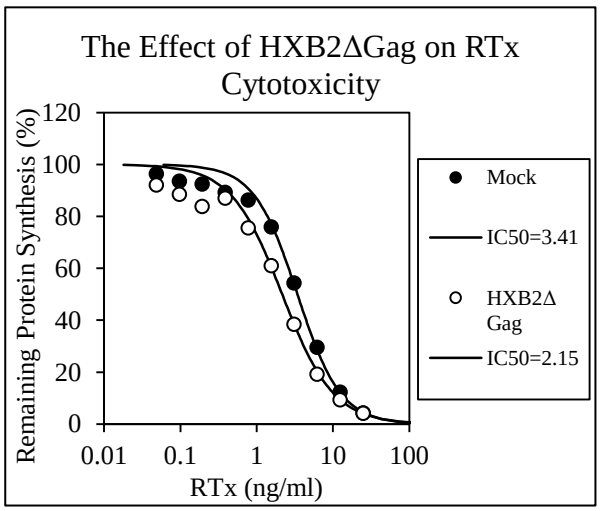
The Effect of HXB2ΔGag on RTx Cytotoxicity
Remaining Protein Synthesis (%)
120
100
80
60
40
20
0
0.01
0.1
1
10
100
RTx (ng/ml)
Mock
IC50=3.41
HXB2Δ Gag
IC50=2.15

F

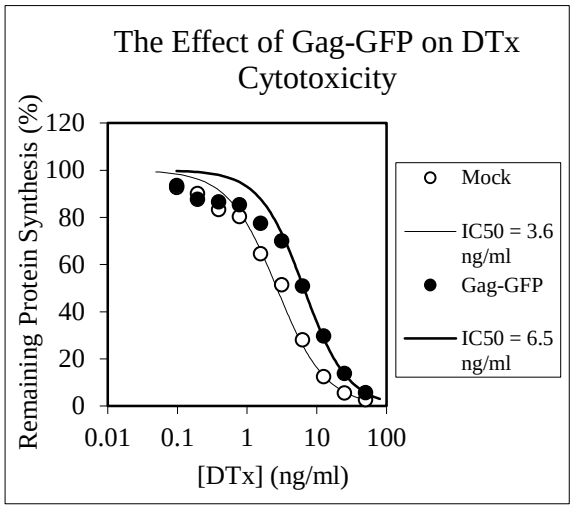
The Effect of Gag-GFP on DTx Cytotoxicity
Remaining Protein Synthesis (%)
120
100
80
60
40
20
0
0.01
0.1
1
10
100
[DTx] (ng/ml)
Mock
IC50 = 3.6 ng/ml
Gag-GFP
IC50 = 6.5 ng/ml

Fi

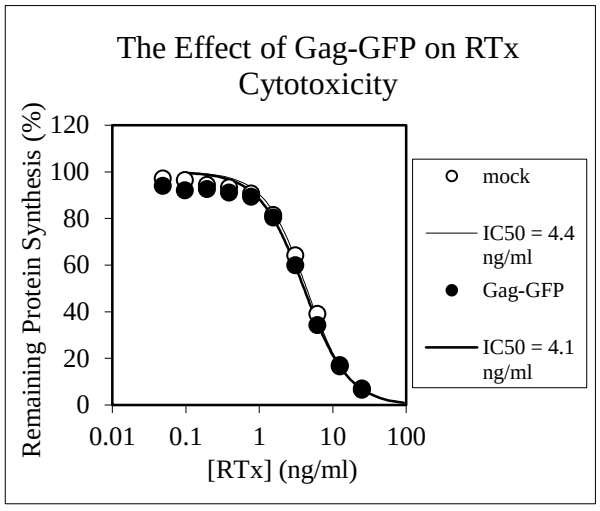
The Effect of Gag-GFP on RTx Cytotoxicity
Remaining Protein Synthesis (%)
120
100
80
60
40
20
0
0.01
0.1
1
10
100
[RTx] (ng/ml)
mock
IC50 = 4.4 ng/ml
Gag-GFP
IC50 = 4.1 ng/ml

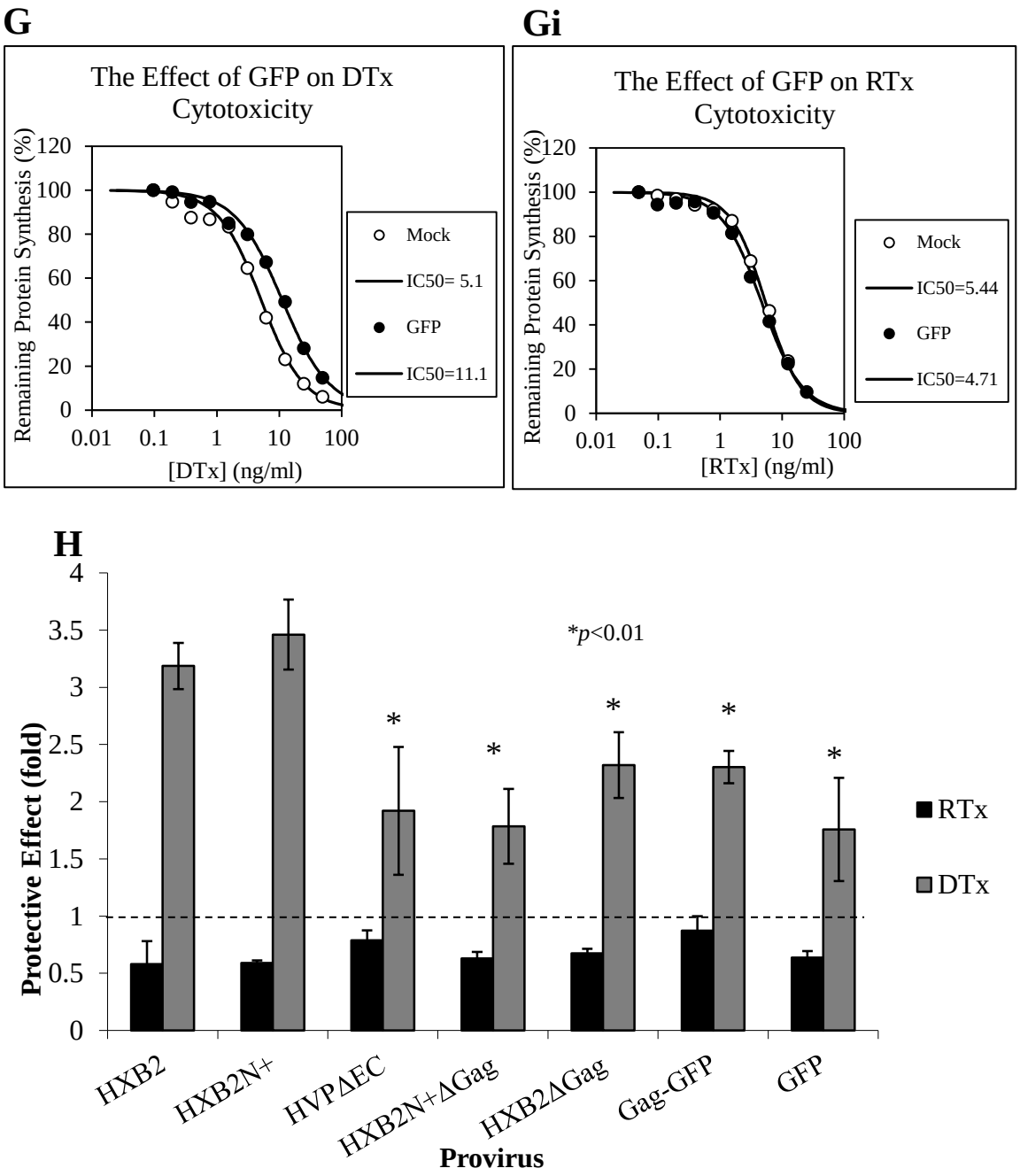

Figure 75: The effect of HIV-1 on DTx/RTx cytotoxicity. A-G- Left panels show DTx cytotoxicity curves, Ai-Gi- Right panels show RTx, from 4 hour toxin challenges of transfected HeLa cells, showing one representative result from 3 repeat experiments. IC50 (concentration in ng/ml at which protein synthesis is inhibited by 50%) is shown to the right of each graph. Proviruses used in experiments are as follows; A-HXB2N$^+$, B- HXB2, C-HVPΔEC, D-HXB2N$^+$ΔGag, E-HXB2ΔGag, F- Gag-GFP, G- GFP pcDNA. H shows a compilation of average protections/sensitisations to toxins from 3 repeat experiments. Statistically significant results, as compared to HXB2N$^+$, are highlighted by an asterisk (p<0.01)

7.2.2 HIV-2 has a Greater Effect on DTx Trafficking than HIV-1

Results gathered in the previous chapter suggest that HIV-2 Gag trafficking and assembly requires intracellular compartments, which are likely to be multivesicular bodies (MVBs)/late endosomes. Similar to HIV-1 Gag, it is also probable that HIV-2 Gag reaches these late endosomal compartments via early endosomal compartments, since in both cases when AP-3 was knocked down, Gag became stuck within intracellular compartments and could not traffic to the PM. Since early endosomal compartments are used in DTx trafficking (Papini et al., 1993; Lemichez et al., 1997), and late endosomes may also play some role, it was predicted that HIV-2 would also interfere with DTx cytotoxicity, but perhaps to a greater extent than HIV-1, since HIV-1 predominantly assembles and buds at the PM. Results gathered from transfecting HeLa cells with the *env* deleted HIV-2 provirus SVRΔNB are shown in Figures 76A, Ai and D, where A and Ai are one representative from repeat experiments. As can be seen, HIV-2 had a large effect on DTx cytotoxicity, and the protective effect was revealed to be 4.6 fold, which was higher than HIV-1 HXB2. T-tests revealed this difference to be significant, indicating that HIV-2 SVRΔNB transfected provirus had a significantly greater protective effect against DTx cytotoxicity than HIV-1 HXB2. The effect for RTx was also a slight sensitisation as with HIV-1; an average of 1.7 fold, similar to that of HIV-1.

Next, to investigate whether the MA domain contributes to this effect, the MA2 provirus was tested. Since this virus is more efficient at particle release than HIV-1, it was predicted that this may have a greater effect on DTx cytotoxicity. The results are shown in Figures 76B, Bi and D. Surprisingly, the protective effect against DTx was revealed to be 3.5 fold; a similar value to that obtained for HIV-1 HXB2. HXB2 was

A

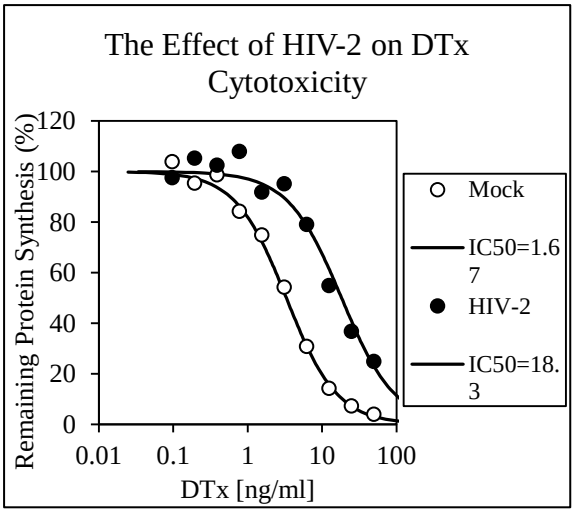
The Effect of HIV-2 on DTx Cytotoxicity
Remaining Protein Synthesis (%)
120
100
80
60
40
20
0
0.01
0.1
1
10
100
DTx [ng/ml]
Mock
IC50=1.67
HIV-2
IC50=18.3

Ai

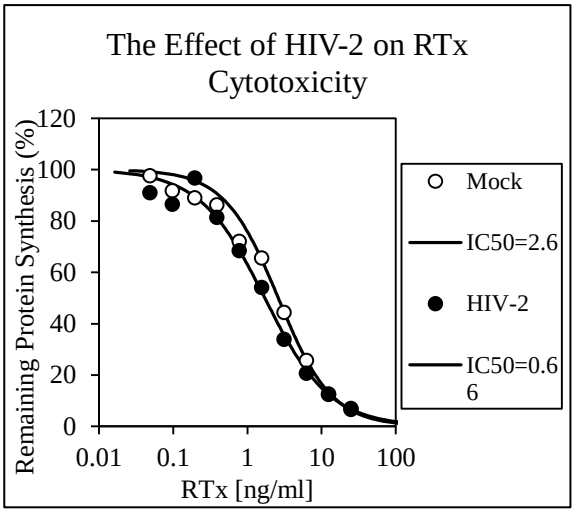
The Effect of HIV-2 on RTx Cytotoxicity
Remaining Protein Synthesis (%)
120
100
80
60
40
20
0
0.01
0.1
1
10
100
RTx [ng/ml]
Mock
IC50=2.6
HIV-2
IC50=0.66

B

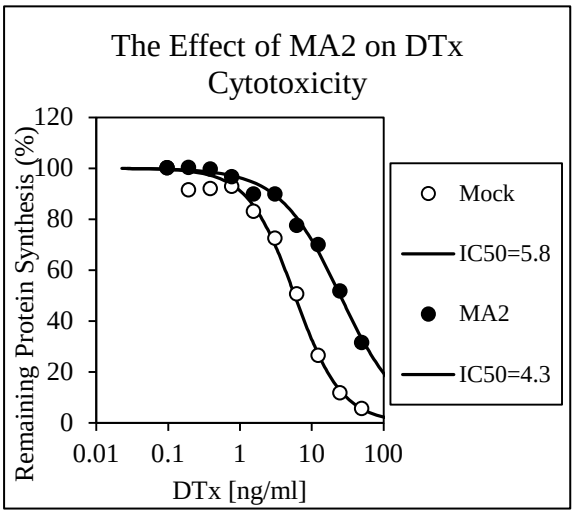
The Effect of MA2 on DTx Cytotoxicity
Remaining Protein Synthesis (%)
120
100
80
60
40
20
0
0.01
0.1
1
10
100
DTx [ng/ml]
Mock
IC50=5.8
MA2
IC50=4.3

Bi

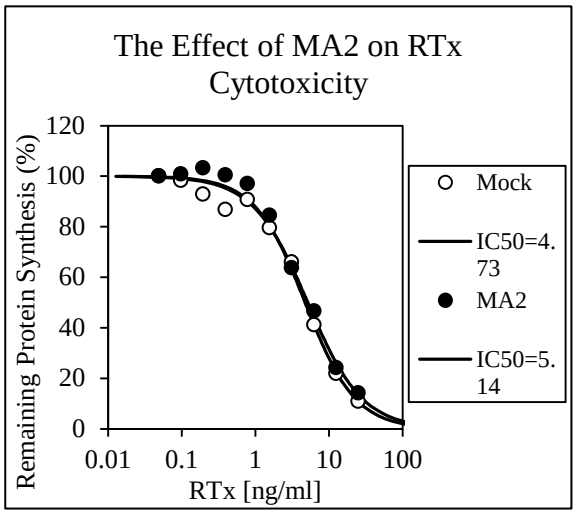
The Effect of MA2 on RTx Cytotoxicity
Remaining Protein Synthesis (%)
120
100
80
60
40
20
0
0.01
0.1
1
10
100
RTx [ng/ml]
Mock
IC50=4.73
MA2
IC50=5.14

C

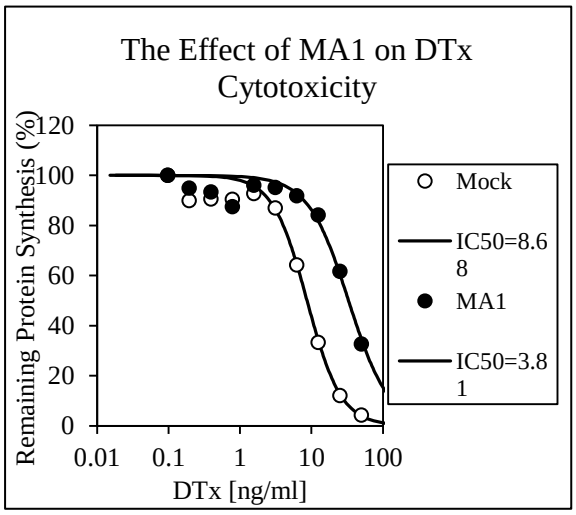
The Effect of MA1 on DTx Cytotoxicity
Remaining Protein Synthesis (%)
120
100
80
60
40
20
0
0.01
0.1
1
10
100
DTx [ng/ml]
Mock
IC50=8.68
MA1
IC50=3.81

Ci

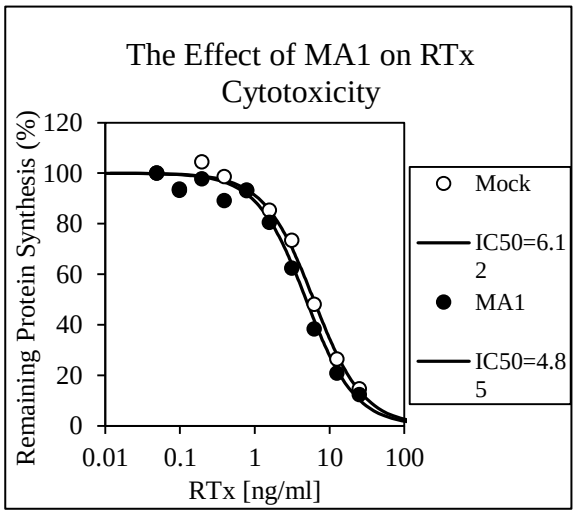
The Effect of MA1 on RTx Cytotoxicity
Remaining Protein Synthesis (%)
120
100
80
60
40
20
0
0.01
0.1
1
10
100
RTx [ng/ml]
Mock
IC50=6.12
MA1
IC50=4.85

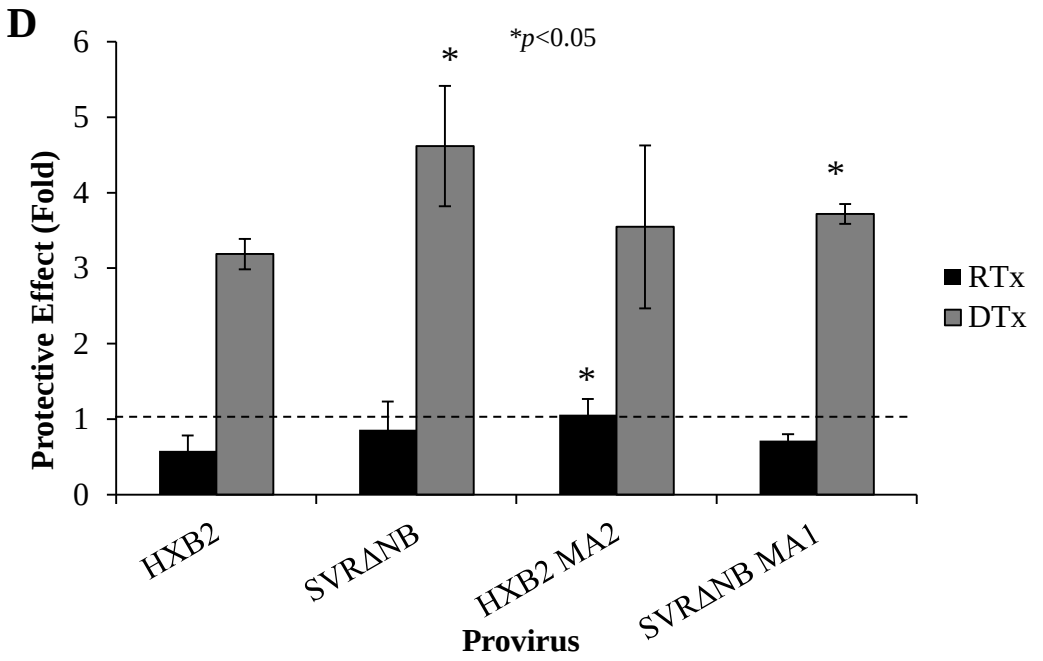

Figure 76: The effect of HIV-2 and chimeric proviruses on DTx/RTx cytotoxicity. A-C- left panels show DTx cytotoxicity curves, Ai-Ci- right panels show RTx, from one representative of 3 repeat experiments. Proviruses used in experiments are as follows; A-HIV-2 (SVRΔNB), B- MA2 (HXB2 MA2), C-MA1 (SVRΔNB MA1). D-Compilation of average protections/sensitisations to toxins. Statistically significant results, as compared to HIV-1 HXB2, are highlighted by an asterisk (p<0.05).

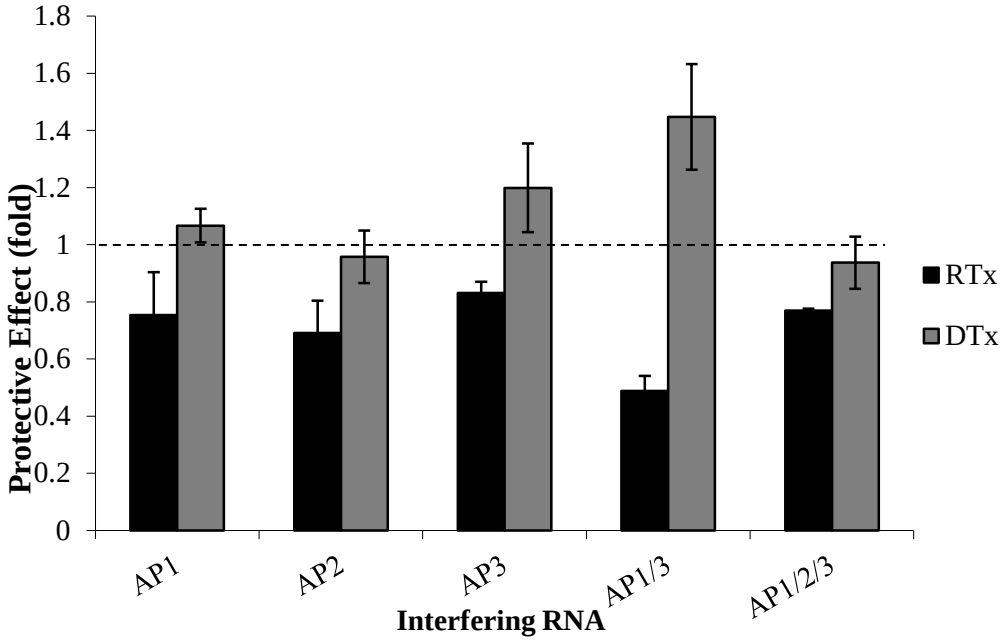

Figure 77: The effect of AP knockdown on DTx/RTx cytotoxicity in siRNA treated HeLa cells. Compiled average protections/sensitisations to DTx and RTx are shown from 3 independent repeat experiments.

used for comparative measures as this was the provirus used to generate both MA1 and MA2. This again indicated that this virus has a similar phenotype to HIV-1 with regards to interactions with the APs, despite containing the MA domain of HIV-2. Another surprising result was that there was no sensitisation to RTx; this is the first transfected construct to have no effect on RTx trafficking. This was not expected, considering one could expect the increase in viral egress seen with this virus to have some effect on general receptor recycling/entry from the PM.

Finally, the MA1 provirus was used to determine whether this behaved in a similar manner to HIV-1 or HIV-2. The results are shown in Figures 76C, Ci and D. The average protective effect against DTx observed for this provirus was found to be 3.7 fold, which although was not as high as with HIV-2, it was still significantly higher than HIV-1 HXB2 ($p<0.05$). This was again indicative that this virus has a similar phenotype to HIV-2, despite containing the MA of HIV-1.

7.2.3 Knocking Down the APs does not Affect DTx Trafficking

To investigate whether the interference of HIV with DTx trafficking is mediated by the APs, the next logical stage was to test whether siRNA induced knockdown of the APs also affected DTx trafficking. This would then infer which AP may be involved in DTx trafficking, and therefore also imply which AP HIV is likely interfering with to cause an interruption in toxin trafficking. The siRNAs directed against AP-1, -2 and -3 were first used to transfect HeLa cells individually. The summarised results are shown in Figure 77. As can be seen, surprisingly no protective effect against DTx was found. A slight sensitisation to RTx, representative of the non-specific effect of transfection seen before, was once again observed. This indicates that RTx remains a suitable control.

Since it is possible that DTx could use several APs to work in a redundant manner efficient trafficking, it was postulated that reducing one AP at a time is not sufficient to produce a significant effect. Therefore, AP-1 and -3, then all 3 siRNAs together were utilised. The results are also summarised in Figure 77. Once again, surprisingly, very little effect/ no effect was seen. When AP-1 and -3 siRNAs were used together, this produced the largest effect against both DTx and RTx. The protection against DTx was still only 1.5 fold, however. This is similar to the result obtained from HVPΔEC, which we would most likely regard as a non-specific effect, especially since when all 3 AP siRNAs were used together, no effect was seen. These results indicate that reducing the APs is not sufficient to interrupt DTx trafficking. However, since in this particular experiment efficient knockdown was not proven, we cannot exclude the possibility that the small protective effects seen were due to inefficient knockdown.

7.2.4 HIV-1 Interferes with Early and Late Stages of DTx Trafficking

Although it has so far been demonstrated that HIV interferes with DTx, but not RTx, it is necessary to gather data which can infer the stage of toxin trafficking that is interrupted. Therefore, in order to gauge an idea as to how HIV is exerting this observed effect on DTx cytotoxicity, toxin time course assays were carried out. In these assays, fixed (high) concentration of toxin was added to a different well of cells every 15 minutes over a period of 3 hours prior to measuring ^{35}S-methionine incorporation. This determines approximately when the first ribosomes start to be inhibited, and the subsequent rate of inhibition. This ascertains whether a delay in toxin trafficking (lag time) is occurring, or a delay in the later stages (intoxication) of the toxin pathway, which would be indicated by an alteration in the gradient of protein synthesis

A

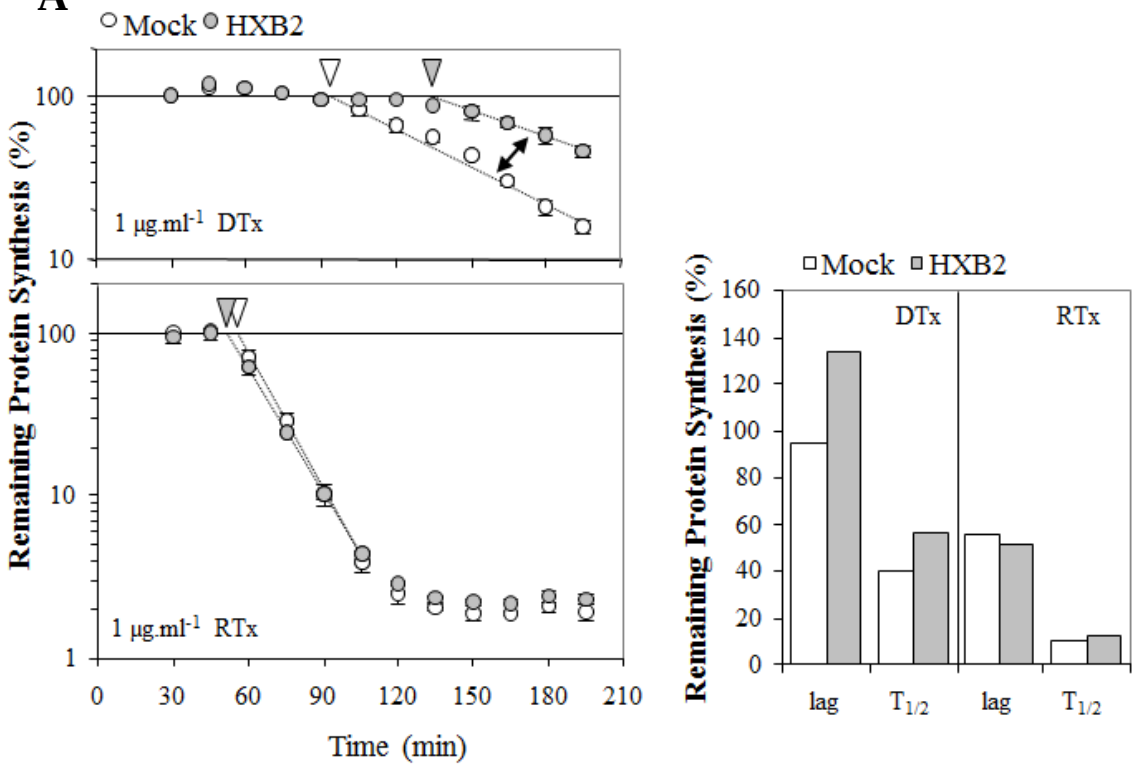

B

Toxin	Transfection	Regression	R^2	lag, min (change)	$T_{1/2}$, min (change)
DTx	Mock	$y = 522.98e^{-0.0175x}$	0.9782	94.54	39.61
	HXB2	$y = 516.56e^{-0.0123x}$	0.9902	133.50 (+38.96)	56.35 (+16.74)
RTx	Mock	$y = 3704.8e^{-0.0654x}$	0.9993	55.23	10.60
	HXB2	$y = 2179.5e^{-0.0589x}$	0.9998	51.34 (-3.9)	11.77 (+1.17)

Figure 78: HIV-1 interferes with DTx trafficking. A- Remaining protein synthesis after toxin challenge for different amounts of time. White and grey arrows indicate transition from the lag phase to the intoxication phase (mock and HXB2, respectively). Black double arrow highlights a change in intoxication rate, as shown by a change in slope gradient. B- Table of calculated changes in toxin trafficking times (lag) and intoxication ($T_{1/2}$).

inhibition. HXB2 provirus was transfected as before and compared to mock-transfected cells. Results are shown in Figure 78.

This Figure shows that a significant increase in lag time occurred in the presence of HIV-1, as compared to mock transfected cells. This was calculated to be approximately 40 minutes (see Figure 78B). This is indicative of a delay in toxin trafficking, likely explains the protective effect observed before. Slightly surprisingly, however, a slight delay (approximately 17 minutes) in the intoxication phase was also observed, as demonstrated by a slight change in the gradient of the slope on the graph, and the change in $T_{1/2}$ times calculated. It may therefore be that the interruption of DTx cytotoxicity is not simply a result of interrupting the normal trafficking pathway of this toxin as presumed, but possibly a combination of effects during early and late stages of this pathway.

This Figure also shows a very slight decrease in the lag time of RTx, which was expected since a slight sensitisation was observed after plasmid transfection. The change in lag time was, however, very modest (4 minutes). This was lower than the expected value from this experiment. Selection of appropriate times of toxin addition is, however, crucial to this experiment, so it remains possible that modest changes were missed, masking real effects.

7.2.5 HIV does not Interfere with VSV-G Trafficking

As mentioned above, trafficking of ts045-VSV-G-EGFP (VSV-G)has been reported to be dependent on AP-3 (Nishimura et al., 2002); in particular, it was found to interact with the δ subunit of AP-3. This is the same subunit which HIV-1 has been proposed to interact with (Dong et al., 2005), although others have disputed this from *in vitro* peptide expression experiments (Kyere et al., 2012). Since direct visualisation of the

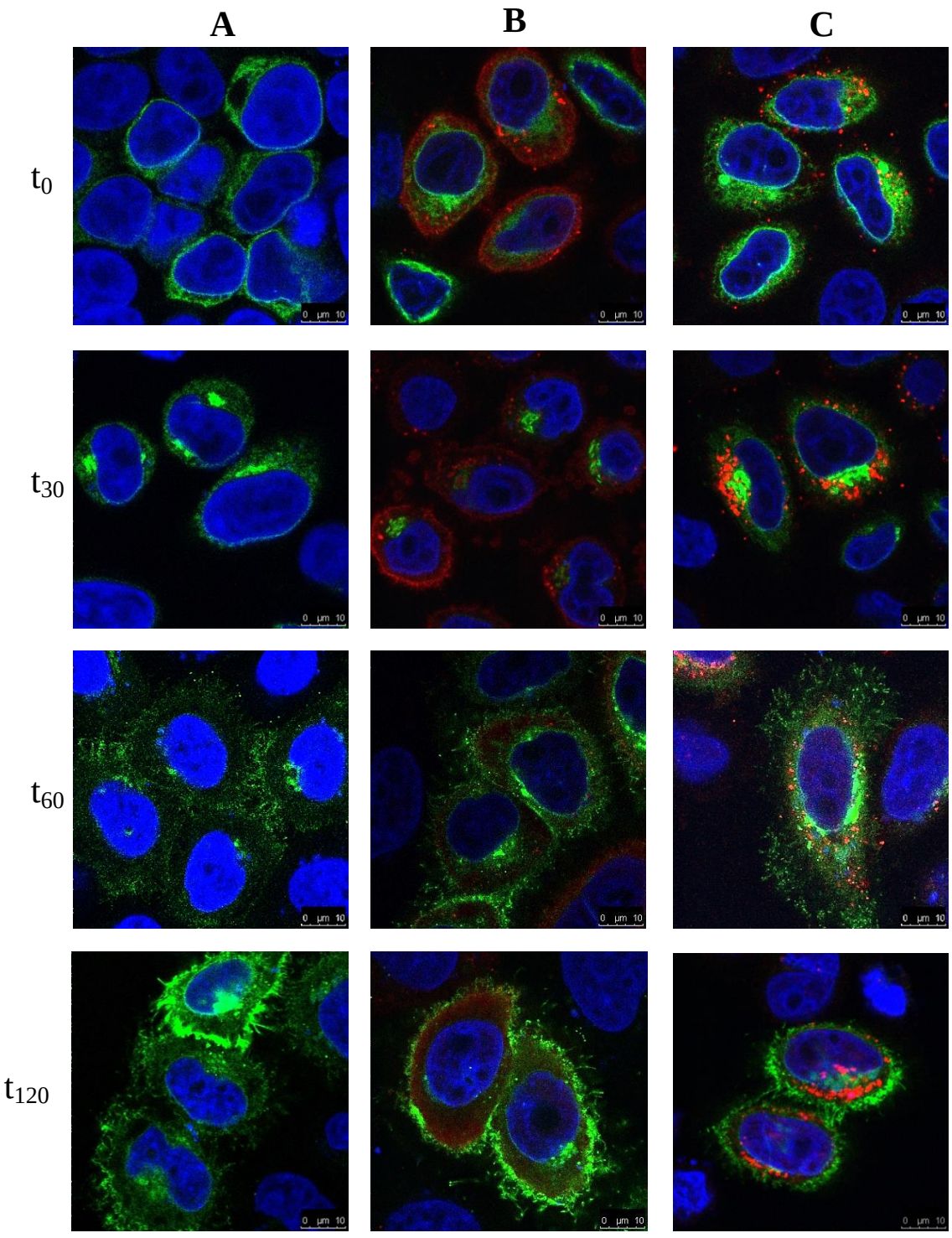

Figure 79: HIV-1 and -2 do not interfere with ts045-VSV-G-EGFP trafficking. Confocal immunofluorescence images of VSV-G-EGFP (green) and HIV Gag (red) in HeLa cells at 0 (t_0), 30 (t_{30}), 60 (t_{60}) and 120 (t_{120}) minutes after shift to 32^{o}C. Panel A- VSV-G trafficking in the absence of HIV provirus. Panel B- VSV-G trafficking in the presence of HIV-1 HXB2. Panel C- VSV-G trafficking in the presence of HIV-2 SVRΔNB.

trafficking of VSV-G is possible, it was thought to be a particularly useful tool for investigating potential interference with an AP-3-dependent trafficking pathway.

The trafficking of the temperature sensitive VSV-G-EGFP protein was followed at 0, 30, 60 and 120 minutes after release from the ER in HeLa cells transfected with HIV-2 HXB2 or HIV-2, by confocal immunofluorescence microscopy. The results are shown in Figure 79.

Panel A shows VSV-G-EGFP fluorescence (green) in the absence of HIV. At t_0, VSV-G could be observed in a perinuclear position, which is likely the ER. At t_{30}, the protein could be observed in a tight juxtanuclear location, which is likely the Golgi/ TGN. AT t_{60}, less was present in the TGN, and some diffuse cytoplasmic staining could be observed. Some had also reached the PM, as shown by some projections around the edge of the cell. By $t_{120,}$ most of the construct was present at the PM, as shown by strong fluorescence around the edge of the cell. Panel B shows VSV-G trafficking in the presence of HIV-1, and panel C shows trafficking in the presence of HIV-2 (Gag immunofluorescence shown in red). As can be seen, VSV-G displayed localisations similar to when the provirus was absent. This suggests that HIV did not interfere with the trafficking of VSV-G. This would support the evidence gathered by Kyere et al. (2012), suggesting that HIV-1 does not interact directly with the AP-3δ subunit, but also infers that HIV-2 may not either. However, Kyere et al. (2012) used a purified AP-3δ fragment *in vitro,* whereas Dong et al. (2005), carried out multiple approaches with intact AP-3 *in vivo.* This was particularly surprising since data gathered in the previous chapter show a strong dependence of HIV-2 trafficking on AP-3. However, this experiment cannot rule out the possibility of AP-3 interactions since it is an indirect assay, and it may simply be that HIV Gag and VSV-G are able to both traffic in an AP-3 mediated manner without competitively interfering with each other.

7.3 Discussion

HIV-1 has evolved the ability to interrupt the trafficking of numerous proteins in order to benefit the virus life cycle. For example, HIV-1 Nef is able to interfere with the trafficking of MHC-I to aid immune evasion (Blagoveshchenskaya et al., 2002) by sequestering it to the TGN. Since data collected in previous chapters demonstrates that both HIV-1 and HIV-2 are able to disrupt the localisation of the adaptor proteins, and require them for trafficking and assembly, the ability of these viruses to interfere with AP dependent trafficking pathways was investigated.

The first trafficking pathway to be investigated was that of Diphtheria toxin (DTx). This toxin is a useful tool since it is known to enter the cell via clathrin-mediated receptor endocytosis, pass into early endosomes, and then enter the cytoplasm after endosomal acidification. Since we know both HIV-1 and -2 interact with AP-3, which is involved in endosomal trafficking, this seemed an appropriate assay.

Results obtained from these experiments clearly demonstrate the ability of HIV-1 to interfere with the DTx trafficking pathway, as demonstrated by a protective effect. Protection against DTx meant that there is an interference with toxin action at some stage, i.e. it was not able to as efficiently cause a cessation in protein synthesis in the presence of HIV. Sensitisation to RTx were observed throughout, meaning that there was an increase in toxin action, i.e. a more efficient cessation in protein synthesis.

It was also discovered through the use of mutant viruses that Gag was necessary, but not sufficient for the interruption in DTx cytotoxicity. Since Gag deleted proviruses caused a small protective effect, this means that the presence of other viral components exert some effect, but that the majority of the effect is Gag driven. A possible explanation for the fact that Gag-GFP could not substantially protect against DTx is

that Gag, in the absence of other viral proteins, behave differently. This could subvert the need to pass through endosomes, and therefore reduces the disruption of DTx trafficking. Viral Nef was also found to be dispensable for the protective effects observed, which was surprising since Nef too interacts with the APs.

A possible explanation for the observed protective effect against DTx is sequestration of the APs by Gag. DTx may require AP-3 to travel along the endosomal pathway before it enters the cytoplasm if this occurs from late endosomes. A requirement for AP-1 may be involved in DTx receptor recycling if it transits through the Golgi, although it may cycle directly from endosomes without the APs/clathrin, and AP-2 would also be required for receptor mediated endocytosis. It is possible that HIV could sequester the APs as a consequence of Gag interactions, therefore making them unavailable for utilisation by DTx. However, the siRNA cytotoxicity assays demonstrate that it is possibly more complex than merely sequestering the APs, as a reduction in the APs does not appear to interfere with DTx trafficking. This was surprising especially since AP-2 knockdown should disrupt clathrin-mediated endocytosis; however, it may be that the siRNAs are not capable of removing all AP molecules present in the cell, and that only a few molecules are required to assist DTx trafficking, since a very small amount of toxin is capable of exerting a cytotoxic effect. Another explanation could be that the presence of Gag on endosomal membranes prevents the translocation of DTx into the cytosol.

Not surprisingly, it was found that HIV-2 had a significantly larger effect on DTx trafficking than HIV-1. Since previous results indicate that HIV-2 alters the localisation of AP-3, requires this protein for trafficking and assembly, and also likely involves the endosomal pathway for Gag trafficking, this was logical. The most likely explanation is that the presence of HIV-2 Gag in endosomal compartments (M. Marongiu, I. Portman

and E. C. Anderson, unpublished results) either prevents the entry of DTx into these compartments, or causes a failure in endosomal acidification required for cytoplasmic entry. MA1 was also found to have a significantly larger effect on DTx as compared with HIV-1. This makes sense since MA1 is not capable of releasing viral particles; this would cause an intracellular accumulation, which will be more likely to interfere with intracellular pathways. Confocal immunofluorescence microscopy in HeLa cells also demonstrated that this virus gets stuck around the edge of the cell in clathrin concentrated areas, which could have detrimental effects on clathrin-mediated endocytosis. MA2, however, exerted a similar effect to HIV-1, further indicating that this virus adopts a similar trafficking phenotype to HIV-1. Since this virus has a higher release efficiency than HIV-1, it is also likely that this results in a decrease in intracellular Gag, and therefore a lower burden on cellular trafficking pathways.

With regards to time course assays, the results gained from DTx assays were as expected; there was a significant (~40 minute) decrease in trafficking of the toxin, but a small effect on intoxication was also observed. There are several possible explanations for the results observed. Firstly, it may be that HIV present at the PM interferes with AP-2- dependent receptor mediated endocytosis of DTx. Secondly, it is possible that HIV Gag localised to endosomal membranes may prevent DTx from trafficking down the endosomal pathway or translocating into the cytosol. Finally, if AP-1 facilitates DTx receptor recycling back to the surface, it is possible that Gag may interfere with this since we saw a change in the localisation of AP-1 in HIV-1 transfected cells (see chapter 3.2.4ii). The small decrease in intoxication rate seen could be due to the perturbation of the delivery of a facilitating enzyme necessary for DTx activation, such as furin. Or it may be that there is a defect in endosomal maturation, also caused by an

interference with AP-3. Repeat experiments would be necessary to determine whether this effect is indeed significant, however.

The ts045-VSV-G-EGFP results showed that HIV did not alter its trafficking. This was puzzling and unexpected, since it has been demonstrated that both Gag and VSV-G interact with the AP-3δ subunit. It was therefore assumed that, through competition, HIV may inhibit VSV-G trafficking from the ER to the PM. This was not the case as can be seen from the results. It is possible that Gag is not present in high enough quantities to inhibit the trafficking of VSV-G to the PM, as some AP-3 subunits are still available for utilisation. It is possible, however, that subtle changes in trafficking times do occur, but are missed by the time points selected for this experiment. Alternatively, since HIV is able to use VSV-G as an envelope in the absence of Env, it may be that these molecules are capable of co-trafficking; therefore no disruption would be seen.

7.4 Future Work

The most obvious limitation of this study is the absence of repeat time course assays. This was due to a limited availability of toxin, and could not be avoided. Unfortunately, therefore, repeat experiments utilising different time intervals was not possible. This means that the sensitisation to RTx was not well characterised, and it was not possible to confirm the possible delays in the intoxication phase of DTx.

An obvious gap in the results presented in this chapter is the absence of HIV-2 Gag deleted proviruses. Although it would be assumed that these follow the same pattern as HIV-1, it would be interesting to see whether an absence of HIV-2 Gag also removes the interference with DTx.

Future experiments involving siRNAs should also ensure that knockdown is efficient via Western blot, which was lacking in this chapter. Since AP-2 knockdown in

particular did not produce the expected effect of reducing DTx cytotoxicity by inhibiting entry, it is likely that knockdown was not sufficient.

Although confocal microscopy failed to reveal an interruption in VSV-G trafficking, this study was somewhat limited. Despite the observation that the construct was localised to the previously described areas at each designated time point, this experiment failed to show what happens to the construct between time points. It is therefore possible that, in the presence of HIV, VSV-G trafficked at a different speed to when it was absent. For example, it is possible that VSV-G reaches the PM fully by 100 minutes, but not until 110/120 minutes in the presence of HIV. Real-time confocal microscopy would have been a useful tool to investigate this.

CHAPTER 8: DOES HIV-1 AFFECT VESICLE RECYCLING WITHIN ASTROCYTES?

8.1 Introduction

Individuals infected with HIV not only suffer a severely impaired immune system, but many will experience neurological complications later on in the disease process. These neurocognitive complications have been collectively categorised as HIV-associated neurocognitive disorders (HAND), which defines three categories of dysfunction; asymptomatic neurocognitive impairment, mild neurocognitive disorder, and HIV-associated dementia (HAD), with the latter being the most severe manifestation (Kaul, 2009). Approximately 60% of HIV infected individuals experience some neurological impairment and prior to the widespread use of HAART, up to 30% of patients would suffer HAD. Symptoms include a range of motor and cognitive impairments, ranging from diminished short term memory, leg weakness and behavioural and personality changes (Gonzalez-Scarano and Martin-Garcia, 2005; Ghafouri et al., 2006).

HIV enters the CNS during early stages of infection, shortly after systemic viral dissemination. The favourite hypothesis for viral invasion is the "Trojan horse" hypothesis, whereby HIV enters host cells that are destined for the brain. These cells are predominantly monocyte-derived macrophages, which are highly efficient at crossing the blood brain barrier (BBB). There is some evidence that free viral particles may also enter the brain through the BBB via a similar mechanism to adsorptive endocytosis, mediated by the Env glycoprotein (Kramer-Hämmerle et al., 2005; Aquaro et al., 2008; Banks et al., 2011).

Within the CNS, HIV preferentially infects perivascular macrophages and microglia; these cells permit productive infection. Some lines of evidence have suggested that neurons may be infected by HIV; however, this remains controversial and the damage

that occurs within these cells is likely mediated by the inflammatory molecules secreted by infected cells (Sharma and Bhattacharya, 2009). Another cell line which has been the focus of much interest is astrocytes. Astrocytes are latently rather than productively infected, and thus do not produce new virions after an initial burst of viral protein production when first infected; they do represent a viral reservoir, however. Initial PCR investigation of astrocytic populations in HAD patients revealed infection in only 1-3% of the population, whereas the development of highly sensitive methods detected gene expression in 19% of $GFAP^+$ (glial fabrillary acidic protein; a marker for astrocytes) cells (Churchill et al., 2009).

Astrocytes represent an important aspect of HAD for numerous reasons. Firstly, they are the most abundant cell type present within the brain, constituting 40% of the total nervous system cell population, outnumbering neurons 10-50:1 (Brack-Werner, 1999). Secondly, astrocytes play a pivotal role in brain functioning, forming an essential part of the tripartite synapse, releasing a number of neurotransmitters and neurotrophins essential for regulating neuronal synaptogenesis and synaptic activity. Astrocytes are also essential for brain homeostasis, mopping up excess glutamate and converting it into glutamine, preventing excessive neuronal excitation (Wang et al., 2004). Finally, latent infection of astrocytes, or exposure of astrocytes to either progeny virions or extracellular gp120 also alters global astrocyte gene expression, causing glutamate catabolism to become compromised, the induction of apoptotic protein synthesis, excitotoxic neuronal death and impaired glutamate uptake and release (Wang et al., 2004; Dou et al., 2006; Churchill et al., 2009).

Within these cells, HIV expression is restricted to early gene products, such as Nef and Rev (Aquaro et al., 2008); Gag expression was found to be dramatically less than that in HeLa cells (Gorry et al., 1999). Replication within astrocytes is down-regulated at

several different stages of the life cycle, including virus entry, reverse transcription, nucleocytoplasmic HIV-1 RNA transport, translation of viral RNA, and maturation of progeny virions (Gorry et al., 2003). One such example, proposed to account for low Gag expression, is that it is mainly the multiply spliced, smaller (2kb) transcripts are able to enter the cytoplasm from the nucleus due to a cell determined block in the nucleus-cytoplasmic Rev shuttling, causing nuclear retention of Rev-dependent mRNAs and their subsequent degradation (Gorry et al., 1998; Aquaro et al., 2008). It was also found that translation of *gag* and *env* transcripts was inefficient; only Tat and Rev were efficiently translated from their native mRNAs (Gorry et al., 1999).

Many of the hypotheses which have been so far proposed with regards to how astrocytic infection impairs CNS function are speculative, due to a lack of suitable experimental systems. One such hypothesis is that infected astrocytes may become impaired in their role in neuronal support. Astrocytes, unlike previously believed, play an active role in brain signalling, behaving as both secretory and receptive elements to numerous transmitters (Volkandt, 2002). They can release a variety of transmitters including ATP and glutamate in response to increased intracellular Ca^{2+} levels (Montana et al., 2006).

As mentioned in the introduction (chapter 1.5.3) AP-1, -2 and -3 are extensively involved in neurotransmitter recycling. Although adaptor protein mediated vesicle recycling has not been studied within astrocytes, it was revealed that astrocytes do indeed express at least AP-2 (Miñana et al., 2001).

A summation of this evidence led to the following hypothesis; if vesicle recycling in astrocytes occurs in an AP dependent manner, can HIV infection in astrocytes perturb this process via interference with the APs? If so, perhaps this may contribute to the loss of neuronal function observed in HAD, and therefore the motor/cognitive symptoms

observed. This chapter aimed at developing techniques to investigate the potential effects of HIV on vesicle recycling pathways within a human astrocytoma cell line.

8.2 Results

8.2.1 U373 MG Cells Express Gag from a Gag-GFP Construct

Due to the Rev associated block of protein expression, proteins from larger splice products have not been reported to be synthesised to high levels in astrocytes. Transfection of astrocytes with a Rev-independent Gag-GFP plasmid (Hermida-Matsumoto and Resh, 2000) should bypass this block and allow synthesis of Gag proteins. To test this theory, both Gag-GFP and GFP plasmids were used to transfect human astrocytoma (U373 MG) cells, which were viewed under the confocal microscope. The results are shown in Figure 80.

As can be seen, both GFP and Gag-GFP were expressed well in this cell line 24 hours post-transfection. GFP expressing cells increased at 48 hours as compared with samples taken at 24 hours; the same could not be said for Gag-GFP, however. As can be seen in Figure 80D, both untransfected U373 MG cells and Gag-GFP expressing cells were sparse and some had very altered morphologies. The nucleus also appeared to have disintegrated in some cells, as shown by the loss of defined round nuclei, replaced with a diffuse DAPI staining.

Although this is an artificial system as Gag is not predicted to be expressed at high levels in astrocytes, and therefore this is not representative of an *in vivo* situation, this does suggest that Gag expression in astrocytes has a detrimental effect on astrocyte morphology and viability.

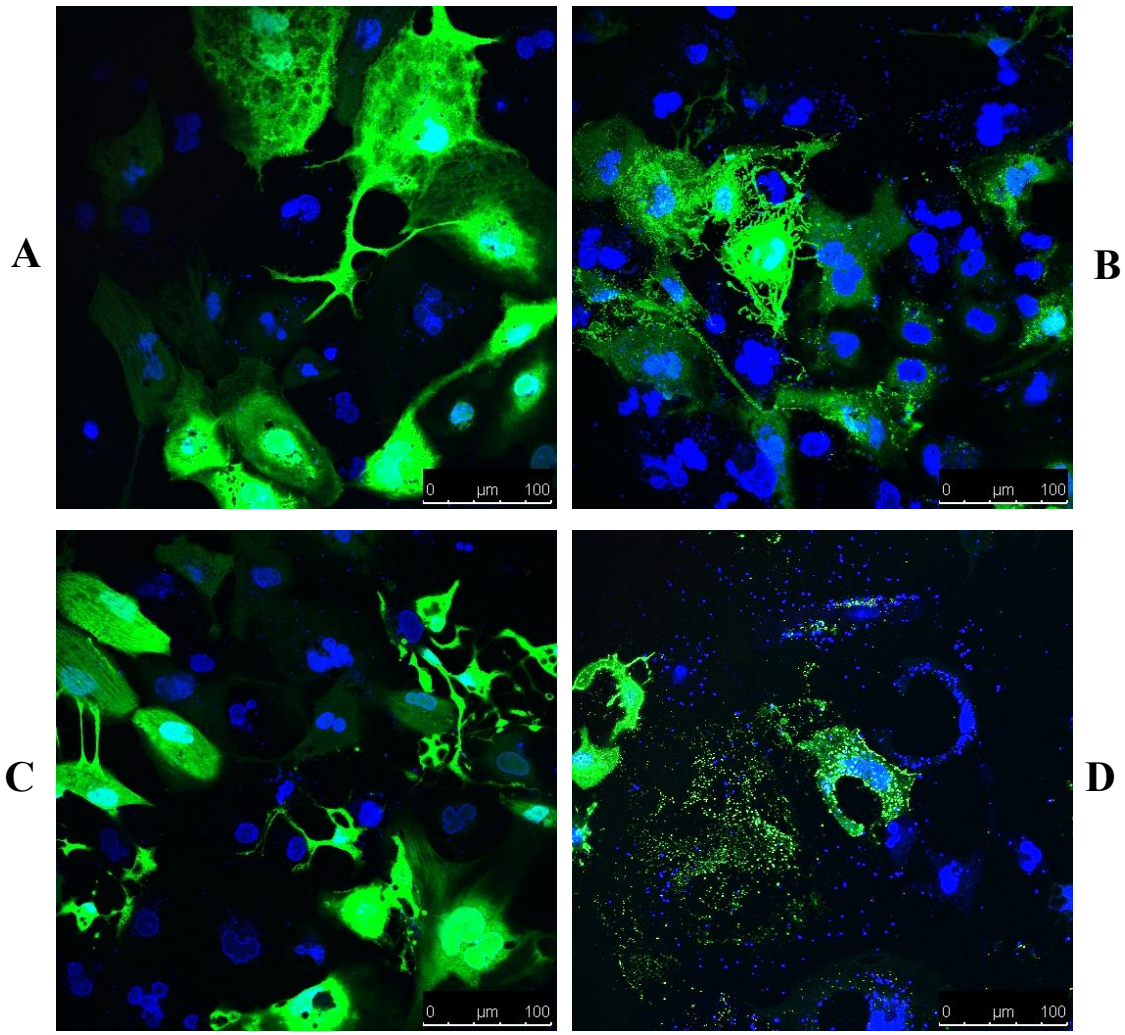

Figure 80: GFP and Gag-GFP expression in U373 MG cells. Confocal immunofluorescence images of U373 MG cells 24 (A, B) and 48 hours (C, D) post-transfection with GFP (A and C) or Gag-GFP (B and D) expression plasmids. Blue stain= DAPI.

8.2.2 HIV-1 Gag and Nef are Expressed in Provirus-Transfected U373 MG Cells

The ability of astrocytes to produce Nef in high quantities when infected with HIV-1 has been previously described (Ranki et al., 1995). Although Gag expression has been detected in transfected astrocyte cell lines, inefficient translation of *gag* transcripts, amongst other things, leads to a decrease in Gag protein expression when compared with non-neuronal cell lines (Gorry et al., 1999). Transfection of astrocytes with proviral DNA will bypass viral entry and reverse transcription, but not nucleocytoplasmic RNA transport or mRNA translation. To determine whether transfected U373 MG cells do indeed express Nef in high quantities, and to establish whether Gag expression can be detected despite blocks in translation, U373 MG cells were transfected with the HXB2N^{+} HIV-1 provirus and analysed by both Western blot and by confocal immunofluorescence microscopy, using anti-HIV-1 p24 and anti-HIV-1 Nef antibodies for viral protein detection. The results are shown in Figure 81.

Figure 81A shows a Western blot of cellular Gag collected at 24 and 48 hours after transfection of both HeLa and U373 MG cells. As can be seen, although Gag could be detected, it was present at much lower levels than in HeLa cells. These levels were comparable since equal amounts of protein were loaded into each lane of the gel. No Gag was detected in supernatant samples, supporting the non-productive nature of these cells (data not shown). Figure 81B shows Nef 24 hours after HIV-1 transfection of U373 MG cells only. As can be seen, even at 24 hours, a significant amount of Nef was detectable.

Figures 81C and D show confocal immunofluorescence images of Gag and Nef staining, respectively, within transfected U373 MG cells. Nef had a diffuse staining pattern, similar to that of HeLa cells. Gag was a mixture of punctate and diffuse, again

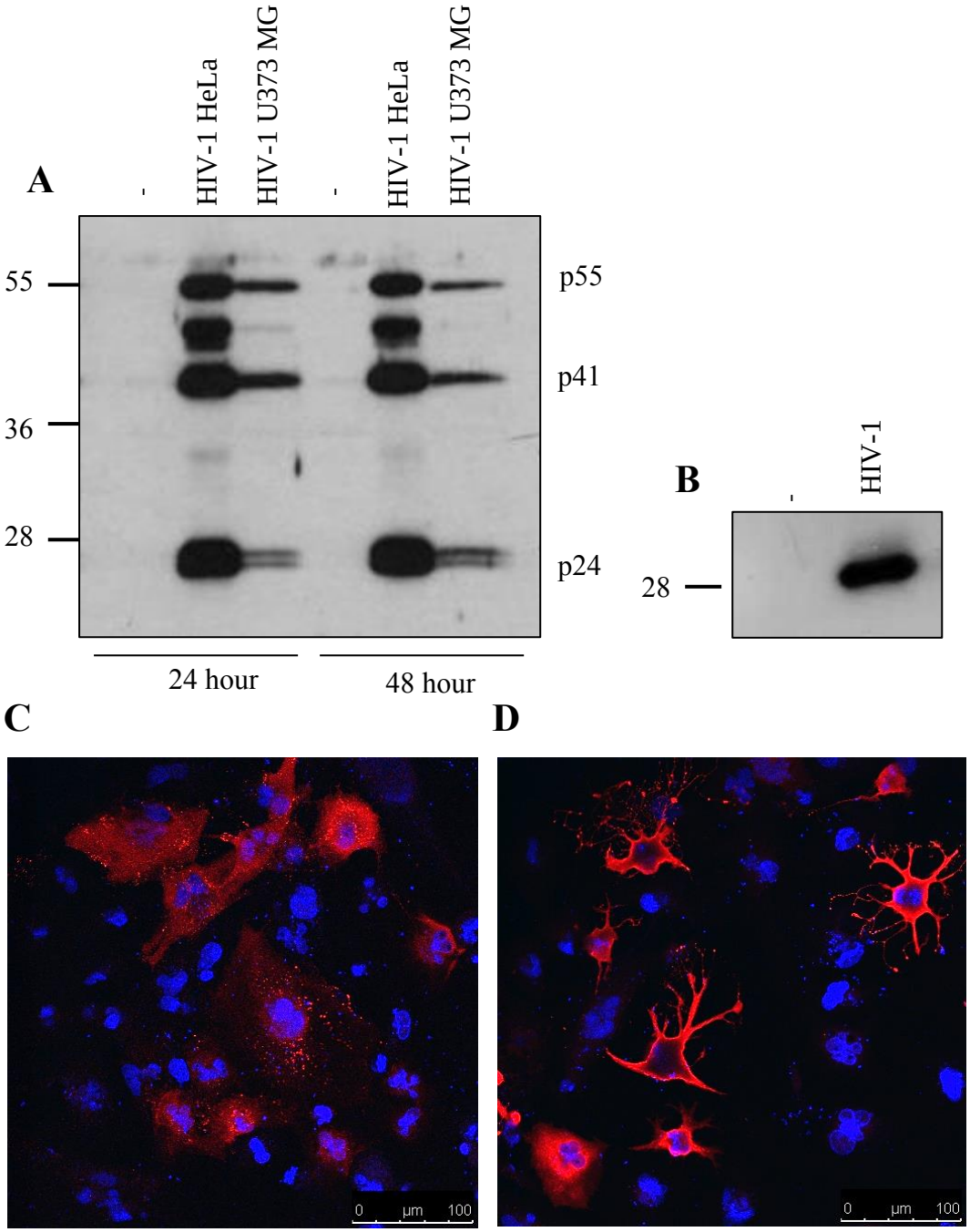

Figure 81: HIV-1 Gag and Nef are expressed in U373 MG cells. A- Western blot of HeLa and U373 MG cell lysates, 24 and 48 hours post transfection with the HIV-1 provirus, using an anti-HIV p24 antibody. B- Western blot U373 MG cell lysates, 24 hours post-transfection with the HIV-1 provirus, using an anti-HIV-1 Nef antibody. C and D- Confocal immunofluorescence images of U373 MG cells transfected with the HIV-1 provirus for 24 hours, stained with anti-HIV-1 p24 and anti-HIV-1 Nef, respectively (red). Blue=DAPI.

reminiscent of staining within HeLa cells. Confocal immunofluorescence microscopy revealed Gag expression in between 10-30% of U373 MG cells, compared to 50-70% of HeLa cells (data not shown).

8.2.3 HIV-2 Gag is Expressed in Significantly Lower Levels than HIV-1 Gag in U373 MG Cells

Evidence for the neuropathology of HIV-2 infections is limited. This is mainly due to the fact that HIV-2 predominantly exists in Western Africa, where diagnostic tests and medical surveillance are limited. Nonetheless, there has been evidence gathered from a number of patients which would support the notion that HIV-2 has a similar impact on the CNS as HIV-1, with patients developing HAD and other neurological conditions such as giant cell encephalitis (Rolfe, 1994).

To investigate whether astrocytes are permissive to HIV-2 through transfection, U373 MG cells were transfected with the HIV-2 provirus and investigated by confocal microscopy, using an anti-SIV p27 antibody as a marker for Gag expression. The results are shown in Figure 82. As can be seen, HIV-2 Gag was clearly expressed in this cell line (82B). The distribution of Gag was slightly different as compared with HIV-1 (Figure 82A); once again we observed a very punctate staining, similar to that in HeLa cells, whereas with HIV-1 we saw a mixture of punctate and diffusely stained cells, again reminiscent of the pattern seen in HeLa cells.

Transfected U373 MG cells were also analysed by Western blot using an anti-SIV p27 antibody on harvested cell samples and compared with transfected HeLa cells. The results are shown in Figure 82C.

As can be seen, very little HIV-2 Gag was present in transfected U373 MG cells. The same amount of protein was loaded between HeLa and U373 MG samples, which

demonstrate that HeLa cells produced significantly more than the astrocytes. In addition, the relative expression of HIV-2 in U373 MG compared to HeLa cells appeared to be less than the relative expression of HIV-1 in these cell types (Figure 81A vs. Figure 82C).

In agreement with the Western blot results, when cells expressing Gag were counted using confocal microscopy (Figure 82D), HIV-1 transfection produced significantly more Gag expressing cells than HIV-2 ($p<0.05$) at 24 hours. At 48 hours, however, there was no significant difference despite there being >10% more Gag expressing cells in the HIV-1 transfection ($p>0.05$). This could perhaps be due to the toxicity of HIV on these cell lines, destroying many apoptosed Gag expressing cells, which would then be washed away during the fixing and staining procedure. It must be mentioned, however, that even in HeLa cells, HIV-1 transfection gives significantly more Gag expressing cells than HIV-2 (data not shown).Therefore this decrease in HIV-2 expression is not an astrocyte-specific mechanism.

8.2.4 U373 MG Cells Express Adaptor Proteins -1, -2 and -3

As mentioned in the introduction, AP-2 has been detected in astrocytes (Miñana et al., 2001). To investigate whether they express AP-1 and -3 also, confocal immunofluorescence microscopy was carried out on U373 MG cells, using anti-AP-1 and -3 antibodies. As Figures 83A and B demonstrate, these proteins are clearly abundantly expressed within astrocytes. For further confirmation, Western blot analysis was carried out on both U373 MG and HeLa cell lysates, using antibodies against all 3 adaptor proteins. As Figure 83C shows, all 3 adaptor proteins are expressed within this cell line. Abundances of these proteins in comparison to HeLa cells cannot be

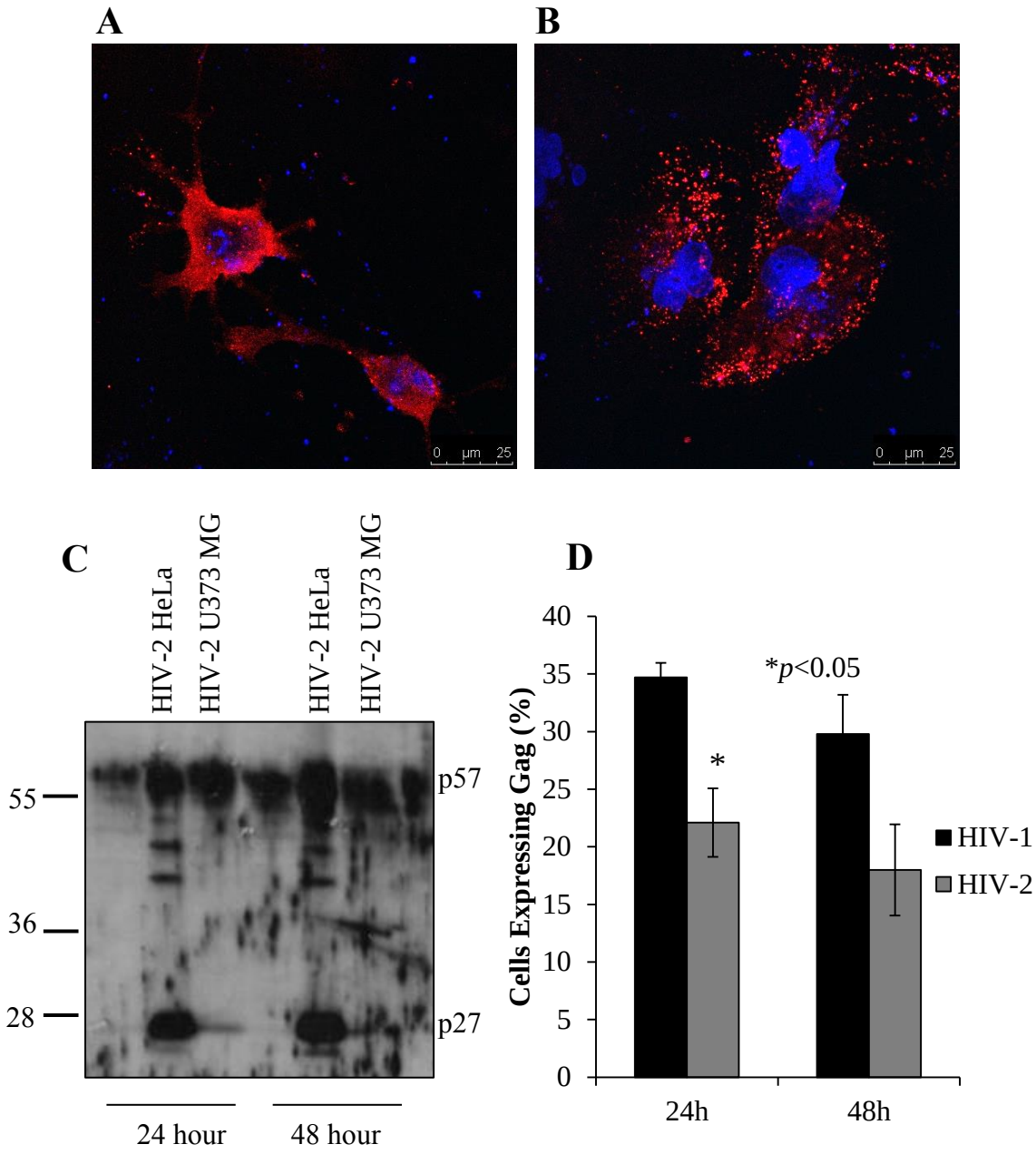

Figure 82: HIV-2 Gag is expressed in transfected U373 MG cells at significantly lower levels than HIV-1. A and B- Confocal immunofluorescence images of U373 MG cells transfected for 24 hours with HIV-1 and HIV-2 proviruses, respectively. Anti-HIV-1 p24 and anti-SIV p27 antibodies were used for Gag detection (red). Blue=DAPI. C- Western blot of HeLa and U373 MG cell lysates, 24 and 48 hours post-transfection with the HIV-2 provirus, using anti-SIV p27 antibody. D- Quantification of HIV-1 and HIV-2 Gag expressing U373 MG cells, 24 and 48 hours post proviral transfection, gathered from 3 independent repeat experiments. Statistically significant differences between HIV-1 and HIV-2 are highlighted by an asterisk ($p<0.05$).

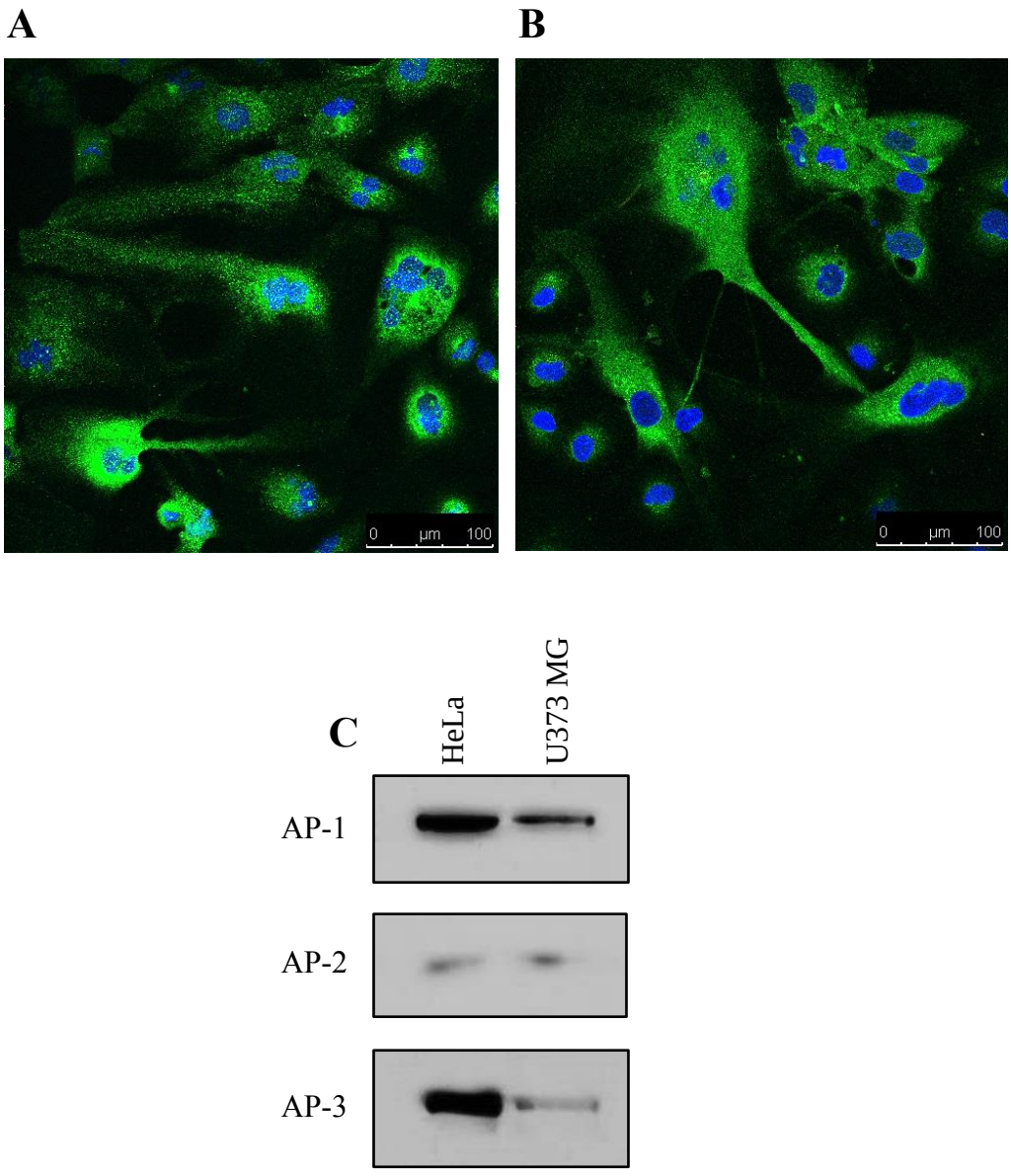

Figure 83: U373 MG cells express adaptor proteins -1, -2 and -3. A and B- Confocal immunofluorescence images of U373 MG cells stained with anti AP-1γ and AP-3δ, respectively (green). Blue stain= DAPI. C- Western blot of harvested HeLa and U373 MG cell lysates. Membranes were probed with anti AP-1γ, AP-2μ or AP-3δ antibodies.

extrapolated since samples were collected directly by using SDS-protein sample buffer to increase concentration, therefore total protein concentrations could not be measured.

Since it has been discovered that HIV-1 infection of astrocytes leads to impaired glutamate uptake and release (Wang et al., 2003), it was postulated whether this could be due to HIV interfering with glutamate receptor recycling, since it is likely that this process will be at least AP-2 mediated. AMPA receptors are ionotropic glutamate receptors that are found in both neurons and astrocytes. They are tetrameric heteromers composed of 4 subunits of GluR1, GluR2, GluR3 and GluR4, which form ligand gated ion channels (Chang et al., 2012). Extensive investigation of the U373 MG cell line by Western blot analysis revealed that this cell line does not express GluR1 or GluR2 in detectable amounts (data not shown). It remains to be elucidated, however, whether they may express GluR3 or GluR4; however, since GluR2 is usually the common subunit of this receptor, coupled with different combinations of the other subunits, it seems unlikely.

8.2.5 HIV-1 Interferes with Astrocytic Vesicle Recycling

Mechanisms of investigating synaptic vesicle recycling and vesicle endocytosis/exocytosis events has been revolutionised since the advent of styryl dyes. Previously, no such experimental system existed whereby examinations of single vesicle events taking place within a cellular process could be studied.

Styryl dyes possess a hydrophilic head attached to a lipophilic tail; this allows the unique property of reversible insertion into the outer leaflet of lipid surface membranes without permeating the vesicle, which is due to two cationic charges located in the head group (Betz et al., 1996; Cousin and Robinson, 1999; Amaral et al., 2011). These dyes are not fluorescent when in aqueous solution, however, they increase in fluorescence

100-fold when partitioned into membranes; this means that fluorescent labelling is limited to outer leaflets of plasma membranes the inner leaflet and recycling vesicles (Cousin and Robinson, 1999; Khvotchev and Kavalati, 2008).

Many styryl dyes have been developed; FM1-43 is one of the more popular dyes since it possesses a short half-time in membrane, which allows dye that has not been internalised to be quickly washed off. This dye can be used to investigate vesicle recycling; after incubation of a cell line with this dye, it inserts into the outer leaflet of the PM, and after stimulation of exocytosis it becomes internalised during vesicle retrieval. Leftover dye is washed off, and what remains reflects fluorescently labelled vesicles. By recording uptake of the dye, insight is given into vesicle endocytosis. Stimulation of exocytosis allows release of the vesicles upon a second round of stimulation, which can be measured by loss of fluorescence (Cousin and Robinson, 1999).

This technique therefore seemed an appropriate and direct way to investigate whether HIV-1 is able to vesicle recycling within astrocytes; does HIV prevent dye uptake, therefore interfering with endocytosis, which is likely through interactions with AP-2/AP-1 (Kim and Ryan, 2009)? Or does HIV-1 prevent destaining (loss of fluorescence), thereby interfering with vesicle exocytosis, which AP-3 has been implicated in (Nakatsu et al., 2004; Scheuber et al., 2006)?

To test this, four conditions were investigated; mock-transfected cells, the Gag-GFP expression construct, a GFP only control, and HIV-GFP (pNL4-3-EGFP). This proviral construct expresses all of the structural, regulatory and accessory proteins of HIV-1 except Env, because a form of enhanced GFP (EGFP) has been inserted into the *env* open reading frame. Vesicle recycling was investigated using the styryl dye FM1-43 and two receptor agonists; UTP and TFLLR-NH_2. UTP is a P2Y receptor agonist; P2Y

receptors are a family of G protein-coupled receptors, and TFLLR-NH_2 is a PAR1 (Protease-activated receptor) agonist (Huang, 2007; Jacobson et al., 2009).

Mock-transfected and Gag-GFP transfected cells were investigated first. Cells were pre-loaded with FM1-43 for 1 hour to stain vesicles. Cells were selected for recordings using a 2-photon microscope, and vesicle exocytosis (destaining) was stimulated by the addition of TFLLR-NH_2 for five minutes. ImageJ was then utilised to measure changes in fluorescence over time from multiple regions of interest per cell, which were expressed as percentages of peak fluorescence. A recording taken from a mock transfected cell is shown in Figure 84.

As can be seen, the addition of TFLLR-NH_2 successfully stimulated vesicle exocytosis, as demonstrated by a loss of fluorescence. This experiment was repeated and the same pattern was seen; however, due to differences in numbers of frames recorded from these repeat experiments, the results could not be compiled into one graph. UTP alone was also found to stimulate a loss of fluorescence (data not shown).

Next, Gag-GFP transfected cells were investigated using the same protocol. The results are shown in Figure 85. As can be seen, in multiple experiments, the presence of Gag-GFP severely compromised vesicle exocytosis upon stimulation by TFLLR-NH_2. Although a decrease in fluorescence was observed over time, this was found to be only a 20% loss of total fluorescence, as compared with 50% in mock transfected cells. This demonstrates that the presence of HIV-1 Gag disrupted the normal vesicle recycling process within astrocytes. The response of FM1-43 stained Gag-GFP transfected cells to other agonists, UTP and anandamide (AEA, a cannabinoid neurotransmitter), was also investigated, and once again only very modest losses of fluorescence could be observed (data not shown).

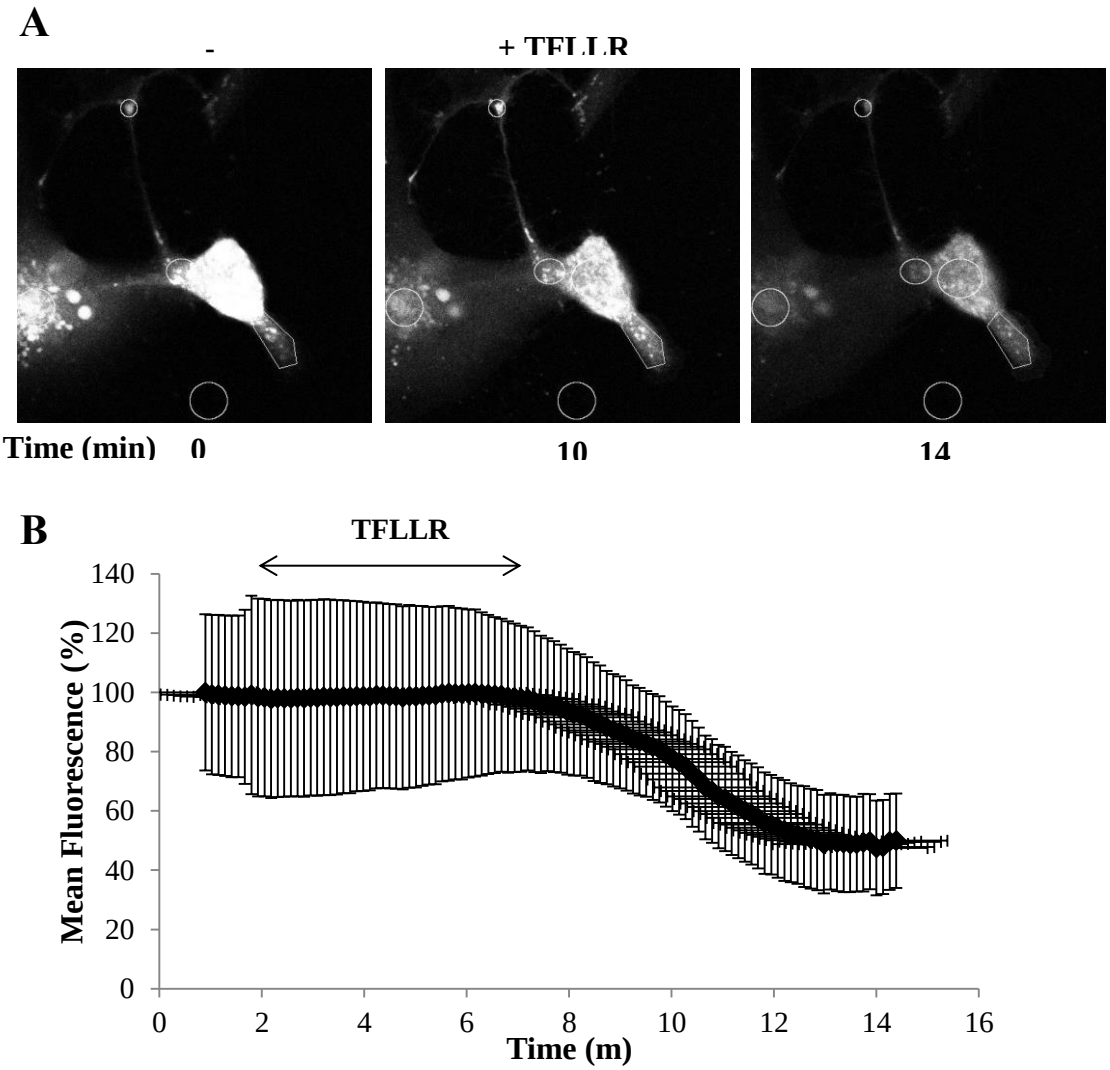

Figure 84: TFLLR-NH_2 stimulates vesicle exocytosis in U373 MG cells. U373 cells were grown on glass coverslips and mock-transfected for 24 hours, followed by pre-loading with FM1-43 for 1 hour to allow dye uptake. Cells were viewed using a 2-photon microscope, and coverslips were perfused with a hypotonic solution containing TFLLR-NH_2 from 2 minutes into the experiment for 5 minutes, followed by a wash. A- Confocal fluorescence images of vesicles containing FM1-43 at 0, 10 and 14 minutes. Changes in fluorescence intensity over time were then calculated for individually selected regions of interest (ROIs) (see circles in panel A) using ImageJ. Background fluorescence was subtracted from each value. This was then plotted, and the result from 1 cell is demonstrated in B, with values expressed as percentages of peak of fluorescence.

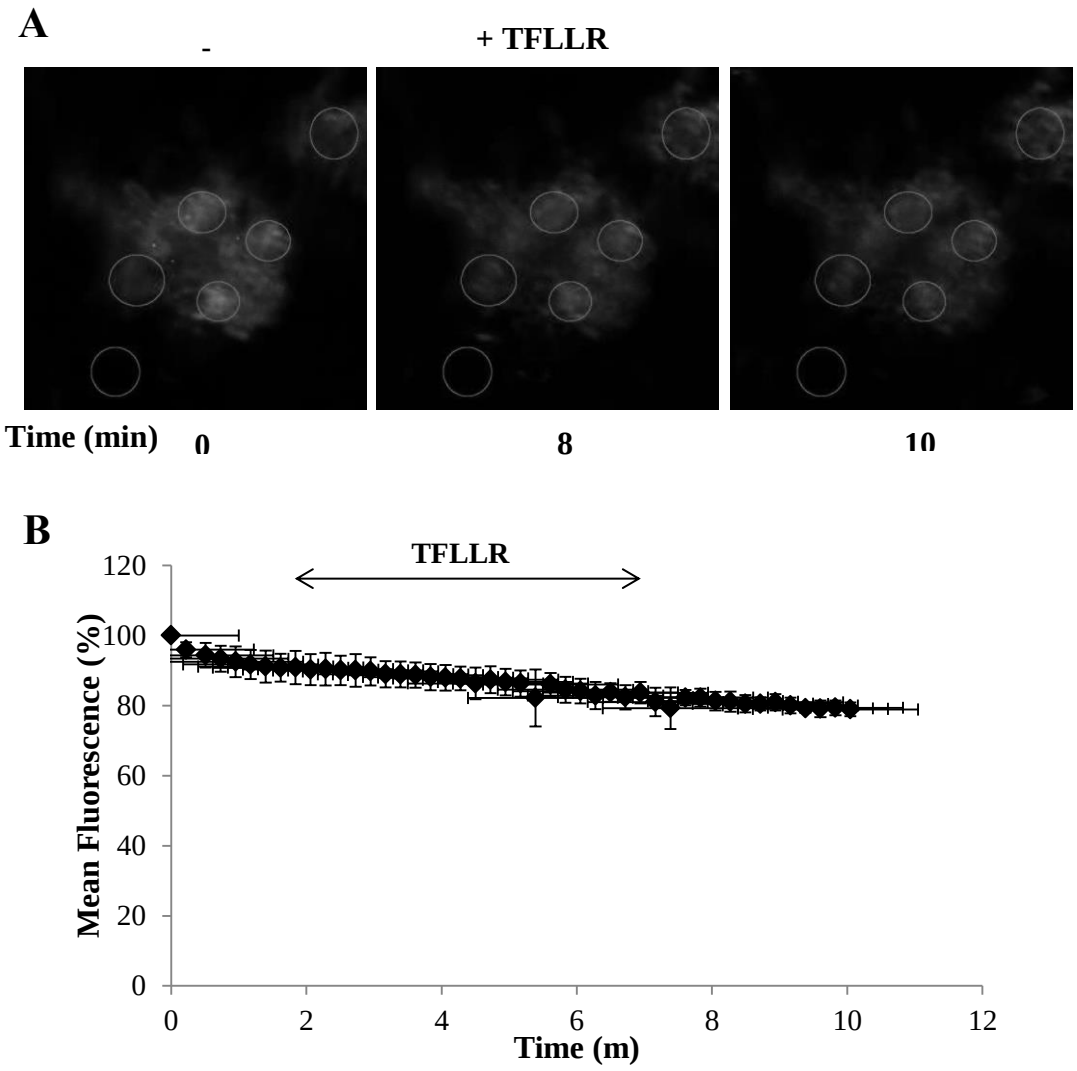

Figure 85: Gag-GFP compromises vesicle exocytosis in U373 MG cells. U373 cells were grown on glass coverslips and transfected with Gag-GFP for 24 hours, followed by pre-loading with FM1-43 for 1 hour to allow dye uptake. Cells were viewed using a 2-photon microscope, and cells expressing GFP were selected for recordings. Coverslips were perfused with a hypotonic solution containing TFLLR-NH_2 from 2 minutes into the experiment for 5 minutes, followed by a wash. A- Confocal fluorescence images of vesicles containing FM1-43 at 0, 8 and 10 minutes. Changes in fluorescence intensity over time were then calculated for individually selected ROIs (see circles in panel A) using ImageJ. Background fluorescence was subtracted from each value. This was then plotted, and the results from 3 independent experiments are demonstrated in B, with values expressed as percentages of peak of fluorescence.

To take this further, the HIV-GFP provirus was used, with GFP pcDNA used as a control for these experiments. Dye uptake, as well as destaining, was also investigated in these experiments to look at both vesicle endocytosis and exocytosis. Cells were transfected for 24 hours, and cells expressing GFP were selected for recordings using a 2-photon confocal microscope. FM1-43 plus UTP was added cells to stimulate dye uptake (vesicle staining), followed by the addition of the two agonists together (TFLLR-NH_2 and UTP) to stimulate vesicle exocytosis. ImageJ was then used as before to measure changes in fluorescence over time for defined regions of interest. The results for GFP transfected cells are shown in Figure 86.

A relatively slow increase in fluorescence was observed in these cells; it took 25-30 minutes to reach peak fluorescence (Figure 86B). Dye uptake was found to be initially slow, with a rapid increase approximately 8 minutes prior to reaching peak fluorescence. This was followed by a rapid decrease in fluorescence when UTP and TFLLR-NH_2 were added together; meaning vesicle exocytosis was efficient and occurring to compensate for the increase in endocytosis. A total loss of fluorescence was not observed; fluorescence decreased by 40% after stimulation of vesicle exocytosis, which was 30% higher than the initial fluorescence values. The error bars at the initial stages of the experiment were also large, as one cell fluoresced much more rapidly than others. The second stage of the experiment, however, displayed very small error bars and was therefore more reliable.

The HIV-GFP provirus was next investigated, and the results are shown in Figure 87. As can be seen, the pattern of staining and destaining was strikingly different from that of GFP only transfected cells. An initial burst of fluorescence upon dye and agonist addition was observed, followed by a long period of slow increase. Since dye uptake was evidently very rapid, FM1-43 was only added for 10 minutes, as oppose to 20

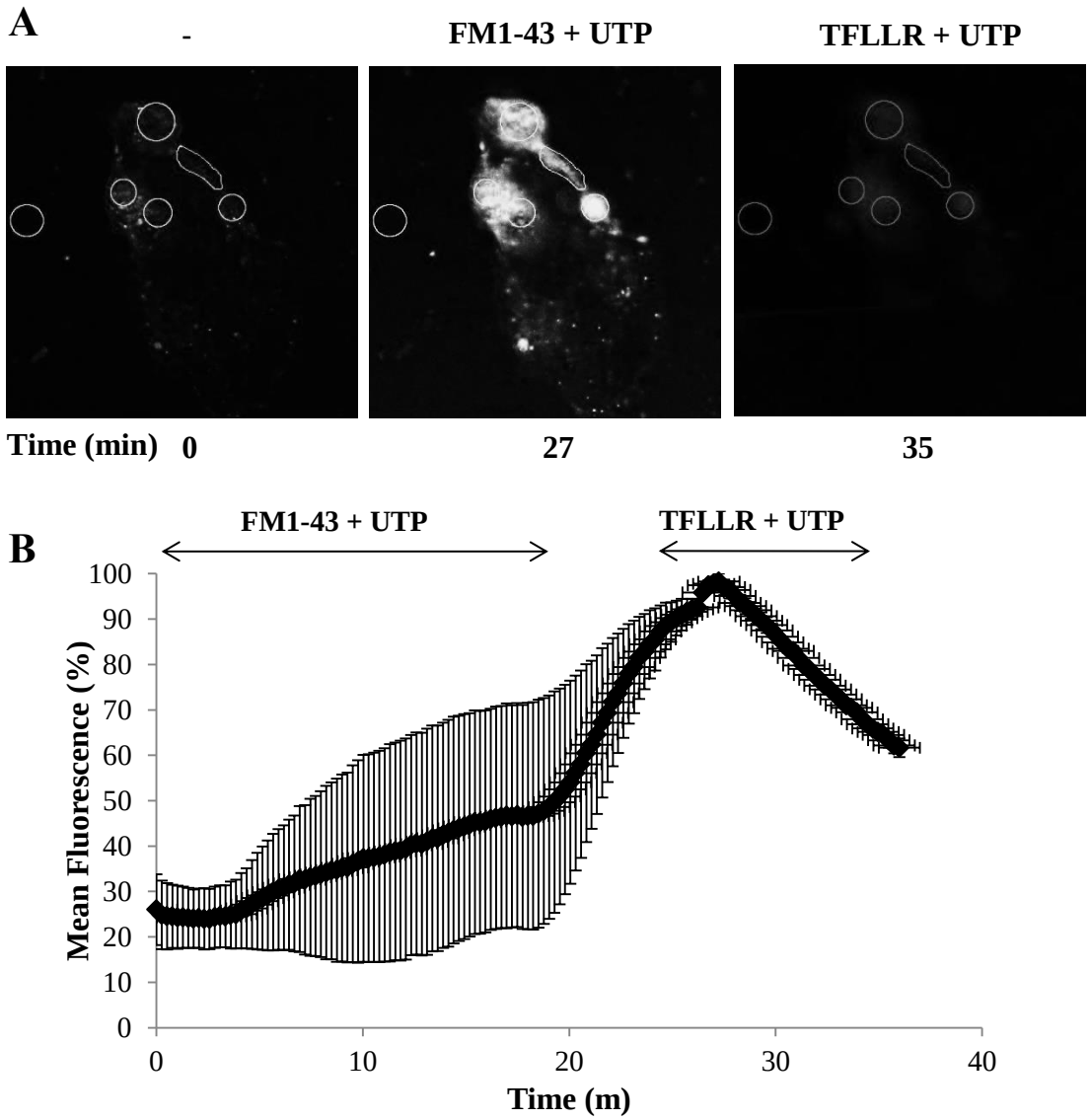

Figure 86: Vesicle recycling in GFP only transfected cells. U373 cells were grown on glass coverslips and transfected with GFP DNA for 24 hours. Cells were viewed using a 2-photon microscope, and cells expressing GFP were selected for recordings. Coverslips were perfused with a hypotonic solution containing FM1-43 and UTP for 20 minutes to allow uptake of dye (A-left and middle, 0 and 27 minutes, respectively). Cells were then washed for 10 minutes, and then perfused with TFLLR-NH_2 and UTP for 10 minutes to allow vesicle de-staining (A-right, 35 minutes). Changes in fluorescence intensity over time were then calculated for individually selected ROIs (see circles in panel A) using ImageJ. Background fluorescence was subtracted from each value. This was then plotted, and the results from 3 cell recordings are demonstrated in B, expressed as percentages of the peak of fluorescence.

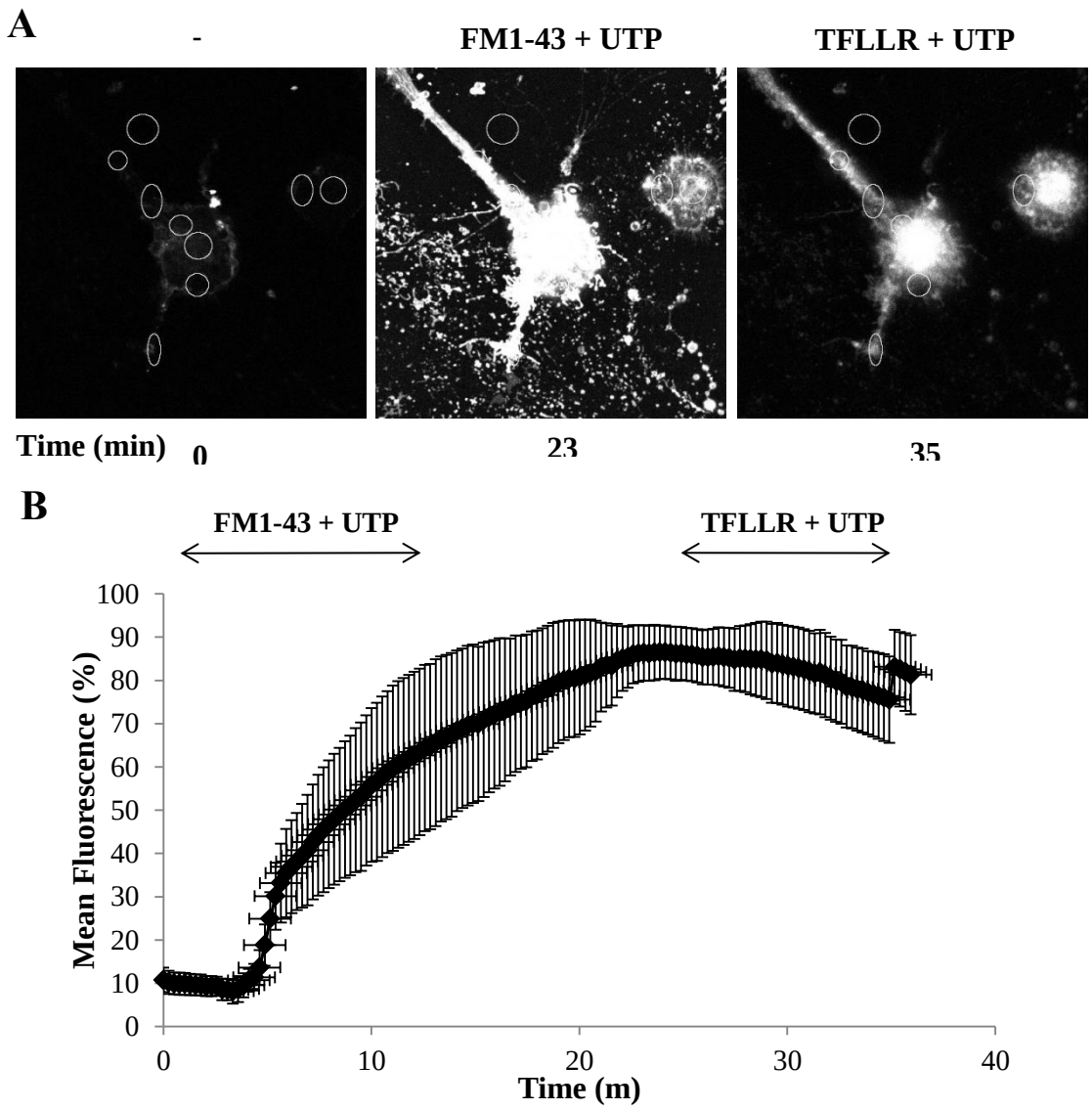

Figure 87: Vesicle recycling in HIV-GFP transfected cells. U373 cells were grown on glass coverslips and transfected with pNL4-3-EGFP for 24 hours. Cells were viewed using a 2-photon microscope, and cells expressing GFP were selected for recordings. Coverslips were perfused with a hypotonic solution containing FM1-43 and UTP for 10 minutes to allow uptake of dye (A-left and middle, 0 and 23 minutes, respectively). Cells were then washed for 10 minutes, and then perfused with TFLLR-NH_2 and UTP for 10 minutes to allow vesicle de-staining (A-right, 35 minutes). Changes in fluorescence intensity over time were then calculated for individually selected ROIs (see circles in panel A) using ImageJ. Background fluorescence was subtracted from each value. This was then plotted, and the results from 4 cell recordings are demonstrated in B, expressed as percentages of the peak of fluorescence.

minutes (used in GFP experiments), to prevent over staining. Peak fluorescence was reached by approximately 22 minutes; around 2-3 minutes faster than GFP only. Following this, a very gradual decrease in fluorescence during stimulation with UTP and TFLLR was observed, unlike the rapid more drop we saw in GFP only cells. Fluorescence only dropped by approximately 15% of the peak of fluorescence by the end of the experiment; 25% less than GFP only transfected cells. The recording did not continue for an extended period after the agonist was added because the maximum amount of recording time for the software was reached.

These results support the results gathered in Gag-GFP transfected cells, and indicate that the presence of HIV-1 proteins does indeed have an effect on vesicle recycling. It is difficult to deduce whether the effect on dye uptake is reliable since the error bars were large in GFP-only cells, but certainly the patterns of vesicle staining and destaining were markedly different between these two treatments. The second half of the experiment (destaining) was perhaps more accurate since error bars for both conditions were small.

8.2.6 HIV-1 does not Affect Calcium Waves

Astrocytes are capable of a type of intercellular communication based on the propagation of calcium (Ca^{2+}) waves. Calcium waves are defined as a localised increase in cytosolic Ca^{2+}, followed by a succession of similar events in a wave-like fashion. These may be restricted to individual cells (intracellular), or alternatively may spread to neighbouring cells (intercellular) by one of two proposed mechanisms. These are direct communication through adjacent cytosols via diffusion through gap junctions, or receptor mediated activation via gliotransmitter release, presumably ATP. Intracellular calcium waves involve a cascade of events following G protein coupled receptor

activation, which ultimately leads to release of Ca^{2+} from the ER (Scemes and Giaume, 2008)

Mechanisms have been developed that allow direct visualisation of calcium waves, through the use of fluorescently labelled calcium probes. One such probe is the genetically encoded probe known as GCaMP, which was forged by connecting DNA encoding EGFP to a fragment of myosin light chain kinase sequence and the calcium binding calmodulin (CaM) DNA. When Ca^{2+} binds to the expressed CaM, it induces conformational changes which subsequently trigger a change in EGFP that in turn leads to a change in fluorescence intensity (Nakai et al., 2001).

In order to visualise calcium waves within the U373 MG cell line, a modified GCaMP construct was used; Sy-GCaMP-mCh. This construct is mCherry tagged, as oppose to GFP, to complement the GFP tagged constructs already used in this chapter.

It is possible that HIV-1 could interfere with the propagation of Ca^{2+} waves through two different mechanisms. HIV-1 could interfere with G protein coupled receptor expression, possibly through interference with receptor recycling and targeting it for degradation, such as with MHC-I. We would not expect HIV-1 to be able to affect the release of Ca^{2+} stores from the ER since results gathered do not suggest that HIV interferes with ER trafficking. Alternatively, HIV-1 could interfere with gliotransmitter signalling between astrocytes, thus preventing calcium wave propagation.

To investigate the possibility of HIV interfering with calcium waves, U373 MG cells were grown on glass coverslips and co-transfected with Sy-GCaMP-mCh and either GFP and HIV-GFP for 24 hours. A Sy-GCaMP only control was also used. Cells were visualised using a 2 photon confocal microscope, and were stimulated using different

agonists for defined time periods; these were as anandamide (AEA), UTP and TFLLR-NH_2.

The results for Sy-GCaMP only are shown in Figure 88. As can be seen, the addition of various stimulants did trigger visible Ca^{2+} waves in this cell line; increases and decreases in fluorescence could be seen over time (Figure 88A). To quantify this, recordings were taken from several individual cells using ImageJ, selecting multiple regions of interest (ROIs), as shown by the circles in Figure 88A. ImageJ was used to calculate changes in fluorescence (pixels) over time, correcting for background fluorescence; this was converted into a percentage of peak fluorescence. The average change in fluorescence over time is shown in Figure 88B. The error bars were fairly large as some cells appeared more responsive than others, possibly because some cells were connected via hemichannels and were therefore able to spread waves between each other. The initial large loss of fluorescence was likely attributable to release of readily available calcium pools, whereas the subsequent increases and decreases were likely from using reserve pools and were therefore smaller, although some calcium (as $CaCl_2$) was added in the wash solution.

Next, GFP only transfected cells were used as a control (see Figure 89), since the HIV provirus used also expresses GFP. Once again, calcium waves could be propagated within this cell line. Although the oscillations in fluorescence appeared moderate in comparison to GCaMP only expressing cells, it is worth mentioning that only two agonists were used in this experiment, as opposed to three, and that the most dramatic changes in fluorescence observed in the previous experiment were when the agonist AEA was added. This agonist was not used in these experiments, and therefore provides a likely explanation for the results observed.

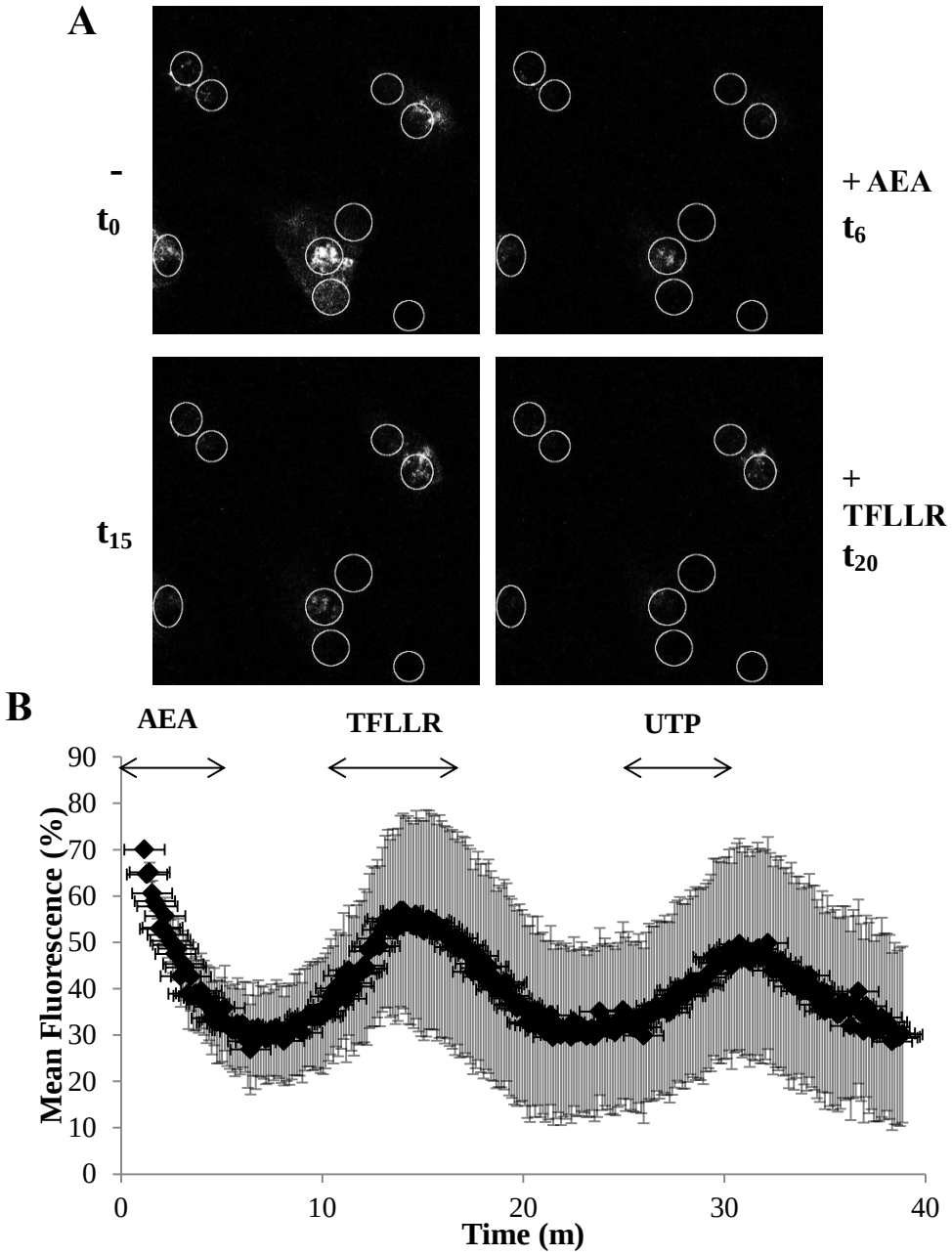

Figure 88: Calcium waves can be propagated in U373 MG cells. Sy-GCaMP-mCherry only transfected U373 MG cells were visualised on a 2 photon microscope. Cells expressing mCherry were selected for analysis. Slides were perfused with AEA for five minutes, followed by TFLLR-NH_2 for five minutes, and finally UTP. A- Confocal images of Sy-GCaMP-mCherry fluorescence at 0, 6, 15 and 20 minutes. Washes with a hypotonic solution were included in between stimulations. Recordings from multiple cells were analysed by ImageJ using multiple ROIs (circles in A), including a background area. Changes in fluorescence over time were calculated and expressed as percentages of the peak of fluorescence (B).

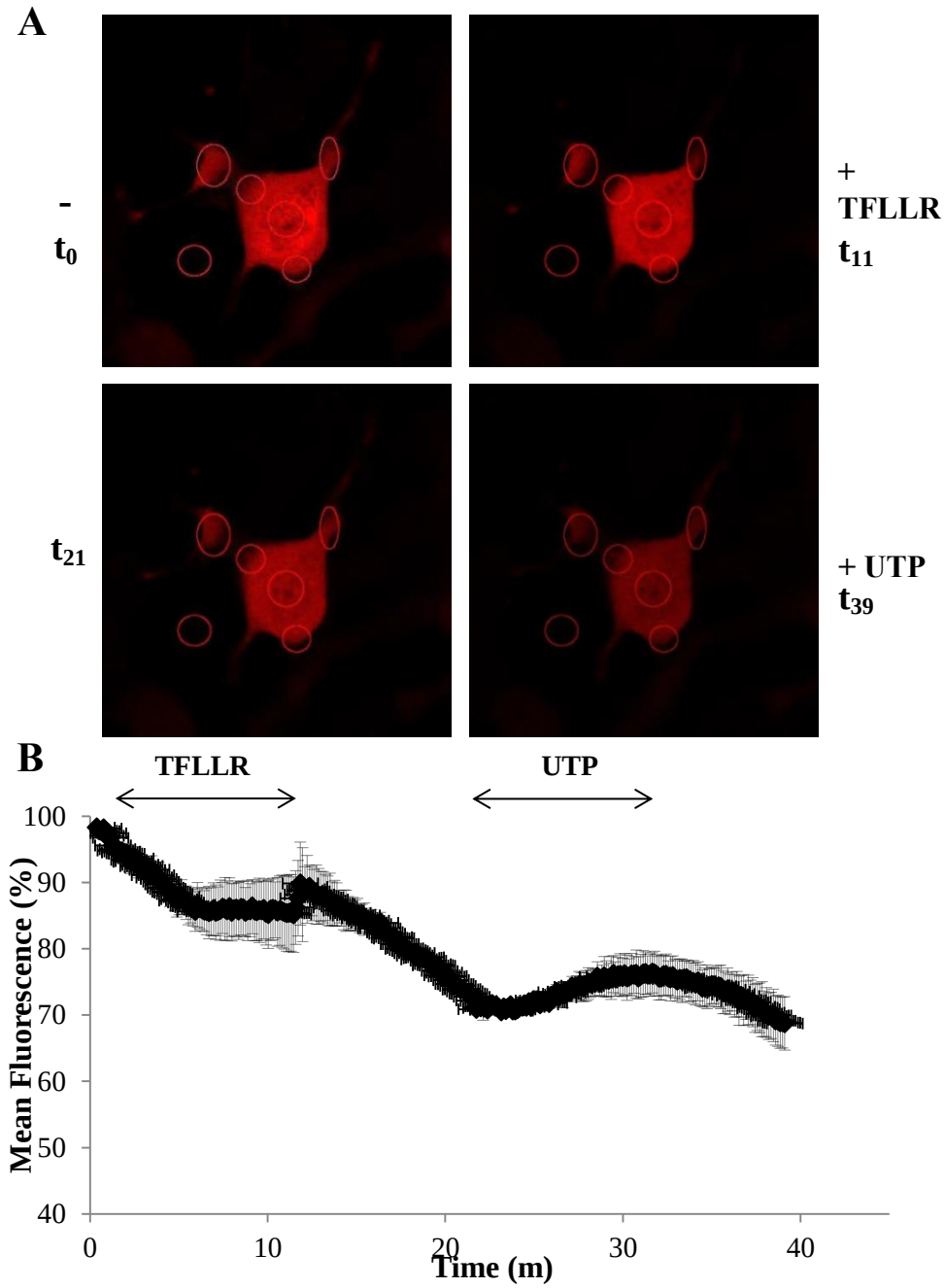

Figure 89: GFP does not affect calcium waves. Sy-GCaMP and GFP transfected U373 MG cells were visualised on a 2 photon microscope. Cells expressing both GFP and mCherry were selected for analysis. Slides were perfused with TFLLR-NH_2 for ten minutes, and finally UTP. Washes with a hypotonic solution were included in between stimulations. A- Confocal images of Sy-GCaMP-mCherry fluorescence at 0, 11, 21 and 39 minutes. Recordings from multiple cells were analysed by ImageJ using multiple ROI's (circles in A), including a background area. Changes in fluorescence over time were calculated and expressed as percentages of the peak of fluorescence (B).

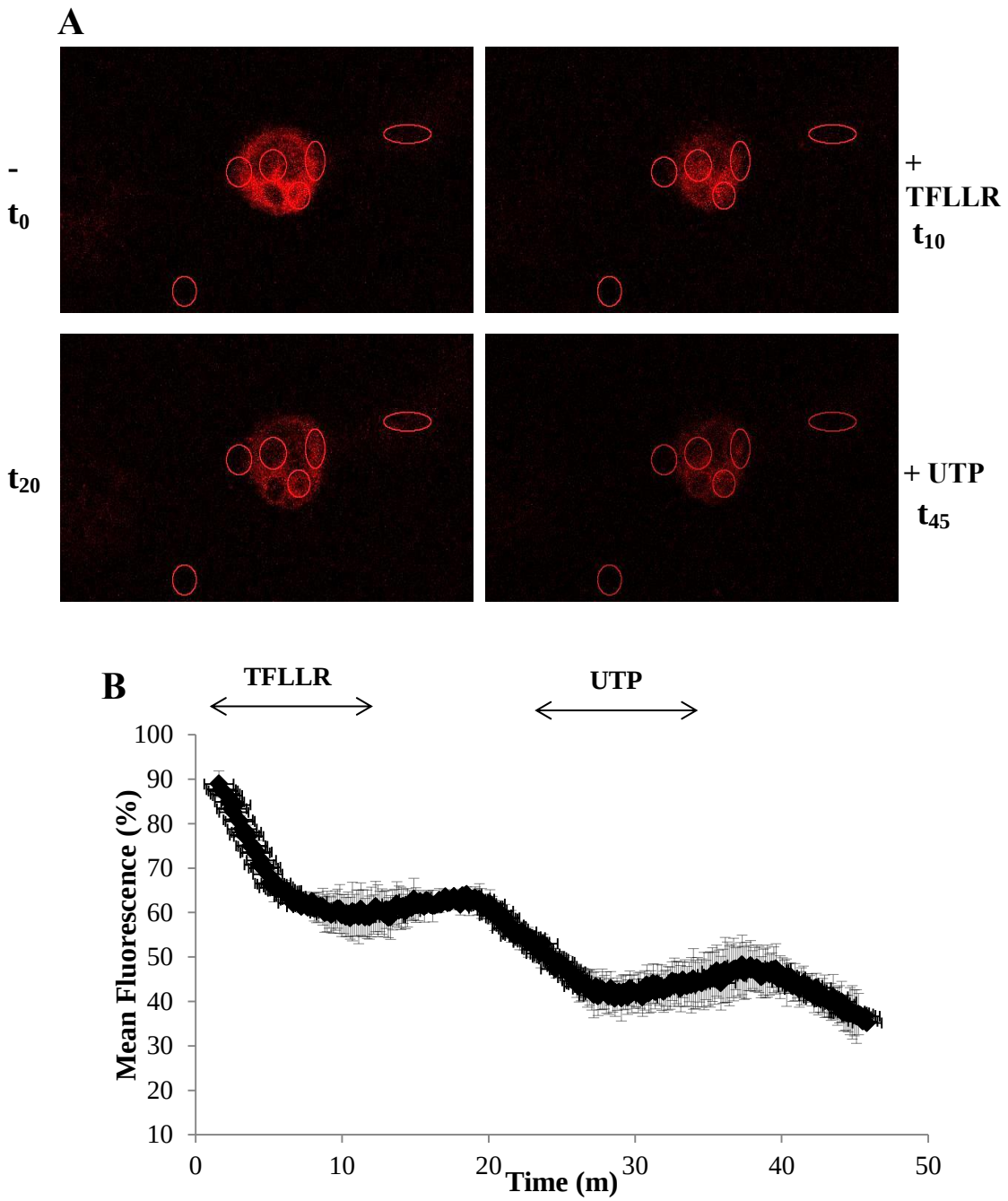

Figure 90: HIV does not affect calcium waves. Sy-GCaMP and HIV-GFP transfected U373 MG cells were visualised on a 2 photon microscope. Cells expressing both GFP and mCherry were selected for analysis. Slides were perfused with TFLLR-NH_2 for ten minutes, and finally UTP. Washes with a hypotonic solution were included in between stimulations. A- Confocal images of Sy-GCaMP-mCherry fluorescence at 0, 10, 20 and 45 minutes. Recordings from multiple cells were analysed by ImageJ using multiple ROIs (circles in A), including a background area. Changes in fluorescence over time were calculated and expressed as percentages of the peak of fluorescence (B).

When HIV-GFP was transfected into cells (see Figure 90), a similar pattern to that of GFP only transfected cells was observed. Again the oscillations were smaller than that of cells only expressing GCaMP, but calcium waves were indeed propagated. The error bars for these two conditions were also much smaller than that of GCaMP only cells, and therefore may represent a more reliable data set. Since the results were similar to that of GFP transfected cells, this suggests that HIV does not interfere with calcium waves within astrocytes.

8.3 Discussion

Various hypotheses have been suggested for the development of neurological symptoms in HIV infected individuals. The CNS is a complex, multi-faceted system, and it seems most likely that the conditions observed are due to a variety of HIV induced effects, as opposed to one. This chapter aimed to shed light on the role of astrocyte infection in the development of HIV associated dementia; particularly, drawing links between the trafficking perturbations of AP dependent pathways observed in other cell lines utilised within this thesis. Since we know that both AP-1, -2 and -3 are critical to vesicle recycling within neurons, it seemed an appropriate extrapolation that similar mechanisms exist within astrocytes.

Having first established that the cell line chosen for experimentation (U373 MG) did indeed express these 3 APs (Figure 83), and was capable of expressing Gag (and Nef) from both transfected Gag-GFP (Figure 80) and a HIV-1 proviral plasmid (Figure 81), methods were chosen to investigate vesicle recycling. Direct visualisation of vesicle endocytosis and exocytosis through the use of fluorescent dyes was used to investigate the potential of HIV-1 to interfere with these specific trafficking pathways, having

already established the ability of HIV to interfere with DTx trafficking within HeLa cells (as described in chapter 7).

Difficulties arose in the fine tuning of early experiments; establishing optimum concentrations of FM1-43 and length of agonist addition proved arduous. Having attempted various protocols, the addition of the agonist TFLLR-$NH2_2$ after dye pre-loading was selected for examination of mock transfected and Gag-GFP transfected cells. There was a striking difference in the response to this agonist between these two experimental conditions (Figure 84 vs Figure 85); Gag-GFP transfected cells exhibited only a very modest and slow loss of fluorescence in comparison to mock transfected cells, which displayed a relatively rapid loss of fluorescence.

These results would suggest that the presence of HIV-1 Gag can indeed interfere with the recycling of gliotransmitter vesicles within astrocytes. This is, however, not necessarily representative of an *in vivo* situation since Gag will be expressed in much lower levels during HIV-1 infection, since transfection of this construct bypasses numerous blocks of HIV-1 replication. These results do, however, raise the possibility of a similar situation arising in HIV infected individuals, and demonstrate the capability of a Gag-mediated effect. Interestingly, as shown in chapter 7, the Gag-GFP construct displayed little interference with the trafficking of DTx in HeLa cells, suggesting different mechanisms operating within these two cell lines. Since HeLa cells are undoubtedly a more robust cell line, it is possible that they are inherently hardier, and therefore transfection of the astrocytoma cell line is more likely to produce toxic effects. Gag-GFP transfected U373 MG cells often had altered morphologies, as shown by confocal microscopy (Figure 80), which would support the notion that overexpression of Gag is toxic to these cells, which would of course affect normal cell functioning.

To investigate this apparent effect further, a HIV-GFP provirus was used (Figure 87), alongside a GFP only control (Figure 86). This provirus expresses all the viral proteins (except Env), including Nef, which is also known to interact with the APs and can disturb trafficking pathways, for example of the transferrin receptor (Craig et al., 2000; Madrid et al., 2005). Both dye uptake and dye release were investigated in these experiments. When just release events (loss of fluorescence) are taken into account, a similar pattern to that in Gag-GFP transfected cells could be observed; severely compromised vesicle destaining when compared to the control. When dye uptake is also taken into account, we also saw a difference between HIV-GFP and GFP only transfected cells; interestingly, HIV-GFP transfected cells displayed more rapid dye uptake, reminiscent of the slight sensitisation to RTx described in chapter 7. Since these two processes will be governed by different adaptor proteins; possibly AP-2 (and/or AP-1) and AP-3, respectively, it is suggestive of interference in more than one trafficking pathway within astrocytes.

As mentioned, vesicle release (exocytosis) events involve AP-3 in neuronal cells (Nakatsu et al., 2004; Scheuber et al., 2006); and therefore this likely occurs in astrocytes also. DTx trafficking may be dependent on AP-3 (see chapter 7), and both HIV-1 and HIV-2 significantly interrupted this pathway in HeLa cells, in a Gag dependent manner. This is suggestive of a universal effect of HIV on AP-3-dependent trafficking pathways. Despite HIV not being able to productively infect astrocytes, it does not necessarily mean that newly synthesised Gag and Nef proteins do not traffic in the same manner to assembly sites, or at least engage with the adaptor proteins, rendering them unavailable for cellular processes such as synaptic vesicle biogenesis. However, since astrocytes transfected with HIV proviruses, or indeed infected astrocytes *in vivo*, express very limited amounts of viral Gag proteins, it does beg the

question whether the effects observed are indeed Gag mediated. However, Nef is expressed in high levels in astrocytes *in vivo* and *in vitro,* which may be suggestive of Nef mediated interference. Nef was found to be dispensable for the interruption of DTx trafficking, but certainly what happens in one cell may not mirror what happens in another. At this stage, it remains unknown how HIV-1 interrupts with vesicle exocytosis events, therefore more research is required.

Vesicle uptake (endocytosis), as mentioned, is governed by AP-2 in neuronal cells, and in its absence, AP-1 may act to replace it (Kim and Ryan, 2009). AP-2 has an inhibitory effect on HIV-1 particle release in productively infected cells such as HeLa; this may also occur in astrocytes, however it is unlikely that this is the sole reason for the inability of HIV to egress since it evidently does not abolish particle release in other cell lines. It was therefore surprising to see that the presence of HIV appeared to increase dye uptake in U373 cell lines, in comparison to GFP transfected cells. It seems plausible that the presence of actively trafficking HIV particles may cause an increase of AP-1 at the plasma membrane, which therefore may make this protein more readily available to mediate vesicle endocytosis. That being said, since the error bars for this part of the experiment were very large for GFP transfected cells, it still remains a possibility that HIV does not significantly increase vesicle uptake. More experiments are therefore required to investigate whether this is a real effect.

What do these results mean with regards to HIV associated neurocognitive disorders? The idea that astrocytes merely provide a neuronal support network is outdated, and they have been discovered to play many crucial and active roles in brain functioning. Astrocytes release numerous transmitters, including glutamate, ATP and D-serine, which regulate neuronal excitability and synaptic transmission (Hamilton and Attwell, 2010). Both D-serine and glutamate release by astrocytes are essential for neuronal

NMDA receptor function, which in turn is essential for the induction of long-term synaptic plasticity (the ability of synapses to strengthen or weaken over time), which is crucial for learning and memory (Halassa et al., 2007). More specifically, it was found that the release of D-serine from astrocytes upon neuronal stimulation was critical for long-term potentiation (the long lasting enhancement of signal transmission between neurons), which underlies synaptic plasticity, to occur in the hippocampus; a major component of the brain responsible for consolidation of short-term memory into long-term memory and spatial navigation (Yang et al., 2003). We could therefore envisage that if HIV perturbs the release of these transmitters, synaptic plasticity would be compromised, therefore affecting short-term memory; one of the symptoms commonly associated with HAD patients.

Interestingly, recent evidence has started to suggest a role for astrocytes in motor function, and it is anticipated that much future research will begin to answer questions in this area. Rhythmic motor behaviours, such as locomotion, are controlled by neuronal cells named central pattern generators (CPGs). Within the spinal cord, numerous transmitters are responsible for modulating the CPGs involved in locomotion. These include ATP, adenosine and endocannabinoids (Christensen et al., 2013). We know that astrocytes are capable of releasing ATP (Montana et al., 2006), but recent evidence gathered suggests that astrocytes can also release the endocannabinoids AEA alongside homo-γ-linolentlethanolamide and docosatetraenylethanolamide (Walter et al., 2002). It therefore also seems plausible that an interference with the release of these transmitters by astrocytes may also affect locomotion, which we could postulate may contribute to the loss of motor function observed in some HAD patients. I should hasten to add, however, that conclusions drawn are speculative, and it remains a difficulty in neuroscience to definitively draw

links between what happens at the cell level and physiological manifestations. However, this research certainly has the potential to shed light on some grey areas with respect to the neurological manifestations of HIV infection. Since the brain is a complex system, it seems likely that symptoms result from not one, but an amalgamation of numerous different virological consequences on cell function.

Astrocytes are also capable of communication through calcium signalling. The synaptic release of particular neurotransmitters from neighbouring neurons, such as glutamate, can lead to an increase in intracellular Ca^{2+} in astrocytes, which triggers the release of glutamate from these cells, which in turn causes glutamate receptor mediated Ca^{2+} increases in nearby neurons (Fellin and Carmignoto, 2004). It was found that exposure of astrocytes to either HIV-1 particles, or gp120 alone, impaired glutamate uptake and release, which was attributed to the concomitant decrease in expression of the glutamate transporter EEAT2 (Wang et al., 2003). Since results in this chapter suggest that Ca^{2+} signalling is not impaired in HIV transfected astrocytes compared to GFP transfected astrocytes (Figure 90 vs Figure 89), it would suggest that this is not an additional factor contributing to the loss of glutamate signalling by astrocytes during HIV infection. It would also support data collected from RTx cytotoxicity assays and VSV-G trafficking assays, in which HIV did not interfere with ER trafficking, since propagation of Ca^{2+} waves involves release of Ca^{2+} pools from the ER.

8.4 Future Work

This chapter has provided novel insights into possible mechanisms behind the development of neurological complications in HIV infected individuals. In particular, results have demonstrated that HIV-1 causes perturbation of vesicle recycling within astrocytes, which may be a possible contribution to short-term memory loss in

individuals suffering with HAND. The research carried out in this chapter is, however, very much in its infancy, and requires more rigorous investigation. However, work carried out certainly provides a firm backbone for the continuation of research in this novel field.

Fine tuning of protocols in this chapter meant that, despite using 3 agonists, not enough data was gathered to draw conclusions for UTP and AEA in mock transfected and Gag-GFP transfected cells, therefore repeat experiments are required following the same protocol that was used for TFLLR-NH_2. More experiments are also required to investigate the effects of HIV on dye uptake; these experiments were not performed in mock transfected or Gag-GFP transfected cells, and the error bars for GFP transfected cells were large, possibly indicating unreliability in the current data set.

An obvious gap in research is the lack of studies using HIV-2. Since these studies were novel and HIV-1 expressed Gag better than HIV-2, and success was not guaranteed, it was decided to conduct experiments utilising only HIV-1. An HIV-2-GFP construct could be made and utilised for future experiments as a useful tool for comparative means; with data gathered so far, it would suggest that these viruses likely would not produce identical effects.

An interesting direction to take this chapter forward would be to investigate individual vesicle trajectories within these different conditions. It would be interesting to see whether the presence of HIV specifically slowed down individual vesicle movement, as compared with control cells. This would be a relatively simple analysis using software on ImageJ; vesicle labelling is more problematic. A sister construct to the SyGCaMP-mCherry used in this chapter, SyPhy-mCherry, which labels individual vesicles could be used to carry on research.

Another interesting set of experiments would be to investigate receptor recycling on astrocytes. This could be carried out using biotinylation, whereby receptors on the cell surface are labelled, and then compared with the total pool of receptors after stimulation. It had been our intention to test receptor recycling of the glutamate receptor; unfortunately, since it was discovered that U373 MG down-regulate glutamate receptor expression, it was not possible to conduct these experiments on this cell line. Therefore, a suggestion would be to attempt this experiment in a cell line which does express glutamate receptors. Alternatively, it would be interesting to see if, in a co-culture of astrocytes and neurons, the presence of HIV inhibited the uptake of receptors on neuronal surfaces, which would also likely affect synaptic plasticity.

This leads to a further limitation of this work; the use of an astrocytoma cell line, rather than primary astrocytes or astrocyte/neuron co-culture. HIV does not infect rodent cells, which rules out the use of rodent-derived primary cells, and would necessitate the use of human tissue. In the future, stem cell technology may aid these experiments.

CHAPTER 9: CONCLUSIONS

9.1 Conclusions and Future Work

This thesis aimed at shedding light on the interactions between HIV-1 and not only the clathrin adaptor proteins, but adaptor protein dependent trafficking pathways. The trafficking pathways adopted by newly synthesised HIV-2 Gag proteins were also scrutinised. This chapter will summarise the conclusions drawn from results gathered and how these have contributed to research in this field.

Firstly, results gathered through confocal immunofluorescence microscopy and Western blot of AP siRNA treated cells supported the hypothesis that HIV-1 traffics to the PM via an endosomal intermediate, and that AP-1 and AP-3 likely function in different stages of the HIV-1 trafficking process. AP-1 most likely facilitates the direction of newly synthesised Gag molecules to endosomes, since Gag in cells where AP-1 was knocked down appeared more diffuse; whereas AP-3 may facilitate the delivery of these compartments to the PM, since Gag in cells where AP-3 was knocked down appeared more punctate. In both cases, PM Gag staining was virtually abolished.

Next, novel research investigating HIV-2 trafficking found that this virus traffics, and interacts with the APs, in a different manner to HIV-1. Confocal immunofluorescence microscopy studies demonstrated that HIV-1 and HIV-2 Gag display different cellular localisations. The punctate pattern observed in HIV-2 transfected HeLa cells, in comparison to the diffuse staining seen with HIV-1, was suggestive of the potential of this virus to assemble within intracellular compartments, which has been observed with HIV-1 but only in macrophage cell lines. Further investigation of viral protein levels after siRNA mediated knockdown of the adaptor proteins found that HIV-2 was more dependent on AP-3, which is involved in endosomal cargo trafficking, than AP-1 for

efficient particle assembly and release, whereas HIV-1 presented similar dependencies on the two proteins. The novel adaptor protein AP-5, which associates with late endosomes, also facilitated HIV-2 particle assembly and release, but did not affect HIV-1.

Interestingly, however, HIV-1 and HIV-2 both affected the localisation of AP-1, but produced strikingly different effects; HIV-1 appeared to condense AP-1 into a tight juxtanuclear position, possibly the Golgi/TGN, although this was not formally identified. HIV-2, however, caused AP-1 to adopt a somewhat tubular appearance. Although this remains uncertain, it may indicate a role for AP-1 in transporting newly synthesised HIV-2 Gag molecules to cytoskeletal elements such as actin or microtubules for efficient trafficking, which would support the novel role also found for AP-1 (and AP-3) in the transport of lipoplexes, which may involve delivery of cytoskeletal motor molecules, such as kinesin KIF4, to cargo. The identity of the compartments to which AP-1 was relocalised to was not discovered, however, because colocalisation studies with cellular markers were not performed.

The depletion of cellular Gag observed in the absence of AP-1 or -3, in both HIV-1 and HIV-2 transfected cells, indicated that when newly synthesised Gag molecules are unable to efficiently traffic and assemble into particles, total Gag levels fall. This suggests degradation by cellular mechanisms. Results indicated that this was not due to lysosomal or proteasomal degradation, or the formation of aggregates which were not recovered by the method of lysis adopted, or inhibition of translation; therefore the fate of Gag in AP-1/-3 deficient cells remains to be elucidated.

Further evidence to support a role of intracellular compartments in the trafficking of HIV-2 Gag was gathered through the use of Diphtheria toxin, which enters the cell via clathrin mediated endocytosis, which is therefore likely AP-2 mediated. From here, it

traffics to the early endosome, and possibly uses AP-3 in trafficking to the late endosome, prior to escape to the cytosol. Although HIV-1 Gag perturbed the toxicity of DTx, HIV-2 Gag was found to have a significantly larger protective effect. Earlier investigation of adaptor protein levels during HIV-1 transfection indicated that the disruption of DTx trafficking was not due to altered AP expression. It was therefore speculated that the observed protective effects of HIV Gag on cells to DTx challenge could be due to AP sequestration by HIV Gag molecules, possibly preventing the availability of the APs to facilitate efficient DTx trafficking, especially if some DTx is using a late endosomal compartment to enter the cytosol. Alternatively, the presence of Gag on internal membranes, such as early endosomes, might interfere with endosomal acidification or the emergence of DT A fragment across the endosomal membrane. These possibilities were not explored.

Further analysis by confocal immunofluorescence microscopy revealed a strong colocalisation and re-distribution of AP-3 by HIV-2 in HeLa cells, which was not observed in HIV-1 transfected cells. While the speculation that increased AP-3 sequestration in the presence of Gag may explain the interference with DTx entry and toxicity, there may be other explanations. These data also, however, suggested that the pronounced intracellular distribution of HIV-2 Gag could be due to the re-internalisation budding particles at the plasma membrane following restriction by tetherin, rather than a preference for assembly within intracellular compartments. Utilisation of a tetherin-deficient cell line (HEK 293T) revealed that although HIV-2 Gag became more diffuse, punctate staining was still the dominant phenotype. Therefore tetherin restriction is not solely responsible for the increased intracellular localisation of HIV-2 Gag in non-macrophage cell lines. Inhibition of endocytosis by AP-2 knockdown and expression of a Rab5 dominant negative construct further

demonstrated that the presence of HIV-2 Gag within intracellular compartments was not due to internalisation of released virions. Electron microscopy studies revealed the presence of HIV-2 immature particles within intracellular compartments in HEK 293T cells, further verifying the ability of this virus to assemble within intracellular compartments in non-macrophage cells. Confocal immunofluorescence demonstrated these to be CD81 (and CD63) positive compartments, which HIV-1 Gag did not localise to.

So HIV-1 and HIV-2 Gag differ in their trafficking pathways, but what could this mean in terms of the disease caused by these two viruses? As discussed in chapter 6.1, HIV-2 is overall less pathogenic than HIV-1, and a considerably higher proportion of infected individuals are classed as long term non-progressors. This has been linked to lower plasma viraemia levels in the majority of HIV-2 patients in comparison to HIV-1. There have been several theories proposed to account for this, such as a less efficient ability to evade immune responses. Since results gathered in this thesis propose that HIV-2 can begin to assemble within LEs/MVBs in non-macrophage cell lines, and a higher proportion of Gag is present within these compartments than HIV-1, it may be that this could also contribute to the decrease in pathogenicity of HIV-2. This is because it is possible that some of these compartments enter a degradative pathway, for example by fusing with lysosomes, as oppose to being recycled to the PM for release. This could result in a lower efficiency of viral particle release in comparison to HIV-1, which we speculate could also contribute to a decrease in plasma viraemia levels.

Although current literature suggests that the AP binding sites of HIV-1 Gag lie within the MA domain, the use of chimeric viruses suggested that other AP binding sites may exist. For example, depletion of AP-2 in MA2 transfected cells greatly enhanced particle release, as was the case with HIV-1, indicating that AP-2 has a negative effect

on MA2 release. This is in contrast to HIV-2, where release was not found to be inhibited by AP-2. The MA domain was previously described to drive Gag localisation and membrane binding, however, results gathered here through the use of chimeric viruses would suggest that other factors are also required for Gag localisation since MA2 Gag displayed a similar appearance to HIV-1 in HEK 293T cells.

The final stage of this project aimed at investigating the ability of HIV to cause a global disruption in trafficking pathways, through the use of an astrocytoma cell line. This was based on the following observations: AP-1, -2 and -3 are involved in neuronal vesicle recycling (Nakatsu et al., 2004; Scheuber et al., 2006; Kim and Ryan, 2009); AP deficiencies in mice lead to defects in learning and memory (Glyvuk et al., 2010); astrocytes, but not neurons, are infected in HIV patients (Churchill et al., 2009; Sharma and Bhattacharya, 2009); similar vesicle recycling mechanisms are presumed to exist in astrocytes; HIV infected patients suffering neurological complications often experience memory loss (Gonzalez-Scarano and Martin-Garcia, 2005; Ghafouri et al., 2006). Through the use of fluorescent dyes, it was possible to ascertain that HIV was indeed capable of disrupting vesicle recycling in astrocytes; in particular, vesicle exocytosis events. Since vesicle biogenesis and exocytosis has been shown to be regulated by AP-3 in neuronal cells, (Nakatsu et al., 2004; Scheuber et al., 2006), this may suggest that HIV globally interferes with AP-3 dependent trafficking pathways, since DTx may also traffic in an AP-3 dependent manner.

In summary, this research has demonstrated that although there are common aspects between the trafficking pathways adopted by HIV-1 and HIV-2, these two viruses may indeed differ not only in their interactions with the clathrin adaptor proteins, but also in their mechanisms of transport to, and preferred location of assembly sites, and thus in their ability to interfere with AP dependent trafficking pathways.

Future work to continue research is necessary in several areas. Firstly, it would be interesting to understand why HIV-1 and HIV-2 adopt different cellular trafficking pathways, since they share 60% amino acid sequence similarity in their Gag proteins (Dilley et al., 2011). Mutational analysis may provide some insights here. It is also particularly important to provide more robust evidence of the involvement of endosomes in the trafficking of HIV-2, for example by direct visualisation of a fluorescently labelled virus.

Second, confirmation of the suggested existence of AP binding sites other than those described in MA and Nef is needed to verify findings about the behaviour of the MA chimeric viruses.

Finally, this project has provided some foundations for research into insights behind the contributions to neurological manifestations during HIV infection. As mentioned, research is very much in its infancy, but now that protocols have been established, continuation of work should not be problematic.

9.2 Contributions to the Field

This research has contributed to the field in several ways. Firstly, it has highlighted differences in the trafficking of HIV-1 and HIV-2, which was previously unknown, and in doing so has also suggested that current literature on the AP binding sites within Gag may be outdated. Particularly, results herein have posited the possible presence of ulterior AP binding sites besides those currently described in MA. Results from the use of chimeric viruses may also indicate that the current theory of MA being solely responsible for Gag localisation to be oversimplified. Results gathered also stand to support, rather than dispute, the current hypothesis for HIV-1 Gag trafficking; that Gag travels to the PM via an endosomal intermediate, but also highlight the different roles

the adaptor proteins AP-1 and -3 play. AP-1 likely facilitates Gag delivery to endosomes, whereas AP-3 likely assists in the trafficking of Gag from early to late endosomal compartments, therefore indirectly assisting the PM delivery of Gag.

Secondly, a novel role for the clathrin adaptor proteins in the trafficking of lipoplexes has been unravelled. This is particularly interesting since these proteins have not been implicated in this role previously, and due to the nature of the cargo usually transported by the APs, this was particularly surprising.

Finally, this research has demonstrated a global ability of HIV to interfere with AP dependent pathways, even in cells that are not productively infected. This shows us that the APs are not solely involved in assisting particle assembly, but that a complex interplay of different APs likely exists in order to direct both the trafficking, localisation and formation of new virus particles. Although studies carried out using an astrocytoma cell line are preliminary and require further work, it was intriguing to discover that HIV-1 is able to perturb vesicle recycling within this cell line.

REFERENCES

(2010). UNAIDS Report on the Global AIDS Epidemic 2010. [online] Available from: http://www.unaids.org/globalreport/documents/20101123_GlobalReport_full_en.pdf (Accessed 03.01.2012).

(2012). UNAIDS Report on the Global AIDS Epidemic 2012. [online] Available from: http://www.unaids.org/en/media/unaids/contentassets/documents/epidemiology/2012/gr2012/20121120_UNAIDS_Global_Report_2012_en.pdf (Accessed 28.08.2013).

Adamson, C. S. and Freed, E. O. (2007). Human immunodeficiency virus type 1 assembly, release, and maturation. *Advances in Pharmacology*, **55**, 347-87.

Aguilar, R. C., Boehm, M., Gorshkova, I., Crouch, R. J., Tomita, K., Saito, T., Ohno, H. and Bonifacino, J. S. (2001). Signal-binding specificity of the mu4 subunit of the adaptor protein complex AP-4. *The Journal of Biological Chemistry*, **276**, 13145-13152.

Alberts, B., Johnson, A., Lewis, J., Raff, M., Roberts, K. and Walter, P. (2002). Molecular Biology Of The Cell, Fourth Edition (New York: Garland Science).

Aletrari, M. O., McKibbin, C., Williams, H., Pawar, V., Pietroni, P., Lord, J. M., Flitsch, S. L., Whitehead, R., Swanton, E., High, S. and Spooner, R. A. (2011). Eeyarestatin 1 interferes with both retrograde and anterograde intracellular trafficking pathways. *PloS one*, **6**, e22713.

Alroy, I., Tuvia, S., Greener, T., Gordon, D., Barr, H. M., Taglicht, D., Mandil-Levin, R., Ben-Avraham, D., Konforty, D., Nir, A., Levius, O., Bicoviski, V., Dori, M., Cohen, S., Yaar, L., Erez, O., Propheta-Meiran, O., Koskas, M., Caspi-Bachar, E., Alchanati, I., Sela-Brown, A., Moskowitz, H., Tessmer, U., Schubert, U. and Reiss, Y. (2005). The trans-Golgi network-associated human ubiquitin-protein ligase POSH is essential for HIV type 1 production. *Proceedings of the National Academy of Sciences of the United States of America*,**102**, 1478-1483.

Amaral, E., Guatimosim, S. and Guatimosim, C. (2011). Using the fluorescent styryl dye FM1-43 to visualize synaptic vesicles exocytosis and endocytosis in motor nerve terminals. *Methods in Molecular Biology*, **689**, 137-48.

Anderson, E. C. and Lever, A. M. L. (2006). Human immunodeficiency virus type 1 Gag polyprotein modulates its own translation. *Journal of Virology*, **80**, 10478-10486.

Andrew, A. and Strebel, K. (2010). HIV-1 Vpu targets cell surface markers CD4 and BST-2 through distinct mechanisms. *Molecular Aspects of Medicine*, **31**, 407-417.

Aquaro, S., Svicher, V., Ronga, L., Perno, C. F. and Pollicita, M. (2008). HIV-1-associated dementia during HAART therapy. *Recent Patents on CNS Drug Discovery*, **3**, 23-33.

Aral, S. O. (1993). Heterosexual transmission of HIV - the role of other sexually-transmitted infections and behavior in its epidemiology, prevention and control. *Annual Review of Public Health*, **14**, 451-467.

Arhel, N. J. and Kirchhoff, F. (2009). Implications of Nef: Host Cell Interactions in Viral Persistence and Progression to AIDS. *HIV Interactions with Host Cell Proteins*, **339**, 147-175.

Arts, E. J. and Hazuda, D. J. (2012). HIV-1 Antiretroviral Drug Therapy. *Cold Spring Harbour Perspectives in Medicine*, **2**.

Ayouba, A., Akoua-Koffi, C., Calvignac-Spencer, S., Esteban, A., Locatelli, S., Li, H., Li, Y., Hahn, B. H., Delaporte, E., Leendertz, F. H. and Peeters, M. (2013). Evidence for continuing cross-species transmission of SIVsmm to humans: characterization of a new HIV-2 lineage in rural Cote d'Ivoire. *Aids*, **27**, 2488-91.

Balasubramaniam, M. and Freed, E. O. (2011). New Insights into HIV Assembly and Trafficking. *Physiology*, **26**, 236-251.

Banks, W. A., Freed, E. O., Wolf, K. M., Robinson, S. M., Franko, M. and Kumar, V. B. (2001). Transport of Human Immunodeficiency Virus Type 1 Pseudoviruses across the Blood-Brain Barrier: Role of Envelope Proteins and Adsorptive Endocytosis. *Journal of Virology*, **75**, 4681-91.

Barbieri, M. A., Roberts, R. L., Mukhopadhyay, A. and Stahl, P. D. (1996). Rab5 regulates the dynamics of early endosome fusion. *Biocell*, **20**, 331-8.

Barois, N. and Bakke, O. (2005). The adaptor protein AP-4 as a component of the clathrin coat machinery: a morphological study. *Biochemical Journal*, **385**, 503-510.

Basu, V. P., Song, M., Gao, L., Rigby, S. T., Hanson, M. N. and Bambara, R. A. (2008). Strand transfer events during HIV-1 reverse transcription. *Virus Research*, **134**, 19-38.

Batonick, M., Favre, M., Boge, M., Spearman, P., Honing, S. and Thali, M. (2005). Interaction of HIV-1 Gag with the clathrin-associated adaptor AP-2. *Virology*, **342**, 190-200.

Beck, K. A. and Keen, J. H. (1991). Interaction of the phosphoinositide cycle intermediates with the plasma membrane-associated clathrin assembly protein AP-2. *Journal of Biological Chemistry*, **266**, 4442-4447.

Berkowitz, R. D., Alexander, S., Bare, C., Linquist-Stepps, V., Bogan, M., Moreno, M. E., Gibson, L., Wieder, E. D., Kosek, J., Stoddart, C. A. and McCune, J. M. (1998). CCR5- and CXCR4-utilizing strains of human immunodeficiency virus type 1 exhibit differential tropism and pathogenesis in vivo. *Journal of Virology*, **72**, 10108-10117.

Berry, N., Jaffar, S., Schim van der Loeff, M., Ariyoshi, K., Harding, E., N'Gom, P. T., Dias, F., Wilkins, A., Ricard, D., Aaby, P., Tedder, R. and Whittle, H. (2002). Low level viremia and high CD4% predict normal survival in a cohort of HIV type-2-infected villagers. *AIDS Research and Human Retroviruses*, **18**, 1167-73.

Betz, W. J., Mao, F. and Smith, C. B. (1996). Imaging exocytosis and endocytosis. *Current Opinion in Neurobiology*, **6**, 365-71.

Bhatia, S., Patil, S. S. and Sood, R. (2013). Bovine immunodeficiency virus: a lentiviral infection. *Indian Journal of Virology*, **24**, 332-341.

Blagoveshchenskaya, A. D., Thomas, L., Feliciangel, S. F., Hung, C. H. and Thomas, G. (2002). HIV-1 Nef downregulates MHC-I by a PACS-1- and PI3K-regulated ARF6 endocytic pathway. *Cell*, **111**, 853-66.

Boquet, P., Silverman, M. S., Pappenheimer, A. M., Jr. and Vernon, W. B. (1976). Binding of triton X-100 to diphtheria toxin, crossreacting material 45, and their fragments. *Proceedings of the National Academy of Sciences of the Unites States of America*, **73**, 4449-53.

Borrow, P., Shattock, R. J. and Vyakarnam, A. (2010). Innate immunity against HIV: a priority target for HIV prevention research. *Retrovirology*, **7**.

Bos, K., Wraight, C. and Stanley, K. K. (1993). TGN38 is maintained in the trans-Golgi network by a tyrosine-containing motif in the cytoplasmic domain. *EMBO journal*, **12**, 2219-2228.

Bower, M., Palmieri, C. and Dhillon, T. (2006). AIDS-related malignancies: changing epidemiology and the impact of highly active antiretroviral therapy. *Current Opinion in Infectious Diseases*, **19**, 14-19.

Brack-Werner, R. (1999). Astrocytes: HIV cellular reservoirs and important participants in neuropathogenesis. *AIDS*, **3**, 1-22.

Briant, L., Gay, B., Devaux, C. and Chazal, N. (2011). HIV-1 Assembly, Release and Maturation. *World Journal of AIDS*, **1**, 111-130.

Brierley, I. and Dos Ramos, F. J. (2006). Programmed ribosomal frameshifting in HIV-1 and the SARS-CoV. *Virus Research*, **119**, 29-42.

Briggs, J. A. G., Wilk, T., Welker, R., Krausslich, H. G. and Fuller, S. D. (2003). Structural organization of authentic, mature HIV-1 virions and cores. *Embo Journal*, **22**, 1707-1715.

Bunnik, E. M., Swenson, L. C., Edo-Matas, D., Huang, W., Dong, W., Frantzell, A., Petropoulos, C. J., Coakley, E., Schuitemaker, H., Harrigan, P. R. and van't Wout, A. B. (2011). Detection of Inferred CCR5-and CXCR4-Using HIV-1 Variants and Evolutionary Intermediates Using Ultra-Deep Pyrosequencing. *Plos Pathogens*, **7**.

Castro-Nallar, E., Pérez-Losada, M., Burton, G. F. and Crandall, K. A. (2012). The evolution of HIV: Inferences using phylogenetics. *Molecular Phylogenetics and Evolution*, **62**, 777-792.

Chan, D. C., Fass, D., Berger, J. M. and Kim, P. S. (1997). core structure of gp41 from the HIV envelope protein. *Cell*, **89**, 263-273.

Chang, J. J. and Altfeld, M. (2010). Innate Immune Activation in Primary HIV-1 Infection. *Journal of Infectious Diseases*, **202**, S297-S301.

Chang, P. K.-Y., Verbich, D. and McKinney, R. A. (2012). AMPA receptors as drug targets in neurological disease – advantages, caveats, and future outlook. *European Journal of Neuroscience*, **35**, 1908-1916.

Chapuy, B., Tikkanen, R., Mühlhausen, C., Wenzel, D., Von Figura, K. and Höning, S. (2008). AP-1 and AP-3 Mediate Sorting of Melanosomal and Lysosomal Membrane Proteins into Distinct Post-Golgi Trafficking Pathways. *Traffic*, **9**, 1157-1172.

Charneau, P., Mirambeau, G., Roux, P., Paulous, S., Buc, H. and Clavel, F. (1994). HIV-1 reverse transcription - a termination step at the center of the genome. *Journal of Molecular Biology*, **241**, 651-662.

Chaudhuri, R., Lindwasser, O. W., Smith, W. J., Hurley, J. H. and Bonifacino, J. S. (2007). Downregulation of CD4 by human immunodeficiency virus type 1 Nef is dependent on clathrin and involves direct interaction of Nef with the AP2 clathrin adaptor. *Journal of Virology*, **81**, 3877-90.

Chahroudi, A., Bosinger, S. E., Vanderford, T. H., Paiardini, M. and Silvestri, G. (2012). Natural SIV hosts: showing AIDS the door. *Science*, **335**, 1188-93.

Checkley, M. A., Luttge, B. G. and Freed, E. O. (2011). HIV-1 Envelope Glycoprotein Biosynthesis, Trafficking, and Incorporation. *Journal of Molecular Biology*, **410**, 582-608.

Choe, S., Bennett, M. J., Fujii, G., Curmi, P. M., Kantardjieff, K. A., Collier, R. J. and Eisenberg, D. (1992). The crystal structure of diphtheria toxin. *Nature*, **357**, 216-22.

Chen, H. M. and Engelman, A. (1998). The barrier-to-autointegration protein is a host factor for HIV type 1 integration. *Proceedings of the National Academy of Sciences of the United States of America*, **95**, 15270-15274.

Choe, S., Bennett, M. J., Fujii, G., Curmi, P. M., Kantardjieff, K. A., Collier, R. J. and Eisenberg, D. (1992). The crystal structure of diphtheria toxin. *Nature*, **357**, 216-22.

Christensen, R. K., Petersen, A. V. and Perrier, J. F. (2013). How do glial cells contribute to motor control? *Current Pharmaceutical Design*, **19**, 4385-99.

Chukkapalli, V. and Ono, A. (2011). Molecular determinants that regulate plasma membrane association of HIV-1 Gag. *Journal of Molecular Biology*, **410**, 512-524.

Churchill, M. J., Wesselingh, S. L., Cowley, D., Pardo, C. A., McArthur, J. C., Brew, B. J. and Gorry, P. R. (2009). Extensive astrocyte infection is prominent in human immunodeficiency virus-associated dementia. *Annals of Neurology*, **66**, 253-8.

Clark, S. J., Saag, M. S., Decker, W. D., Campbellhill, S., Roberson, J. L., Veldkamp, P. J., Kappes, J. C., Hahn, B. H. and Shaw, G. M. (1991). High titers of cytopathic virus in plasma of patients with symptomatic primary HIV-1 infection. *New England Journal of Medicine*, **324**, 954-960.

Coffin, J. M., Hughes, S. H. and Varmus, H. E. (1997). Retroviruses: Cold Spring Harbor Laboratory Press).

Collier, A. C., Coombs, R. W., Schoenfeld, D. A., Bassett, R. L., Timpone, J., Baruch, A., Jones, M., Facey, K., Whitacre, C., McAuliffe, V. J., Friedman, H. M., Merigan, T. C., Reichman, R. C., Hooper, C. and Corey, L. (1996). Treatment of human immunodeficiency virus infection with saquinavir, zidovudine, and zalcitabine. *New England Journal of Medicine*, **334**, 1011-1017.

Collins, B. M., McCoy, A. J., Kent, H. M., Evans, P. R. and Owen, D. J. (2002). Molecular Architecture and Functional Model of the Endocytic AP2 Complex. *Cell*, **109**, 523-535.

Costin, J. M. (2007). Cytopathic mechanisms of HIV-I. *Virology Journal*, **4**.

Cousin, M. A. and Robinson, P. J. (1999). Mechanisms of synaptic vesicle recycling illuminated by fluorescent dyes. *Journal of Neurochemistry*, **73**, 2227-39.

Craig, H. M., Reddy, T. R., Riggs, N. L., Dao, P. P. and Guatelli, J. C. (2000). Interactions of HIV-1 nef with the mu subunits of adaptor protein complexes 1, 2, and 3: role of the dileucine-based sorting motif. *Virology*, **271**, 9-17.

Craigie, R. and Bushman, F. D. (2012). HIV DNA Integration. *Cold Spring Harbor perspectives in medicine*, **2**.

Crowther, R. A. and Pearse, B. M. F. (1981). Assembly and packing of clathrin into coats. *Journal of Cell Biology*, **91**, 790-797.

Daly, C. J. and McGrath, J. C. (2003). Fluorescent ligands, antibodies, and proteins for the study of receptors. *Pharmacology & Therapeutics*, **100**, 101-118.

Danglot, L. and Galli, T. (2007). What is the function of neuronal AP-3? *Biology of the Cell*, **99**, 349-61.

Das, A. T., Harwig, A. and Berkhout, B. (2011). The HIV-1 Tat Protein Has a Versatile Role in Activating Viral Transcription. *Journal of Virology*, **85**, 9506-9516.

de Marco, A., Heuser, A. M., Glass, B., Krausslich, H. G., Muller, B. and Briggs, J. A. (2012). Role of the SP2 domain and its proteolytic cleavage in HIV-1 structural maturation and infectivity. *Journal of Virology*, **86**, 13708-16.

de Silva, T. I., Cotten, M. and Rowland-Jones, S. L. (2008). HIV-2: the forgotten AIDS virus. *Trends Microbiol*, **16**, 588-95.

de Silva, T. and Weiss, R. A. (2010). HIV-2 Goes Global: An Unaddressed Issue in Indian Anti-Retroviral Programmes. *The Indian Journal of Medical Research*, **132**, 660-662.

Delchambre, M., **Gheysen, D., Thines, D., Thiriart, C., Jacobs, E., Verdin, E., Horth, M., Burny, A. and Bex, F.** (1989). The Gag precursor of simian immunodeficiency virus assembles into virus-like particles. *EMBO Journal*, **8**, 2653-2660.

Delelis, O., Saib, A. and Sonigo, P. (2003). Biphasic DNA synthesis in spumaviruses. *Journal of Virology*, **77**, 8141-6.

DellAngelica, E. C., Ohno, H., Ooi, C. E., Rabinovich, E., Roche, K. W. and Bonifacino, J. S. (1997). AP-3: An adaptor-like protein complex with ubiquitous expression. *EMBO Journal*, **16**, 917-928.

Deneka, M., Pelchen-Matthews, A., Byland, R., Ruiz-Mateos, E. and Marsh, M. (2007). In macrophages, HIV-1 assembles into an intracellular plasma membrane domain containing the tetraspanins CD81, CD9, and CD53. *Journal of Cell Biology*, **177**, 329-41.

B. Descours, A. Cribier, C. Chable-Bessia, D. Ayinde, G. Rice, Y. Crow, A. Yatim, O. Schwartz, N. Laguette, M. Benkirane. (2012). SAMHD1 restricts HIV-1 reverse transcription in quiescent $CD4^+$ T-cells. *Retrovirology*, **9.**

Desjarlais, D. C., Friedman, S. R., Choopanya, K., Vanichseni, S. and Ward, T. P. (1992). International epidemiology of HIV and AIDS among injecting drug-users. *AIDS*, **6**, 1053-1068.

Dilley, K. A., Ni, N., Nikolaitchik, O. A., Chen, J., Galli, A. and Hu, W. S. (2011). Determining the frequency and mechanisms of HIV-1 and HIV-2 RNA copackaging by single-virion analysis. *Journal of Virology*, **85**, 10499-508.

Dimitrov, D. S., Willey, R. L., Sato, H., Chang, L. J., Blumenthal, R. and Martin, M. A. (1993). Quantitation of human-immunodeficiency-virus type-1 infection kinetics. *Journal of Virology*, **67**, 2182-2190.

Dinman, J. D., Ruiz-Echevarria, M. J. and Peltz, S. W. (1998). Translating old drugs into new treatments: ribosomal frameshifting as a target for antiviral agents. *Trends in Biotechnology*, **16**, 190-196.

Dinneen, J. L. and Ceresa, B. P. (2004). Expression of dominant negative rab5 in HeLa cells regulates endocytic trafficking distal from the plasma membrane. *Experimental Cell Research*, **294**, 509-22.

Dismuke, D. J. and Aiken, C. (2006). Evidence for a functional link between uncoating of the human immunodeficiency virus type 1 core and nuclear import of the viral preintegration complex. *Journal of Virology*, **80**, 3712-3720.

Dong, X. H., Li, H., Derdowski, A., Ding, L. M., Burnett, A., Chen, X. M., Peters, T. R., Dermody, T. S., Woodruff, E., Wang, J. J. and Spearman, P. (2005). AP-3 directs the intracellular trafficking of HIV-1 Gag and plays a key role in particle assembly. *Cell*, **120**, 663-674.

Donovan, J. J., Simon, M. I., Draper, R. K. and Montal, M. (1981). Diphtheria toxin forms transmembrane channels in planar lipid bilayers. *Proceedings of the National Academy of Sciences of the Unites States of America*, **78**, 172-176.

Dore, G. J. and Cooper, D. A. (2001). Bridging the divide: global inequities in access to HIV/AIDS therapy. *Medical Journal of Australia*, **175**, 570-572.

Dorfman, T., Luban, J., Goff, S. P., Haseltine, W. A. and Gottlinger, H. G. (1993). Mapping of functionally important residues of a cysteine-histidine box in the human-immunodeficiency-virus type-1 nucleocapsid protein. *Journal of Virology*, **67**, 6159-6169.

Dou, H. Y., Morehead, J., Bradley, J., Gorantla, S., Ellison, B., Kingsley, J., Smith, L. M., Chao, W., Bentsman, G., Volsky, D. J. and Gendelman, H. E. (2006). Neuropathologic and neuroinflammatory activities of HIV-1-infected human astrocytes in murine brain. *Glia*, **54**, 81-93.

Douek, D. C., Picker, L. J. and Koup, R. A. (2003). T cell dynamics in HIV-1 infection. *Annual Review of Immunology*, **21**, 265-304.

Drazin, R., Kandel, J. and Collier, R. J. (1971). Structure and Activity of Diphtheria Toxin II. Attack by Trypsin at a Specific Site Within The Intact Toxin Molecule. *The Journal of Biological Chemistry*, **240**, 1504-1510.

Duncan, C. J. A. and Sattentau, Q. J. (2011). Viral Determinants of HIV-1 Macrophage Tropism. *Viruses-Basel*, **3**, 2255-2279.

Dunn, D. T., Newell, M. L., Ades, A. E. and Peckham, C. S. (1992). Risk of human-immunodeficiency-virus type-1 transmission through breast-feeding. *Lancet*, **340**, 585-588.

Egan, M. A., Carruth, L. M., Rowell, J. F., Yu, X. and Siliciano, R. F. (1996). Human immunodeficiency virus type 1 envelope protein endocytosis mediated by a

highly conserved intrinsic internalization signal in the cytoplasmic domain of gp41 is suppressed in the presence of the Pr55gag precursor protein. *Journal of Virology*, **70**, 6547-56.

Elouahabi, A. and Ruysschaert, J. M. (2005). Formation and intracellular trafficking of lipoplexes and polyplexes. *Mol Ther*, **11**, 336-47.

Endo, Y. and Tsurugi, K. (1988). The RNA N-glycosidase activity of ricin A-chain. The characteristics of the enzymatic activity of ricin A-chain with ribosomes and with rRNA. *Journal of Biological Chemistry*, **263**, 8735-8739.

Escola, J.-M., Kleijmeer, M. J., Stoorvogel, W., Griffith, J. M., Yoshie, O. and Geuze, H. J. (1998). Selective Enrichment of Tetraspan Proteins on the Internal Vesicles of Multivesicular Endosomes and on Exosomes Secreted by Human B-lymphocytes. *Journal of Biological Chemistry*, **273**, 20121-20127.

Este, J. A. and Telenti, A. (2007). HIV entry inhibitors. *Lancet*, **370**, 81-88.

Fackler, O. T. and Baur, A. S. (2002). Live and let die: Nef functions beyond HIV replication. *Immunity*, **16**, 493-497.

Farina, F., Pierobon, P., Delevoye, C., Monnet, J., Dingli, F., Loew, D., Quanz, M., Dutreix, M. and Cappello, G. (2013). Kinesin KIFC1 actively transports bare double-stranded DNA. *Nucleic Acids Research*, **41**, 4926–4937.

Farnet, C. M. and Haseltine, W. A. (1991). Determination of viral-proteins present in the human-immunodeficiency-virus type-1 preintegration complex. *Journal of Virology*, **65**, 1910-1915.

Fauci, A. S. (1988). The human immunodeficiency virus - infectivity and mechanisms of pathogenesis. *Science*, **239**, 617-622.

Fellin, T. and Carmignoto, G. (2004). Neurone-to-astrocyte signalling in the brain represents a distinct multifunctional unit. *The Journal of Physiology*, **559**, 3-15.

Ferguson, S., Raimondi, A., Paradise, S., Shen, H., Mesaki, K., Ferguson, A., Destaing, O., Ko, G., Takasaki, J., Cremona, O., O' Toole, E. and De Camilli, P. (2009). Coordinated Actions of Actin and BAR Proteins Upstream of Dynamin at Endocytic Clathrin-Coated Pits. *Developmental cell*, **17**, 811-822.

Folsch, H., Pypaert, M., Maday, S., Pelletier, L. and Mellman, I. (2003). The AP-1A and AP-1B clathrin adaptor complexes define biochemically and functionally distinct membrane domains. *The Journal of cell biology*, **163**, 351-62.

Forgac, M. (2007). Vacuolar ATPases: rotary proton pumps in physiology and pathophysiology. *Nat Rev Mol Cell Biol*, **8**, 917-29.

Forshey, B. M., von Schwedler, U., Sundquist, W. I. and Aiken, C. (2002). Formation of a human immunodeficiency virus type 1 core of optimal stability is crucial for viral replication. *Journal of Virology*, **76**, 5667-5677.

Fotin, A., Cheng, Y., Grigorieff, N., Walz, T., Harrison, S. C. and Kirchhausen, T. (2004). Structure of an auxilin-bound clathrin coat and its implications for the mechanism of uncoating. *Nature*, **432**, 649-53.

Frankel, A. D. and Young, J. A. T. (1998). HIV-1: Fifteen proteins and an RNA. *Annual Review of Biochemistry*, **67**, 1-25.

Freed, E. O. and Martin, M. A. (1995). The role of human-immunodeficiency-virus type-1 envelope glycoproteins in virus-infection. *Journal of Biological Chemistry*, **270**, 23883-23886.

Friedrich, B., Li, G., Dziuba, N. and Ferguson, M. R. (2010). Quantitative PCR used to Assess HIV-1 Integration and 2-LTR Circle Formation in Human Macrophages, Peripheral Blood Lymphocytes and a CD4+ Cell Line. *Virology Journal*, **7**.

Friedrich, B. M., Dziuba, N., Li, G., Endsley, M. A., Murray, J. L. and Ferguson, M. R. (2011). Host factors mediating HIV-1 replication. *Virus Research*, **161**.

Friend, D. S., Papahadjopoulos, D. and Debs, R. J. (1996). Endocytosis and intracellular processing accompanying transfection mediated by cationic liposomes. *Biochimica et Biophysica Acta (BBA) - Biomembranes*, **1278**, 41-50.

Fujii, K., Munshi, U. M., Ablan, S. D., Demirov, D. G., Soheilian, F., Nagashima, K., Stephen, A. G., Fisher, R. J. and Freed, E. O. (2009). Functional role of Alix in HIV-1 replication. *Virology*, **391**, 284-292.

Fuller, S. D., Wilk, T., Gowen, B. E., Krausslich, H. G. and Vogt, V. M. (1997). Cryo-electron microscopy reveals ordered domains in the immature HIV-1 particle. *Current Biology*, **7**, 729-738.

Ganser-Pornillos, B., Yeager, M. and Sundquist, W. I. (2008). The Structural Biology of HIV Assembly. *Current Opinion in Structural Biology*, **18**, 203-217.

Gao, F., Bailes, E., Robertson, D. L., Chen, Y., Rodenburg, C. M., Michael, S. F., Cummins, L. B., Arthur, L. O., Peeters, M., Shaw, G. M., Sharp, P. M. and Hahn, B. H. (1999). Origin of HIV-1 in the chimpanzee Pan troglodytes troglodytes. *Nature*, **397**, 436-441.

Geretti, A. M. (2006). HIV-1 subtypes: epidemiology and significance for HIV management. *Current Opinion in Infectious Disease*, **19**, 1-7.

Ghafouri, M., Amini, S., Khalili, K. and Sawaya, B. E. (2006). HIV-1 associated dementia: symptoms and causes. *Retrovirology*, **3**.

Ghanam, R. H., Samal, A. B., Fernandez, T. F. and Saad, J. S. (2012). Role of the HIV-1 Matrix Protein in Gag Intracellular Trafficking and Targeting to the Plasma Membrane for Virus Assembly. *Frontiers in microbiology*, **3.**

Gifford, R. J. (2012). Viral evolution in deep time: lentiviruses and mammals. *Trends in Genetics*, **28**, 89-100.

Gilbert, M. T. P., Rambaut, A., Wlasiuk, G., Spira, T. J., Pitchenik, A. E. and Worobey, M. (2007). The emergence of HIV/AIDS in the Americas and beyond.*Proceedings of the National Academy of Sciences*, **104**, 18566-18570.

Gladnikoff, M., Shimoni, E., Gov, N. S. and Rousso, I. (2009). Retroviral Assembly and Budding Occur through an Actin-Driven Mechanism. *Biophysical Journal*, **97**, 2419-28.

Glyvuk, N., Tsytsyura, Y., Geumann, C., D'Hooge, R., Huve, J., Kratzke, M., Baltes, J., Boening, D., Klingauf, J. and Schu, P. (2010). AP-1/sigma1B-adaptin mediates endosomal synaptic vesicle recycling, learning and memory. *The EMBO Journal*, **29**, 1318-30.

Goedert, J. J. (2012). HIV-associated lung cancer: ambiguities and challenges. *Aids*, **26**, 1031-1033.

Goff, S. P. (1990). Retroviral Reverse Transcriptase: Synthesis, Structure and Function. *journal of acquired immune deficiency syndromes*, **3**, 817-831.

Gomez, C. and Hope, T. J. (2005). The ins and outs of HIV replication. *Cellular Microbiology*, **7**, 621-626.

Gonzalez-Scarano, F. and Martin-Garcia, J. (2005). The neuropathogenesis of AIDS. *Nature Reviews Immunology*, **5**, 69-81.

Gorry, P., Purcell, D., Howard, J. and McPhee, D. (1998). Restricted HIV-1 infection of human astrocytes: potential role of nef in the regulation of virus replication. *Journal of Neurovirology*, **4**, 377-86.

Gorry, P. R., Howard, J. L., Churchill, M. J., Anderson, J. L., Cunningham, A., Adrian, D., McPhee, D. A. and Purcell, D. F. (1999). Diminished production of human immunodeficiency virus type 1 in astrocytes results from inefficient translation of gag, env, and nef mRNAs despite efficient expression of Tat and Rev. *Journal of Virology*,**73**, 352-61.

Gorry, P. R., Ong, C., Thorpe, J., Bannwarth, S., Thompson, K. A., Gatignol, A., Vesselingh, S. L. and Purcell, D. F. (2003). Astrocyte infection by HIV-1: mechanisms of restricted virus replication, and role in the pathogenesis of HIV-1-associated dementia. *Current HIV Research*, **1**, 463-73.

Gottlieb, G. S. and Sow, P. S. H., S. E.Ndoye, I.Redman, M.Coll-Seck, A. M.Faye-Niang, M. A.Diop, A.Kuypers, J. M.Critchlow, C. W.Respess, R.Mullins, J. I.Kiviat, N. B. (2002). Equal Plasma Viral Loads Predict a Similar Rate of CD4± T Cell Decline in Human Immunodeficiency Virus (HIV) Type 1- and HIV-2-Infected Individuals from Senegal, West Africa. *Journal of Infectious Diseases*, **185**, 905-914.

Göttlinger, H. G. (2001). HIV-1 Gag: a molecular machine driving viral particle assembly and release. *HIV Compendium*.

Gousset, K., Ablan, S. D., Coren, L. V., Ono, A., Soheilian, F., Nagashima, K., Ott, D. E. and Freed, E. O. (2008). Real-time visualization of HIV-1 GAG trafficking in infected macrophages. *Plos Pathogens*, **4**.

Greenspan, A. and Castro, K. G. (1990). Heterosexual Transmission of HIV Infection. *Siecus Report*, **19**, 1-27.

Griffin, S. D., Allen, J. F. and Lever, A. M. (2001). The major human immunodeficiency virus type 2 (HIV-2) packaging signal is present on all HIV-2 RNA species: cotranslational RNA encapsidation and limitation of Gag protein confer specificity. *Journal of Virology*, **75**, 12058-69.

Groom, H. C. T., Anderson, E. C. and Lever, A. M. L. (2009). Rev: beyond nuclear export. **90**, 1303-1318.

Grossman, Z., Meier-Schellersheim, M., Paul, W. E. and Picker, L. J. (2006). Pathogenesis of HIV infection: what the virus spares is as important as what it destroys. *Nature Medicine*, **12**, 289-295.

Grulich, A. E., Wan, X. N., Law, M. G., Coates, M. and Kaldor, J. M. (1999). Risk of cancer in people with AIDS. *AIDS*, **13**, 839-843.

Guyader, M., Emerman, M., Sonigo, P., Clavel, F., Montagnier, L. and Alizon, M. (1987). Genome organization and transactivation of the human-immunodeficiency-virus type-2. *Nature*, **326**, 662-669.

Haigwood, N. L. and Stamatatos, L. (2003). Role of neutralizing antibodies in HIV infection. *AIDS*, **17**.

Halassa, M. M., Fellin, T. and Haydon, P. G. (2007). The tripartite synapse: roles for gliotransmission in health and disease. *Trends in Molecular Medicine*, **13**, 54-63.

Hamilton, N. B. and Attwell, D. (2010). Do astrocytes really exocytose neurotransmitters? *Nature Reviews Neuroscience*,**11**, 227-38.

Han, Y. H., Moon, H. J., You, B. R. and Park, W. H. (2009). The effect of MG132, a proteasome inhibitor on HeLa cells in relation to cell growth, reactive oxygen species and GSH. *Oncol Rep*, **22**, 215-21.

Hansmann, A., Schim van der Loeff, M. F., Kaye, S., Awasana, A. A., Sarge-Njie, R., O'Donovan, D., Ariyoshi, K., Alabi, A., Milligan, P. and Whittle, H. C. (2005). Baseline plasma viral load and CD4 cell percentage predict survival in HIV-1- and HIV-2-infected women in a community-based cohort in The Gambia.*J Acquir Immune Defic Syndr*, **38**, 335-41.

Harrich, D. and Hooker, B. (2002). Mechanistic aspects of HIV-1 reverse transcription initiation. *Reviews in Medical Virology*, **12**, 31-45.

Harrison, G. P., Miele, G., Hunter, E. and Lever, A. M. (1998). Functional analysis of the core human immunodeficiency virus type 1 packaging signal in a permissive cell line. *Journal of Virology*, **72**, 5886-5896.

Hearps, A. C. and Jans, D. A. (2006). HIV-1 integrase is capable of targeting DNA to the nucleus via an importin alpha/beta-dependent mechanism. *Biochemical Journal*, **398**, 475-484.

Henne, W. M., Boucrot, E., Meinecke, M., Evergren, E., Vallis, Y., Mittal, R. and McMahon, H. T. (2010). FCHo Proteins Are Nucleators of Clathrin-Mediated Endocytosis. *Science*, **328**, 1281-1284.

Hermida-Matsumoto, L. and Resh, M. D. (2000). Localization of Human Immunodeficiency Virus Type 1 Gag and Env at the Plasma Membrane by Confocal Imaging. *Journal of Virology*, **74**, 8670-8679.

Hirst, J., Barlow, L. D., Francisco, J. C., Sahlender, D. A., Seaman, M. N. J., Dacks, J. B. and Robinson, M. S. (2011). The Fifth Adaptor Protein Complex. *Plos Biology*, **10**, e1001170

Hirst, J., Irving, C. and Borner, G. H. H. (2013). Adaptor Protein Complexes AP-4 and AP-5: New Players in Endosomal Trafficking and Progressive Spastic Paraplegia. *Traffic*, **14**, 153-164.

Hirst, J. and Robinson, M. S. (1998). Clathrin and adaptors. *Biochimica et Biophysica Acta (BBA) - Molecular Cell Research*, **1404**, 173-193.

Homann, S., Smith, D., Little, S., Richman, D. and Guatelli, J. (2011). Upregulation of BST-2/Tetherin by HIV infection in vivo. *Journal of Virology*, **85**, 10659-68.

Holm, G. H. and Gabuzda, D. (2005). Distinct mechanisms of CD4(+) and CD8(+) T-cell activation and bystander apoptosis induced by human immunodeficiency virus type 1 virions. *Journal of Virology*, **79**, 6299-6311.

Horenkamp, F. A., Breuer, S., Schulte, A., Luelf, S., Weyand, M., Saksela, K. and Geyer, M. (2011). Conformation of the Dileucine-Based Sorting Motif in HIV-1 Nef Revealed by Intermolecular Domain Assembly. *Traffic*, **12**, 867-877.

Huotari, J. and Helenius, A. (2011). Endosome maturation. *Embo j*, **30**, 3481-500.

Hryckiewicz, K., Bura, M., Kowala-Piaskowska, A., Bolewska, B. and Mozer-Lisewska, I. (2011). HIV RNA Splicing. *HIV & AIDS Review*, **10**, 61-64.

Huang, S. C. (2007). Protease-activated receptor-1 (PAR1) and PAR2 but not PAR4 mediate relaxations in lower esophageal sphincter. *Regulatory Peptides*, **142**, 37-43.

Ivanchenko, S., Godinez, W. J., Lampe, M., Kraeusslich, H.-G., Eils, R., Rohr, K., Braeuchle, C., Mueller, B. and Lamb, D. C. (2009). Dynamics of HIV-1 Assembly and Release. *Plos Pathogens*, **5**.

Iversen, T. G., Skretting, G., Llorente, A., Nicoziani, P., van Deurs, B. and Sandvig, K. (2001). Endosome to Golgi transport of ricin is independent of clathrin and of the Rab9- and Rab11-GTPases. *Mol Biol Cell*, **12**, 2099-107.

Jacks, T., Power, M. D., Masiarz, F. R., Luciw, P. A., Barr, P. J. and Varmus, H. E. (1988). Characterization of ribosomal frameshifting in HIV-1 gag-pol expression. *Nature*, **331**, 280-283.

Jacobson, K. A., Ivanov, A. A., de Castro, S., Harden, T. K. and Ko, H. (2009). Development of selective agonists and antagonists of P2Y receptors. *Purinergic Signalling*, **5**, 75-89.

Janeway, C. A., Travers, P., Walport, M. and Shlomchik, M. J. (2001). Immunobiology: The Immune System in Health and Disease. 5th edition.

Jia, B., Serra-Moreno, R., Neidermyer, W., Rahmberg, A., Mackey, J., Fofana, I. B., Johnson, W. E., Westmoreland, S. and Evans, D. T. (2009). Species-specific activity of SIV Nef and HIV-1 Vpu in overcoming restriction by tetherin/BST2. *PLoS Pathogens*, **5**, e1000429.

Johnson, S. F. and Telesnitsky, A. (2010). Retroviral RNA Dimerization and Packaging: The What, How, When, Where, and Why. *Plos Pathogens*, **6**.

Joshi, A., Garg, H., Nagashima, K., Bonifacino, J. S. and Freed, E. O. (2008). GGA and arf proteins modulate retrovirus assembly and release. *Molecular Cell*, **30**, 227-238.

Jouvenet N., Neil, S. J. D., Bess, C., Johnson, M. C., Virgen C. A., Simon, S. M. and Bieniasz, P. D (2006). Plasma Membrane Is the Site of Productive HIV-1 Particle Assembly. *PLoS Biology*, **4**, (12): e435. doi:10.1371/journal.pbio.0040435

Kajaste-Rudnitski, A., Pultrone, C., Marzetta, F., Ghezzi, S., Coradin, T. and Vicenzi, E. (2010). Restriction factors of retroviral replication: the example of Tripartite Motif (TRIM) protein 5α and 22. *Amino Acids*, **39**, 1-9.

Karn, J. (1999). Tackling Tat. *Journal of Molecular Biology*, **293**, 235-254.

Katz, R. A. and Skalka, A. M. (1994). The retroviral enzymes. *Annual Review of Biochemistry*, **63**, 133-173.

Kaul, M. (2009). HIV-1 associated dementia: update on pathological mechanisms and therapeutic approaches. *Current Opinion in Neurology*, **22**, 315-20.

Kaye, J. F. and Lever, A. M. L. (1998). Nonreciprocal packaging of human immunodeficiency virus type 1 and type 2 RNA: a possible role for the p2 domain of Gag in RNA encapsidation. *Journal of Virology*, **72**, 5877-5885.

Kelly, B. T., McCoy, A. J., Spate, K., Miller, S. E., Evans, P. R., Honing, S. and Owen, D. J. (2008). A structural explanation for the binding of endocytic dileucine motifs by the AP2 complex. *Nature*, **456**, 976-79.

Khvotchev, M. and Kavalali, E. T. (2008). Pharmacology of neurotransmitter release: measuring exocytosis. *Handbook of Experimental Pharmacology*, 23-43.

Kim, S. H. and Ryan, T. A. (2009). A Distributed Set of Interactions Controls Functionality in the Role of AP-2 as a Sorting Adaptor in Synaptic Vesicle Endocytosis. *The Journal of Biological Chemistry*, **284**, 32803-12.

Kim, S. H. and Ryan, T. A. (2009). Synaptic vesicle recycling at CNS synapses without AP-2. *The Journal of Neuroscience*, **29**, 3865-74.

Kirchhausen, T. (1999). Adaptors for clathrin-mediated traffic. *Annual Review of Cell and Developmental Biology*, **15**, 705-732.

Kirchhausen, T. (2000). Clathrin. *Annual Review of Biochemistry*, **69**, 699-727.

Kirchhausen, T. and Harrison, S. C. (1981). Protein organisation in clathrin trimers. *Cell*, **23**, 755-761.

Kirsch, T. and Beevers, L. (1993). Uncoating of clathrin-coated vesicles by uncoating ATPase from developing peas. . *Plant Physiology*, **103**, 205-212.

Knysz, B., Szetela, B. and Gladysz, A. (2007). Pathogenesis of HIV-1 Infection: Chosen Aspects. *HIv & AIDS Review*, **6**, 7-11.

Kramer-Hammerle, S., Rothenaigner, I., Wolff, H., Bell, J. E. and Brack-Werner, R. (2005). Cells of the central nervous system as targets and reservoirs of the human immunodeficiency virus. *Virus Research*, **111**, 194-213.

Kyere, S. K., Mercredi, P. Y., Dong, X., Spearman, P. and Summers, M. F. (2012). The HIV-1 matrix protein does not interact directly with the protein interactive domain of AP-3δ. *Virus Research*, **162**, 411-414.

Laga, M., Diallo, M. O. and Buve, A. (1994). Inter-relationship of sexually transmitted diseases and HIV: where are we now? *AIDS*, **8 (supp. 1)**, S119–S124.

Laguette, N., Bregnard, C., Benichou, S. and Basmaciogullari, S. (2010). Human immunodeficiency virus (HIV) type-1, HIV-2 and simian immunodeficiency virus Nef proteins. *Molecular Aspects of Medicine*, **31**, 418-433.

Laguette, N., Sobhian, B., Casartelli, N., Ringeard, M., Chable-Bessia, C., Segeral, E., Yatim, A., Emiliani, S., Schwartz, O. and Benkirane, M. (2011). SAMHD1 is the dendritic- and myeloid-cell-specific HIV-1 restriction factor counteracted by Vpx. *Nature*, **474**, 654-7.

Lahouassa, H., Daddacha, W., Hofmann, H., Ayinde, D., Logue, E. C., Dragin, L., Bloch, N., Maudet, C., Bertrand, M., Gramberg, T., Pancino, G., Priet, S., Canard, B., Laguette, N., Benkirane, M., Transy, C., Landau, N. R., Kim, B. and Margottin-Goguet, F. (2012). SAMHD1 restricts the replication of human

immunodeficiency virus type 1 by depleting the intracellular pool of deoxynucleoside triphosphates. *Nature Immunology*, **13**, 223-8.

Lau, A. W. and Chou, M. M. (2008). The adaptor complex AP-2 regulates post-endocytic trafficking through the non-clathrin Arf6-dependent endocytic pathway. *Journal of Cell Science*, **121**, 4008-4017.

Le Rouzic, E. and Benichou, S. (2005). The Vpr protein from HIV-1: distinct roles along the viral life cycle. *Retrovirology*, **2**.

Lee, M. R., Shin, J. N., Moon, A. R., Park, S. Y., Hong, G., Lee, M. J., Yun, C. W., Seol, D. W., Piya, S., Bae, J., Oh, J. W. and Kim, T. H. (2008). A novel protein, MUDENG, induces cell death in cytotoxic T cells. *Biochemical and Biophysical research Communications*, **370**, 504-508.

Lemey, P., Pybus, O. G., Rambaut, A., Drummond, A. J., Robertson, D. L., Roques, P., Worobey, M. and Vandamme, A. M. (2004). The molecular population genetics of HIV-1 group O. *Genetics*, **167**, 1059-68.

Lemey, P., Pybus, O. G., Wang, B., Saksena, N. K., Salemi, M. and Vandamme, A.-M. (2003). Tracing the Origin and History of the HIV-2 Epidemic. *Proceedings of the National Academy of Sciences in the Unites States of America*, **100**, 6588-6592.

Lemichez, E., Bomsel, M., Devilliers, G., vanderSpek, J., Murphy, J. R., Lukianov, E. V., Olsnes, S. and Boquet, P. (1997). Membrane translocation of diphtheria toxin fragment A exploits early to late endosome trafficking machinery. *Molecular Microbiology*, **23**, 445-57.

Leroux, C., Cadore, J. L. and Montelaro, R. C. (2004). Equine Infectious Anemia Virus (EIAV): what has HIV's country cousin got to tell us? *Veterinary Research*, **35**, 485-512.

Levy, J. A. (1993). Pathogenesis of human-immunodeficiency-virus infection. *Microbiological Reviews*, **57**, 183-289.

Lewthwaite, P. and Wilkins, E. (2009). Natural History of HIV/AIDS. *Medicine*, **37**, 333-337.

Li, G., D'Souza-Schorey, C., Barbieri, M. A., Roberts, R. L., Klippel, A., Williams, L. T. and Stahl, P. D.(1995). Evidence for phosphatidylinositol 3-kinase as a regulator of endocytosis via activation of Rab5. *Proc Natl Acad Sci U S A*, **92**, 10207-11.

Li, M. and Craigie, R. (2006). Virology - HIV goes nuclear. *Nature*, **441**, 581-582.

Li, Y., Kar, A. K. and Sodroski, J. (2009). Target Cell Type-Dependent Modulation of Human Immunodeficiency Virus Type 1 Capsid Disassembly by Cyclophilin A. *Journal of Virology*, **83**, 10951-10962.

Liu, B., Dai, R., Tian, C. J., Dawson, L., Gorelick, R. and Yu, X. F. (1999). Interaction of the Human Immunodeficiency Virus Type 1 Nucleocapsid with Actin. *Journal of Virology*, **73**, 2901-2908.

Liu, H., Liu, Y., Liu, S., Pang, D. W. and Xiao, G. (2011). Clathrin-mediated endocytosis in living host cells visualized through quantum dot labeling of infectious hematopoietic necrosis virus. *Journal of Virology*, **85**, 6252-6262.

Liu, L., Sutton, J., Woodruff, E., Villalta, F., Spearman, P. and Xinhong, D. (2012). Defective HIV-1 Particle Assembly in AP-3 Deficient Cells Derived from

Patients with Hermansky-Pudlak Syndrome Type 2. *Journal of Virology*, **20**, 11242-11253.

Llano, M., Vanegas, M., Fregoso, O., Saenz, D., Chung, S., Peretz, M. and Poeshla, E. M. (2004). LEDGF/p75 determines cellular trafficking of diverse lentiviral but not murine oncoretroviral integrase proteins and is a component of functional lentiviral preintegration complexes. *Journal of Virology*, **78**, 9524–9537.

Llorente, A., Lauvrak, S. U., van Deurs, B. and Sandvig, K. (2003). Induction of direct endosome to endoplasmic reticulum transport in Chinese hamster ovary (CHO) cells (LdlF) with a temperature-sensitive defect in epsilon-coatomer protein (epsilon-COP). *J Biol Chem*, **278**, 35850-5.

Lowe, G. D. O. (1987). Hemophilia, blood products and HIV-infection. *Scottish Medical Journal*, **32**, 109-111.

Lu, M., Blacklow, S. C. and Kim, P. S. (1995). A trimeric structural domain of the HIV-1 transmembrane glycoprotein. *Nature Structural Biology*, **2**, 1075-1082.

Lubben, N. B., Sahlender, D. A., Motley, A. M., Lehner, P. J., Benaroch, P. and Robinson, M. S. (2007). HIV-1 Nef-induced Down-Regulation of MHC Class I Requires AP-1 and Clathrin but Not PACS-1 and Is Impeded by AP-2. *Molecular Biology of the Cell*, **18**, 3351-3365.

Luo, L. Z., Li, Y. and Kang, C. Y. (1990). Expression of Gag precursor protein and secretion of virus-like Gag particles of HIV-2 from recombinant baculovirus-infected insect cells. *Virology*, **179**, 874-880.

MacNeil, A., Sarr, A. D., Sankale, J. L., Meloni, S. T., Mboup, S. and Kanki, P. (2007). Direct evidence of lower viral replication rates in vivo in human immunodeficiency virus type 2 (HIV-2) infection than in HIV-1 infection. *Journal of Virology*, **81**, 5325-30.

Mahieux, R. and Gessain, A. (2003). HTLV-1 and associated adult T-cell leukemia/lymphoma. *Reviews in Clinical Experimental Hematology*, **7**, 336-61.

Malim, M. H. and Emerman, M. (2008). HIV-1 accessory proteins - Ensuring viral survival in a hostile environment. *Cell Host & Microbe*, **3**, 388-398.

Margottin, F., Bour, S. P., Durand, H., Selig, L., Benichou, S., Richard, V., Thomas, D., Strebel, K. and Benarous, R. (1998). A novel human WD protein, h-beta TrCP, that interacts with HIV-1 Vpu connects CD4 to the ER degradation pathway through an F-box motif. *Molecular Cell*, **1**, 565-574.

Marno, K. M., Ogunkolade, B. W., Pade, C., Oliveira, N. M., O'Sullivan, E. and McKnight, A. (2014). Novel restriction factor RNA-associated early-stage anti-viral factor (REAF) inhibits human and simian immunodeficiency viruses. *Retrovirology* **11**, 3.

Marsh, M., Pelchen-Matthews, A. (2000). Endocytosis in viral replication. *Traffic*, **7**, 525-532

Martinez, N. W., Xue, X., Berro, R. G., Kreitzer, G. and Resh, M. D. (2008). Kinesin KIF4 Regulates Intracellular Trafficking and Stability of the Human Immunodeficiency Virus Type 1 Gag Polyprotein. *Journal of Virology*, **82**, 9937-9950.

Martinez-Steele, E., Awasana, A. A., Corrah, T., Sabally, S., van der Sande, M., Jaye, A., Togun, T., Sarge-Njie, R., McConkey, S. J., Whittle, H. and Schim van der Loeff, M. F. (2007). Is HIV-2- induced AIDS different from HIV-1-associated AIDS? Data from a West African clinic. *Aids*, **21**, 317-24.

Mateyak, M. K. and Kinzy, T. G. (2013). ADP-ribosylation of translation elongation factor 2 by diphtheria toxin in yeast inhibits translation and cell separation. *Journal of Biological Chemistry*, **288**, 24647-55.

Mattapallil, J. J., Douek, D. C., Hill, B., Nishimura, Y., Martin, M. and Roederer, M. (2005). Massive infection and loss of memory CD4(+) T cells in multiple tissues during acute SIV infection. *Nature*, **434**, 1093-1097.

McCann, E. M. and Lever, A. M. (1997). Location of cis-acting signals important for RNA encapsidation in the leader sequence of human immunodeficiency virus type 2. *Journal of Virology*, **71**, 4133-7.

McCutchan, F. E. and Jackson, H. M. (2003). HIV-1 Global Distribution. [online] Available from: http://www.pbs.org/wgbh/pages/frontline/aids/atlas/clade.html (Accessed 05.01.2012).

McCutchan, F. E. (2006). Global epidemiology of HIV. *Journal of Medical Virology*, **78 Suppl 1**, S7-s12.

McGlynn, J. (1983). 'Gay compromise syndrome'. *Nursing mirror*, **156**, 20-2.

McMahon, H. T. and Mills, I. G. (2004). COP and clathrin-coated vesicle budding: different pathways, common approaches. *Current Opinion in Cell Biology*,**16**, 379-391.

McMahon, H. T. and Boucrot, E. (2011). Molecular mechanism and physiological functions of clathrin-mediated endocytosis. *Nat Rev Mol Cell Biol*, **12**, 517-33.

Mehle, A., Goncalves, J., Santa-Marta, M., McPike, M. and Gabuzda, D. (2004). Phosphorylation of a novel SOCS-box regulates assembly of the HIV-1 Vif-Cul5 complex that promotes APOBEC3G degradation. *Genes & Development*, **18**, 2861-2866.

Miele, G., Mouland, A., Harrison, G. P., Cohen, E. and Lever, A. M. (1996). The human immunodeficiency virus type 1 5' packaging signal structure affects translation but does not function as an internal ribosome entry site structure. *Journal of Virology*, **70**, 944-951.

Mills, I. G. (2007). The interplay between clathrin-coated vesicles and cell signalling. *Seminars in Cell & Developmental Biology*, **18**, 459-470.

Minana, R., Duran, J. M., Tomas, M., Renau-Piqueras, J. and Guerri, C. (2001). Neural cell adhesion molecule is endocytosed via a clathrin-dependent pathway. *The European Journal of Neuroscience*, **13**, 749-56.

Misumi, S., Inoue, M., Dochi, T., Kishimoto, N., Hasegawa, N., Takamune, N. and Shoji, S. (2010). Uncoating of Human Immunodeficiency Virus Type 1 Requires Prolyl Isomerase Pin1. *Journal of Biological Chemistry*, **285**, 25185-25195.

Montana, V., Malarkey, E. B., Verderio, C., Matteoli, M. and Parpura, V. (2006). Vesicular transmitter release from astrocytes. *Glia*, **54**, 700-715.

Morikawa, Y., Hinata, S., Tomoda, H., Goto, T., Nakai, M., Aizawa, C., Tanaka, H. and mura, S. (1996). Complete Inhibition of Human Immunodeficiency Virus

Gag Myristoylation Is Necessary for Inhibition of Particle Budding. *Journal of Biological Chemistry*, **271**, 2868-2873.

Motley, A., Bright, N. A., Seaman, M. N. and Robinson, M. S. (2003). Clathrin-mediated endocytosis in AP-2-depleted cells. *J Cell Biol*, **162**, 909-18.

Muchiri, J. M., Rigby, S. T., Nguyen, L. A., Kim, B. and Bambara, R. A. (2011). HIV-1 Reverse Transcriptase Dissociates during Strand Transfer. *Journal of Molecular Biology*, **412**, 354-364.

Murphy, J. (2011). Mechanism of Diphtheria Toxin Catalytic Domain Delivery to the Eukaryotic Cell Cytosol and the Cellular Factors that Directly Participate in the Process. *Toxins*, **3**, 294-308.

Naglich, J. G., Metherall, J. E., Russell, D. W. and Eidels, L. (1992). Expression cloning of a diphtheria toxin receptor: identity with a heparin-binding EGF-like growth factor precursor. *Cell*, **69**, 1051-61.

Nakai, J., Ohkura, M., Imoto, K. (2001). A high signal-to-noise Ca2+ probe composed of a single green fluorescent protein. *Nature Biotechnology*, **19**, 137-141.

Nakatsu, F. and Ohno, H. (2003). Adaptor protein complexes as the key regulators of protein sorting in the post-Golgi network. *Cell Structure and Function*, **28**, 419-429.

Nakatsu, F., Okada, M., Mori, F., Kumazawa, N., Iwasa, H., Zhu, G., Kasagi, Y., Kamiya, H., Harada, A., Nishimura, K., Takeuchi, A., Miyazaki, T., Watanabe, M., Yuasa, S., Manabe, T., Wakabayashi, K., Kaneko, S., Saito, T. and Ohno, H. (2004). Defective function of GABA-containing synaptic vesicles in mice lacking the AP-3B clathrin adaptor. *Journal of Cell Biology*, **167**, 293-302.

Neil, S. J., Zang, T. and Bieniasz, P. D. (2008). Tetherin inhibits retrovirus release and is antagonized by HIV-1 Vpu. *Nature*, **451**, 425-30.

Newell-Litwa, K., Seong, E., Burmeister, M. and Faundez, V. (2007). Neuronal and non-neuronal functions of the AP-3 sorting machinery. *Journal of Cell Science*, **15**, 531-541.

Nguyen, D. G., Booth, A., Gould, S. J. and Hildreth, J. E. (2003). Evidence that HIV budding in primary macrophages occurs through the exosome release pathway. *Journal of Biological Chemistry*, **278**, 52347-54.

Nicol, M. Q., Mathys, J. M., Pereira, A., Ollington, K., Ieong, M. H. and Skolnik, P. R. (2008). Human immunodeficiency virus infection alters tumor necrosis factor alpha production via Toll-like receptor-dependent pathways in alveolar macrophages and U1 cells. *Journal of Virology*, **82**, 7790-8.

Nishimura, N., Plutner, H., Hahn, K. and Balch, W. E. (2002). The delta subunit of AP-3 is required for efficient transport of VSV-G from the trans-Golgi network to the cell surface. *Proceedings of the National Academy of Sciences of the United States of America*, **99**, 6755-60.

Noble, B., Abada, P., Nunez-Iglesias, J. and Cannon, P. M. (2006). Recruitment of the Adaptor Protein 2 Complex by the Human Immunodeficiency Virus Type 2 Envelope Protein Is Necessary for High Levels of Virus Release. *Journal of Virology*, **80**, 2924-2932.

Nyamweya, S., Hegedus, A., Jaye, A., Rowland-Jones, S., Flanagan, K. L. and Macallan, D. C. (2013). Comparing HIV-1 and HIV-2 infection: Lessons for viral immunopathogenesis. *Reviews in Medical Virology*, **23**, 221-240.

Ohno, H. (2006). Clathrin-associated adaptor protein complexes. *Journal of Cell Science*, **119**, 3719-3721.

Ohno, H. (2006). Physiological roles of clathrin adaptor AP complexes: Lessons from mutant animals. *Journal of Biochemistry*, **139**, 943-948.

Ohno, H., Aguilar, R. C., Yeh, D., Taura, D., Saito, T. and Bonifacino, J. S. (1998). The medium subunits of adaptor complexes recognize distinct but overlapping sets of tyrosine-based sorting signals. *Journal of Biological Chemistry*, **273**, 25915-25921.

Oldridge, J. and Marsh, M. (1998). Nef - an adaptor adaptor? *Trends in Cell Biology*, **8**, 302-305.

Olusanya, O., Andrews, P. D., Swedlow, J. R. and Smythe, E. (2001). Phosphorylation of threonine 156 of the mu2 subunit of the AP2 complex is essential for endocytosis in vitro and in vivo. *Current Biology*, **11**, 896-900.

Ono, A. (2009). HIV-1 assembly at the plasma membrane: Gag trafficking and localization. *Future Virology*, **4**, 241-257.

Ono, A. (2007). Subcellular locations at which HIV-1 assembles. *Uirusu*, **57**, 9-18.

Ono, A., Ablan, S. D., Lockett, S. J., Nagashima, K. and Freed, E. O. (2004). Phosphatidylinositol (4,5) bisphosphate regulates HIV-1 Gag targeting to the plasma membrane. *Proceedings of the National Academy of Sciences of the Unites States of America*, **101**, 14889-14894.

Ono, A. and Freed, E. O. (2004). Cell-type-dependent targeting of human immunodeficiency virus type 1 assembly to the plasma membrane and the multivesicular body. *Journal of Virology*, **78**, 1552-1563.

Ono, A. and Freed, E. O. (2001). Plasma membrane rafts play a critical role in HIV-1 assembly and release. *Proceedings of the National Academy of Sciences of the United States of America*, **98**, 13925-13930.

Ono, A., Orenstein, J. M. and Freed, E. O. (2000). Role of the Gag matrix domain in targeting human immunodeficiency virus type 1 assembly. *Journal of virology*, **74**, 2855-2866.

Ortiz-Lazareno, P. C., Hernandez-Flores, G., Dominguez-Rodriguez, J. R., Lerma-Diaz, J. M., Jave-Suarez, L. F., Aguilar-Lemarroy, A., Gomez-Contreras, P. C., Scott-Algara, D. and Bravo-Cuellar, A.(2008). MG132 proteasome inhibitor modulates proinflammatory cytokines production and expression of their receptors in U937 cells: involvement of nuclear factor-kappaB and activator protein-1. *Immunology*, **124**, 534-41.

Owen, D. J., Collins, B. M. and Evans, P. R. (2004). Adaptors for clathrin coats: Structure and function. *Annual Review of Cell and Developmental Biology*, **20**, 153-191.

Owen, D. J. and Luzio, J. P. (2000). Structural insights into clathrin-mediated endocytosis. *Current Opinion in Cell Biology*, **12**, 467-474.

Pace, M. J., Agosto, L., Graf, E. H. and O'Doherty, U. (2011). HIV reservoirs and latency models. *Virology*, **411**, 344-354.

Pajonk, F., Himmelsbach, J., Riess, K., Sommer, A. and McBride, W. H. (2002). The Human Immunodeficiency Virus (HIV)-1 Protease Inhibitor Saquinavir Inhibits Proteasome Function and Causes Apoptosis and Radiosensitization in Non-HIV-associated Human Cancer Cells. *Cancer Research*, **62**, 5230-5235.

Pantaleo, G., Graziosi, C. and Fauci, A. S. (1993). The immunopathogenesis of human-immunodeficiency-virus infection. *New England Journal of Medicine*,**328**, 327-335.

Papini, E., Rappuoli, R., Murgia, M. and Montecucco, C. (1993). Cell Penetration of Diphtheria Toxin. *The Journal of Biological Chemistry*, **268**, 1567-1574.

Pauwels, R. (2004). New non-nucleoside reverse transcriptase inhibitors (NNRTIs) in development for the treatment of HIV infections. *Current Opinion in Pharmacology*, **4**, 437-446.

Peckham, C. and Gibb, D. (1995). Current concepts - mother-to-child transmission of the human-immunodeficiency-virus. *New England Journal of Medicine*, **333**, 298-302.

Peden, A. A., Oorschot, V., Hesser, B. A., Austin, C. D., Scheller, R. H. and Klumperman, J. (2004). Localization of the AP-3 adaptor complex defines a novel endosomal exit site for lysosomal membrane proteins. *Journal of Cell Biology*, **164**, 1065-76.

Pelchen-Matthews, A., Kramer, B. and Marsh, M. (2003). Infectious HIV-1 assembles in late endosomes in primary macrophages. *Journal of Cell Biology*,**162**, 443-455.

Pereira, L. A., Bentley, K., Peeters, A., Churchill, M. J. and Deacon, N. J. (2000). A compilation of cellular transcription factor interactions with the HIV-1 LTR promoter. *Nucleic Acids Research*, **28**, 663-668.

Perlman, M. and Resh, M. D. (2006). Identification of an intracellular trafficking and assembly pathway for HIV-1 Gag. *Traffic*, **7**, 731-745.

Perera, S. S. and Saksena, N. K. (2012). Innate, Adaptive and Intrinsic Immunity in Human Immunodeficiency Virus Infection. *American Journal of Infectious Diseases*, **8**, 132-148.

Pertel, T., Hausmann, S., Morger, D., Zuger, S., Guerra, J., Lascano, J., Reinhard, C., Santoni, F. A., Uchil, P. D., Chatel, L., Bisiaux, A., Albert, M. L., Strambio-De-Castillia, C., Mothes, W., Pizzato, M., Grutter, M. G. and Luban, J. (2011). TRIM5 is an innate immune sensor for the retrovirus capsid lattice. *Nature*, **472**, 361-5.

Peter, F. (1998). HIV nef: The mother of all evil? *Immunity*, **9**, 433-437.

Picker, L. J. (2006). Immunopathogenesis of acute AIDS virus infection. *Current Opinion in Immunology*, **18**, 399-405.

Plantier, J.-C., Leoz, M., Dickerson, J. E., De Oliveira, F., Cordonnier, F., Lemee, V., Damond, F., Robertson, D. L. and Simon, F. (2009). A new human immunodeficiency virus derived from gorillas. *Nature Medicine*, **15**, 871-872.

Pollard, V. W. and Malim, M. H. (1998). The HIV-1 Rev protein. *Annual Review of Microbiology*, **52**, 491-532.

Popov, S., Rexach, M., Zybarth, G., Reiling, N., Lee, W. A., Ratner, L., Lane, C. M., Moore, M. S., Blobel, G. and Bukrinsky, M. (1998). Viral protein R regulates nuclear import of the HIV-1 pre-integration complex. *Embo Journal*, **17**, 909-917.

Popov, S., Strack, B., Sanchez-Merino, V., Popova, E., Rosin, H. and Gottlinger, H. G. (2011). Human immunodeficiency virus type 1 and related primate lentiviruses engage clathrin through Gag-Pol or Gag. *Journal of virology*, **85**, 3792-801.

Popper, S. J., Sarr, A. D., Travers, K. U., Gueye-Ndiaye, A., Mboup, S., Essex, M. E. and Kanki, P. J.(1999). Lower human immunodeficiency virus (HIV) type 2 viral load reflects the difference in pathogenicity of HIV-1 and HIV-2. *J Infect Dis*, **180**, 1116-21.

Presley, J. F., Cole, N. B., Schroer, T. A., Hirschberg, K., Zaal, K. J. and Lippincott-Schwartz, J. (1997). ER-to-Golgi transport visualized in living cells. *Nature*, **389**, 81-5.

Quinn, T. C. (1996). Global burden of the HIV pandemic. *Lancet*, **348**, 99-106.

Ranki, A., Nyberg, M., Ovod, V., Haltia, M., Elovaara, I., Raininko, R., Haapasalo, H. and Krohn, K. (1995). Abundant expression of HIV Nef and Rev proteins in brain astrocytes in vivo is associated with dementia. *AIDS*, **9**, 1001-1008.

Raposo, G., Moore, M., Innes, D., Leijendekker, R., Leigh-Brown, A., Benaroch, P. and Geuze, H. (2002). Human Macrophages Accumulate HIV-1 Particles in MHC II Compartments. *Traffic*, **3**, 718-729.

Ratner, L., Fisher, A., Jagodzinski, L. L., Mitsuya, H., Liou, R. S., Gallo, R. C. and Wong-Staal, F. (1987). Complete nucleotide sequences of functional clones of the AIDS virus. *AIDS Res Hum Retroviruses*, **3**, 57-69.

Remy, G. (1998). HIV-2 infection throughout the world. A geographical perspective. *Sante*, **8**, 440-6.

Resh, M. D. (2005). Intracellular trafficking of HIV-1 Gag: How Gag interacts with cell membranes and makes viral particles. *Aids Reviews*, **7**, 84-91.

Rey, O., Canon, J. and Krogstad, P. (1996). HIV-1 Gag protein associates with F-actin present in microfilaments. *Virology*, **220**, 530-534.

Ribeiro, R. M., Hazenberg, M. D., Perelson, A. S. and Davenport, M. P. (2006). Naive and memory cell turnover as drivers of CCR5-to-CXCR4 tropism switch in human immunodeficiency virus type 1: Implications for therapy. *Journal of Virology*, **80**, 802-809.

Richardson, J. H., Child, L. A. and Lever, A. M. (1993). Packaging of human immunodeficiency virus type 1 RNA requires cis-acting sequences outside the 5' leader region. *Journal of Virology*, **67**, 3997-4005.

Ricotta, D., Conner, S. D., Schmid, S. L., von Figura, K. and Höning, S. (2002). Phosphorylation of the AP2 μ subunit by AAK1 mediates high affinity binding to membrane protein sorting signals. *The Journal of Cell Biology*, **156**, 791-795.

Rink, J., Ghigo, E., Kalaidzidis, Y. and Zerial, M. (2005). Rab conversion as a mechanism of progression from early to late endosomes. *Cell*, **122**, 735-49.

Robert J, G. Viral evolution in deep time: lentiviruses and mammals. *Trends in Genetics*, **28**, 89-100.

Robinson, J. G., Redford, K. H. and Bennett, E. L. (1999). Wildlife Harvest in Logged Tropical Forests. *Science*, **284**, 595-596.

Robinson, M. S. (1994). The role of clathrin, adaptors and dynamin in endocytosis. *Current Opinion in Cell Biology*, **6**, 538-544.

Robinson, M. S. and Bonifacino, J. S. (2001). Adaptor-related proteins. *Current Opinion in Cell Biology*, **13**, 444-453.

Robinson, M. S. (2004). Adaptable adaptors for coated vesicles. *Trends in Cell Biology*, **14**, 167-174.

Rodgers-Farmer, A. Y. (1999). HIV risk factors, HIV antibody testing, and AIDS knowledge among African Americans age 55 years and older. *Social Work in Health Care*, **29**, 1-17.

Roeth, J. F., Williams, M., Kasper, M. R., Filzen, T. M. and Collins, K. L. (2004). HIV-1 Nef disrupts MHC-I trafficking by recruiting AP-1 to the MHC-I cytoplasmic tail. *Journal of Cell Biology*, **167**, 903-13.

Rolfe, M. (1994). HIV-2 and its Neurological Manifestations. *South African Journal of Medicine*, **84**, 503-505.

Romani, B., Engelbrecht, S. and Glashoff, R. H. (2010). Functions of Tat: the versatile protein of human immunodeficiency virus type 1. *Journal of General Virology*, **91**, 1-12.

Saad, J. S., Miller, J., Tai, J., Kim, A., Ghanam, R. H. and Summers, M. F. (2006). Structural basis for targeting HIV-1 Gag proteins to the plasma membrane for virus assembly. *Proceedings of the National Academy of Sciences of the Unites States of America*, **103**, 11364-11369.

Saad, J. S., Ablan, S. D., Ghanam, R. H., Kim, A., Andrews, K., Nagashima, K., Soheilian, F., Freed, E. O. and Summers, M. F. (2008). Structure of the myristylated human immunodeficiency virus type 2 matrix protein and the role of phosphatidylinositol-(4,5)-bisphosphate in membrane targeting. *Journal of Molecular Biology*, **382**, 434-447.

Sackett, K. and Shai, Y. (2002). The HIV-1 gp41 N-terminal heptad repeat plays an essential role in membrane fusion. *Biochemistry*, **41**, 4678-4685.

Sakuma, R., Mael, A. A. and Ikeda, Y. (2007). Alpha Interferon Enhances TRIM5α-Mediated Antiviral Activities in Human and Rhesus Monkey Cells. *Journal of Virology*, **81**, 10201-10206.

Sandvig, K., Skotland, T., van Deurs, B. and Klokk, T. I. (2013). Retrograde transport of protein toxins through the Golgi apparatus. *Histochemistry and Cell Biology*, **140**, 317-26.

Sandvig, K., Torgersen, M. L., Engedal, N., Skotland, T. and Iversen, T. G. (2010). Protein toxins from plants and bacteria: probes for intracellular transport and tools in medicine. *FEBS Letters*, **584**, 2626-34.

Sandvig, K. and van Deurs, B. (1996). Endocytosis, intracellular transport, and cytotoxic action of Shiga toxin and ricin. *Physiology Reviews*, **76**, 949-66.

Sandvig, K. and van Deurs, B. (1996). Endocytosis, intracellular transport, and cytotoxic action of Shiga toxin and ricin. *Physiol Rev*, **76**, 949-66.

Sarafianos, S. G., Das, K., Tantillo, C., Clark, A. D., Ding, J., Whitcomb, J. M., Boyer, P. L., Hughes, S. H. and Arnold, E. (2001). Crystal structure of HIV-1 reverse transcriptase in complex with a polypurine tract RNA : DNA. *EMBO Journal*, **20**, 1449-1461.

Sarafianos, S. G., Marchand, B., Das, K., Himmel, D. M., Parniak, M. A., Hughes, S. H. and Arnold, E. (2009). Structure and Function of HIV-1 Reverse Transcriptase: Molecular Mechanisms of Polymerization and Inhibition. *Journal of Molecular Biology*, **385**, 693-713.

Sauter, D., Hue, S., Petit, S. J., Plantier, J. C., Towers, G. J., Kirchhoff, F. and Gupta, R. K. (2011). HIV-1 Group P is unable to antagonize human tetherin by Vpu, Env or Nef. *Retrovirology*, **8**, 103.

Sauter, D., Schindler, M., Speckt, A., Landford, W. M., Münch, J., Kim, K.-A., Votteler, J., Schubert, U., Bibollet-Ruche, F., Keele, B. F., Takehisa, J., Ogando, Y., Ochsenbauer, C., Kappes, J. C., Ayouba, A., Peeters, M., Learn, G. H., Shaw, G., Sharp, P. M., Bieniasz, P., Hahn, B. H., Hatziioannou, T. and Kirchoff, F. (2009). The evolution of pandemic and non-pandemic HIV-1 strains has been driven by Tetherin antagonism. *Cell host and microbe*, **6**, 409-421.

Savasta, A. M. (2004). HIV: Associated transmission risks in older adults - An integrative review of the literature. *Janac-Journal of the Association of Nurses in Aids Care*, **15**, 50-59.

Scemes, E. and Giaume, C. (2006). Astrocyte Calcium Waves: What They Are and What They Do. *Glia*, **54**, 716-25.

Schaller, M., Krnjaic, N., Niewerth, M., Hamm, G., Hube, B. and Korting, H. C. (2003). Effect of antimycotic agents on the activity of aspartyl proteinases secreted by Candida albicans. *Journal of Medical Microbiology*, **52**, 247-9.

Schep, L. J., Temple, W. A., Butt, G. A. and Beasley, M. D. (2009). Ricin as a weapon of mass terror--separating fact from fiction. *Environment International*, **35**, 1267-71.

Scheuber, A., Rudge, R., Danglot, L., Raposo, G., Binz, T., Poncer, J.-C. and Galli, T. (2006). Loss of AP-3 function affects spontaneous and evoked release at hippocampal mossy fiber synapses. *Proceedings of the National Academy of Sciences*, **103**, 16562-16567.

Schierup, M. H. and Hein, J. (2000). Recombination and the Molecular Clock. *Molecular Biology and Evolution*,**17**, 1578-1579.

Schild, G. C. and Minor, P. D. (1990). Human immunodeficiency virus and AIDS: challenges and progress. *The Lancet*, **335**, 1081-1084.

Schubert, U., Ott, D. E., Chertova, E. N., Welker, R., Tessmer, U., Princiotta, M. F., Bennink, J. R., Krausslich, H.-G. and Yewdell, J. W. (2000). Proteasome inhibition interferes with Gag polyprotein processing, release, and maturation of HIV-1 and HIV-2. *Proceedings of the National Academy of Sciences of the United States of America*, **97**, 13057-13062.

Seong, E., Wainer, B. H., Hughes, E. D., Saunders, T. L., Burmeister, M. and Faundez, V. (2005). Genetic analysis of the neuronal and ubiquitous AP-3 adaptor complexes reveals divergent functions in brain. *Molecular Biology of the Cell*, **16**, 128-140.

Sha, J., He, Y. and Liu, X. (2009). HIV Nef Increasing Viral Particle Infectivity may be Through Affecting the Protein transport of HIV Factors or Host Cellular Factors which Promote Viral Assembly or Budding. *Bioscience Hypotheses*, **2**, 85-87.

Sharp, P. M., Bailes, E., Chaudhuri, R. R., Rodenburg, C. M., Santiago, M. O. and Hahn, B. H. (2001). The origins of acquired immune deficiency syndrome viruses: where and when? *Philosophical Transactions of the Royal Society of London. Series B: Biological Sciences*, **356**, 867-876.

Sharp, P. M., Bailes, E., Robertson, D. L., Gao, F. and Hahn, B. H. (1999). Origins and Evolution of AIDS Viruses. *The Biological Bulletin*, **196**, 338-342.

Sharp, P. M. and Hahn, B. H. (2011). Origins of HIV and the AIDS Pandemic. *Cold Spring Harbor Perspectives in Medicine*, **1**.

Sharp, P. M., Robertson, D. L. and Hahn, B. H. (1995). Cross-species transmission and recombination of AIDS viruses. *Philosophical Transactions of the Royal Society of London Series B-Biological Sciences*, **349**, 41-47.

Sherer, N. M., Lehmann, M. J., Jimenez-Soto, L. F., Ingmundson, A., Horner, S. M., Cicchetti, G., Allen, P. G., Pypaert, M., Cunningham, J. M. and Mothes, W. (2003). Visualization of Retroviral Replication in Living Cells Reveals Budding into Multivesicular Bodies. *Traffic*, **4**, 785-801.

Sherer, N. M., Swanson, C. M., Hué, S., Roberts, R. G., Bergeron, J. R. C. and Malim, M. H. (2011). Evolution of a Species-Specific Determinant within Human CRM1 that Regulates the Post-transcriptional Phases of HIV-1 Replication. *PLoS Pathogens*, **7**, e1002395.

Shi, G., Faúndez, V., Roos, J., Dell'Angelica, E. C. and Kelly, R. B. (1998). Neuroendocrine Synaptic Vesicles Are Formed In Vitro by Both Clathrin-dependent and Clathrin-independent Pathways. *The Journal of Cell Biology*, **143**, 947-955.

Shi, Y., Brandin, E., Vincic, E., Jansson, M., Blaxhult, A., Gyllensten, K., Moberg, L., Brostrom, C., Fenyo, E. M. and Albert, J. (2005). Evolution of human immunodeficiency virus type 2 coreceptor usage, autologous neutralization, envelope sequence and glycosylation. *J Gen Virol*, **86**, 3385-96.

Sierra, S., Kupfer, B. and Kaiser, R. (2005). Basics of the virology of HIV-1 and its replication. *Journal of Clinical Virology*, **34**, 233-244.

Simoes, S., Slepushkin, V., Pires, P., Gaspar, R., Pedroso de Lima, M. C. and Duzgunes, N. (2000). Human serum albumin enhances DNA transfection by lipoplexes and confers resistance to inhibition by serum. *Biochim Biophys Acta*, **1463**, 459-69.

Simmen, T., Honing, S., Icking, A., Tikkanen, R. and Hunziker, W. (2002). AP-4 binds basolateral signals and participates in basolateral sorting in epithelial MDCK cells. *Nature Cell Biology*, **4**, 154-159.

Simon, F., Matheron, S., Tamalet, C., Loussert-Ajaka, I., Bartczak, S., Pepin, J. M., Dhiver, C., Gamba, E., Elbim, C., Gastaut, J. A. and et al. (1993). Cellular and plasma viral load in patients infected with HIV-2.*Aids*, **7**, 1411-7.

Simpson, F., Bright, N. A., West, M. A., Newman, L. S., Darnell, R. B. and Robinson, M. S. (1996). A novel adaptor-related protein complex. *The Journal of Cell Biology*, **133**, 749-760.

Simpson, F., Peden, A. A., Christopoulou, L. and Robinson, M. S. (1997). Characterization of the Adaptor-related Protein Complex, AP-3. *The Journal of Cell Biology*, **137**, 835-845.

Sleiman, D., Goldschmidt, V., Barraud, P., Marquet, R., Paillart, J.-C. and Tisné, C. (2012). Initiation of HIV-1 Reverse Transcription and Functional Role of nucleocapsid-mediated tRNA/viral genome interactions. *Virus Research*, **169**, 324-329.

Smythe, E. and Ayscough, K. R. (2003). The Ark1/Prk1 family of protein kinases. *EMBO reports*, **4**, 246-251.

Soriano, V., Gomes, P., Heneine, W., Holguin, A., Doruana, M., Antunes, R., Mansinho, K., Switzer, W. M., Araujo, C., Shanmugam, V., Lourenco, H., Gonzalez-Lahoz, J. and Antunes, F. (2000). Human immunodeficiency virus type 2 (HIV-2) in Portugal: clinical spectrum, circulating subtypes, virus isolation, and plasma viral load. *J Med Virol*, **61**, 111-6.

Sorkin, A. (2004). Cargo recognition during clathrin-mediated endocytosis: a team effort. *Current Opinion in Cell Biology*, **16**, 392-399.

Sterjovski, J., Roche, M., Churchill, M. J., Ellett, A., Farrugia, W., Gray, L. R., Cowley, D., Poumbourios, P., Lee, B., Wesselingh, S. L., Cunningham, A. L., Ramsland, P. A. and Gorry, P. R. (2010). An altered and more efficient mechanism of CCR5 engagement contributes to macrophage tropism of CCR5-using HIV-1 envelopes. *Virology*, **404**, 269-278.

Stolp, B. and Fackler, O. T. (2011). How HIV Takes Advantage of the Cytoskeleton in Entry and Replication. *Viruses*, **3**, 293-311.

Stowell, D. (2006). HIV genome. [online] Available from: http://www.mcld.co.uk/hiv/?q=HIV%20genome (Accessed 20.07.2013).

Stratigos, J. D. and Tzala, E. (2000). Global epidemiology of HIV infections and AIDS. *Clinics in Dermatology*, **18**, 381-387.

Strebel, K. (2013). HIV accessory proteins versus host restriction factors. *Current Opinion in Virology*, **3**, 692-699.

Stremlau, M., Owens, C. M., Perron, M. J., Kiessling, M., Autissier, P. and Sodroski, J. (2004). The cytoplasmic body component TRIM5αrestricts HIV-1 infection in Old World monkeys. *Letters to Nature*, **427**, 848-843.

Sundquist, W. I. and Kräusslich, H.-G. (2012). HIV-1 Assembly, Budding and Maturation. *Cold Spring Harbor Perspectives in Medicine*, **2**.

Suzuki, Y. and Craigie, R. (2007). The road to chromatin - nuclear entry of retroviruses. *Nature Reviews Microbiology*, **5**, 187-196.

Suzuki, Y., Suzuki, Y. (2011). *Viral Gene Therapy*. **In**: Gene Regulatable Lentiviral Vector System. InTech.

Taylor MJ, Perrais D, Merrifield CJ. (2011) A High Precision Survey of the Molecular Dynamics of Mammalian Clathrin-Mediated Endocytosis. *PLoS Biology* 9(3): e1000604

Tebit, D. M. and Arts, E. J. (2011). Tracking a century of global expansion and evolution of HIV to drive understanding and to combat disease. *The Lancet Infectious Diseases*, **11**, 45-56.

Takeuchi, J. S., Perche, B., Migraine, J., Mercier-Delarue, S., Ponscarme, D., Simon, F., Clavel, F. and Labrosse, B. (2013). High level of susceptibility to human TRIM5alpha conferred by HIV-2 capsid sequences. *Retrovirology*, **10**, 50.

Theos, A. C., Tenza, D., Martina, J. A., Hurbain, I., Peden, A. A., Sviderskaya, E. V., Stewart, A., Robinson, M. S., Bennett, D. C., Cutler, D. F., Bonifacino, J. S., Marks, M. S. and Raposo, G. (2005). Functions of adaptor protein (AP)-3 and AP-1 in tyrosinase sorting from endosomes to melanosomes. *Molecular Biology of the Cell*, **16**, 5356-72.

Tilton, J. C. and Doms, R. W. (2010). Entry inhibitors in the treatment of HIV-1 infection. *Antiviral Research*, **85**, 91-100.

Ungewickell, E., Ungewickell, H., Holstein, S. E., Lindner, R., Prasad, K., Barouch, W., Martin, B., Greene, L. E. and Eisenberg, E. (1995). Role of auxilin in uncoating clathrin-coated vesicles. *Nature*, **378**, 632-5.

Ungewickell, E. J. and Hinrichsen, L. (2007). Endocytosis: clathrin-mediated membrane budding. *Current Opinion in Cell Biology*, **19**, 417-425.

Vandegraaff, N., Devroe, E., Turlure, F., Silver, P. A. and Engelman, A. (2006). Biochemical and genetic analyses of integrase-interacting proteins lens epithelium-derived growth factor growth factor related protein 2 function and (LEDGF)/p75 and hepatoma-derived (HRP2) in preintegration complex HIV-1 replication. *Virology*, **346**, 415-426.

van der Loeff, M. F., Larke, N., Kaye, S., Berry, N., Ariyoshi, K., Alabi, A., van Tienen, C., Leligdowicz, A., Sarge-Njie, R., da Silva, Z., Jaye, A., Ricard, D., Vincent, T., Jones, S. R., Aaby, P., Jaffar, S. and Whittle, H. (2010). Undetectable plasma viral load predicts normal survival in HIV-2-infected people in a West African village. *Retrovirology*, **7**, 46.

Veazey, R. S., Marx, P. A. and Lackner, A. A. (2001). The mucosal immune system: primary target for HIV infection and AIDS. *Trends in Immunology*, **22**, 626-633.

Vonderheit, A. and Helenius, A. (2005). Rab7 associates with early endosomes to mediate sorting and transport of Semliki forest virus to late endosomes. *PLoS Biol*, **3**, e233.

Wacker, I., Kaether, C., Kromer, A., Migala, A., Almers, W. and Gerdes, H. H. (1997). Microtubule-dependent transport of secretory vesicles visualized in real time with a GFP-tagged secretory protein. *Journal of Cell Science*, **110**, 1453-1463.

Waguri, S., Dewitte, F., Le Borgne, R., Rouille, Y., Uchiyama, Y., Dubremetz, J. F. and Hoflack, B. (2003). Visualization of TGN to endosome trafficking through fluorescently labeled MPR and AP-1 in living cells. *Molecular biology of the cell*, **14**, 142-155.

Walker, N., Grassly, N. C., Garnett, G. P., Stanecki, K. A. and Ghys, P. D. (2004). Estimating the global burden of HIV/AIDS: what do we really know about the HIV pandemic? *Lancet*, **363**, 2180-2185.

Walter, L., Franklin, A., Witting, A., Moller, T. and Stella, N. (2002). Astrocytes in culture produce anandamide and other acylethanolamides. *The Journal of Biological Chemistry*, **277**, 20869-20876.

Walter, V. (2002). Vesicular release mechanisms in astrocytic signalling. *Neurochemistry International*, **41**, 301-306.

Wang, F.-x., Huang, J., Zhang, H., Ma, X. and Zhang, H. (2008). APOBEC3G upregulation by alpha interferon restricts human immunodeficiency virus type 1 infection in human peripheral plasmacytoid dendritic cells. *Journal of General Virology*, **89**, 722-730.

Wang, Z., Pekarskaya, O., Bencheikh, M., Chao, W., Gelbard, H. A., Ghorpade, A., Rothstein, J. D. and Volsky, D. J. (2003). Reduced expression of glutamate transporter EAAT2 and impaired glutamate transport in human primary astrocytes exposed to HIV-1 or gp120. *Virology*, **312**, 60–73.

Wang, Z. Y., Trillo-Pazos, G., Kim, S. Y., Canki, M., Morgello, S., Sharer, L. R., Gelbard, H. A., Su, Z. Z., Kang, D. C., Brooks, A. I., Fisher, P. B. and Volsky, D. J. (2004). Effects of human immunodeficiency virus type 1 on astrocyte gene expression and function: Potential role in neuropathogenesis. *Journal of Neurovirology*, **10**, 25-32.

Wei, B. L., Denton, P. W., O'Neill, E., Luo, T., Foster, J. L. and Garcia, J. V. (2005). Inhibition of Lysosome and Proteasome Function Enhances Human Immunodeficiency Virus Type 1 Infection *Journal of Virology*, **79**, 5705-5712.

Weiss, E. R. and Goettlinger, H. (2011). The Role of Cellular Factors in Promoting HIV Budding. *Journal of Molecular Biology*, **410**, 525-533.

Weller, S. C. (1993). A meta-analysis of condom-effectiveness in reducing sexually-transmitted HIV. *Social Science & Medicine*, **36**, 1635-1644.

Welsch, S., Keppler, O. T., Habermann, A., Allespach, I., Krijnse-Locker, J. and Krausslich, H.-G. (2007). HIV-1 Buds Predominantly at the Plasma Membrane of Primary Human Macrophages. *Plos Pathogens*, **e36**.

Wertheim, J. O. and Worobey, M. (2009). Dating the age of the SIV lineages that gave rise to HIV-1 and HIV-2. *PLoS Comput Biol*, **5**, e1000377.

Wigge, P., Kohler, K., Vallis, Y., Doyle, C. A., Owen, D., Hunt, S. P. and McMahon, H. T. (1997). Amphiphysin heterodimers: potential role in clathrin-mediated endocytosis. *Mol Biol Cell*, **8**, 2003-15.

Worobey, M., Gemmel, M., Teuwen, D. E., Haselkorn, T., Kunstman, K., Bunce, M., Muyembe, J. J., Kabongo, J. M., Kalengayi, R. M., Van Marck, E., Gilbert, M. T. and Wolinsky, S. M. (2008). Direct evidence of extensive diversity of HIV-1 in Kinshasa by 1960. *Nature*, **455**, 661-4.

Wu, Y. (2004). HIV-1 gene expression lessons from provirus and non-integrated DNA. *Retrovirology*, **1**.

Yamamoto, J. K., Sanou, M. P., Abbott, J. R. and Coleman, J. K. (2010). Feline immunodeficiency virus model for designing HIV/AIDS vaccines. *Current HIV Research*, **8**, 14-25.

Yang, Y., Ge, W., Chen, Y., Zhang, Z., Shen, W., Wu, C., Poo, M. and Duan, S. (2003). Contribution of astrocytes to hippocampal long-term potentiation through release of d-serine. *Proceedings of the National Academy of Sciences of the United States of America*, **100**, 15194-15199.

Ylinen, L. M., Keckesova, Z., Wilson, S. J., Ranasinghe, S. and Towers, G. J. (2005). Differential restriction of human immunodeficiency virus type 2 and simian immunodeficiency virus SIVmac by TRIM5alpha alleles. *J Virol*, **79**, 11580-7.

Young, A. (2007). Structural insights into the clathrin coat. *Seminars in Cell and Developmental Biology*, **18**, 448-458.

Zeigerer, A., Gilleron, J., Bogorad, R. L., Marsico, G., Nonaka, H., Seifert, S., Epstein-Barash, H., Kuchimanchi, S., Peng, C. G., Ruda, V. M., Del Conte-Zerial, P., Hengstler, J. G., Kalaidzidis, Y., Koteliansky, V. and Zerial, M. (2012). Rab5 is necessary for the biogenesis of the endolysosomal system in vivo. *Nature*, **485**, 465-70.

Zhang, H., Zhou, Y., Alcock, C., Kiefer, T., Monie, D., Siliciano, J., Li, Q., Pham, P., Cofrancesco, J., Persaud, D. and Sliciano, R.F. Novel Single-Cell-Level Phenotypic Assay for Residual Drug Susceptibility and Reduced Replication Capacity of Drug-Resistant Human Immunodeficiency Virus Type 1. *J of Virology* **78**:1718-1729, 2004.

Zhang, F., Zang, T., Wilson, S. J., Johnson, M. C. and Bieniasz, P. D. (2011). Clathrin Facilitates the Morphogenesis of Retrovirus Particles. *PLoS Pathogens*, **7**, e1002119.

Zuhorn, I. S., Kalicharan, R. and Hoekstra, D. (2002). Lipoplex-mediated Transfection of Mammalian Cells Occurs through the Cholesterol-dependent Clathrin-mediated Pathway of Endocytosis. *Journal of Biological Chemistry*, **277**, 18021-18028.